Fall 11-1-2019

# CHARACTERIZING PHOTOBIOREGENERATIVE TECHNOLOGY FOR SIMULTANEOUS THERMAL CONTROL AND AIR REVITALIZATION OF SPACECRAFT AND SURFACE HABITATS

Emily E. Matula
emily.matula@colorado.edu

# CHARACTERIZING PHOTOBIOREGENERATIVE TECHNOLOGY FOR SIMULTANEOUS THERMAL CONTROL AND AIR REVITALIZATION OF SPACECRAFT AND SURFACE HABITATS

by

EMILY ELIZABETH MATULA

B.S., University of Michigan, 2012

M.Eng., University of Michigan, 2014

A thesis submitted to the

Faculty of the Graduate School of the

University of Colorado in partial fulfillment

of the requirement for the degree of

Doctor of Philosophy

Department of Smead Aerospace Engineering Sciences

2019

This thesis entitled:

Characterizing Photobioreactor Technology for Simultaneous Thermal Control and Air Revitalization of Spacecraft and Surface Habitats

written by Emily Elizabeth Matula

has been approved for the Department of Smead Aerospace Engineering Sciences

_____

Dr. James A. Nabity, Associate Professor
Bioastronautics, Smead Aerospace Engineering Sciences
University of Colorado - Boulder

_____

Dr. David Klaus, Professor
Bioastronautics, Smead Aerospace Engineering Sciences
University of Colorado - Boulder

Date_____

The final copy of this thesis has been examined by the signatories, and we find that both the content and the form meet acceptable presentation standards of scholarly work in the above-mentioned discipline.

Matula, Emily Elizabeth (Ph.D., Aerospace Engineering Sciences)

Characterizing Photobioreactor Technology for Simultaneous Thermal Control and Air Revitalization of Spacecraft and Surface Habitats

Thesis directed by Associate Professor James A. Nabity

Algal photobioreactors have been researched as potential solutions to air revitalization in a spacecraft cabin environment by absorbing $CO_2$ and producing $O_2$ through photosynthesis. This photosynthesis, and consumption of produced biomass, theoretically provides a closed-loop solution for long-duration spaceflight. Addressing multiple spaceflight requirements simultaneously with algae has the potential to reduce launch mass, power and volume of future Environmental Control and Life Support (ECLS) systems. Additionally, inoculating algal culture into a water-based thermal cooling loops (flight-proven standard of active cooling found on the International Space Station (ISS)) could incorporate simultaneous air revitalization and thermal control into a common system. However, this imparts rapid, extreme thermal swings on algal cells not evolved for culture in a transient thermal environment. Therefore, the effect of dynamic thermal environments on the $CO_2/O_2$ turnover of algae was characterized to provide a first-order assessment of system feasibility. This research characterizes the effect of dynamic environments, both transient thermal environments and varying levels of $CO_2$ concentration, on metabolic processes of the algal culture. Experiments using Antarctic algal species were included to investigate if cold-acclimated algae are more efficient than *Chlorella* at $CO_2/O_2$ turnover in the active cooling environment. The simultaneous heat and mass transfer coefficients of a nonporous, gas-permeable membrane were characterized, and membrane models developed for future design considerations. A photobioreactor system was designed with considerations for gravity-independence, prototyped, and tested using parameters defined by the ISS cabin environment. A failure modes and effect analysis distilled lessons learned from the previous experiments, which also informs the use of algae for bioregenerative life support. In conclusion, the resulting values from the previous characterization experiments, along with values found in literature, were used to make a first-order mass-balance comparison between current ISS ECLSS and photobioregenerative technologies. This work serves as an initial evaluation of the feasibility for using an algal photobioreactor for simultaneous air revitalization and active thermal control of a spacecraft or surface habitat.

DEDICATION

To Andrew, whose patience is more than I deserve

To those who believed in me, giving me the opportunity to get started

To those who did not, giving me the drive to finish

ACKNOWLEDGEMENTS

I would like to first thank my PhD Advisor, Dr. James A. Nabity. I will be forever grateful that he was willing to take a chance on a Michigan grad he had never met before, as his first PhD student. His support of my research, academic, and personal endeavors have advanced my career further than I thought possible. I am also thankful to the rest of my committee, Dr. David Klaus, Dr. Torin Clark, Dr. William Lewis, Dr. Daniel Barta, and Dr. Jeffery Thayer. Their patience in answering (sometimes mundane) questions while I navigated unfamiliar research territory, and willingness to identify and offer resources for experiments and data reduction increased the quality of my research and my understanding of phycology and bioastronautics.

A particular thank you to the NASA Space Technology Research Fellowship (NSTRF) program, who provided funding for this work and my tenure at the University of Colorado. Through the NSTRF program I was first paired with my mentor, Dr. Daniel Barta, who selflessly made time to be engaged in my research and provide valuable feedback on my progress. He also introduced me to research at NASA in bioregenerative ECLSS and expanded my network by connecting me to Dr. Oscar Monje and Dr. Brad Bebout -both of whom were influential in the direction of my experiments. I am thankful that these researchers, and their lab groups (including Dr. Leslie Bebout, Dr. Craig Everroad, and Angela Detweiler) were willing to readily provide guidance to a visiting PhD student.

Thank you to Dr. James McCutchan and his group at CIRES (Chase Bergeson, Stefan Petersen, and Jennifer Roberson) for allowing me to use their FireSting probes, but also to use their equipment and lab space to conduct experiments.

Many thanks to Dr. Diane McKnight, Dr. Michael Gooseff, and the McMurdo Long-Term Ecological Research (MCM-LTER) group for allowing me to be involved in the 2018-2019 season and the privilege to support the mission of the LTER. My experience provided a me a direct introduction to extremophilic algae and the team's insight into Dry Valley ecology strengthened my research.

My sincerest thanks to the BioServe group, not only was I allowed to use their lab spaces but they also made me feel as though I was part of their group, including me in discussions and taking my research timelines into consideration (their respect for my research was not required, but I will never forget it).

First, I'd like to thank Tom Vance for being the real MVP, our goal to hit all the breakfast and triple D spots in Boulder gave me something to look forward to and was always the break I needed.

Thank you to: Anyone who knows Art Mann -the author of Danger Skies, they are like a brother to me and were always there during my roughest times. Dennice and Ariel, my DMV buddies, my first friends in Boulder, and providers of cute pet pictures. Sheena Patterson, giving me your calm ear and steady thoughtfulness to get through all levels of higher education. Jordan Holquist, who was willing to listen to anything that would come after a chuckle, pause, and chair swivel -I know that he's only here for the Paragon Dessert Bar. Mike Lotto for getting me back into the range and pushing and prodding to make me better. Kimia Seyedmadani for checking-in and always remembering me. Daniel Case for giving me a different perspective and making me remember that there is always life beyond grad school. Jordan Dixon, Carlos Pinedo, and Bari Suri for being ready to swap stories and provide a laugh whenever I needed it. Matt Rhode and Adrian Stang for allowing me to invade the shop to ask for construction advice but also to be a pain in their rear. Tobias Niederwieser for letting me bounce photobioreactor ideas around and keeping me on my toes. Chris Massina for being my champion at NASA and having my back. The Graf family for opening up their house to me and introducing me to the joy of Popeyes. Meals on Wheels of Boulder for making me feel useful and loved when sometimes I otherwise felt stagnant. Kimberly Coseglia for showing me what a rockstar feminist looks like and letting me fiddle with Miss Fickle the little motorcycle (she saved my mental state on many an occasion). Thank you to the Bioastronautics group for being my home away from home and my family away from family -to anyone who stopped to chat with me in the lab while I hung out at AETHER or took cell counts, your distraction was always needed and appreciated.

A very heartfelt thank you to my parents, Val and Lisa Matula for showing me what persistence, love, and support looks like -they are the reason I know the moon and stars. My remaining bit of sanity is thanks to my brother John Matula, who kept me laughing through the very last moment. A hug, no pats, to Keith and Maria Rosine for being my cheerleaders from afar -very "note-necessary". I am thankful for my grandparents, aunts, uncles, and cousins who always encouraged me and made feel that what I was doing was very important to them.

Finally, to my husband Andrew Rosine, I love you, thank you, we made it.

This work was funded by a NASA Space Technology Research Fellowship, NNX15AP52H

Table of Contents

## List of Tables

## List of Figures

# Chapter 1 Introduction

## 1.1 Research Motivation

In an effort to take our species outside of Low Earth Orbit (LEO), NASA is now building the infrastructure and launch vehicles for future long-duration human spaceflight missions. When including humans in mission designs, Environmental Control and Life Support Systems (ECLSS) are required for crew viability. Since these flights could be beyond LEO, with minimal return capabilities, the ECLSS is required to be robust while adhering to volume, power, and mass constraints. The Life Support Section (TA6) of NASA's 2015 Technology Roadmap stated that one of the roadmap goals was to "develop technologies that enable long-duration, deep-space human exploration with minimal resupply consumables"(NASA 2015).

Current and heritage technologies providing atmospheric revitalization rely on the use of consumable products and some also generate waste. This approach can quickly become mass or volume prohibitive, as the system scales with mission duration. Other researched methods for atmospheric revitalization have included biological-based systems, such as algal photobioreactors. The Technology Roadmap states that "algae and bacteria may also provide benefits for carbon dioxide removal, oxygen production…" (NASA 2015). Biological-based systems have the capacity of providing this closed-loop capability while addressing multiple functions of an ECLSS, potentially reducing system mass, power, or volume. One such additional functionality is the use of an algal system for active thermal control of the cabin environment. Algae are typically cultured in a water-based medium with properties similar to the water used in the ISS cooling loops. So, it is conceivable that if the algal medium were used as the working fluid in the thermal loop, the algal photobioreactor could be used to control spaceflight thermal loads while simultaneously addressing atmospheric revitalization through photosynthesis. This research reviews the state-of-the-art for ECLSS, bioregenerative technologies with the potential for life support, and potential culture and system failure modes. Then characterizes the effects of dynamic thermal environments and $CO_2$ concentrations on the $CO_2/O_2$ turnover capabilities of algae. Finally, utilizing the results of a literature review while considering the results of the dynamic environment experiments, mass-balance comparisons assesses the overall operational feasibility of a notional system in a spacecraft or surface habitat environment.

### 1.2 Overview of Objectives

This dissertation demonstrates initial technical feasibility of utilizing a biological system for simultaneous air revitalization and thermal control of inhabited environments in an effort to further close the carbon loop. The research focused on the $CO_2/O_2$ turnover capabilities of an algal culture when subjected to environmental thermal cycles reflective of a water-based spacecraft thermal control loop. The executed experiments contribute to this feasibility study and explore the system operational boundaries. Resulting experimental data, and cases from the literature, inform system reliability. Both open and closed system experiments were performed in an effort to characterize traits of the biological portion of the system, without influence of confounding variables. First-order system mass balances were developed to uncover possible challenges with system scaling, and to understand the influence of design and operational conditions on the algal culture.

This work addressed the following research objectives:

1. *Investigate the reliability of an algal photobioreactor system used in nominal cabin atmospheric and thermal environments through literature surveys and experimental results.*
2. *Determine the influence of steady-state and dynamic environmental temperatures on the algal system's $CO_2$ removal and reduction, $O_2$ regeneration, and cell growth rate.*
3. *Characterize the effects of time-varying the input $CO_2$ concentrations on an algal photobioreactor system's $CO_2$ removal, $O_2$ regeneration, and metabolic rates.*
4. *Characterize simultaneous heat and mass transfer capabilities of a non-porous membrane suitable for gravity independent gas transfer.*
5. *Develop a bench-top algal system, designed to minimize gravity effects, that allows for the study of closed-loop simultaneous algal air revitalization and thermal control.*
6. *Consider the first-order feasibility of an algal photobioreactor system as a closed loop $CO_2$ reduction and $O_2$ regeneration system under nominal spacecraft cabin atmospheric and temperature conditions.*

### 1.3 Dissertation Overview

Chapter 2 provides a history of atmospheric revitalization technologies used to support human spaceflight. Included are issues pertaining to the current ISS technology, prompting the need for closed-loop systems for long

duration spaceflight. Utilization of algal systems in enclosed environments was also included in Chapter 2's survey to establish the current state-of-the-art. Chapter 3 describes how an algal photobioreactor may provide environmental control and life support (ECLS). It then assesses the reliability of the proposed photobioreactor-based ECLSS by reviewing failure causes and modes of both an algal culture and the support hardware with associated risk assessments. This informs considerations for future experiments, explains culture response to the presented environments, and addresses Objective 1. Chapter 4 characterizes the metabolic response of algae to a range of steady-state temperature environments, replicating literature results and suggesting an operational envelope for the bioregenerative system to address Objective 2. Figure 1 portrays how parametric experimental results reported in Chapters 5,6, and 7 informs the design a comprehensive system-level experiment that investigated concurrent air revitalization and active thermal control. Chapter 5 responds to Objective 2 by subjecting algal cultures to temperature cycles, simulating a spacecraft thermal control loop, while measuring culture metabolic response. Chapter 6 continues the study of algal metabolic response to transient environments. The culture was exposed to dynamic environmental concentrations of $CO_2$, imitating changes in cabin gas concentration. The $CO_2$ to $O_2$ turnover-rate of the culture was measured during these changes, which addresses Objective 3. Chapter 7 shifts focus from the biological aspect of the air revitalization/thermal control approach to the supporting hardware, therefore, responding to Objective 4. Here, an assessment of the simultaneous heat and mass transfer capabilities of a nonporous membrane was conducted. Chapter 8, addressing Objective 5, utilizes the results of both the biological and supporting hardware experiments to develop a bench-top bioreactor with minimal gravity-dependence for supporting simultaneous air revitalization and active thermal control. The unit was tested within the operational regimes experienced by the ISS environment. Lessons learned from this unit informed suggestions for a photobioreactor design for spaceflight, presented in this chapter. Chapter 9 provides an initial feasibility assessment of an algal photobioreactor installation, responding to Objective 6. The assessment was performed through first-order sizing calculations using mass-balance equations, and system considerations and comparisons to currently used ISS technologies. Chapter 9 also includes a review of operational regimes for the proposed photobioreactor, based off of the results of the presented experiments, while knowledge gaps for biological ECLSS are identified. Chapter 10 expands the scope of this photobioreactor research by investigating the use of species native to extreme environments, and how they may be predisposed to efficient spaceflight utilization. Here, preliminary replications

of previous temperature cycling experiments are conducted with Antarctic chlorophytes. In conclusion, Chapter 11 summarizes the presented research by reviewing experimental results, discussing the possible feasibility of implementing the proposed system in a spaceflight environment, and detailing future research required to continue assessing an algal photobioreactor's potential for supporting multifunctional ECLSS in a spacecraft or surface habitat.

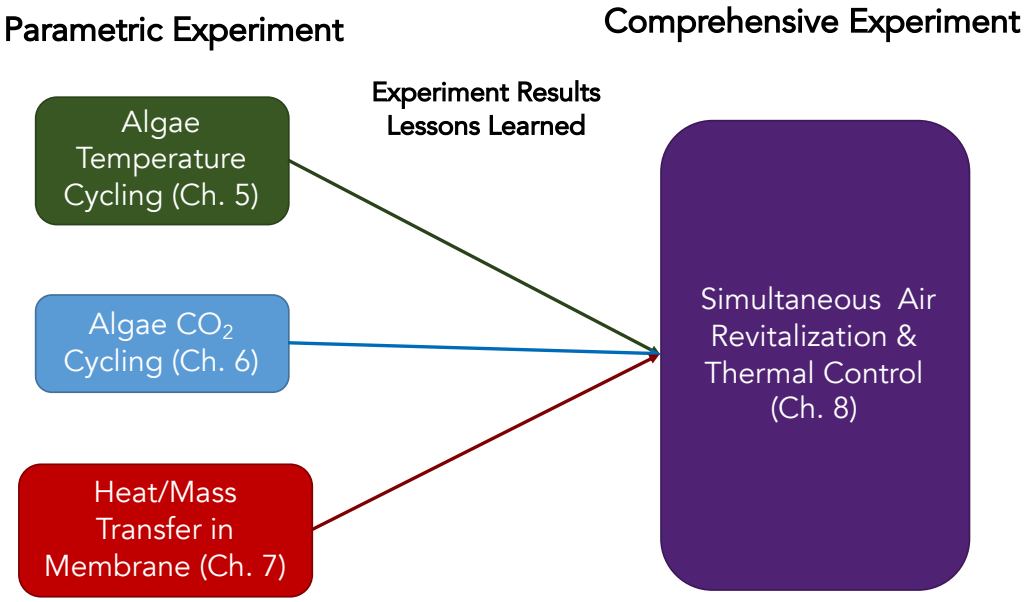


**Figure 1. Illustration of parametric experiments used to inform the design of a photobioreactor system for study of simultaneous air revitalization and active thermal control**

# Chapter 2 Research Rationale and Background

## 2.1 Introduction

Environmental Control and Life Support Systems (ECLSS) provide the most fundamental physiological needs for all manned spaceflight missions. One of these, atmosphere revitalization, requires the removal of carbon dioxide ($CO_2$) and replenishment of oxygen ($O_2$) to maintain a breathable atmosphere. There are various ways to fulfill this need, depending on the duration and distance of the mission. One approach for short duration missions (<16 days), $CO_2$ could be absorbed with Lithium-Hydroxide (LiOH), and $O_2$ could be generated by a chemical system (perchlorate oxygen candle) or carried up in cylinders (Metcalf et al. 2012; Meck et al. 2001). These expendable systems have been repeatedly spaceflight-proven (Cronyn, Watkins, and Alexander 2012). Expendables may be acceptable for short duration missions due to the ability for resupply from Earth. Long duration missions may require closed-loop, regenerable systems because of their potential for smaller launch mass when compared to an open-loop system with consumables as cargo. Technologies that provide multiple functionalities, or capabilities in addition to the primary purpose, could further reduce this launch mass. With future missions projected to extend farther out into space, regenerable technologies become increasingly important to meet the needs of the crew.

## 2.2 Problem Statement

NASA has made it clear through their dialogue in the 2014 Strategic Plan that they intend to pursue longer duration missions and travel farther from the Earth than before. As the Strategic Plan states, “NASA is expanding human exploration by developing the capability to transport humans to and from deep space…using innovative technologies” and “due to available flight trajectories, astronauts will either have to leave within 30 days or stay on the surface [of Mars] for more than 500 days…they will need to be self-sufficient.” Consequently, in the 2015 NASA Technology Roadmap TA 6: Human Health, Life Support, and Habitation Systems document, NASA has also acknowledged the need for “high-reliability processes…increased self-sufficiency…and minimized logistics supply” to sustain manned missions beyond Low Earth Orbit (LEO). The request for reliable processes can be mapped to the need to produce “Systems that remove metabolically-generated carbon dioxide from the spacecraft atmosphere to

safe levels for the crew, and deliver the carbon dioxide to onboard processes dedicated to the recovery of oxygen." (NASA 2015).

Current $CO_2$ removal and reduction and $O_2$ generation technologies for long duration spaceflight, such as those that have been used on the International Space Station (ISS), include the use of a Carbon Dioxide Removal Assembly (CDRA), Carbon Dioxide Reduction Assembly (CRA), and Oxygen Generation Assembly (OGA). These systems require the regular resupply of materials and consumables. For example, the CDRA/Sabatier reactor vents methane as a waste, thereby consuming hydrogen to recover some of the $O_2$ from $CO_2$. Secondly, historical failure rates associated with the with the overall air revitalization system were higher than initially estimated, as the CDRA system previously failed approximately 90 days compared to the calculated 1,000 days (Flynn, M. personal communication, October 14, 2014, Gentry and Cover 2015).

The purpose of this research was to characterize the $CO_2/O_2$ turnover of an algal photobioreactor for simultaneous air revitalization and active thermal control, addressing the concern about air revitalization NASA outlined in TA6. Terrestrial designs have shown photosynthetic-based systems can provide a relatively reliable, closed-loop solution for $CO_2$ removal and $O_2$ resupply (Smernoff, Wharton, and Averner 1987). Photosynthetic-based systems have potential full closure of the carbon loop, can operate within nominal cabin temperatures, do not require the use of hazardous materials (such as pure hydrogen gas), passively respond to dynamic environments, and offer multifunctional capabilities. Time between system maintenance of algal cultures used terrestrially for biodiesel and pharmaceuticals are longer than a mission to the Martian surface, suggesting the potential for system reliability (Chisti 2007). Feasibility of using an algal photobioreactor for atmospheric revitalization and thermal control in a spacecraft and habitat environment was informed through benchtop experiments characterizing algal response (through cell health and $CO_2/O_2$ turnover rates) to transient cabin environments.

### 2.3 Background of Current Spacecraft ECLSS and Appropriate Biological Technologies

This section reviews the rationale for investigating biological systems as a replacement for current physicochemical ones. First, the human metabolic requirements that an ECLSS addresses when planning for human spaceflight are presented. Then, the current physicochemical technologies that address the air revitalization and thermal control requirements are described, along with their shortcomings. Lastly, photosynthetic systems are

detailed, with their promise to overcome drawbacks associated with physicochemical systems. Only the air revitalization and thermal control capabilities of the photobioreactor system area reviewed, since it was the focus of the conducted research.

### 2.3.1 Human Spaceflight Requirements

When humans are included in spaceflight mission designs, considerations need to be made to keep them "alive, healthy, and happy"(D. M. Klaus 2004). Figure 2 depicts the most basic of crew metabolic inputs and outputs needed for the crew.

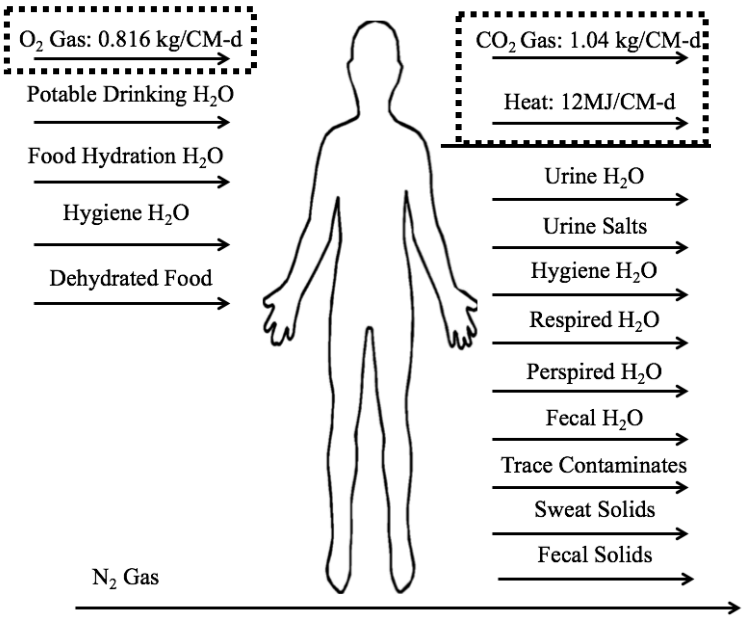


**Figure 2. Basic human inputs and outputs for metabolic functioning as presented by Anderson et al. 2018. Those to be considered for the researched air revitalization and thermal control photobioreactor have been boxed in a dashed line.**

While all aspects of the human metabolic inputs and outputs are presented in the Figure 2, those parameters considered as part of the algal photobioreactor system researched for ECLSS use have been highlighted. The Baseline Values and Assumptions Document (BVAD) produced by NASA provides rates and values for each of these metabolic functions as well as cabin thresholds (Anderson et al. 2018). Those cabin thresholds that influence air revitalization and thermal control concepts are presented in Table 1.

**Table 1. Thresholds for a human spaceflight cabin as presented by Anderson et al.2018**

| Cabin Characteristic | Acceptable Range or Threshold, Nominal |
|---|---|
| Oxygen Content | 18-23.1 kPa |
| Carbon Dioxide Content | 0.031-0.71 kPa, 0.4 kPa |
| Relative Humidity | 25-70%, 60% |
| Temperature | 291.5-299.8 K, 295.2 K |
| Pressure | 48.0-192.7 kPa, 70.3 kPa |

### 2.3.2 Current ECLSS Technology

Air revitalization system size scales with mission duration and crew size; as a result, the system may become so large that it becomes mission prohibiting due to mass and volume constraints. The Apollo-era missions were a maximum of 14 days with a 3-person crew. Given this short duration mission and small crew size, non-regenerable technologies were used. Lithium hydroxide (LiOH) canisters removed carbon dioxide ($CO_2$) and onboard tanks replenished atmospheric oxygen ($O_2$). As the missions and crew numbers increased during the Shuttle-era, and eventually into the ISS-era, the "carry it with you" approach to air revitalization became too massive to remain cost effective to launch. Regenerable technologies for atmospheric revitalization became necessary as the mission durations became longer and more mass prohibitive. Currently, the ISS uses a multi-component, partly regenerable system for removing $CO_2$ and providing $O_2$. This includes molecular sieve absorption of $CO_2$ (Carbon Dioxide Removal Assembly, CDRA) and reduction of $CO_2$ and hydrogen into water and methane (CRA), and the production of $O_2$ and hydrogen from water electrolysis (Knox and Stanley 2015).

The CDRA system was thought to only require maintenance no more than once every three years, when first brought online, but due to zeolite dust contamination and pump failure, the system failed, on average, more than four times in a year. A study reviewing the theoretical maximum failure rates of the CDRA system stated that it was calculated to have a rate of one failure approximately every 170 days, which was the highest rate when compared to other technologies (Jones 2011; Sherif and Knox 2005). CDRA reliability expressed as a concern by both NASA ISS on-orbit reports and a NASA representative (Flynn, M., personal communication, October 14, 2014, Metcalf et al. 2012). It was observed that the actual mean time between failures was 90 days. Each of these repairs requires extra consumables, including crew time.

For a Sabatier reaction, the major consumable is hydrogen, a hazardous byproduct of water electrolysis, delivered to the system. Sabatier-produced methane is currently vented overboard, but candidate technologies are being considered for utilization of this waste methane. The Sabatier reaction is exothermic, which means it produces heat during the chemical reaction. The resulting reaction temperature can exceed 500 °C, while insulated, the insulation required to protect the crew is an additional launch mass. A portion of the waste heat is used to warm up the Sabatier reactants before initiation through the reaction, while the rest of the heat must be removed by a condensing heat exchanger. In addition to these wastes, the low recovery rate of $O_2$ (approximately 50%) also reduces the overall effectiveness of the system (Samplatsky et al. 2011; Metcalf et al. 2012).

Most items in the spacecraft cabin create heat and necessitate the need for a cooling system to keep the cabin within the set temperature range. Cabin cooling capabilities are provided by a system that uses clean water loops to remove heat from the cabin. The heat from the water is transferred to an ammonia loop (via an Interface Heat Exchanger, IFHX), then to a radiator, from which the heat is rejected into space (The Boeing Company, n.d.). Having two separate cooling loops, the Moderate Temperature Loop (MTL) and the Low Temperature Loop (LTL), allows for quicker heat removal, depending on the area's temperature requirements and allowable temperature swings.

The cabin thermal control system, while it does employ pumps and valves, is relatively reliable and does not have any current overarching issues. When expanding the focus from the cabin aspect of the system to the entire cooling loop, there are health concerns about using ammonia and impending leaks. However, this is not included in the focus of the current research overview.

The active thermal aspect of this research is relatively well-established, as liquid-cooling loops have been included in spaceflight designs since the Gemini program (Peterson 1987). Therefore, while the influence of the thermal system on algae was considered, the principle focus of this dissertation was on the biological aspects of the algal photobioreactor for air revitalization and active thermal control.

### 2.4 History of Investigated Concept

The thought of trying to use photosynthetic organisms to sequester $CO_2$ and regenerate $O_2$ in a cabin environment is not novel. NASA and others have researched the idea of using water-based bioregenerative systems

since 1958; their first experiments involved the use of *Lemnaceae* or duckweed. Unfortunately, due to the state of culturing technology at the time, i.e. inefficient lighting systems, they were unable to design a system to fit within their mass and power constraints for flight (Welch 1963). However, the technology was ground-proven in 1961 by the Soviet Union. One man's entire $CO_2$ limits and $O_2$ requirements were sustained with 30L of algae (*Chlorella*) for 30 days. The Russian's BIOS III, a closed ecosystem inhabited by humans, attained the highest terrestrial-test closure level of 91%, but it also incorporated the use of some higher plants. Since then, two shuttle missions have flown with closed-loop aquarium experiments that included algae. The algae reproduced more than two culture generations and were able to support the fish contained in the aquarium (Eckart 1995). The European Space Agency (ESA) has continued the idea of a comprehensive approach to biological-based ECLSS. The Micro-Ecological Life Support System Alternative (MELiSSA) based its system designs off of a lake eco-structure, incorporating higher plants and micro-bacteria in a similar concept as the aquariums. However, the MELiSSA concept structures the regenerable loop into compartments -each one isolated from the other in an effort to simplify the behaviors of each area. While this may increase the need for support hardware (for system isolation and upkeep), it may increase efficiency in system response, as each area could be tuned to cabin events (Lasseur 2011).

Early designs for spaceflight used terrestrial culturing techniques employing a multiphase flow for provision of water and nutrients to the algal cells. $CO_2$ provision relied on sparging, or bubbling, of gases through the medium, which is difficult to control in a microgravity environment. In the 1990's the commercialization of gas-permeable membranes was able to provide gas diffusion into the liquid stream, without bubble formation. Since then, various photobioreactor designs have been developed for spaceflight applications, all including gas-permeable membranes for $CO_2$ provision and $O_2$ removal of the algal stream (Javanmardian and Palsson 1991; Jochen Keppler et al. 2018). Researchers at the University of Stuttgart developed and launched a membrane-based photobioreactor, for culturing the algae *C. vulgaris* aboard the ISS. The bioreactor uses a $CO_2$ slip stream from the European Space Agency's (ESA) Life Support Rack (LSR) to support the culture. Under investigation is culture's response to microgravity through optical density (culture density), $O_2$ production, and $CO_2$ consumption measurements (Jochen Keppler et al. 2018).

Recently, NASA Ames Research Center investigated using algal systems for multifunctional purposes during spaceflight. The "Water Walls" system involved the use of semipermeable bags to clean wastewater, house algae

for bioregeneration of the atmospheric environment, and contained solid waste for radiation shielding. The technology hoped to also serve as a food source and passive buffer of the cabin thermal environment (Cohen, Flynn, and Matossian 2013). The design was immature with respect to operation under thermal load. As stated in its most recent publication, "Detailed calculations have not been completed yet because experimental work to measure the heat transfer in the bags in the cabin environment remains ahead of us" (Cohen, Flynn, and Matossian 2013). The experimentation presented in this dissertation investigated active thermal capabilities, related to the thermal control discussed by Flynn.

### 2.4.1 Photosynthetic ECLSS

To gain a better understanding for why algal photobioreactors (PBRs) should be considered for ECLSS use, a study of their cellular functioning should first be presented. Photosynthesis, a simplified version presented in Eq. 1, uses carbon dioxide, water, and energy from illumination (photons) to produce glucose and oxygen.

$$6CO_2 + 12H_2O + photons \rightarrow C_6H_{12}O_6 + 6O_2 + 6H_2O \quad (1)$$

As the equation shows, theoretically 100% of the $O_2$ in $CO_2$ can be recovered. While the $O_2$ produced in the equation is supplied by splitting water molecules, it equates to the same amount as provided in the $CO_2$. However, since algal cells are not perfectly efficient systems, there are some losses that should be included. Typically, algal cells are able to fix approximately 90% of the $CO_2$ dissolved into the medium (Ammann and Fraser-Smith 1968). When the biomass is consumed by the crew, and thereby consuming the reduced carbon from $CO_2$, it provides a closed-loop solution to carbon.

Unabsorbed solar spectrum presents an additional efficiency loss, as chlorophylls only absorb in the 400-700nm wavelength regime (Nakajima, Hanawa, and Tsuchiya 2015). As stated by the Food and Agriculture Organization of the United Nations,

> *"…effectively allowing only 45% of total solar energy to be utilized for photosynthesis. Furthermore, fixation of one $CO_2$ molecule during photosynthesis, necessitates a quantum requirement of ten (or more), which results in a maximum utilization of only 25% of the PAR absorbed by the photosynthetic system. On the basis of these limitations, the theoretical maximum efficiency of solar energy conversion is approximately 11%"* (Miyamoto 1997).

So while 90% of the $CO_2$ in the algal stream is fixed by the cells, and theoretically 100% of $O_2$ is regenerated from the $CO_2$, it requires large amounts of energy at specific wavelengths of light (+2,870 kJ/mol is required for the synthesis of glucose) to produce an economical regeneration stream (Whitmarsh and Govindjee 1999). Using LEDs or fluorescent lights tuned to provide these specific wavelengths is one way to increase photosynthetic efficiency.

Passive adaptability to dynamic environments is another advantage of implementing algal cultures in a spacecraft habitat. Positive correlation of photosynthesis rates to human respiration rates is an example of beneficial environmental response. Increased human respiration (i.e. during exercise) may result in a rise in cabin $CO_2$ concentration, cellular response to this $CO_2$ increase is an escalation in $O_2$ production. Consequently, additional $O_2$ is required by the humans during exercise (Singh and Singh 2014; Anderson et al. 2018).

Benefits of utilizing an algal culture for food provision is attributed to its growth dynamics. Algal biomass potentially provides nutritional supplementation due to its protein, fat, carbohydrate, and nutrient content (United States Department of Agriculture 2016). Its high harvest index (ratio of edible to total biomass), of nearly 100%, fast doubling time (as low as 12hrs) lend algal biomass, and high edible biomass to volume ratio lend algal biomass to be an efficient nutritional source.

### 2.5 Conclusions

The research presented in this dissertation investigated the feasibility of using an algal photobioreactor as a closed-loop air revitalization and active thermal control system for the spacecraft cabin and surface habitat environment. First-order feasibility of this system was developed through identification of possible failure modes and rates, mass-balance comparisons between resulting photobioreactors and current ECLSS, and characterization of photobioreactor system operation through experimentation. This research idea stems from NASA's 2015 Technology Roadmap goal to identify closed-loop technologies that are appropriate for long duration human spaceflight missions. Using the combined system was originally considered by Dr. Michael Flynn's group at NASA Ames, but they did not pursue the thermal control aspect due to project scope, and their system utilized passive instead of active thermal control. The Technology Readiness Level (TRL) of this concept of photobioreactor-based combined air revitalization and active thermal control at its initiation was a level 1, meaning basic principles were observed and reported surrounding the idea. Now, at the completion of this research series, levels vary between 2

and 4 for different aspects of the system (Mai 2015). Research results could not only provide insight on a potential closed-loop system for spaceflight but could also contribute to the overall understanding of algal metabolic functioning in a transient thermal and atmospheric environment.

# Chapter 3 Photobioreactor Failure Modes and Mitigation Methods

## 3.1 Introduction

Missions supporting deep space initiatives will be farther from Earth than ever before and will need to rely on Earth-independent technologies. NASA has put forth a Technology Roadmap, identifying areas requiring technological advancements to support these missions (NASA 2015). Most relevant to this research are areas focused on atmosphere and water revitalization, and the reliability and robustness of space flight systems. As stated in the Technology Roadmap,

> *"Increasing closure of water and oxygen loops can pay significant dividends to deep-space missions, but only if the systems involved have the demonstrated reliability needed to avoid mission costs associated with large stored reserves; large, redundant systems; and large inventories of replacement hardware. Overall system reliability and potential reductions in spare equipment should be addressed at both the subsystem (hardware) and complete system levels, Design and operational simplicity, combined with process robustness to unforeseen circumstances and conditions, need to be regarded among the most important measures of "goodness" as candidate technologies are developed and compared."*(NASA 2015)

Environmental Control and Life Support Systems (ECLSS) are expected to have a certain degree of robustness, including reliability, resilience, and survivability (Escobar, Nabity, and Klaus 2017). However, in low Earth orbit (LEO), the approach to achieve robust systems has been through redundancy, and regular provision of spare components, equipment, and consumables. As missions travel farther from Earth, it becomes exceedingly difficult to launch these components with the same frequency of today. NASA has identified the need to improve robustness of closed-loop technologies.

> *"The overarching sub-goal for environmental control, life support, and habitation is to develop and demonstrate highly reliable capabilities needed to sustain humans for long periods of time in deep space with minimal reliance on Earth-supplied consumables, expendables, replacement equipment, and crew intervention and maintenance, coupled with capabilities to efficiently use in-situ resources and recycle, reuse, and repurpose consumable and expendables. "*(NASA 2015)

Including closed-loop systems could reduce required consumables, allowing the launch mass to be re-appropriated for other deliverables. Biological life support systems have the potential for closing the atmospheric and water revitalization loops through metabolic and photosynthetic processes. In particular, algal systems have capabilities with potential to address multiple ECLSS functions simultaneously. Engineers are considering space flight systems that incorporate algal cultures, by use of photobioreactors, for long duration space flight (Javanmardian and Palsson 1992). Through photosynthesis algae consume $CO_2$ and produce usable $O_2$, and the produced biomass can be consumed by humans, to some extent (Powell, Nevels, and McDowell 1961; Wells et al. 2017). Furthermore, studies have also shown algae's ability to process human fecal and urine waste streams, as waste contains nutrients required for biomass production (L. Wang et al. 2010). Allowing algal cultures to convert human metabolic wastes into usable products for the crew could further close the ECLSS loop. However, if the biomass is used for waste stream management, it would probably not be consumed by humans for food safety reasons.

Understanding the potential failure mechanisms of an algal photobioreactor-based ECLSS architecture through identification of required algal inputs and outputs establishes design requirements for any photobioreactor. Here, the effects, inherent risks, including both probability and severity, and potential causes of failure are identified, thereby providing information to guide a risk assessment of algal photobioreactors. Previous studies have presented areas of special consideration when designing a photobioreactor for bioregenerative ECLSS but have not estimated the likelihood or severity of a system failure (I. Wagner et al. 2016). This chapter has included such an overview to indicate areas that require additional research before inclusion in missions or areas where the potential reliability of a bioregenerative system could be beneficial. Figure 3 gives a visual representation of the structure of this chapter. The relationship between crew and current ISS ECLSS technologies are defined and compared to a photobioreactor able to perform the same function. The potential ECLSS failure modes and effects are produced from the photobioreactor and ISS comparison. Causes of these photobioreactor failure modes are placed into two groups, those dependent on algal cell physiology and those dependent on the spaceflight environment, culture application, and supporting hardware. Possible countermeasures or mitigation strategies for each failure are outlined. Finally, areas requiring further experimentation to identify additional potential failure causes are established. This work should serve as an initial resource for Failure Modes and Effects Analysis (FMEA) of an algal photobioreactor-based ECLSS.

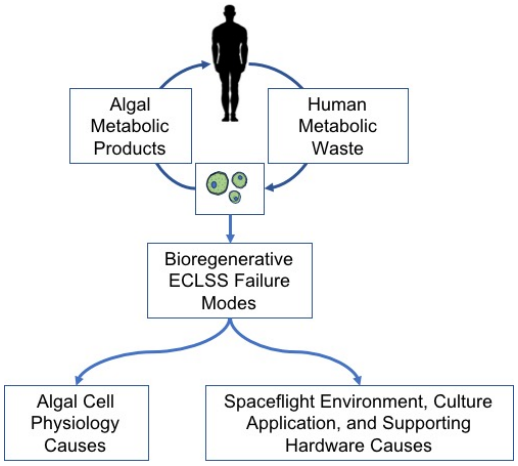


**Figure 3. Chapter organization, starting with an overview of human/algal ECLSS interactions, then failure causes flowing directly from biological ECLSS failure modes**

### 3.2 Background

With its first full-time crew docking in 2000, the International Space Station (ISS) is presently the longest operated, continuously inhabited spacecraft (Borsche 2005). Thus, ECLSS technologies found on the ISS are the current standard for addressing human metabolic functions on long duration space flights. Each of the identified ECLSS technologies are briefly described for later comparison to the algal photobioreactor technology able to provide similar functionality. The rationale regarding bioregenerative ECLSS and an overview of previous bioregenerative flight experiments are included as reference.

Table 2 presents the human metabolic functions addressed by the ECLSS, and the current ECLSS technology keeping the cabin within its tolerable ranges (values for ISS ranges available in 2018 NASA Life Support Baseline Values and Assumptions Document -BVAD) (Richard S. Williams 2015; Anderson et al. 2018). Table 2 also presents

the failure modes of an ECLSS, and the consequence of failure. The described modes and effects are valid regardless of system execution (e.g. whether physicochemical or bioregenerative).

**Table 2. Characteristics of crewed space flight cabin, current ECLSS technologies, associated potential algal functions, failure modes of cabin environment, and failure effect to crew.**

| Human Metabolic Function | Cabin Environmental Ranges | ISS ECLSS Addressing Human Function | Algal Function in Photobioreactor | Failure Mode | Failure Effect |
|---|---|---|---|---|---|
| Respired $CO_2$ | 0-0.5% $CO_2$ Cabin Concentration | CDRA removes $CO_2$ | Consumes $CO_2$ | $CO_2$ concentration exceeds allowable limit | $CO_2$ toxicity can cause hypercapnia and death |
| $O_2$ Consumption | 15.71-24.27% $O_2$ Cabin Concentration | OGA, produces $O_2$ | Production of $O_2$ through photosynthesis | $O_2$ concentration outside of allowable range | Onset of hypoxia, hyperoxia or increased risk of fire |
| Heat Production | 17.85-26.85°C Cabin Temperature | ATCS, transports heat | Algal water medium used as heat transfer medium | Cabin temperature outside of allowable range | Hyperthermia or hypothermia |
| Water Consumption | 2.5 kg/CM-d, Water Consumption | WPA, provides potable water | Culture consumes pollutants as a step towards potable water | Fails to consume enough pollutants | Dehydration or dehumidification of cabin, overloading wastewater treatment |
| Wastewater Production | 3.25 kg/CM-d, Wastewater Production include solid waste | WPA, cleans wastewater | Culture consumes nitrogen and phosphorous components found in waste | Contaminants exceed allowable levels | Overloading of wastewater treatment technologies |
| Food Consumption | 1.51 kg/CM-d, Food Consumption | Transported Food | Produced biomass is consumed for nutrition | Insufficient production of food; nutritional quality fails to meet standards | Crew malnutrition; starvation |
| Radiation Exposure | 6000 m/Gy Allowable Radiation Dose -Skin | Passive Material Shielding | Algal water medium used as radiation shielding | Radiation protection inadequate | Radiation poisoning, Increased risk of cancer |

### 3.2.1 ISS Current ECLSS Technologies

Technologies presented here represent the current state-of-the-art for ISS ECLSS operation. Proposed systems, or those currently being flown as space flight experiments are not included.

#### 3.2.1.1 Air Revitalization

The current ISS air revitalization system (in regard to processing respired $CO_2$ into useable $O_2$) compromises several major subassemblies: The Carbon Dioxide Removal Assembly, Carbon Dioxide Reduction Assembly, Oxygen Generation Assembly (OGA), Water Processor Assembly and Urine Processor Assembly. Each is briefly described below.

##### 3.2.1.1.1 Carbon Dioxide Removal Assembly (CDRA)

The Carbon Dioxide Removal Assembly (CDRA) removes the $CO_2$ from the crewed environment by flowing a stream of cabin air through desiccant and $CO_2$ adsorbent beds. The scrubbed air is passed through a second desiccant bed before returning to the crewed environment. When the zeolite adsorbent is saturated with $CO_2$, the air stream is diverted to a second $CO_2$ adsorbent bed, and the first bed is regenerated using a pressure/swing method. The released $CO_2$ is then be fed into a Sabatier system for reduction for recovery of $O_2$ (Sherif and Knox 2005; Knox and Stanley 2015; Coutts et al. 2015),

##### 3.2.1.1.2 Carbon Dioxide Reduction Assembly

The $CO_2$ captured by CDRA is provided to the Sabatier system with OGA-supplied hydrogen to synthesize $H_2O$ and methane $CH_4$. The water is stored either for potable use or to be reduced into oxygen and hydrogen by electrolysis. At this time, methane is treated as a waste product and vented overboard (Abney and Mansell 2011; Gatens et al. 2015; Samplatsky et al. 2011).

##### 3.2.1.1.3 Oxygen Generation Assembly

Water electrolysis currently produces the ISS's oxygen and hydrogen. Either the Sabatier system or the wastewater processing system supplies the required water. Current is passed through an electrochemical cell inserted into the water stream. The cathode reduces water to produce $H_2$, while the water around the anode oxidizes and produces $O_2$. This is by use of a proton exchange membrane, transporting the hydrated protons from the anode to the cathode side (Zoulias et al. 2004; Abney and Mansell 2011).

#### 3.2.1.2 Wastewater Processing

##### 3.2.1.2.1 Urine Processor Assembly

Water from flush water and urine is treated by the Urine Processor Assembly (UPA). Phosphoric acid (originally sulfuric acid) and chromium trioxide are first added to the wastewater to control microbial growth. The distillation assembly is the core of the UPA. It evaporates wastewater at a low pressure, the vapor then condenses on the walls of the assembly. Leftover brine (e.g. salts from urine) is stored in a Temporary Urine Brine Storage System (TUBSS) and the distilled water is directed to the WPA for further processing (Gentry and Cover 2015; Anderson et al. 2018; Bagdigian and Cloud 2005).

##### 3.2.1.2.2 Water Processor Assembly

The Water Processor Assembly (WPA) treats water recovered from humidity condensate and the UPA. The water is pumped through particulate beds, multifiltration beds, a catalytic reactor, and an ion exchange bed before being stored in a potable tank (Gentry and Cover 2015).

#### 3.2.1.3 Food Provision

The current approach to food provision is to carry enough for the duration of the mission or provide resupply launches. Early in the space program, food was processed into paste form and stored in squeeze tubes. Early food was unappetizing, which led to the replacement by retort-stabilized and dehydrated food (Logan 2004). The freeze-dried meals save on storage volume, have increased shelf life, and do not need refrigeration. Unfortunately, the dehydrated food does have an eventual expiration, leftover packaging contributes to waste, and the food fails to have the full sensory effect of fresh produce. Every few months, resupply launches deliver limited quantities of fresh food to the ISS. These types of launches may not be possible for a mission to Mars, so preliminary experiments involving produce growth are currently being conducted on the ISS (Anderson et al. 2018; Logan 2004; Massa et al. 2015).

#### 3.2.1.4 Radiation Shielding

Passive shielding is the current method for radiation protection. Multiple layers of material line the inside of the spacecraft as a “wall” between radiation and the crew. In reality, all materials on board can contribute to total radiation shielding but are not selected primarily for their shielding qualities. Rather, they are chosen for other

attributes or characteristics important to the component or subsystem design. Typical radiation protection designs today incorporate High Density Polyethylene (HDPE) (and to some extent, water and stored food) since it is relatively light-weight and hydrogen-rich -a key element for efficient radiation protection. However, the material is combustible. Current combustibility considerations have the HDPE wrapped in an aluminum foil ("Polyethylene (PE) Typical Properties Generic HDPE | UL Prospector" 2016; Simonsen and Nealy 1991; Richard S. Williams 2015).

#### 3.2.1.5 Thermal Control

The ISS uses clean water loops embedded in the cabin walls to remove heat generated by equipment and the crew. The heat collected by the water is transferred to an ammonia loop (via an Interface Heat Exchanger, IFHX), then to a radiator, from which the heat is rejected into space. Having two separate cooling loops that address two separate cabin areas (experiment racks and general cabin environment) allows for quicker heat removal, depending on the area's temperature requirements and allowable temperature swings (Patel et al. 2001; Chambliss et al. 2003).

Additional temperature control is provided by the Common Cabin Air Assembly (CCAA). The ISS cabin atmosphere circulates through the CCAA for temperature and humidity control, as well as particulate removal via filtration. A condensing heat exchanger dehumidifies the air stream, thereby lowering its dewpoint. A bypass loop provides for control over both the temperature and humidity of the air stream delivered back to the cabin (Gentry 2016), (Broyan, Welsh, and Cady 2010; NASA 2010).

### 3.3 Bioregenerative ECLSS

Bioregenerative technologies have the capability to provide robust ECLSS by being adaptable to a dynamic environment, while also providing a potential closed-loop solution. NASA desires the investigation of bioregenerative technologies, and in particular photosynthetic-based systems, for atmosphere revitalization. "Processes that take advantage of metabolic pathways available in organisms like algae and bacteria may also provide benefits for carbon dioxide removal, oxygen production, and air purification" (NASA 2015). While NASA acknowledges the use of algae for air revitalization, an algal culture could potentially address many important human metabolic needs (except for humidity control). Table 2 develops the analogous relationships between current ISS ECLSS and algal culture functionality. The algae biological functions could revitalize the atmosphere, treat wastewater, and produce biomass with potential to supplement crew nutritional needs; while the culturing media

could be used as a coolant within a thermal control loop and augment the radiation shielding. The presented case references a water-based media, instead of a solid media, like agar. ECLSS functions have the potential to be addressed simultaneously with one volume of algae, making a photobioreactor a multifunctional system. The engineering and design of a photobioreactor to provide complete loop closure or multifunctional operation is beyond the scope of this chapter, but its capabilities should still be noted. However, as previously stated, if the reliability and robustness of the photobioreactor system is such that it requires more support than the current ECLSS technologies, then the initial mass savings and potential for closed-loop functionality becomes irrelevant. Therefore, identifying the possible failure modes, causes, and effects of the photobioreactor ECLSS are necessary to determine system robustness.

### 3.4 Flown Algal Experiments

The idea of using biology, and in particular photosynthetic algae, to provide ECLSS capabilities to a crewed cabin is not new or novel. NASA started investigating the use of algae for air revitalization in the 1950 and early 1960s, but unfortunately did not have the illumination methods to produce an efficient enough culturing system for the application to fit within flight mass and power constraints (Miller and Ward 1966; Gitelson, Lisovsky, and MacElroy 2003). In the late 1960's closed-loop bioregenerative air revitalization was ground-proven by the Soviet Union. One man's $CO_2$ scrubbing and $O_2$ provision needs were met with 30L of the algae *Chlorella* for 30 days (Eckart 1996).

Since then, various experiments have been flown to understand the response of algal cultures to the space environment (e.g. microgravity and radiation). While the results of many studies were inconclusive and not published, some experiments showed a reduction in growth rate despite sustained photosynthetic productivity. Clumping and aggregation of cells have also been reported in those samples that were not actively mixed during spaceflight (Niederwieser, Kociolek, and Klaus 2018).

So far, no complete air revitalization system using algae for $CO_2$ turnover has been flight tested. However, a group from the University of Stuttgart currently has an experimental unit on the ISS that takes a slip stream of $CO_2$ from the ESA's LSR to supply their novel algal-based air revitalization system. Their goal with this experiment is to

demonstrate long-term operation, compatibilities with other established ECLSS systems, and characterize algal culture response to the spaceflight environment (Bretschneider et al. 2016).

### 3.5 Methods

First, classification of a failure mode, cause, and effect was established to provide a framework for the review. The definitions in Table 3 come from Langford (1995), Garvey (2009), and the Project Management Institute (2004). Table 4 delineates the qualitative scale for likelihood and severity that is used to assess risk in this chapter. Unfortunately, the lack of data characterizing mean time between failures of algal experiments prevents a more quantitative assessment of risk. The literature also indicates that few spaceflight experiments have been conducted with algal systems (Niederwieser, Kociolek, and Klaus 2018). Likelihood was determined from the number of times the failure was reported in the surveyed literature, recurrence of the environment that prompted these failures, and from the author's experience with culturing algae. Severity was established by examining the contingency plans for the particular failure, and then estimating the resources needed to correct the issue.

**Table 3. Classification of failure terms for this study**

| Term | Definition |
|---|---|
| Failure Mode | The specific manner or way by which a failure occurs in terms of failure of the item |
| Failure Cause | Defects in requirements, design, process, quality control, handling or part application, which are the underlying cause of sequence of causes that initiate a process that leads to a failure mode over a certain time. |
| Failure Effect | Immediate consequences of a failure on operation, function or functionality, or status of some item |
| Likelihood | Probability of occurrence |
| Severity | Consequences of incident |
| Detection | The means of detection of the failure mode by maintainer, operator or built in detection system, including estimated dormancy period (if applicable) |
| Mitigation | Acts to decrease the probability of occurrence or impact of a threat. |
| Contingency | Responses designed for use only if certain events occur. |

**Table 4. Classification of likelihood and severity for presented study. Volume/volume (v/v) is the comparison of algal culture density post-failure, compared to pre-failure.**

| Risk Assessment | Qualitative Value | Rationale |
|---|---|---|
| Likelihood | Improbable | -Not observed in personal experiments<br>-No occurrences reported in literature<br>-Stimulating environment rarely occurs |
| | Occasional | - Personally-observed in experiments once<br>- <5 occurrences reported in literature<br>-Stimulating environment occurs <5 times per mission |
| | Frequent | -Personally-observed in multiple experiments<br>- >5 occurrences reported in literature<br>-Stimulating environment occurs >5 times per mission |
| Severity | Negligible | -System or culture can recover within a day of correction<br>-Corrective action takes < 1 day<br>- <25% v/v culture re-establishment required |
| | Critical | -System or culture can recover within a week<br>-Corrective action takes < 1 week<br>- 25%-50% v/v culture re-establishment required |
| | Catastrophic | -System or culture requires >2 weeks of re-establishing<br>-Corrective action takes >1 week<br>-Extensive (> 50% v/v) culture volume re-establishment required |

This chapter presents failures documented in the literature, along with their realized causes of failure. The failure modes review was limited to the algal genus *Chlorella* for all of the failure examples. This is due to the extensive documentation of cellular physiology and bench-top experiments, available for the genus. Additionally, the majority of the limited spaceflight experiments included *Chlorella* (Niederwieser, Kociolek, and Klaus 2018). In this chapter, two categories are sufficient to group failure causes (those issues stemming from culturing algae, and those originating from the system and system hardware). These failures can occur in benchtop experiments as well as larger-scale terrestrial operations.

This chapter is organized in the following order, ECLSS failure modes and subsequent effects are identified, causes of these modes are established with respect to the bioregenerative system or the system hardware, and finally the likelihood and impact of the causes are estimated. Current countermeasures or contingency efforts for individual failures are presented. Incorporating countermeasures into the design reduces the risk of failure. The chapter concludes by identifying areas in need of further investigation and suggesting research that could advance the robustness of photobioreactors for use in space habitats.

### 3.6 Failure Modes, Causes, and Effects Associated with Culturing Algae

The failure modes presented in Table 5 can originate from algal cell physiology. While table 4 presents similar information to that of table 1, it should be noted that the failure mode column on the right is specific to an algal culture and culturing technique. Culture response to the environment can result in failure to meet ELCSS requirements, regardless of proper design and operation of support hardware. Identifying causes associated with the culture biology ensures future application's hardware includes proper detection methods. An algal culture fails when it does not perform within its designed functionality range (e.g. not removing enough $CO_2$ or providing enough $O_2$) over the course of a specified duration. Mitigation and contingency plans are presented for all identified failures.

**Table 5. Failure modes of algal culture based on algal cellular physiology, mapped to human metabolic function**

| Human Metabolic Function | Algal Function in Photobioreactor | Failure Mode of Algal Culture |
|---|---|---|
| *Respired $CO_2$* | Consumes $CO_2$ | Algae cannot metabolize or fix enough $CO_2$ to keep cabin levels below the upper limit |
| *$O_2$ Consumption* | Produces $O_2$ through photosynthesis | Algae is not able to produce enough $O_2$ to keep with human demands |
| *Heat Production* | Algal water medium used as heat transfer coolant | Medium is unable to remove heat, and keep cabin within required temperature range |
| *Water Consumption* | Culture "treats" water by consuming pollutants | Algae cannot provide water for crew needs |
| *Wastewater Production* | Culture consumes nitrogen and phosphorous components found in waste | Algae cannot treat wastewater at a rate sufficient to provide potable water for crew use |
| *Food Consumption* | Produces edible and nutritional biomass | Biomass is not safe for consumption or fails to meet nutritional needs, or is not produced at a high enough rate |
| *Radiation Exposure* | Algal water medium used as radiation shielding | Medium is unable to provide enough shielding |

#### 3.6.1 Photosynthesis Process

To understand failures associated with the photosynthetic process, the global equation (Eq. 1) provides insight, however this simple equation neglects intermediate steps important to the process. As Cloot explained, a high-level overview of photosynthesis describes a two-stage process.

*"The first stage, also called the "light reaction," is characterized by a series of reactions requiring light, where the energy is used for the reduction of nicotinamide adenine di-nucleotide phosphate (NADP) and for the photophosphorylation of adenosine diphosphate (ADP) into a high-energy compound: adenosine triphosphate (ATP). The second stage, that does not require light, combines the reducing power of NADP and the energy of ATP to promote the reduction of carbon dioxide $CO_2$ and produce carbohydrates as well as proteins and fats"* (Cloot 1994).

Equations 2 and 3 are for the light independent and dependent cycles, respectively, that support the photosynthetic reaction. Reagents in these included equations demonstrate the need for additional nutrients in the photosynthetic process. Neglecting supplementation of these nutrients over time could result in a culture failure by limiting nutrients required to complete cell sustainment through photosynthesis (Kimball 2011).

Global Equation (Eq. 1 repeated):

$$6CO_2 + 12H_2O + photons \rightarrow C_6H_{12}O_6 + 6O_2 + 6H_2O \quad (1)$$

Intermediate Two-stage Process:

$$3CO_2 + 9ATP + 6NADPH + 6H^+ \rightarrow C_3H_6O_3phosphate + 9ADP + 8P_i + 6NADP^+ + 3H_2O \quad (2)$$

$$2H_2O + 2NADP^+ + 3ADP + 3P_i + photons \rightarrow 2NADPH + 2H^+ + 3ATP + O_2 \quad (3)$$

where *ATP*, *NADPH*, *ADP*, $P_i$, and *NADP* are all products as intermediate steps in the overall photosynthetic process, and contain either nitrogen, phosphorous or both. Indicating that a source of nitrogen and phosphorous needs to be available to algae to promote adequate growth. Additional trace elements not captured in the photosynthetic equation are also required. These elements include iron, magnesium, sodium, potassium, and calcium, depending on the cultured species (Mandalam and Palsson 1998a). The glucose formed in the overall photosynthetic process makes other components of the cell including cellulose, lipids, or protein. Allowing this balanced system to become unstable through input disparity, leads to some of the most common culture failures.

#### 3.6.1.1 Resource Limitations, including Irradiance, Carbon Dioxide, and Nutrients

One of the most commonly encountered causes of failures are limited inputs. Referencing the previously presented photosynthetic equations, Table 6 presents those inputs utilized by the algal cells and that have the possibility of becoming limiting reagents. The limiting input depends on local environmental conditions. The

processes governing algae growth are constantly responding to environmental changes, in an effort to establish a new balance. Typically, a reduction in growth rate or viable cell count is the response, as the limited input can restrict cell metabolic function. The input can be adjusted to correct the imbalance, but unless a stable system results, a different input may limit growth, requiring further action.

**Table 6. List of potential limiting inputs referenced from photosynthetic equations.**

| Limiting Input |
|---|
| $CO_2$ |
| Photons |
| Nitrogen |
| Phosphorous |
| $H_2O$ |
| Trace Elements |

#### 3.6.1.2 Irradiance and $CO_2$

Dr. Blackman (1905) identified the relationship between photosynthetic inputs, outputs, and light intensity. He concluded that the photosynthetic process had both light dependent and independent reactions. Blackman went on to specify the relationship between increasing temperature (or supplied $CO_2$ content) and light provision to photosynthetic rate (Campbell and Reece 2008). Figure 4 illustrates the factors responsible for limiting photosynthetic rate at various light intensities. Temperature and $CO_2$ content were also varied to understand the relationship between the three inputs (Kimball 2011). Each scenario results in a "dark-limited phase" meaning that the light independent reactions could not occur quickly enough to support the increased light intensity. Introducing periods of darkness (through baffles, mixing, and flashing lights) counteracts this, allowing the light independent reactions to occur, and can increase biomass production when compared to constantly irradiated cultures (Figure 5) (Liao et al. 2014).

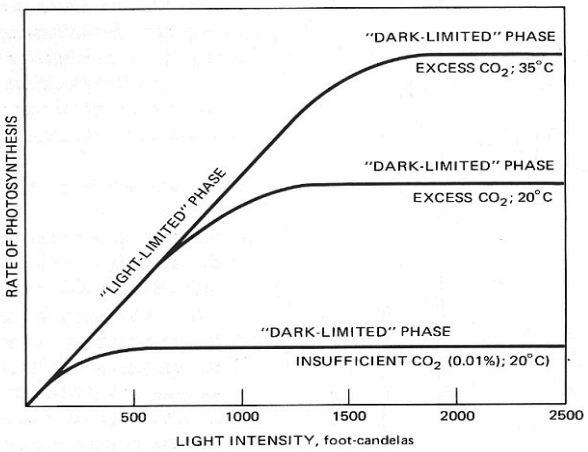


**Figure 4. Photosynthetic rate as a function of light intensity, with various CO2 concentrations and temperatures (selected from (Kimball 2011).**

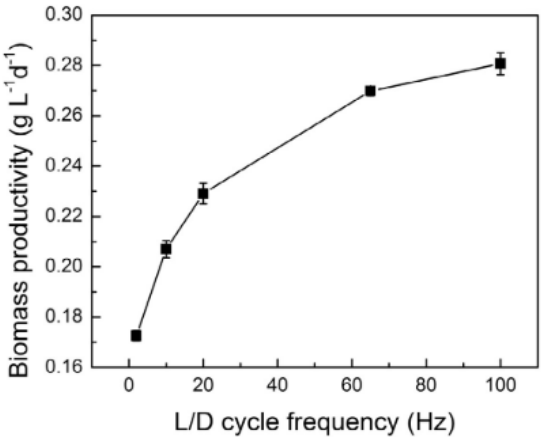


**Figure 5. Effect of light/dark cycle frequency on the performance of the periodically shaded tubular photobioreactor (selected from (Liao et al. 2014).**

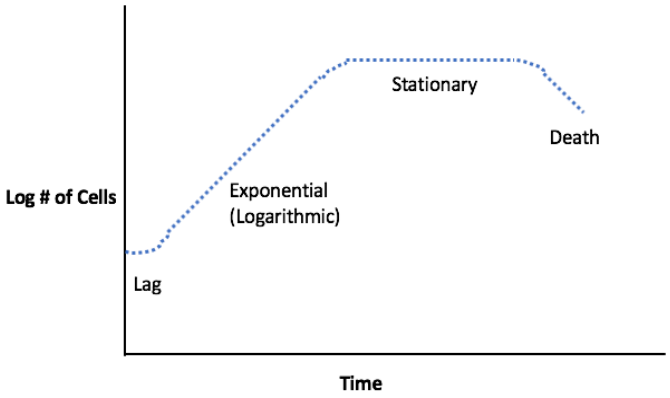


**Figure 6. Viable cell count over the course of a culturing period in batch mode. Specific growth periods are labeled. (Modified from (OrbitBiotech 2018)).**

Increasing light intensity becomes necessary as the culture density continues to increase through the growth period. Typically, if dissolved $CO_2$ is in abundance, and the medium temperature is warm enough, the culture becomes light-limited. The culture can become dense enough that the cells begin to self-shade, so the penetration length of irradiance fails to reach the inner cells of the culture (I. Wagner et al. 2016). Reduction in photosynthetic rate or viable cell count can occur, as the cells become unable to sustain themselves. This commonly occurs with batch culturing, where the biomass is harvested after reaching a particular density. illustrates the growth cycle of a batch culture using constant environmental conditions. The number of viable cells begins to increase until the cells begin to self-shade, and a reduction in functioning cells occurs. Continuous culturing of the cells, constantly replenishing medium and removing excess biomass, sustains a steady viable cell density (OrbitBiotech 2018). A continuous culturing system would be reflected by an extended stationary phase in Figure 6.

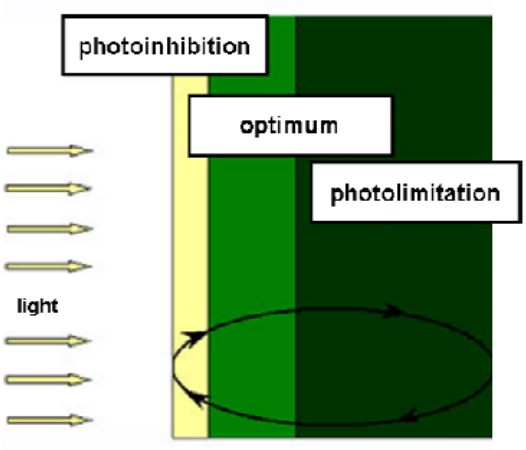


**Figure 7. Flashing light effect executed through culture mixing. (Selected from (Buchert and Belz 2012), modified from (Degen et al. 2001)).**

Mixing or stirring (through gas sparging, mechanical pumping, or paddle-stirring) can reduce the effects of self-shading, as the cells are moved through illuminance of the lighting system (Figure 7). This results the previously presented “flashing light” effect, which can increase biomass production (Figure 5).

Activating the light dependent reactions requires the provision of photons to the system. Palsson suggests approximately eight photons of light may be required for the formation of one $O_2$ molecule, and that environmental factors such as temperature can influence photosynthesis.

*"…eight photons of light (quanta) may be required for the formation of one oxygen molecule, and environmental conditions such as temperature have a strong influence on the efficiency of photosynthesis. The minimum photon requirement for Chlorella cells was estimated to be in the range of 5-6 hv/O2¬"* (Javanmardian and Palsson 1991)

This establishes a correlation between an increase in produced oxygen to the increase in provided photons. The sensitivity to irradiance is clear in Figure 8, adapted from Červený et al., 2009. While it is not the response of Chlorella to variations in irradiance, Scenedesmus q. is within the same division, Chlorophyta (green algae). Figure 8 illustrates the increase in dissolved $O_2$, and decrease in dissolved $CO_2$, as the intensity of irradiance increases. Subsequently, minimum photosynthetic rates are recorded when the irradiance is turned off (Červený et al. 2009). The experiment completed by Červený referenced diel illumination cycles for the irradiance duration, although, it should be noted that periods of darkness are not required for culturing most algae. Chlorella can be cultivated for long durations using continuous irradiance (Sharma, Singh, and Vijendra 2011). Which this has the potential to provide crews with un-interrupted atmospheric revitalization.

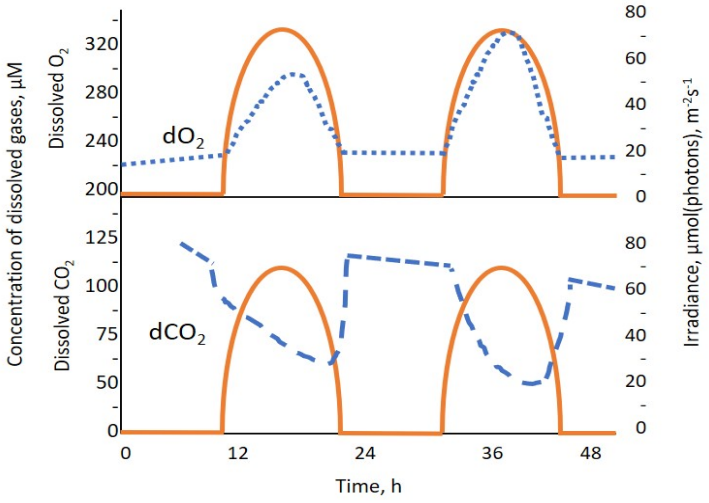


**Figure 8. In each panel, the irradiance is indicated with a solid line. Top panel: Concentration of $O_2$ (dotted line) dissolved in the algal suspension of the bioreactor during two days of *Scenedesmus q.* growth. The increase of dissolved $O_2$ during day and its decrease at night are due to the photosynthetic and of respiratory activities of the algal cells. Bottom panel: Concentration of dissolved $CO_2$ (dashed line) in the algal suspension during two days of *Scenedesmus q.* growth. (Selected from (Červený et al. 2009)).**

Typically, intensity is first considered when trying to increase the number of photons hitting culture cells. Figure 9 establishes a correlation between light intensity and culture growth rate (Y. Zhao et al. 2013). While it is apparent

that light (photons) needs to be included in the algal culturing process; each species requires a specific optimal intensity and spectrum. Figure 9 also reveals the dependence of the culture growth rate to the wavelength of light. Figure 10 provides an explanation for this dependence by presenting the photosynthetic action spectrum; which relates the rate of photosynthesis to each wavelength in the visible spectrum. Photons excite cell electrons into their next energy level, progressing the photosynthetic process (Nakajima, Hanawa, and Tsuchiya 2015). The Chlorella absorption spectrum overlaid on the photosynthetic action spectrum shows that while one of its peak requirements lay in the red wavelengths, it also has a significant absorption peak in the blue wavelength range. This suggests that specific species of algae may have particular spectral preferences for optimal growth. Since these peaks are typical of chlorophyll a and b absorption, this is absorption spectrum is common across green algae (Nakajima, Hanawa, and Tsuchiya 2015; Algae Research and Supply 2019). Figure 9 reveals that the dry mass of Chlorella cultures grown in red-spectrum lighting are consistently higher than those grown at other wavelengths and confirms the positive correlation between peak absorption, shown in Figure 10, and biomass production. Ensuring that the culture is receiving the proper wavelengths for the species and enough intensity to support the required culture density keeps the culture functioning within the required ECLSS range, in terms of irradiance. First understanding the irradiance requirements of the culture helps mitigate this failure, but the ability to increase irradiance should be available as a contingency plan.

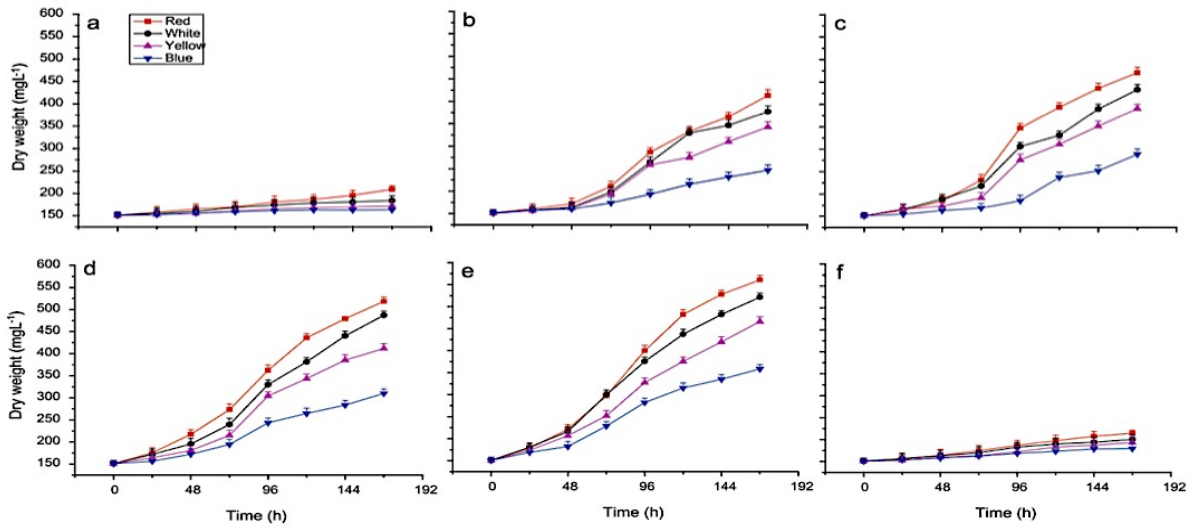


**Figure 9. Microalgae dry weight (grown with 28% $CO_2$) over time at various light wavelengths (red, white, yellow, and blue), and intensities: (a) 400, (b) 800, (c) 1200, (d) 1600, (e) 2000, (f) 2400 μmol $m^{-1}s^{-2}$ (selected from (Y. Zhao et al. 2013).**

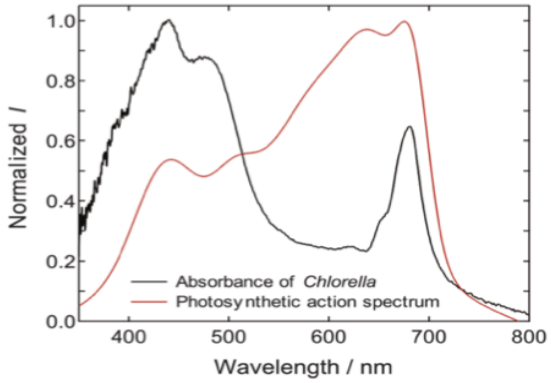


**Figure 10. Absorbance spectrum of *Chlorella* dispersion and the typical photosynthetic action spectrum (selected from (Nakajima, Hanawa, and Tsuchiya 2015).**

#### 3.6.1.3 Nutrients

Needs of the culture differ depending if they are open-container (e.g. raceway ponds) or closed-container systems (e.g. a recirculating flow within a tubular reactor). Studying the provision of nitrogen and phosphorous to open and closed systems provides prime examples. Dissolved atmospheric nitrogen ($N_2$) can be utilized by select species of prokaryotes (i.e. few within the phylum cyanobacteria) (S. C. Wagner 2011). However, it is not in the preferred nitrogen form for eukaryotic algae (i.e. *Chlorella*) (Dixon and Kahn 2004). *Chlorella* assimilate already fixed nitrogen (such as $NO^-_3$ and $NH^+_4$) typically found in fertilizer runoff or urban waste streams, which can be abundant

in an outdoor open-container system ("Algae and the Nitrogen Cycle" 2012). However, Hao et al. found that the quantities of nitrogen and phosphorous can be in a closed-loop system, unless controlled (Hao et al. 2012). Wang confirms this in the results of their batch-culture experiment using *Chlorella* to consume nitrogen and phosphorous from municipal wastewater streams (L. Wang et al. 2010). Figure 11 illustrates the reduction of phosphorous and nitrogen concentrations, and the correlating increase in optical density, as an indicator of increased biomass. Growth of biomass reached a stagnation point after the concentrations of phosphorous and nitrogen reached a certain threshold. Major nutrients (e.g. nitrogen or phosphorus) could be supplied through human urine as a contingency plan, or as a designed mitigation plan, unless already a standard part of the system operation.

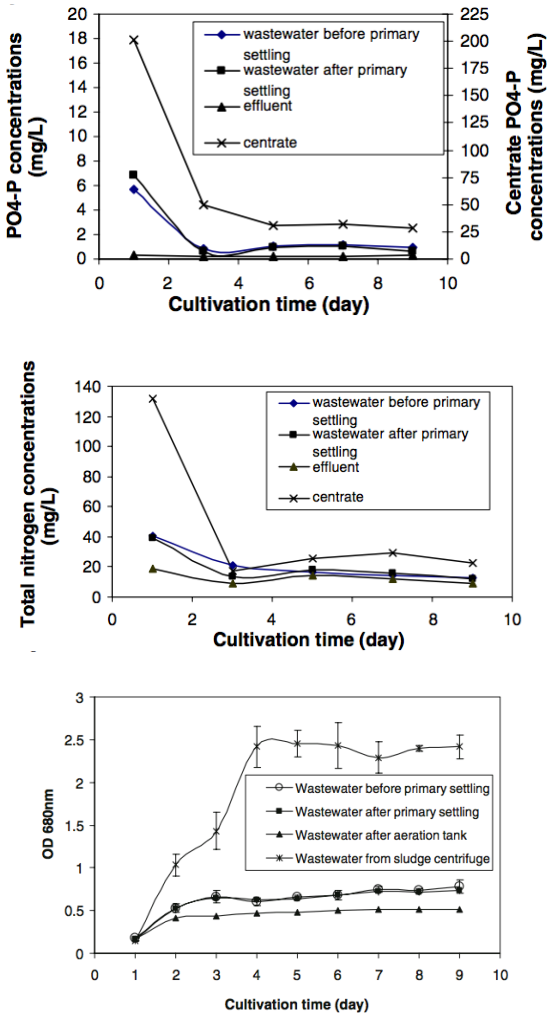


**Figure 11. Nutrient evolution during the culture period. (top) Trends of ammonium nitrogen ($NH_3$–N) in wastewaters #1 (before primary settling), #2 (after primary settling), and #4 (centrate -nutrient-rich wastewater effluent). (middle) Trends of TN in the four wastewaters. (bottom) Optical density for growth curves of four wastewaters (selected from (L. Wang et al. 2010).**

### 3.6.2 Cellular Stressors

Previously presented causes of failure were dependent upon the photosynthetic reaction, and its constituents. The following causes of failure, while still focused on the physiology of the algal cell and culture, extend beyond the photosynthetic reaction and include other aspects of cell functioning.

#### 3.6.2.1 Excess $O_2$ Accumulation

Much like any living organism, if algae are in close proximity to high concentrations of their waste ($O_2$) for extended periods of time, there is a reduction in culture viability. Algal cells are constantly respiring, the process of

reducing stored glucose for energy, which requires $O_2$ for the reduction. The amount of oxygen produced during photosynthesis may be sufficient for fulfilling the respiratory requirement. However, in unsealed systems, it is more likely the ambient environmental oxygen that contributes most to respiration, as the dissolved concentration, via Henry's law, would be higher than that evolved from photosynthesis. Figure 12 is similar to Blackwell's light intensity and photosynthetic relationship figure, but includes values for the oxygen evolution rates, given a particular set of environmental conditions (Melis 2009). Respiration is evident at zero light intensity, "as respiration is the only cellular bioenergetic activity, consuming about 3 mmol $O_2$ [mol Chl]$^{-1}$ s$^{-1}$" (Melis 2009). However, if the $ppO_2$ is allowed to build up while irradiated, the specific growth rate of *Chlorella,* and other algal species begins to slow (Ogawa, Fujii, and Aiba 1980). As stated by Raso and van Genugten,

> *Oxygen inhibits growth, since it competes with the carbon dioxide for the Rubisco enzyme involved in the CO2 fixation to generate biomass…There are two mechanisms largely responsible for the deleterious effects on growth of the microalgae: the competitive effect of O2 on Rubisco (photorespiration) and photo-inhibition which causes cell damage of photosystem II by the generation of reactive oxygen species. Photorespiration only takes place during the dark reaction of photosynthesis and is thus independent of the light conditions used, while the Reactive Oxygen Species (ROS) are formed if the algae receive excessive amounts of light in the light reaction of the photosynthesis* (Raso et al. 2011).

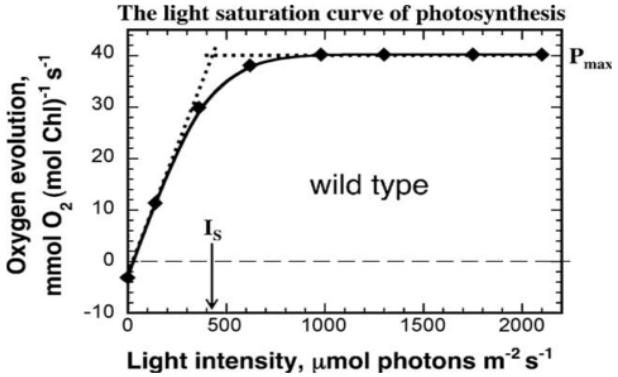


**Figure 12. Plotted is the rate of photosynthesis ($O_2$ evolved per mol Chl per s) as a function of light intensity for wild type algae. Photosynthesis saturates at intensity IS (about 400 μmol photons m$^{-2}$ s$^{-1}$). For reference, full sunlight intensity = 2200– 2500 μmol photons m$^{-2}$ s$^{-1}$ (selected from (Melis 2009)).**

The primary conclusion of the quoted study being that exorbitant oxygen accumulation can be the byproduct of excessive irradiance. Figure 13 illustrates a reduction in oxygen production as the concentration of dissolved oxygen increases. The figure also shows the effect of $CO_2$ level on photosynthesis. Increasing $CO_2$ concentration does reduce the photosynthesis inhibition effect of excess oxygen, yet when $O_2$ concentrations exceed 40%, there is a reduction in the counteraction (Turner and Brittain 1962). Referring back to Figure 9 illuminating the culture with 2,400 μmol $m^{-1}s^{-2}$ reduces the harvested dry weight. The reduction in biomass indicates the culture could not support the initiated photosynthesis, or coexist with the produced oxygen, and slowed its growth rate. Active removal of oxygen can alleviate the stress on photorespiration but requires shading or a reduction in irradiation to relieve photo-inhibition (Turner and Brittain 1962).

If the system is sized properly, a buildup of oxygen should not occur, as cultures would not be irradiated past saturation levels and gas removal system would be sized to accommodate production rates. However, if the system is operated in a low-pressure "Exploration Atmosphere" (where the oxygen concentration is 34% of 8.2psia), it may be a high enough $O_2$ concentration to affect culture metabolism. A buildup of oxygen could also occur if the gas removal system were to fail, allowing the dissolved oxygen concentration to increase. In both cases, illuminance and dissolved oxygen concentration should be reduced to sustain culture viability.

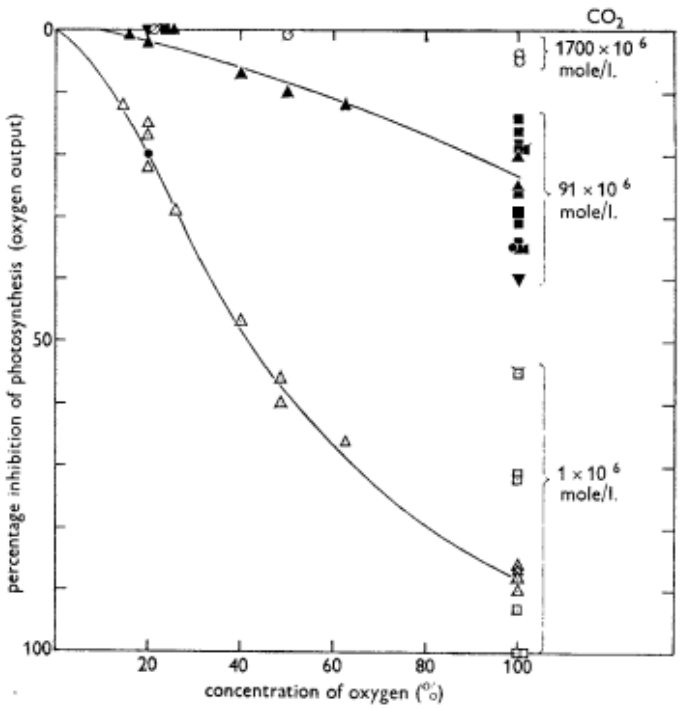


**Figure 13. Oxygen inhibition of photosynthesis in *Chlorella* as a function of oxygen and carbon dioxide concentration. Open triangles/open circles with center dots = $1x10^6$ mole $L^{-1}$ $CO_2$, closed triangles/closed squares = $91x10^6$ $L^{-1}$ $CO_2$, open circles = $1700 x10^6$ $L^{-1}$ $CO_2$ (selected from (Turner and Brittain 1962)).**

#### 3.6.2.2 Bacterial, Grazer, and Viral Infections

Research has shown, and confirmed by stable ecological systems, that algae and bacteria can co-exist, and in some cases algae can benefit from the association (Luz et al. 2016). A literature survey indicated that there is at least one predatory bacterium that causes dead *Chlorella* cells to lyse but did not mention damage to live cells. An additional way bacterium can impair algal growth is through competition for oxygen in a limited resource environment. Cole describes the change in the culturing environment due to bacterial respiration

> *If the supply of organic matter is sufficient, aerobic respiration can use up the supply of dissolved oxygen. Although some algal taxa are capable of photosynthesis (using only photosystem I) under anaerobic conditions, most taxa would be inhibited by the lack of oxygen* (Cole and Cole1 1982).

This consideration is crucial for low-density cultures or cultures that experiences extended periods without irradiation, as the bacterial respiration in addition to the algal respiration could choke out the culture. Algae provide organic material, suitable for bacterial consumption, constantly. As described by Krall and Kok, “all algae secrete some soluble organic material during growth, shed some insoluble material in the process of cell division, and leave

products of autolysis of dead cells in the medium. These may cause excessive foaming and provide substrates for bacterial growth"(Krall and Kok 1960). Proper cleaning procedures that help to establish an axenic culture can assist in establishing a stable, dense enough culture before inoculating with supportive bacteria.

Typically, grazers (or protozoa) and viruses actively target live *Chlorella* cells. However, protozoan, like *Pterioochromonas malhamensis*, can consume either live or dead *Chlorella* cells, as well as symbiotic bacteria. Excessive cellular consumption can lead to a culture crash within a few days (Ma et al. 2017). If subjected to a viral infection, without active control, this system may become unbalanced in a photobioreactor. The infection could decimate the algal population, providing food for the protozoan population, therefore increasing the microorganism population and making it difficult for the algal culture to re-establish.

Viruses, like PBCV-1, attach to the outside of the live *Chlorella* cell wall, burrowing itself into the membrane, and release its DNA into the host cell, the host is reprogrammed to produce viral RNAs, and then lysis of the cell occurs, and the progeny virions are released. This cycle is repeated, and the live algal cells are destroyed through infection, and ultimately lysis (Van Etten et al. 1985).

The extent of the bacterial, grazer, or viral contamination may require entire culture (algal and bacterial) extermination, and algal culture re-establishment. A decrease in photosynthetic rate and change in coloration of the algal culture indicates possible contamination.

#### 3.6.2.3 Chemical Contamination

While conducting an initial cleaning of photobioreactor components is critical for removing extraneous bacteria or remaining residue from manufacturing, culture-compatible methods and chemicals must be used. Using typical laboratory cleaning procedures, such as diluted sodium hypochlorite (bleach), can leave behind harmful residues, if not removed properly. Neutralization or removal of chemical residue may be difficult if the photobioreactor includes areas that are not consistently penetrated with rinsing. A hydrogen peroxide solution gave the best results during personally conducted experiments examining residue-free cleaning techniques of Pyrex beakers. Referencing sanitizing methods for soilless cultivation (i.e. hydroponics) indicated that component exposure to UV, ozone, or concentrations of hydrogen peroxide reduces pathogens (Fisher 2009). Hydrogen peroxide was selected for preparation of experiments for this dissertation due to the availability of hydrogen peroxide,

compatibility with photobioreactor materials, and chemical decomposition into oxygen and water (residue-free). Other solutions included dilutions of bleach, hydrochloric acid, or isopropyl alcohol. All other solutions, except for hydrogen peroxide, resulted in loss of culture.

Additionally, if produced algal biomass is being utilized for human nutritional supplementation, edibility of the biomass must be ensured. Cleaning activities may not be the only source of chemical contamination. Photobioreactor operation itself may result in contamination, including possible chemical leaching of plumbing materials due to material degradation over time. Introducing human waste streams, or other operational water streams, into the photobioreactor can contribute organic and inorganic contaminants not typically found in media composition. This may include caffeine, antibiotics, other compounds excreted or produced by humans, and chemical leeching from plumbing. Bioaccumulation and algal cell surface coating of these compounds may be of concern, if the biomass is to be consumed. These compounds, antibiotics in particular, may inhibit the growth of certain species of algae or cyanobacteria (Qian et al. 2010). However, bioremediation of antibiotics has been observed in *Chlorella* for certain antibiotics, indicating that algae treatment of human metabolic and non-metabolic wastes cannot be generalized (Xiong, Kurade, and Jeon 2017).

#### 3.6.2.4 Heavy Metal Contamination

Algal cultures require heavy metals, including zinc and copper, as micronutrients for metabolic and developmental pathways (Tomsett and Thurman 1988). Yet, exposure to high levels of these heavy metals (and others) are toxic to cultures. As explained by Mallick,

> *Toxicity mechanisms include the blocking of functional groups of important molecules, e.g. enzymes, polynucleotides, transport systems for essential nutrients and ions, displacement and/or substitution of essential ions from cellular sites, denaturation and inactivation of enzymes, and disruption of cell and organellar membrane integrity. In addition, metals are also pointed to exert toxic effects through free radical formation…* (Mallick 2004).

These oxygen-derived free radicals can be in the form of ROS, including $O_2$, $H_2O_2$, and $^{-}OH$. Since these compounds can attack cell constituents like amino acids, proteins, carbohydrates, nucleic acids, and lipids; it reduces the overall functionality and efficiency of the cell (Mallick 2004). Preliminary experiments conducted in the 1960's

characterized the detriment to photosynthetic and respiration rates, as depicted in Figure 14 (McBrien and Hassall 1967). The figure also corroborates that some amount of copper is required for proper algal growth, as the respiration rate is higher than 100% in media with copper concentrations <15 μg/mg biomass. However, the photosynthetic rate is reduced by about 20% with the same amount of copper.

When constructing photobioreactors, avoiding materials such as copper or alloys that contain copper, like brass or bronze, reduces the possibility of copper dissolving into the culture. Instead, certain stainless-steel grades, certain plastics, coated materials, or glass is preferred, since these materials do not prompt detrimental culture effects.

Non-metabolic waste streams may also include heavy metals (e.g. lead from plumbing or run-off from experiments), which could be introduced to a photobioreactor tasked with waste-water remediation. Excessive concentrations of heavy metals (e.g. lead, cadmium, zinc, and chromium) can be lethal to *Chlorella* and accumulates in biomass until that threshold is exceeded (Bajguz 2000; Travieso et al. 1999). This may pose a threat to the human, if the biomass were to be consumed. Heavy metals could then be passed on to the human, possibly inflicting heavy metal poisoning.

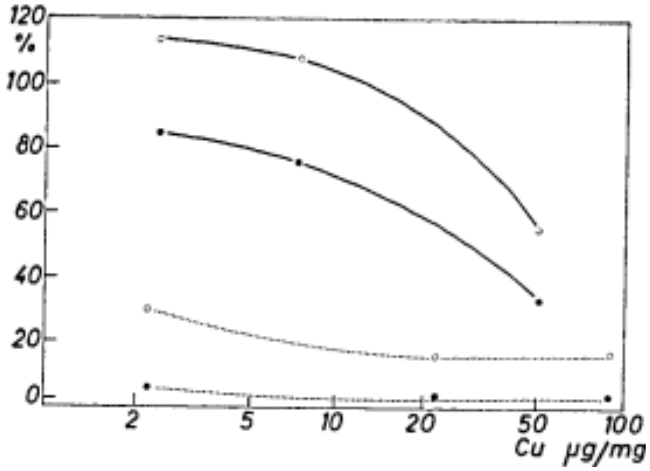


**Figure 14. Respiration and photosynthesis of cells treated with copper under aerobic and anaerobic conditions. Ordinate: Rates of respiration and photosynthesis as percentage of control. Abscissa: Amount of copper applied in μg/mg DW cells. Open circles = Respiration, Closed circles = Photosynthesis; Full lines = Aerobic conditions; Dotted lines = Anaerobic conditions (selected from (McBrien and Hassall 1967)).**

#### 3.6.2.5 Media pH

The algal media's transient pH is influenced by the metabolic functioning of the cell, alkalinity of various salts, and dissolved $CO_2$ concentration. Algae require a carbon source for photosynthesis and prefer aqueous $CO_2$ (carbonic acid). If the cell consumes a majority of the present carbonic acid, it transitions to utilizing available bicarbonate, finally consuming carbonate, if necessary (Gerardi 2018). Figure 15 illustrates the predominance of the three different inorganic species, dependent on pH, figure modified from Wolf-Gladrow et al. 2007. This figure alone suggests an optimal pH of 2-6 for culturing algae, due to the dominance of aqueous $CO_2$ (Wolf-Gladrow et al. 2007). The experimental results of Mayo, presented in Figure 16, support this idea. Maximum growth rates were documented in the 4-6 pH range. However, Mayo also documented a marked decrease in growth rates when the pH went below 4, or above 8 (A. W. Mayo and Noike 1994). Referring to Figure 15, hydrogen or hydroxide ions dominate at the pH extremes. These ions can raise or lower cellular membrane pH from approximately neutral, hampering $CO_2$ fixation (Khalil et al. 2010).

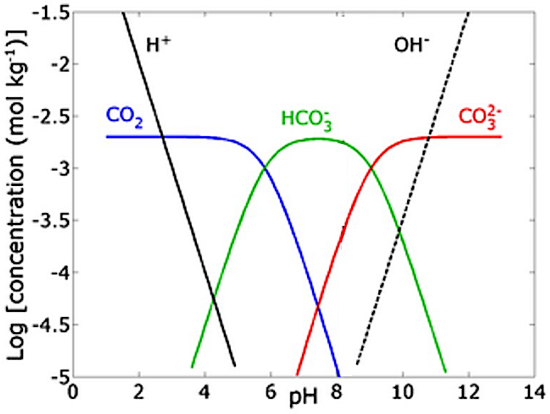


**Figure 15. A Bjerrum plot of the log of concentrations (molar) of various inorganic carbon species as a function of pH in a closed system for a value of total inorganic carbon of $10^{-3}$ mol $L^{-1}$.**

Active pH control in algal media occurs through provision of the three predominate inorganic species, but also stoichiometric balancing of media. Algal medium increases in pH over time as the various carbon sources are consumed, and algae release hydroxide ions while capturing $H^+$ inside the thylakoid membrane, using carbon capturing mechanisms (Kumar et al. 2015). Excess provision of $CO_2$ reduces the pH below viable thresholds.

However, nitrogen sources (e.g. nitrate, ammonium) can be introduced to buffer the inorganic species and stabilize the pH within previously established ranges (Scherholz and Curtis 2013).

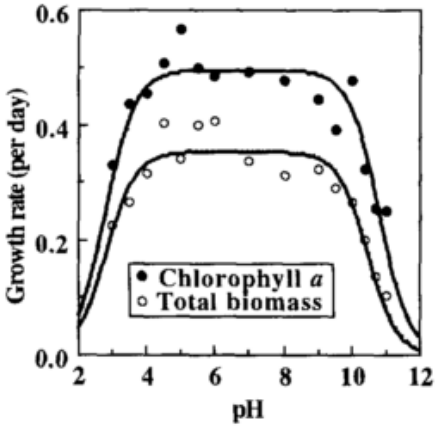


**Figure 16. Effect of pH on growth rate of *C. vulgaris* and total biomass (selected from (A. W. Mayo and Noike 1994)).**

#### 3.6.2.6 Environmental Temperature

While temperature is not an input into the photosynthetic equation, Blackman did record the effect of temperature on photosynthetic rate as depicted in Figure 4. Lower-than-optimum environmental temperatures can reduce carboxylase activity in the cell. The photosynthetic apparatus may then be absorbing more photons than can be utilized in carbon fixation. In an effort to protect itself, the cell may change its photochemistry to reduce the amount of light absorbed to off-set the reduction in carboxylase activity (Öquist 1983). This reduction in photosynthetic rate has a direct effect on the overall culture growth rate.

Figure 17 illustrates the correlation of an increase in growth rate with the increase of media temperature (Dauta et al. 1990). However, there is a threshold temperature for photosynthesis (approximately 22-38°C, depending on the species), as noted in Figure 17. Increasing past this temperature inhibits the charge-separation activity and inactivates the oxygen evolving capability of photosystem II (PSII), resulting in the production of oxygen free radicals, which can damage cellular biochemical compounds (Ras, Steyer, and Bernard 2013).

While the culture is still functional, and may acclimate to extreme temperatures over time, precautions should be taken to keep the cultures within the temperature range that results with the desired photosynthetic rate (Öquist 1983).

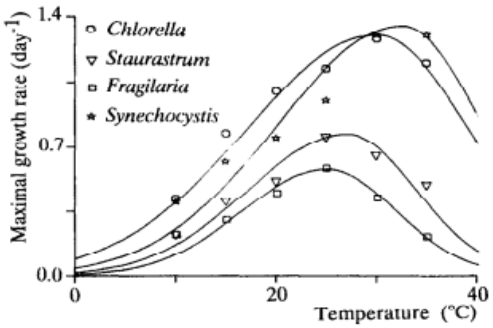


**Figure 17. Variation of maximum growth rate versus temperature for *Chlorella,* Fragilaria*, Staurastrum, and Synechocystis* (selected from (Dauta et al. 1990)).**

### 3.6.2.7 Cellular Resiliency

In the microgravity environment, it is important to agitate the culture medium, ensuring waste products are removed from the cell's immediate surroundings, nutrients are provided to the cells, and that cells are irradiated properly (D. Klaus 1998). Typically, pumps provide these mixing actions during spaceflight; Figure 18 shows the benefit of increased photosynthetic activity from using a rotary pump to actively mix the culture. However, a fast mixing speed imparts a greater shear force to the cell, which lowers the photosynthetic activity (Leupold et al. 2013). Different types of pumps use different mixing mechanisms, some of which can be damaging to algal cells. Figure 19 compares cell vitality to pump cycles through various types of pumps. Those pumps relying on blades or spinning propellers to move medium resulting in lower cell viability over time is due to the amount of shear stresses found at the blade tips. Pumps relying on positive displacement, like the diaphragm pump or the peristaltic pump had higher cell viabilities due to the lower stresses imparted on the cells, a similar result is discussed for *Chlorella* cells in Bretschneider et al. 2016 (Bretschneider et al. 2016; J Keppler 2015). Studies have also shown that the amount of damage imparted on a culture due to mixing is also species specific. For example, *Chlorella* has been shown to sustain higher high critical stress value than *Spirulina*. This is in part due to *Chlorella's* compact, unicellular physiology, while *Spirulina* is typically a long, multicellular spiral (Bronnenmeier and Märkl 1982).

For these reasons, pump selection should carefully consider the spaceflight application, while causing minimal stress to the culture to preserve cell viability without sacrificing mixing.

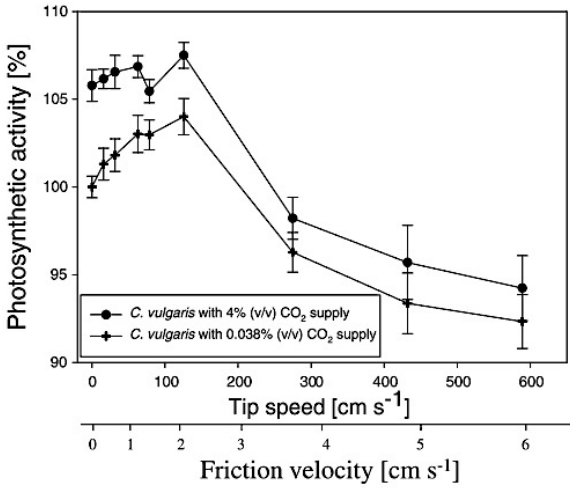


**Figure 18. Dependencies between the photosynthetic activity of C. vulgaris and the tip speed during aeration of $CO_2$-enriched air of 0.038 and 4% $CO_2$ (v/v) in the culture medium. PA is given as arithmetic mean and standard deviation from continuous measurements during a period of 304 minutes of constant tip speed (n=20). TS was increased stepwise after each measuring period. PA of 100% corresponds to the unstirred culture at 0.038% $CO_2$ (selected from (Leupold et al. 2013)).**

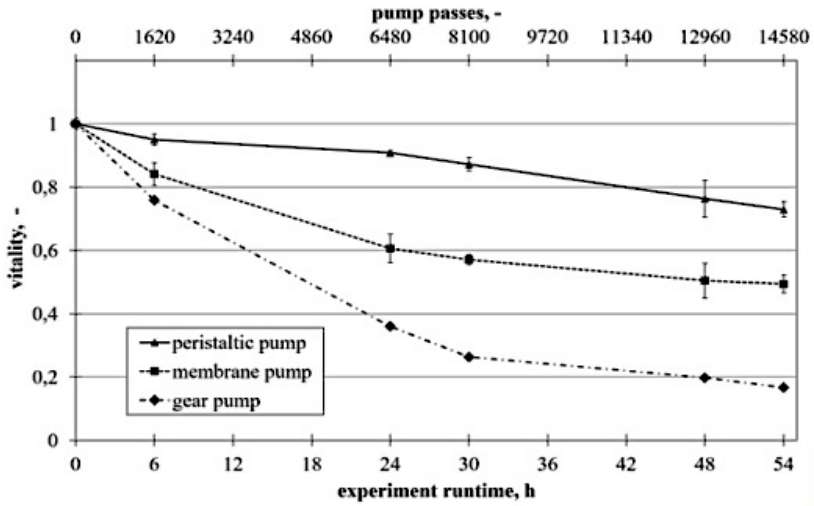


**Figure 19. Remaining vitality of sample cultures (10mL) with each pump running at 45 mL $min^{-1}$ (selected from (Bretschneider et al. 2016; J Keppler 2015)).**

**Table 7. Failure modes of the algal culture with their associated causes. Proposed mitigation or contingency plan is included but is understood that advancements in culturing technology can modify these suggestions.**

| Identifier | Failure Mode of Algal Culture | Cause of Failure Mode of Algal Culture | Mitigation or Contingency Plan |
|---|---|---|---|
| A | Algae cannot metabolize enough $CO_2$ to keep the cabin levels below the upper limit | -Improper irradiance level<br>-Photobioreactor outside allowable temperature range<br>-Copper or heavy metal contamination<br>-Insufficient cell density or culture capacity<br>-Nutritionally stressed | -Functional requirements for the culture need to be defined, and supporting growth environment ranges determined<br>-Ensure no copper or copper-alloy components are incorporated in system design<br>-Determine lacking inputs, increase accordingly |
| B | Algae is not able to produce enough $O_2$ to keep with human demands | -Improper irradiance level<br>-Not enough $CO_2$ is being consumed or provided<br>- Photobioreactor outside allowable temperature range<br>-Copper contamination<br>-Bacterial contamination is consuming excess $O_2$<br>-Insufficient cell density or culture capacity<br>-Nutritionally stressed | -Functional requirements for the culture need to be defined, and supporting growth environment ranges determined<br>-Ensure no copper or copper-alloy components are incorporated in system design<br>-Culture should be sterilized before use to reduce bacterial oxygen consumption<br>-Determine lacking inputs, increase accordingly |
| C | Algae is unable to consume wastes at a rate to provide enough clean water | -Insufficient micronutrients<br>-Concentration of wastes are too high for culture density<br>-Bacterial contamination from waste affects efficiency<br>-Insufficient cell density or culture capacity<br>-Nutritional Imbalance<br>-Copper or heavy metal contamination<br>-Insufficient irradiance level | -Provide micronutrients to support waste removal or dilute solution<br>-Sterilize waste before introducing into culture |
| D | Biomass is not produced at a rate appropriate for human consumption | -Insufficient irradiance, $CO_2$, or nutrients<br>- Photobioreactor outside allowable temperature range | -Functional requirements for the culture need to be defined, and supporting growth environment ranges determined<br>-Determine lacking inputs, increase accordingly |
| E | Overall cell viability | -Insufficient irradiance, $CO_2$, or nutrients<br>-Copper contamination<br>-Excess irradiance or $O_2$ in medium<br>-Medium bacterial contamination<br>-Physical destruction of cells<br>- Photobioreactor outside allowable temperature range | -Functional requirements for the culture need to be defined, and supporting growth environment ranges determined<br>-Ensure no copper/copper-alloy, or other toxic elements (e.g. lead, mercury) components are incorporated in system design<br>-Determine lacking inputs, increase accordingly<br>-Shade culture or reduce irradiance |

### 3.6.3 Causes of Failure Stemming from Culture

Table 7 presents a condensed version of the failure modes affecting culture functionality with causes directly stemming from algal cell physiology and cellular stressors. Suggested mitigation and contingency methods are included. Figure 20 allows for the failure modes of an algal culture to be compared, with consideration for failure causes. It indicates that robust mitigation or contingency efforts should be taken when considering algae for $CO_2$ reduction or $O_2$ provision. Human consumption of algal biomass products is indicated with a question mark due to the uncertainty of a qualitative assessment of failure likelihood and severity. Establishment requires additional research. This is with the assumption that the biomass is safe for human consumption. The edibility status of the biomass depends on the use-case of the photobioreactor, and needs to be considered during the design process. The establishment of failure likelihood and severity depends, in part, on how much biomass is consumed per day. If the biomass products are consumed as nutritional supplementation or food additives, failure of the culture has less of an impact than if the products were used as a substantial part of an astronaut diet.

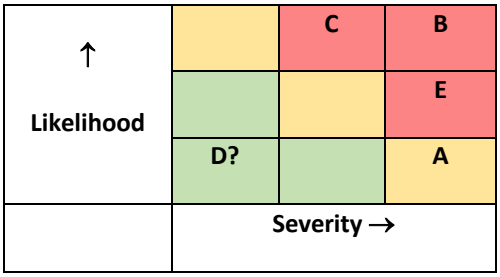


**Figure 20. The likelihood and severity matrix of the failure modes identified in Table 5. Failure modes of algal culture based on algal cellular physiology, mapped to human metabolic function. (Question mark indicates areas that require more research to establish definite severity and likelihood, definitions of A-D are in Table**

### 3.7 Causes of Failure Associated with Spacecraft Environment, Crew/Habitat Interactions, and Equipment

The previous section focused on causes of failure associated with the culture itself, these could happen regardless of the culture application (e.g. air revitalization, waste removal, etc.). This section focuses on failure causes at the system level. This includes causes that are dependent on utilization of the culture, spaceflight environment, and those stemming from the hardware used to execute the application. An algal culture addressing ECLSS functionalities is susceptible to the following application failure causes. Culture systems addressing simultaneous functionalities (e.g. air revitalization with thermal control) are not studied here, but it is assumed that application failure causes are additive. All studied cases assumed that the environment is a spacecraft environment

with a crew of 4-6 people. Table 8 presents the major failure modes associated with the system application, and the effects of these failures on the utilization of the algae. Failures of the application can also include algal cell physiology failure modes and causes, but interaction of the culture with the spacecraft environment is the focus in this section.

**Table 8. ECLSS functions potentially addressed by an algal photobioreactor, with the associated failure mode of that function. Failure effects are included for reference.**

| Algal Photobioreactor Function | Failure Mode of Algal Photobioreactor Application | Failure Effects |
|---|---|---|
| *Air Revitalization -$CO_2$ removal -$O_2$ provision* | Algae medium cannot transfer gases at the required rates | Algae culture becomes $CO_2$ limited and cannot produce sufficient $O_2$ |
| *Heat Transfer* | System or medium fails to transfer heat at the required rate range | Algae culture operates outside of designed temperature boundaries. Temperatures exceed acceptable thresholds. |
| *Biomass Production* | Insufficient irradiance | Algal culture unable to function as efficiently |
| *Cell Viability* | The percentage of viable cells falls below the lower threshold | System can potentially become unstable if death rate exceeds growth rate |

### 3.7.1 Spaceflight Environment

Exposure to the following elements is inevitable during spaceflight. However, mission duration and location determine the extent of influence these spaceflight environmental conditions have on an algal culture.

#### 3.7.1.1 Microgravity Environment

Culturing algae onboard spacecraft poses several challenges related to the microgravity environment: buoyancy-driven forces are absent in micro-gravity, and surface tension and diffusion forces become dominant mechanisms for transport (D. Klaus 1998). Preliminary ground-based studies have used rotating wall vessels and

clinostats to explore the effects of gravity on culture characteristics. These studies showed a significant reduction in growth rate, but no reduction in photosynthetic activity per cell (Mills 2000). This indicates the possible need for including more culture volume for microgravity operation. The ground-based studies also show an increase of ROS, signaling extracellular stress, but the amount of ROS was not enough to cause oxidative damage to the cells (G. Li et al. 2004). Clumping and aggregation of cells was the last major observation from these ground studies (Mills 2000). If cell aggregation is not controlled by vigorous mixing or culturing in continuous mode, it could cause biofilm buildup. Progression of the cell buildup could reduce pump or filter efficiency by fouling, or reduce irradiation penetration length into the culture (Oram 2014),(B. Wang et al. 2008). Additional considerations should be made about the genetic expressions of both algal cells and any predatory biomes (e.g. bacteria, grazers, or viruses) during microgravity flights. A microgravity bacterial study by Zea et al. indicated a reduced lag phase, high final cell count, increased virulence, and reduced susceptibility to antibiotics due to spaceflight-induced genetic mutation (Zea et al. 2016). Changes in genetic expression could affect both the operational efficiency of the algal culture and also the susceptibility of culture failure to contamination effects. However, the timescales and severity by which these mutations could take effect has not been fully researched.

Limited studies have been conducted on culturing algae in microgravity. Results from space flight experiments are not statistically conclusive on the effect of microgravity on cultures. However, a few of the flown experiments experienced a reduction in growth rate, similar to the clinostat ground-studies (G. Wang et al. 2006).

#### 3.7.1.2 Radiation Environment

Use of algal culture for spacecraft radiation shielding provides an additional function by the system. However, ionizing radiation could reduce the cellular growth rate or viability. This is due to the amount of cellular damage that can occur during a solar particle event or through galactic cosmic rays. Excess biomass would be required to buffer against the reduction in growth rate during an event, and to adequately line the cabin walls for crew protection. This could potentially result in large launched mass requirements (Matula and Nabity 2016). Research has mainly focused on terrestrial algal response to alpha and gamma radiation, similar to the radiation provided by nuclear plant meltdowns, but these reactions could be similar to a major radiation event (Vekshina et al. 1969; Barth, Dyer, and Stassinopoulos 2003; Morton and Derse n.d.; Vanhoudt et al. 2012). Studies have shown

that *Chlorella* is able to withstand acute dosages, about 23kr, of gamma rays without significant detriment to viability. However, *Chlorella* was unable to withstand chronic dosages of gamma rays, approximately 5kr/day, without reduction in growth and survival rate (Posner and Sparrow 1964). A relatively low number (<60) of space flight experiments using algae have been conducted but have not resulted in clear conclusions. Of those that have been outside the radiation protection of the Van Allen belts, or in Low Earth Orbit (LEO) for any significant amount of time, none have yielded definite conclusions about algae survival or photosynthetic rates (Niederwieser, Kociolek, and Klaus 2018). However, a recent experiment conducted by the Fraunhofer Institute for Cell Therapy and Immunology, in conjunction the European Space Agency with international partners, sent samples of cryophilic algae found in polar regions to the International Space Station. These cryophilic algae were sampled from their naturally occurring elevated UV environments, found in the polar regions. These cultures were placed on the exterior of the ISS for 16 months, and were exposed to UV-radiation from $4.5x10^6$ kJ/m$^2$ to $8.4x10^6$ kJ/m$^2$ (approximately 1000x polar UV-levels) and temperature swings from -20°C to +50°C (Llabrés and Susana 2010). Two of the five flown cultures survived the experiment, and were able to be re-cultured after being returned from flight (de Vera et al. 2019; Augustin 2017). This suggests that species selected for their ability to resist the effects of radiation terrestrially may be appropriate for spaceflight use.

Generally, the culture may benefit from shielding or establishing denser cultures to offset cell death; in an effort to retain culture viability, avoid crashes, and ultimately system failure, unless species are specifically selected for the radiation environment.

### 3.7.2 Culturing Under Cabin/Habitat Conditions

When utilizing algal culture for ECLSS applications, the culture may be directly integrated into the spacecraft cabin or surface habitat, interacting with the inhabited environmental conditions. The following influences on culture efficiency are dependent on the desired ECLSS purpose.

#### 3.7.2.1 Utilizing Transient Cabin Atmospheric Environments

One of the most attractive characteristics of algae is the ability to reduce $CO_2$ to $O_2$ through photosynthesis. Referencing the photosynthetic equation (Eq.1) presented in the previous section, six $CO_2$ molecules are required for six $O_2$. A human respires approximately 1.04 kg $CM^{-1}day^{-1}$ $CO_2$ and consumes 0.816 kg $CM^{-1}$ $day^{-1}$ of $O_2$ (Anderson

et al. 2015). When the units are converted from kg $CM^{-1}$ $day^{-1}$ to mol $CM^{-1}day^{-1}$, and assumed 100% conversion efficiency, the respired $CO_2$ only produces 0.76 kg of $O_2$. This signals that if algae are the sole oxygen source for human space flight, additional $CO_2$ needs to be provided. However, this is not a desired solution due to cabin environmental requirements. There are two possible solutions to matching the photosynthetic quotient (or assimilation quotient, AQ) of algae and respiratory quotient (RQ) of the crew. First, modifying the crews' diet, through the ratio of included carbohydrates, fats, and proteins, could actively alter their RQ to values reflecting the AQ of the algal system. Respiratory quotients of 0.7 and 1.0 were reported when metabolically oxidizing fats or carbohydrates, respectively (Salisbury, Gitelson, and Lisovsky 1997; Wheeler 2003; Myers 1964). Secondly, the AQ of algae could be adjusted by the type of nitrogen supplied to the media. Using urea resulted in an AQ of 0.82, 0.8 for ammonia, and 0.62 when using nitrate (Krall and Kok 1960). This suggests that using the urea found in the crews' urine as an algal nutritional supplement and increasing the ratio of carbohydrate in the crew diet may help to close the disparity in ratios.

Typical cabin gas streams contain trace elements (e.g. benzene, carbon monoxide, etc.) and could be introduced into the algal stream through gas transfer (Anderson et al. 2018). Algal reactions to these chemicals are relatively unknown. Experimentation is required to determine if the trace element concentrations found in the cabin environment could be detrimental to the culture function. Alternatively, filtration of the gas stream could be conducted to remove elements toxic to algae.

#### 3.7.2.2 Transient Thermal Environment

The algal culture and medium have potential for use in multiple, simultaneous functions. For example, 1) the algae revitalize the atmosphere (consume $CO_2$ while producing $O_2$), 2) harvested biomass is a food or nutrient source, and 3) the medium is used as heat transfer fluid within the cabin. Focusing on the heat transfer application, the medium could experience temperature fluctuations similar to the ISS cooing loop, varying between +4°C and +30°C over a span of tens of minutes to a few hours (Valenzano et al. 2003). Figure 21 illustrates a culture medium temperature response in relation to its position in a cabin cooling loop. Effects of these transient thermal environments on algal metabolic functioning is relatively unknown. Open raceway ponds used for biodiesel can increase +14°C over the course of an afternoon due to solar irradiance without culture detriment, but this is within

the upper range of the algal temperature spectrum (+20°C to +34°C) (Costache et al. 2013). Experiments using various stead-state temperatures ranging from +5°C to +50°C have shown that lower temperatures result in lower growth rate and photosynthetic rate (Bartosh and Banks 2007).

It is hypothesized that the time-averaged metabolic response of temperature-cycled cultures reflects a steady-state, low-temperature oxygen production level. In an effort to offset sluggish growth rates and avoid system failure, algal cultures could be cultivated to a mature density before beginning the cycling or include additional volumes of algae in the design. Disparity in the heat transfer coefficient of water to algal culture is minimal, since algal cell composition is mostly water (approximately 85%) (Kanda and Li 2011). This allows for the assumption that an increase in culture density has a minimal effect on the heat transfer properties of the medium.

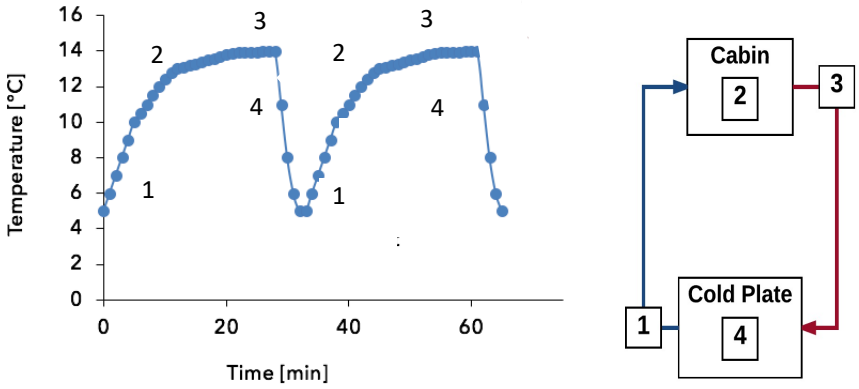


**Figure 21. Graphical representation (left) of the cycle of temperatures experienced by the algal cell if cultured in a medium used for cabin heat transfer (right).**

### 3.7.2.3 Treatment of Urine and Wastewater with Algae

Terrestrially, algae are being used to reduce dissolved nitrogen and phosphorous in wastewater while using the rapidly produced biomass for biodiesel (Jaatinen, Lakaniemi, and Rintala 2015). It might be feasible to use a similar approach in spacecraft. Algae require nitrogen and phosphorous for normal metabolic functioning, found in human grey water and wastewater (Table 9) (Mandalam and Palsson 1998b; Anderson et al. 2018; Hintze et al. 2014). Removing harmful non-organics from the water using algae can be a first step in the water treatment process. Terrestrial experiments have used various dilutions of pasteurized urine (water-to-urine ratios from 200:1 to 2:1) to study its effect on algal metabolic function (Tuantet et al. 2014; Jaatinen, Lakaniemi, and Rintala 2015). Results from these experiments suggest that additional trace nutrients, mostly magnesium, are required to reduce nitrogen and

phosphorous with the highest efficiency, for urine concentrations greater than 100:1 (Tuantet et al. 2014; Zhang et al. 2014). Gitelson suggested that the amount of human urine acceptable to an algal culture for nutrient supplementation can vary from species to species, and even between algal strains (Gitelson, Lisovsky, and MacElroy 2003). This is evident in the literature when identifying the acceptable amount of NaCl (a common component of human urine) for an algal species. The results of Barghbani's experiment using *C. vulgaris* suggested that NaCl concentrations higher than 20g$L^{-1}$ completely inhibited growth, while Shen et al. reported biomass production with concentrations >40g$L^{-1}$ (Barghbani, Rezaei, and Javanshir 2012; Shen et al. 2015). However, overall, increasing urine concentration reduced growth rate. The presence of ammonia in the medium was reported to not have a substantial effect on the viability of the algae, but it did significantly reduce the growth rate when

**Table 9. Composition of optimized growth media, human urine, and urine brine simulant.**

| Major Components | Optimized growth media for *Chlorella v.* (g/L, element amount) | Fresh Human Urine (g/L) | Urine Brine Simulant (g/L) |
|---|---|---|---|
| Urea | – | 13.4 | 70.0 |
| NaCl | N found as $KNO_3$ 0.04 | 8.0 | 11.5 |
| KCl | K found as $KNO_3$ & $KH_2PO_4 \cdot 2H_2O$ 1.37 | 1.64 | 12 |
| $CaSO_4$ | Ca found as $CaCl_2 \cdot 2H_2O$ 0.13 | – | 1.3 |
| $NaNO_3$ | Na found as $Na_2HPO_4 \cdot 2H_2O$ 0.03 | – | 7 |
| $NaH_2PO_4$ | P found as $KH_2PO_4$ & $Na_2HPO_4 \cdot 2H_2O$ 0.21 | P found as $K_3PO_4$ 0.1 | 5 |
| $K_2SO_4$ | – | 2.63 | 30 |
| **Additional Compounds** | | | |
| Al | Al found as $Al_2(SO_4)_3 \cdot 18H_2O$ 0.28 | – | – |
| Mn | Mn found as $MnCl_2 \cdot 4H_2O$ 3.6 | – | – |
| Mg | Mg found as $MgSO_4 \cdot 7H_2O$ 0.2 | Mg found as $MgSO_4$ & $MgCO_3$ 0.2 | – |
| Cu | Cu found as $CuSO_4 \cdot 5H_2O$ 0.39 | – | – |
| Zn | Zn found as $ZnSO_4 \cdot 7H_2O$ 0.4 | – | – |
| S | S found as $SO_4$ 1.09 | S found as $SO_4$ 0.69 | – |
| Fe | Fe found as $FeSO_4 \cdot 7H_2O$ 0.20 | – | – |

ammonia concentrations were above 750 mg $L^{-1}$ (Zhang et al. 2014),(Tam and Wong 1996). During this growth rate reduction, it is possible that other inputs have become limiting (e.g. $CO_2$ or light). This could be an issue for functions relying on growth of the culture, such as food production using biomass. Typically, waste-water streams are not limited to human metabolic waste but also include other non-metabolic fluid wastes, including hygiene wastewater, humidity condensate, dissolved heavy metals, cleaning chemicals, and water recovered from experiments. It was previously mentioned that below certain thresholds, or when including a particular species, waste content does not pose an issue with operation of the photobioreactor. While bioremediation of some chemicals is possible within the algal biomass, most other compounds are stored, leaving the compounds as potential hazards to humans, if the biomass is consumed (Bajguz 2000). Characterizing the expected waste profile can assist the species selection process and inform the food-safety of the biomass (if consumption is planned).

Currently on the ISS, hazardous chemicals (sulfuric acid and chromium trioxide) pre-treat the wastewater before the filter process to control microbial growth. Unfortunately, using this approach before directly introducing the waste stream to the photobioreactor would likely kill the algal culture (Hörcsik et al. 2007). Instead, waste pasteurization, heating the waste stream above the viability point of the microbes and cooling it before introduction to the algal stream, is suggested.

If using algae to reduce wastewater's excess nitrogen and phosphorous, and depending on the dilution ratio of urine, additional trace elements may be required. Otherwise, the culture growth rate might lag beyond the acceptable threshold, causing failure. The main causes of a culture failure would be due to a lack of needed nutrients or a system failure from lagging reductions due to slow growth rates.

#### 3.7.2.4 Algal Edibility

After defining edibility as "fit to be eaten", it is noted that only certain species of algae can be directly ingested by humans (Oxford 2018). Currently, only a select few algae species are commercially available for human consumption as a health food or nutritional supplement to provide antioxidants and protein (Carlson 2011). However, this consumption is typically in the form of smoothies or additive powders, relying on other ingredients to mask or enhance the algal flavor and is typically not a significant part of a person's diet.

NASA and Roscosmos have both have investigated using algae for long duration space flight nutrition. Both groups also hypothesized the ability to close the carbon loop by using biological life support (Eckart 1996). If using an algal photobioreactor for air revitalization, then consumption of the resulting biomass has the potential to complete the carbon cycle in the spacecraft. The percentage of the astronaut's diet reliant on the produced biomass depends upon the algal species, its safe rate of consumption, and post-harvest processing needed to make it suitable for consumption. Determining the diet inclusion percentage also requires consideration of crew acceptance. Researchers found test subjects tired of direct, long-term consumption of algae, and over time became less willing to eat the biomass (La Vone 2014). Also, only specific species of algae should be considered for human consumption. *Chlorella* cells contain a thick cellulose wall that can be difficult to digest in large quantities (this exact amount varies between users) causing diarrhea and dyspepsia. Post-harvest processing, such as grinding, to break down the wall could mitigate these symptoms (Eckart 1996). Certain species of cyanobacterium, not including *Spirulina*, have the potential to produce mycotoxins, causing diarrhea, vomiting, or death if consumed (Bennett and Klich 2003). While this research uses *Chlorella* as a baseline algal species, it is recognized that other algal species may be more appropriate for mass consumption.

Issues introduced in previous sections arising from using algal photobioreactors for waste stream remediation suggests that the biomass produced from these bioreactors should be evaluated before consumption (e.g. analyze chemical content for heavy metals harmful to humans). In addition, bacterial, viral, or protozoan contamination may also be present, and while microbial contamination may not be detrimental to the algal culture, these contaminants could make the biomass unfit for human consumption.

Failures associated with algal food production is largely due to safety of produced biomass (especially in systems processing waste-water streams), tertiary failures could arise from acceptability issues with human consumers. In order to close the carbon loop, it is important for the algae biomass to be fit for human consumption. Otherwise this biomass becomes an additional waste, reducing the efficiency of the overall system. Ensuring the safety of the biomass, selecting species appropriate for human digestion, and manipulating the biomass to be palatable could circumvent these issues. Further investigation is needed to determine of the amount suitable for crew consumption.

### 3.7.3 Support Equipment

If system hardware fails to fully support the culture, then inevitably both the culture and system fails. Support hardware could include, but are not limited to, items such as pumps, valves, piping, and connectors. These components need to be tolerant of biofilm or other biological buildup. The support hardware should also be capable of working in reduced and micro gravity conditions, as the system may be used on the surface as well as inflight. Culturing materials and hardware need to withstand solar particle events and galactic cosmic rays or be easily repaired or replaced in case of damage during an event.

### 3.7.4 Scaling Issues for Long Duration Spaceflight

While no extensive, closed-loop experimental ECLS algal systems have been launched yet, interest in biodiesel has generated the need for large-scale terrestrial operations to provide biomass as feed stock for fuel production. Lessons learned from designing and operating industrial-scaled culturing operations, could be applied to spacecraft or surface habitat designs.

Insufficient amounts supplied $CO_2$, irradiance, nutrients, and improper culturing temperature are the most commonly cited issue with scaling up operations. A reduction in system efficiency or culture crash occurs when there is a disparity between the requirements of the culture and the resources available. A commonly identified limiting factor was irradiance. As cultures became dense enough to be self-shading, vigorous mixing with increased irradiance was needed to promote continued growth (Hao et al. 2012).

Biofilms could build up within enclosed systems, such as tubular or flat-plate bioreactors, and reduce irradiance. Accumulation could occur within pumps and filters, requiring intermittent cleaning to keep the system running at peak efficiency. Large-scale operations use back-flow methods or scrubbers floating in the line to keep the film down and then shut down once a year to conduct a thorough site-wide cleaning. Typically, designs of culturing farms do not include sharp corners or tight bends, since these could provide flow stagnation points and accumulate biofilm (Bosma et al. 2014). Enough pumps should be included in any design to keep the culture moving and mixing.

Terrestrially, $CO_2$ is introduced to the algal culture typically by gas sparging (bubbling gas through culture). If planned use of the photobioreactor included space flight, gas sparging is not a viable option for gas transfer. Bubble formation in microgravity is chaotic and hard to control or predict, making sparging undesirable as a gas transfer

option in space. Gas-permeable membranes can provide gas transfer without bubble formation, relying on stream concentration and Henry's law to transfer gases. Preliminary terrestrial studies of gas transfer membranes in photobioreactors have shown the capability to successfully culture algae (Lee and Palsson 1995). Examples of these have been reviewed in Chapter 2.4.

Inclusion of gas permeable membranes for gas liquid contacting would offer bubble-free provision of gas to the liquid system through concentration-driven processes. However, if the membrane is non-selective when transferring species, water vapor can enter the gas stream. Depending on the requirements of the cabin environment, additional humidity control may be needed to regulate the water vapor content of the membrane outlet gas stream. Furthermore, the transferred water vapor would actively change the water volume in the photobioreactor, concentrating nutrients and biomass, and possibly changing operation characteristics. Returning the lost water to the photobioreactor by condensing the humidity in the output gas stream may be a potential solution. The phase (gas, liquid, or a combination of both) of water leaving the contactor on the gas-side is dependent on the temperature gradient across the membrane. Water vapor has the potential to condense inside the membrane unit, if the gas temperature drops below the dewpoint while in the unit. This may affect the operation of the contactor and require water-removal procedures or active temperature control of the contactor.

Establishment time is an additional issue associated with larger scale biological systems. Cultures need time to reach their required density, unless already established at the time of launch. Not accounting for this establishment time can be a failure in itself. This also needs to be a consideration when reviewing other modes of failure. If a failure can cause culture extermination or loss of density, then the schedule for corrective action must include the time needed to re-establish the culture.

Large-scale units tend to have difficulty with successfully producing axenic cultures. If a system is not axenic, there is the possibility of the invading microorganism overrunning the system, possibly changing its functionality. This problem is perhaps more prevalent in terrestrial culturing than in space flight due to the source of aeration. Typically, terrestrial aeration systems pump air directly from the surrounding environment, allowing airborne microorganisms to join the culture. Spacecraft environments have much more stringent air quality requirements and use multilayer filters to clean the air, reducing the possibility of airborne microbe contamination. Nonetheless, components should be cleaned before utilization in the spacecraft.

Since the spacecraft environment is dynamic, the production rate of biomass during operation for ECLSS purposes may exceed usage or consumption rate. Excess biomass could be preserved or dried and used as a buffer for when biomass production rate is reduced. If the disproportionate rates are not addressed, the carbon loop may not close, which reduces the value of a bioregenerative system. However, if closure of the carbon cycle is not a mission priority, then biomass could be packed into cabin walls for radiation shielding, provide a source of lipids for biofuels, become feedstock for aquaponics or wet incineration, etc.

Finally, integration of the photobioreactor system into the spacecraft needs to be considered. The requirements of the mission and the requirements of the algal culture indicates acceptable modes of integration. Proposed designs have banks of photobioreactor bags or tubes lining the inside of the spacecraft, as seen in Figure 22 (Cohen, Flynn, and Matossian 2013). Designers have indicated that spreading the volume across the surface area of the cabin accommodates the volume of algae, while spreading the culture thin enough to allow for proper irradiance.

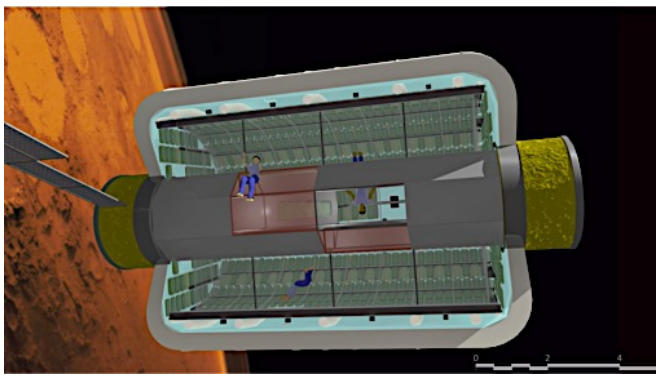

**Figure 22. Proposed integration of photobioreactors into a spacecraft cabin line the walls with light banks and then cover them with culture-containing bags or tubes (selected from (Cohen, Flynn, and Matossian 2013)).**

### 3.7.5 Causes of Failure Stemming from Spaceflight Environment, Cabin/Habitat Conditions, Support Equipment, and Scalability of System

Failure modes, failure causes, likelihood and severity, and mitigation and contingency plans are all presented in Table 10. A notable difference from Figure 20 can be found in the likelihood and severity columns. There are instances where the likelihood of a failure cause is relatively unknown (indicated with an asterisk) and this is due to the proposed spaceflight utilization of the culture. Extensive experimentation of algal cultures in space

flight have not been conducted. Literature searches also provided little insight for estimation of mean time between failures or magnitude of environmental changes on culture health. Figure 23 indicates loss in cell viability as being potentially the most catastrophic failure, primarily due to the re-establishment time of a culture. Depending on the required culture density, this could take upwards of a few weeks. Algal use for human consumption is indicated with a question mark because of the uncertainty associated with estimating the likelihood and severity of failures (limited to post harvest). Uncertainty stems from both the need for more research in the amount palatable to humans and how mission design and planning dictates daily biomass consumption rates. Depending on the utilization and culturing environment of the algae, biomass production rate could exceed consumption/usage rate, or potentially render the biomass unfit for consumption (heavy metal concentrations, bacterial contamination, etc.). Since likelihood and severity of this possibility is reliant on mission-specific requirements and associated system control parameters not considered here, the failure mode is indicated with a question mark.

**Table 10. Failure modes of the algal photobioreactor with their associated causes, likelihood and severity ratings are included, where available. Proposed mitigation or contingency plan are included but advancements in culturing technology may change these plans.**

| Identifier | Failure Mode of Algal Photobioreactor Application | Cause of Failure Mode of Algal Photobioreactor Application | Mitigation or Contingency Plan |
|---|---|---|---|
| F | Membrane is not transferring gas within the required rate range | -Buildup of biomass on membrane surface<br>-Fluid/gas movement through membrane is impeded<br>-Gas-side fouling | -Develop cleaning schedule to remove biomass buildup<br>-Incorporate "emergency" in-vitro cleaning techniques (quick burst of high velocity medium) |
| G | Membrane or medium are not transferring heat at the required rate range | -Buildup of biomass on membrane<br>-Pump failure<br>-External fan or air filter failure | -Develop cleaning schedule to remove biomass buildup<br>-Replacement schedules for pumps |
| H | Algae is not receiving enough irradiance | -Buildup of biomass on light transfer surfaces<br>-Aging bulbs<br>-Pump failure<br>-Electrical system issue<br>-Optical density too high, presence of dead biomass | -Develop cleaning schedule to remove biomass buildup<br>-Replacement schedules for pumps<br>-Determine "warning" signals (decreased $O_2$ production, visible biomass buildup, etc.) to indicate cleaning need |
| I | Algae not palatable or fit for human consumption | -Bacterial contamination | -Maintain reserve culture stock<br>-Vary preparation techniques<br>-Dry algae for later consumption |
| J | The percentage of viable cells goes below the lower threshold | -Pumping damages cells<br>-Utilization pushes growth environment out of optimal ranges<br>-Exposure to radiation environment<br>-Nutritional composition of medium | -Determine "warning" signals (decreased $O_2$ production, decreased viability ratio over time, etc.) to indicate action should be taken<br>-Include redundant systems (algae or otherwise) if a "regrowth" period is needed |
| K | Produced biomass rate exceeds usage/consumption rate (unless nominal operation mode) | -ECLSS utilization pushes growth environment out of optimal ranges<br>-System consuming or utilizing biomass experiences failure | -Dry algae for later consumption<br>-Determine "warning" signals to indicate action should be taken<br>-Tertiary uses for excess biomass should be established (pack walls for radiation shielding, feed aquaponics, etc.) |

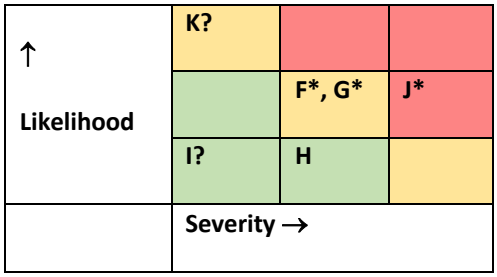


**Figure 23. Established likelihood and severity of the failure modes identified in table 4. (Asterisks indicate likelihood is not established, question marks indicate areas that require more research to establish definite severity and likelihood)**

### 3.8 Discussion

As previously presented, algae are multifunctional organisms, with potential to address most human metabolic needs during space flight. Failures associated with applications supporting human space flight need to be understood for future designs. While research into space flight usage is relatively novel, characterization of algae physiology is well-defined. As a result, a majority of algal vulnerabilities have been established and have associated countermeasures. The advancement of biodiesel has prompted additional research into cultivation methods, which have identified some issues with scaling biomass production. Pilot plants, using culture physiology information, have implemented equipment design and operation changes to mitigate issues with scaling. These lessons learned from the study of phycology and biodiesel production could assist in reducing the likelihood of a failure and increase the reliability of the system.

Terrestrially, algae culturing methods and biological responses are very well-established. However, there are gaps in knowledge with respect to use in a space environment. As presented by Niederweiser, 51 flight experiments have been conducted with algae and have that shown basic biological processes (photosynthesis, respiration, and replication) are sustained, but characterization of the dynamic behavior was not comprehensive (Niederwieser, Kociolek, and Klaus 2018). Additional research is necessary to understand specific cellular response and incorporate results into application designs. Other studies have compiled issues that could arise when using bioregenerative systems for air revitalization and nutritional supplementation, or waste remediation (Nelson et al. 2009; Blüm et al. 1994; Gitelson, Lisovsky, and MacElroy 2003). One study went into more detail by reviewing the feasibility of a bioregenerative life support system that incorporated higher plants for nutritional supplementation,

instead of algal biomass. The unused algal biomass was repurposed to produce a "soil-like" substrate for the higher plants. This design relies on a familiar source of biomass (higher plants) while also taking advantage of the air revitalization and waste management capabilities of algae. Issues with using certain species of algae in conjunction with higher plants were introduced (Tikhomirov et al. 2007). A 1983 NASA report acknowledged three major considerations for algae-based bioregenerative systems: illumination techniques, gas transfer to and from the system, and processing biomass for human consumption (Averner et al. 1983). A majority of the studies surveyed identified areas of issue or design difficulty, but they did not discuss failure modes with suggested means to mitigate failures.

This study not only reviewed areas where bioregenerative systems could be used for additional spaceflight ECLSS, but also the failures that could arise from these applications, with suggested mitigations. Additionally, likelihood and severity were assigned for each of the failures, to indicate to the reader areas for attention when designing bioregenerative systems. The cellular physiology was also included to explain the biological reasoning for some failures and how they could be mitigated.

The study of phycology has not only determined algal cellular function but has also identified associated benefits and shortcomings of various species of algae. *Chlorella* was the focus of this chapter due to the amount of literature available on the species, but others may be more appropriate for certain applications. An example of this relates to selecting a species appropriate for wastewater treatment. Researchers have been interested in using algae for waste remediation terrestrially and in space flight due to its ability to close the carbon loop and efficiently consume the nitrogen-based and phosphorous-based compounds found in human waste. Multiple species have been investigated, including *Chlorella sorokiniana*, *Scenedesmus acuminatus, Chlorella vulgaris*, and *Spirulina plantensis*. A comparison of the results from two similar experiments using human urine for growth media showed that *S. platensis* produced more biomass, had a higher consumption capacity and faster consumption rate of phosphorous and nitrogen than *C. vulgaris* (Jaatinen, Lakaniemi, and Rintala 2015; C. Yang et al. 2008). Meaning, *Spirulina* should be given precedent when considering algae for wastewater remediation to save on system mass, power, and volume. Terrestrial environments analogous to space flight conditions could suggest species well-suited for certain applications. For example, if algae are used for spacecraft thermal control, the culture may be exposed to temperatures below 10°C, an extreme temperature for most algae. While this may be detrimental to most species,

those algae found in the Antarctic thrive at temperatures ranging from -5°C to +15°C, bracketing the operational temperature range for a thermal control system (Morgan-Kiss et al. 2006).

Accommodating a wider range of environmental conditions by including multiple species in a culture may also be appropriate, although some species rely on certain conditions for survival. For example, the aforementioned species from the Antarctic experiences a decrease in cell viability at temperatures greater than +15°C. However, cellular adaptation, through multiple generations, is possible over an extended period of time.

Species adaptation to the environment has been known to the microbiology community as early as 1887. It was concluded that the ciliated protozoa in the fresh waters of New Zealand were basically identical to those found in Europe, while residing in dissimilar environments (Finlay 2014). Examples of temperature adaptation can be found in lab-based experiments using *C. vulgaris*. When compared to the cellular composition of cells grown at 27°C, cells at 5°C exhibited a reduction in chlorophyll per cell, higher ratio of chlorophyll a/b, and a decrease in the content of LHCII polypeptides. These alterations reduce excitation stress on the cell caused by irradiance at cooler temperatures (Maxwell et al. 1994). Other adaptation or coping mechanisms have been cited in regards to changing environmental salinity, UV exposure, low irradiance, and variable pH to increase cellular viability (Morgan-Kiss et al. 2006). Yet, these adaptations may take up to 135 generations to develop, which may be longer than the period of the environmental change (Ras, Steyer, and Bernard 2013). So, while the algal culture could thrive in a new environment, it may take quite a while to do so.

### 3.9 Conclusion

The duration of proposed deep space missions demands a high level of system robustness. Algal photobioreactors have the potential to provide closed loop, bioregenerative ECLSS for space flight missions and therefore, suggest a potential way to address NASA's desire to identify systems with little to no waste or consumables. However, spaceflight environments and conditions could put culture health and growth at risk. Fortunately, extensive research has been conducted for characterizing cellular physiology and developing terrestrial culturing methods. These results provide an appropriate starting point for technology assessment and trade studies of bioregenerative closed-loop technologies. Higher-fidelity failure analysis requires additional flight experiments to gain a better understanding of the real-time response of algae to space flight. Future work should include space

flight experiments to investigate the response of algae cultures to transient changes of lighting, temperature, and $CO_2$ level while in the microgravity environment. Experiments are also needed to characterize a culture's ability to revitalize a cabin atmosphere and transport heat while in the spaceflight environment.

Characterization of algae physiology is typically conducted under steady-state conditions whereas cultures are exposed to time-varying environments if used for ECLSS. As an example, lighting may follow the crew diurnal cycle which has a real-time effect on $O_2$ and $CO_2$ exchange rates. This suggests that a photobioreactor may need its own irradiance source or the application be designed to accommodate cabin lighting schedules with possible supplementation. Determining metabolic responses to these changing conditions may inform additional design considerations for implementation and influence the failure modes and effect analysis.

A major conclusion from this study is that a bioregenerative system has the possibility of multiple failure modes, stemming from both biology and support hardware. Fortunately, biological-based causes are well-known and have established countermeasures. Conversely, the integration of the hardware into a spaceflight setting and its ability to successfully support algal growth requires additional testing and development.

### 3.10 Resulting Presentations and Publications

Journal Paper

**Matula, E. E.,** Nabity, J. A. (2019). "Failure modes, causes, and effects of algal photobioreactors used to control a spacecraft environment", Life Sciences in Space Research, 20, pp. 35-52, 2019.

Conference Paper

**Matula, E. E.,** Nabity, J. A. (2017). "Review of failure modes of a photobioreactor system used for long duration spaceflight environmental control and life support," 47th International Conference on Environmental Systems, Charleston, SC, 2017.

Conference Presentation

47th International Conference on Environmental Systems, "Review of failure modes of a photobioreactor system used for long duration spaceflight environmental control and life support," Charleston, SC, 2017.

# Chapter 4 Characterization of *Chlorella* Metabolism in a Steady-State Temperature Environment

## 4.1 Introduction

The influence of environment temperature on algal processes can be measured through changes in photosynthetic rate, oxygen production rate, or culture doubling time, as introduced in Chapter 3. In this chapter, algae were cultured in steady-state temperatures to characterize culture productivity in temperatures reflective of Low Temperature Loop (LTL) and cabin thermal conditions. The temperatures selected were determined by the boundaries of the utilized environmental lab equipment and the allowable cabin temperature thresholds. This series of experiments informed results of the cycled temperature experiments in subsequent chapters, and a potential culture operational envelope.

## 4.2 Background

Figure 17 of Chapter 3.6.2.6 indicated that algal cells continue to multiply across a range of steady-state environmental temperatures, even as low as +10°C (Dauta et al. 1990). The steady-state environmental temperature envelope used in this Chapter's experiments looked to either maximize heat transfer or air revitalization capabilities. Absorption of environmental heat through liquid cooling loops (like the ISS cabin thermal loop) rely on temperature gradients between the working fluid and the cabin temperature. Heat is absorbed by the loop, when the fluid is cooler than the surrounding environment. The required volume of the working fluid is influenced by this temperature differential. Increasing the temperature delta by operating at the coldest-possible loop temperatures minimizes the required working fluid volume (Incropera et al. 2007). However, if the algal medium is used as the thermal loop working fluid, operating at these low temperatures (<+15°C, maximum temperature of LTL) may reduce the air revitalization capabilities of the culture through a reduction in photosynthesis (Maxwell et al. 1994). Conversely, Figure 17 suggests that culturing algae in medium at approximately +35°C would the maximize growth rate of *Chlorella*. Using the growth rate as a proxy for air revitalization capabilities (since the carbon required for cell replication may come from atmospheric sources), this suggests that optimization of air revitalization capabilities could require warmer media temperatures.

This series of experiments characterized the metabolic response of an algal culture when grown in a steady-state environmental temperature reflective of optimizing heat transfer and reflective of optimizing growth rate as a proxy for air revitalization capabilities.

## 4.3 Materials and Methods

### 4.3.1 Culture and Associated Hardware

*Chlorella vulgaris* was the species selected for exposure to steady-state temperature conditions (*Chlorella vulgaris*, Bacteria-free agar slant, Carolina Biological) due to its heritage in spaceflight experiments and published terrestrial data, for reference. This species is known colloquially as the "lab-rat" of algae, due to its ability to grow in a wide range of pH, temperature, and light regimes. Additionally, this unicellular algae does not produce phycotoxins and can be consumed by humans after minimal processing (Solter and Beasley 2013; Carlson 2011). *Chlorella* was cultured in Bold's (Bristol's) Modified Media (50x Bold Modified Basal Freshwater Nutrient Solution, Sigma Aldrich). The 50x concentrated solution was diluted with Ultrapure water to 1x, and then sterilized by autoclave. A continuous culture was kept in clean, but not sterile, lab conditions. A 1L Pyrex beaker on a magnetic stir plate (AI2801, Apera Instruments), covered lightly with cling wrap placed under a bank of fluorescent bulbs (F40PL/AQ/ECO 49893 Bulb, GE Lighting) maintained the culture.

Each experiment used a sterile, clear 12-well-plate (229111, CellTreat), with only wells B2, B3, B4 filled with 3.5ml of culture with an initial culture density of $1x10^6$ cell/ml. Water levels of wells were marked with an Exacto-knife before covering with a clear, gas-permeable membrane (Sealing membrane, Breathe-Easy). Well-plates were loaded in a clean lab area. Using 12-well-plates allowed for replicates to be executed simultaneously and contained enough culture volume to properly submerge measurement probes.

Temperature control was executed through direct exposure to the Environmental Chamber environment (BioServe Chamber). The plates were placed on stands on an orbital shaker table (7744-01000, Bellco Orbital Shaker) set to 100 RPM kept the culture lifted in the media, reduced media temperature gradients within the well, and promoted gas exchange between the environment and media. The stands kept the distance between the fluorescent light bank and the well-plate constant across all experiments.

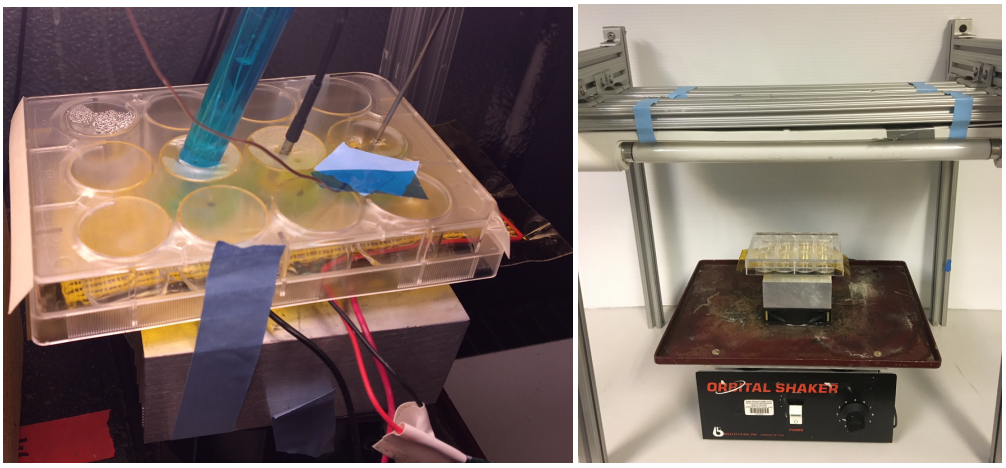


**Figure 24. pH, dissolved oxygen, and temperature probes inserted through membrane (left image). Well-plate and stand on top of orbital shaker table under fluorescent light bank (right image).**

An overhead lighting structure was constructed using 80-20 and fluorescent bulb holders. The 12-in GE fluorescent bulbs (F40PL/AQ/ECO 49893 Bulb, GE Lighting) were installed 8.5-in above the surface of the 12-well-plates, providing approximately 120 μmol $m^{-2}s^{-1}$ for 24-hr illumination. Figure 25 from Dauta et al. suggests that this intensity may maximize growth rate for the tested temperatures (Dauta et al. 1990). Peaks in the lighting spectrum of these bulbs are similar to the absorption peaks of *Chlorella v*, promoting efficient growth (Nakajima, Hanawa, and Tsuchiya 2015; "Spectral Power Distribution Curves" 2016).

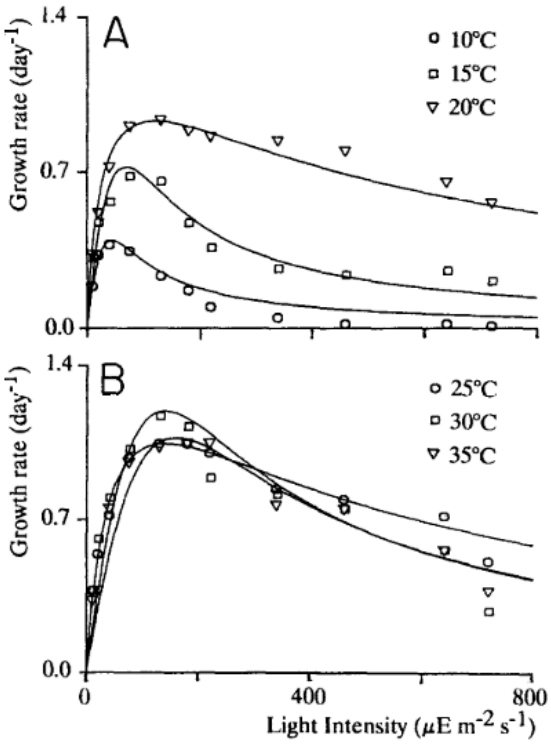


**Figure 25. Observed growth rate versus irradiance levels for A) 10, 15, 20°C (top) B) 25, 30, 35°C (bottom) (selected from (Dauta et al. 1990)).**

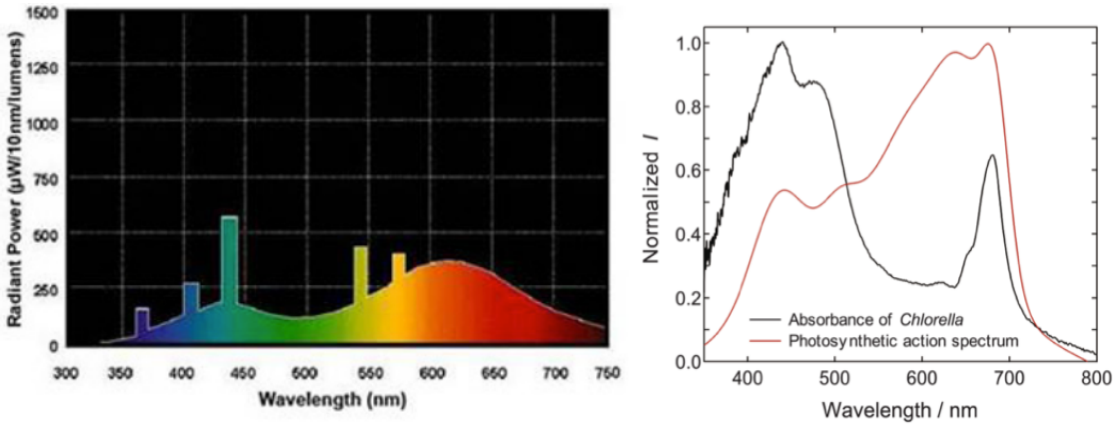


**Figure 26. Emittance spectrum of included GE fluorescent bulbs (left) compared to absorption spectrum of *C. vulgaris* (right) (selected from GE Lighting and (Nakajima, Hanawa, and Tsuchiya 2015)).**

The lighting, shaker table, and Peltier cooler unit were placed in the BioServe Environmental Thermal Control (ETC) unit. The ETC was set to a constant temperature, depending on the requirements of the experiment.

### 4.3.2 Experiment Design

#### 4.3.2.1 Variables and Conditions

The independent variable for this series of experiments was the medium temperature (Table 11Table 12). The lower temperature bound (+10°C) was dictated by the cooling capabilities of the ETC and reflected an LTL operating temperature. While Dauta et al. suggests that +35°C is the optimal temperature for maximum growth rate, the selected upper temperature boundary reflected the maximum allowable cabin temperature (+27°C). The ETC was set to +30°C to ensure the algal medium would reach the desired temperature (Anderson et al. 2018).

**Table 11. Temperature range tested in this experiment, reflecting the operational conditions of a spacecraft thermal and cabin system.**

| Variable | Condition Tested | Temperature Setting (°C) |
|---|---|---|
| Temperature | Low | +10 |
| | High | +27 |

The resulting measured dependent variables were culture density, growth rate, oxygen production, photosynthetic yield, and culture pH. Constants for this set of experiments were the lighting spectrum and intensity, shaking speed, and gas composition within the chamber (assumed standard atmospheric composition and pressure for Boulder, CO).

#### 4.3.2.2 Test Procedure

Experiments were conducted in triplicate, with each plate containing three separate wells running simultaneously, resulting in 9 separate occurrences of each experimental condition found in Table 11. Each run was executed for at least 7 days to capture the exponential growth phase, enabling calculation of growth rate associated with environmental conditions (Table 11). When measurement probes were necessary for the experiment, they were sanitized with a 70% Ethanol bath, rinsed with Ultrapure water, and wiped with a Kimwipe before insertion through the plate's membrane to create a seal around the probe.

#### 4.3.2.3 Measurements

##### 4.3.2.3.1 Continuous Measurements

The microcontroller system was the interface between the sensor sweep in the 12-well-plates and a laptop operating on Windows 7. The pH and temperature measurements were recorded into Microsoft Excel using PLX-DAQ software. All measurements were taken at a sampling rate of 0.2Hz. The pH was measured with an Atlas-

Scientific probe (pH kit, Atlas-Scientific). An Arduino shield (Tentacle Shield, Whitebox Labs) was used to connect the pH sensor to the Arduino. The pH sensor was calibrated before each experimental run using an Atlas buffer kit. Dissolved oxygen was measured with a robust fiber optic, non-consuming dissolved oxygen sensor and compensation temperature probe (Robust Oxygen Probe, PyroScience). Dissolved oxygen measurements were recorded with PyroScience software associated with the probe. The oxygen probes were calibrated before each experimental run using probe-specified air and 3% sodium sulfite solution in DI water.

Before inoculating with algal culture, each of the temperature conditions (+10°C and +27°C) were executed with plain Bristol's media for 3 days to establish an operational baseline for dissolved oxygen and pH. Continuous temperatures for the wells were also recorded using the previously mentioned K-type thermocouple and amplifier.

#### 4.3.2.3.2 Non-continuous Measurements

Initial and final values (at the beginning and end of an experimental run, respectively) of optical density, cell counts, and photosynthetic yield measurements were recorded.

Cell counts and optical density were performed on the same samples taken from the 12-well-plate. A 200µl sample was extracted from the well and placed in the well of a clean 96-well-plate. Optical density measurements were taken first by a photometer (Thermo Scientific Multiskan FC, Fisher Scientific). Readings were taken at 450nm and 690nm to measure absorbance associated with chlorophyll-a and chlorophyll-b, respectively. Before taking each reading, the photometer shook the plate rapidly for 5 seconds to prevent settling of cells. Triplicate measurements were taken of each sample at each wavelength for an average reading. After using the sample to measure optical density, aliquots of the 96 well-plate were diluted with methylene blue as a cell stain. Viability measurements were conducted with methylene blue (0.3% in 30% ethanol, Carolina Biological) after adding the solution to the sample and waiting >2 minutes for the dye to stain dead cells. A hemocytometer (Reichert Bright-Line, Hausser Scientific) was used to conduct these viability measurements through cell counts under a microscope. The five areas in Figure 27 were used to perform cell counts. First a total cell count was taken, including all blue and green cells, then a second count was conducted in the same grid, only considering blue-stained cells (dead). The viability ratio was later

calculated with these counts and used as a reference. An average of the conducted counts multiplied by the dilution ratio and $10^4$cell/ml calculated the culture's cells per milliliter.

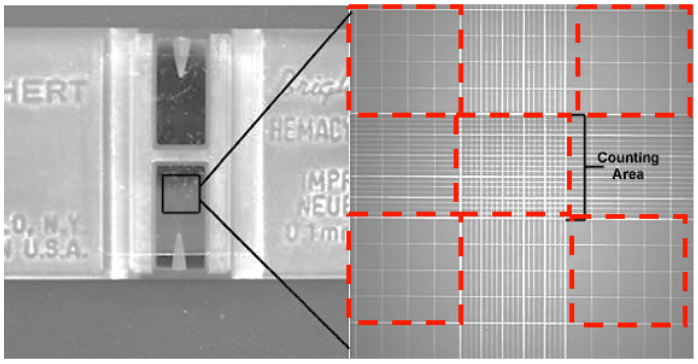


**Figure 27. Hemocytometer grid used for cell counts, 5 areas in dashed outline used to calculate average cell density (image credit, Colorado State University).**

Pulse-amplitude modulated (PAM) chlorophyll fluorometry measurements were conducted (Junior-PAM, Walz) as a non-invasive method of measuring the relative health of the culture. PAM investigates the efficiency (measured on a scale of 0-1, 1 being the highest efficiency) of the cell's photosystem II and requires a dark acclimation period of at least 15 minutes before measuring (measurement instructions, Bebout Lab, NASA Ames). Cultures were allowed to come to a steady state temperature (appropriate for the experimental conditions) and the plates were contained in dark boxes for at least 15 minutes before measuring. The plates were then set on a holding frame to ensure consistent measurement locations. The PAM probe was held to the bottom of the culturing plate, and the saturation pulse was initiated. Prior to each experiment, the PAM was calibrated by measuring a well containing 3.5ml of clean Bristol's media.

Respiration and photosynthetic rate measurements were conducted by allowing plates to come to a steady state temperature (appropriate for the experimental conditions), turning off plate illumination for at least an hour, and then back on for another hour before restarting thermal cycling (if appropriate). The measured drop and increase in dissolved oxygen reflect the reduction in photosynthesis with dark acclimation and then recovery with illumination.

### 4.4 Data Processing

The continuous data were saved in 24-hr increments and the Bristol's dissolved oxygen baseline for that experimental case was subtracted from the collected data. The two-hour block used for measuring respiration and photosynthetic rate were removed for separate processing, and the remaining data was averaged for daily changes in pH and dissolved oxygen for steady state temperatures. The averaged "excess" $O_2$, or $O_2$ with the Bristol's baseline removed, was used to calculate the $O_2$ generation rate per day with the following equation.

$$\Delta O_2 * k_{stir} = [O_2] \tag{4}$$

where $\Delta O_2$ is the excess oxygen present in the media, $gL^{-1}$, $k_{stir}$ is the mass transfer coefficient for a 12-well-plate on an orbital shaker table, $d^{-1}$, and $[O_2]$ is the production rate, $gL^{-1}d^{-1}$ (Ojo et al. 2015; Royce and Thornhill 1991; Boributh et al. 2011). Since the initial culture density was constant for all cases, the calculated $O_2$ rates for each experimental case could be compared.

Culture pH was recorded through the duration of all experiments and is reported here. Optical density, cell viability, and photosynthetic yield measurements were averaged within their triplicate measurements as appropriate (only averaging within like wells -4B with 4B etc., due to the variation of probe footprints in each well, see Figure 33 and the associated standard deviation was also calculated. Cell counts were used to calculate the growth rate over the course of the experiment using the starting and ending cell count values.

Two-way ANOVA with replication was conducted, as appropriate, to determine statistical significance of the compiled results ($p<0.05$, for all tests); Student's t-test (2-tailed, assumed equal variance, independent). The tested null hypothesis was, "The treatment (temperature, axenic status, nutrient addition, etc.) has no statistically significant effect on the measured parameter," for all tested cases. All calculations and compiling of data were conducted with Microsoft Excel 2016 with the Data Analysis package. All presented data points represent averaged triplicate results, and the associated standard deviation as the error bars, unless specifically noted.

### 4.5 Results

Comparison of the metabolic results of the hot and cold experiments is outlined with statistical comparisons, as presented in section 4.4.

#### 4.5.1.1 Oxygen Generation Rate and Culture pH

A comparison of the oxygen production rates from the hot (+27°C) and cold (+10°C) temperature cases is presented in Figure 28. A Student's independent t-test was conducted with the averaged values of each treatment (two tailed, assumed equal variance, $p<0.05$). The subsequent p-value for the t-test indicated that each treatment resulted in significantly different oxygen generation rates, with the hot constant temperature case having the higher production rate (approximately 400% greater at its maximum production rate). The difference between the two generation rates corroborates the suggestion that cooler media temperatures may suppress photosynthesis (Maxwell et al. 1994).

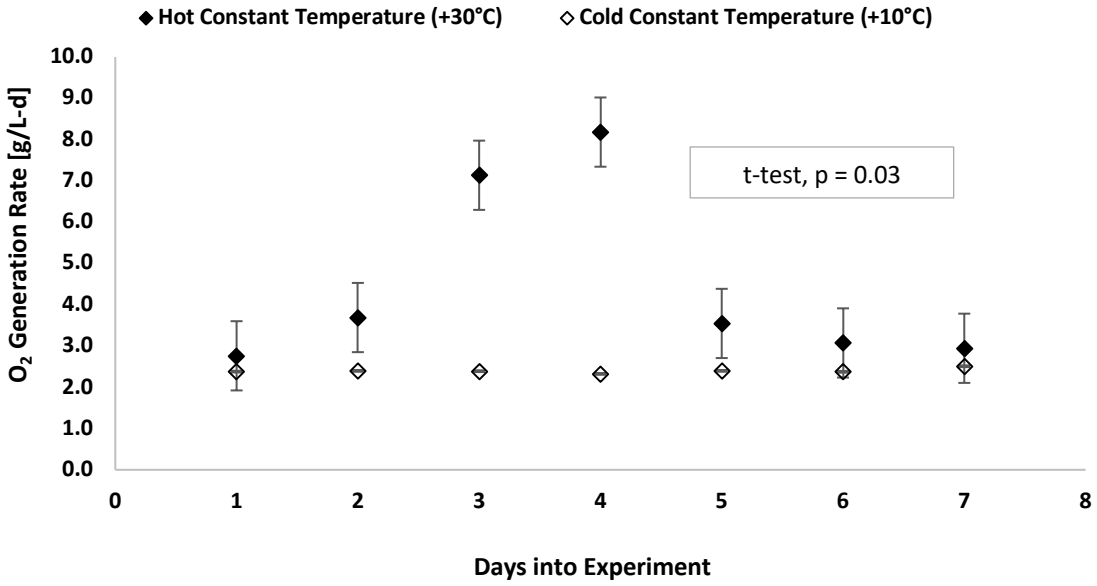


**Figure 28. Dissolved oxygen generation rate for the hot and cold tests across experiment duration. Resulting p-values indicate that there was a statistical difference between the two cases. Each data point is the average of experimental runs at each timestamp. Error bars are the standard deviation resulting from multiple runs. (t-Test, t = 2.48, df = 12, p<0.05)**

The measured pH for each hot and cold case was plotted over the course of the experiment (Figure 29). A Student's independent t-test was conducted with the averaged values of each treatment (two tailed, assumed equal variance, $p<0.05$). The results rejected the null hypothesis with a p-value of 0.002, indicating that there was a significant difference in the pH values between the hot and cold cases. The increase in media pH over time for the hot case suggests that the culture was growing rapidly enough to change the surrounding medium through $CO_2$

uptake and the release of hydroxyl ions (Gerardi 2018). While the cold case may have been growing as well, it was not at a rate measurable through changes in pH.

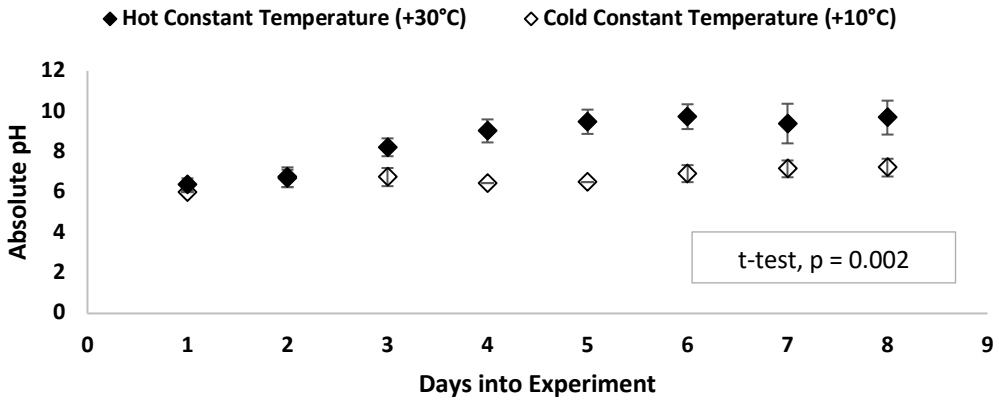


**Figure 29. Measured pH values for hot and cold temperature cases over the course of the experimental runs. The pH values have not been adjusted to account for Bristol's media. Each data point is the average of experimental runs at each timestamp. Error bars are the standard deviation resulting from multiple experiment runs. (t-Test, df = 14, p<0.05)**

#### 4.5.1.2 Photosynthetic Yield

Photosynthetic yield measurements are another proxy for assessing culture health, since efficiently photosynthesizing cultures record photosynthetic yield values closer to one on the 0-1 scale. A two-way ANOVA with replication test was conducted, comparing the two cases but also investigating if time in experiment influenced photosynthetic yield rates ($df = 8$, $p < 0.05$). The null hypothesis was rejected when comparing each case (cold and hot) and between days, indicating that the treatment and time in experiment did have an effect on the resulting photosynthetic yield. The overall (interaction) null hypothesis was rejected, as the hot case had higher photosynthetic yields than the cold case. This continues to support the idea that cooler culturing temperatures reduce overall algal metabolic function. A decrease in photosynthetic yield of the hot case after day 5 suggests that an input to the culture (either available $CO_2$ or nutrients) became limiting and reduced the overall photosynthetic yield of the culture.

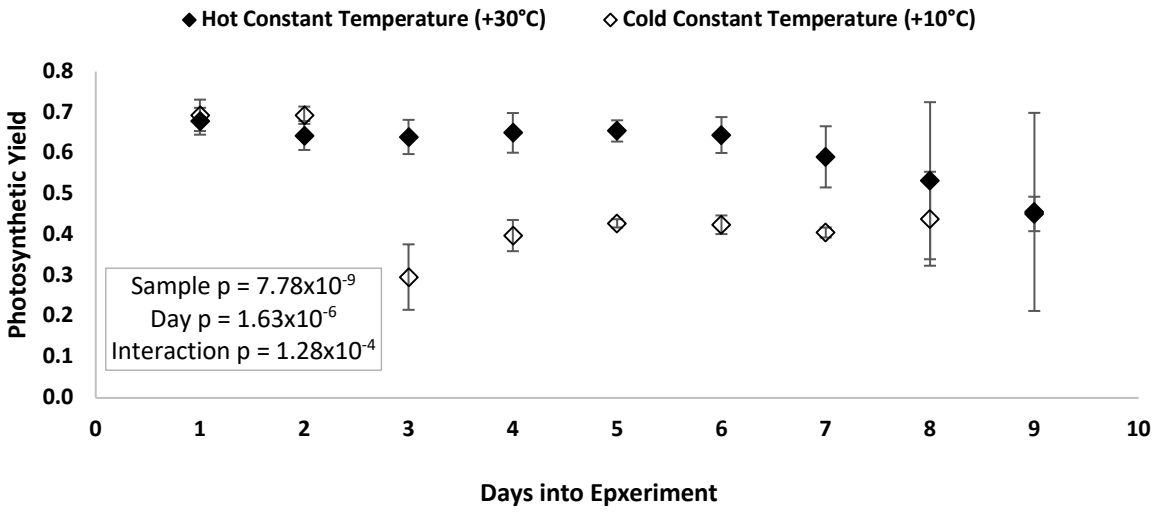


**Figure 30. Photosynthetic yield measurement over the course of the experiment. Each data point is the average of experimental runs at each timestamp. Error bars are the standard deviation resulting from multiple experiment runs. (Two-way ANOVA with replication, df = 8, p<0.05)**

#### 4.5.1.3 Cell and Optical Density Growth Rate

Both cell count and optical density measurements were conducted to determine culture growth rates, which were later used to assess the magnitude of environmental effects. Figure 31 has both the growth rates calculated optical density and cell counts, overlaid to show relative measure agreement. Rates were calculated from beginning and end values, since these cases did not include intermediate sampling. Unfortunately, this also prevented the specific growth rate from being determined, since the onset of exponential growth needs to be identified. Student's independent t-test was executed to compare the tested cases ($df = 2$, $p < 0.05$). While Figure 31 suggests that there is a significant difference in the growth rates between the two temperature cases, the low degrees of freedom cannot support the potential significance. Therefore, the null hypothesis could not be rejected when comparing the optical density and cell count-based growth rates between the two cases.(Hot Constant Temperature OD: $M = 1.6\text{x}10^{-2}$ Abs/d, $SD = 7.5\text{x}10^{-3}$, Cell Count: $M = 7.9\text{x}10^{5}$ cell/mL-d, $SD = 4.0\text{x}10^{5}$); (Cold Constant Temperature OD: $M = 5.4\text{x}10^{-3}$ Abs/d, $SD = 2.8\text{x}10^{-3}$, Cell Count: $M = 9.5\text{x}10^{3}$ cell/mL-d, $SD = 3.9\text{x}10^{4}$).

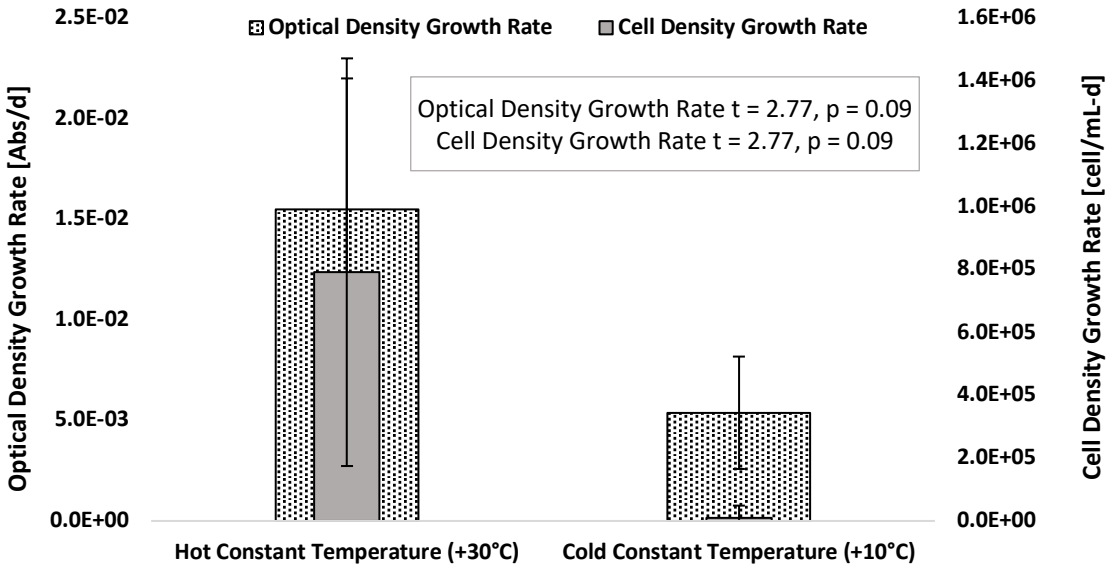


**Figure 31. Comparison of measured optical density and resulting cell counts, converted into rates by calculating daily change for contamination-status cases. Each bar is the average of experimental runs. Error bars are the standard deviation resulting from multiple runs. (t-test, df = 2, $p < 0.05$)**

### 4.6 Discussion

The results of these experiments uphold the suggestions from both Dauta et al. and Maxwell et al., that the metabolic functioning of an algal culture has a positive correlation to the media temperature, when all other inputs are held constant. These outcomes were expected after reviewing literature, including the Blackman relationship (Figure 4) which illustrates the positive correlation.

Algae was cultured at the highest allowable cabin temperature, in an effort to optimize air revitalization capabilities through increased oxygen production and cell growth rates. The oxygen generation rate profile did suggest an increase in production when compared to the cold case. However, over the duration of the experiment, the production rate began to decrease. It is hypothesized that the culture entered its stationary and death period as one of the inputs became limiting; most likely either availability of $CO_2$ or nutrients. This same progression is captured in the pH and photosynthetic yield measurements, as well. Acceleration of the growth profile (Figure 31) indicates that the environmental temperature did have an effect on the culture, since this acceleration is not captured in the cold temperature case.

Culturing algae in the "cold" (+10°C) conditions represented using the algal medium as the working fluid in the thermal control loop but optimizing the system for heat transfer. Oxygen and biomass production indicated that the culture was viable through the duration of the experiment, however, these production rates were significantly less than the temperature case optimal for air revitalization. None of the measured characteristics illustrated easily identifiable transitions into the different growth stages. This suggests that either the culture had an extended lag phase, longer than the duration of the experiment, or the transitions were imperceptible with the conducted measurements.

### 4.7 Conclusion

This set of experiments had two main purposes, to replicate results found in literature establishing the relationship between steady-state media temperature and culture metabolic rates over a range of temperatures that span those of a spacecraft cooling loop, and to characterize the viability of a culture when operated in temperature regimes optimizing either heat transfer or air revitalization.

Temperature control of the algal media was accomplished by placing the culture plates inside of an environmental chamber set to a constant temperature through the duration of the experiment. Dissolved oxygen, pH, and temperature were constantly monitored, while photosynthetic yield measurements were taken daily. Cell counts and optical density measurement were taken at the beginning and end of every experiment, and daily when appropriate.

Results suggest that the culture is viable (producing $O_2$ and biomass) at both the hot and cold temperature cases. However, the cold case resulted in significantly lower oxygen generation rates, measured pH, and photosynthetic yield when compared to the hot case. While the cell production rate also reflected this result, the number of experiment replications could not provide statistical significance. Still, cell production rates referenced in literature under similar environmental conditions corroborates the resulting trends (Dauta et al. 1990). This suggests that if algal medium were used for the working fluid for a spacecraft thermal loop, the culture may not be able to simultaneously address the air revitalization requirements of the spacecraft within the allotted volumetric or mass constraints. The reduction in culture oxygen production rates while operating in the cold environment may necessitate the need to include additional volumes of culture to meet the cabin atmospheric needs. However, the

acceleration of the growth profile recorded in the hot case suggests that modifying culturing temperatures, without changing other inputs, may allow for active control of the culture's production capabilities.

### 4.8 Resulting Publications

No publications are planned at this time

# Chapter 5 Characterization of *Chlorella* Metabolism in a Dynamic Temperature Environment

## 5.1 Introduction

Algal cell physiology has the capability to address multiple human metabolic requirements through photosynthesis and biomass production. Furthermore, selecting certain cultivation approaches could increase the multifunctionality of a culture. For example, growing cells in a liquid medium instead of on a solid substrate could allow the culture to be utilized as heat transfer medium, much like the water-cooling loops found in the ISS cabin today (The Boeing Company, n.d.).

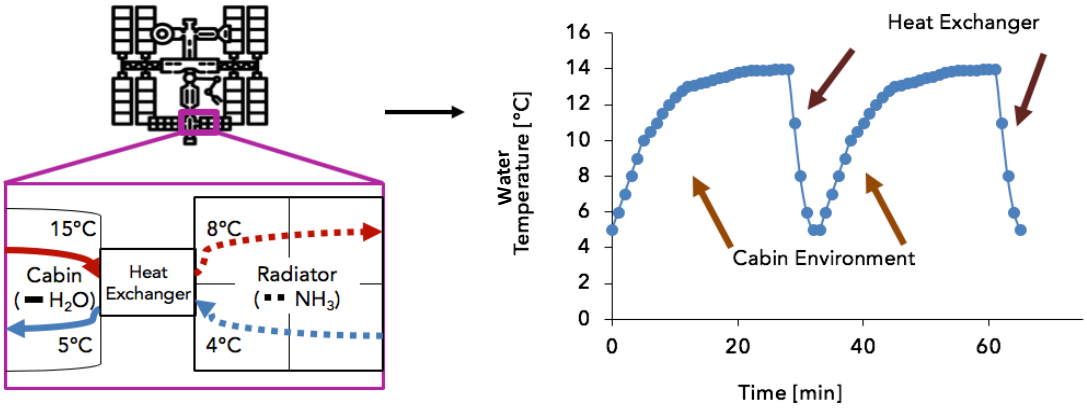


**Figure 32. Temperature cycle experienced by cabin coolant water as it passes through cabin-heat exchanger thermal system. Low Temperature Loop (LTL) temperature regime shown here.**

Theoretically, with the appropriate hardware, one algal photobioreactor system could provide simultaneous air revitalization ($CO_2/O_2$ turnover) and thermal control to a spacecraft cabin (Cohen, Flynn, and Matossian 2013). There are various designs for this type of merged system, including using liquid algal culture as the working fluid in the already established thermal loops, such as the LTL and MTL (Figure 32). Consequently, directly introducing algal cells into the established ISS liquid-cooling loop design and integrating a gas-liquid contactor membrane for $CO_2/O_2$ exchange with the cabin environment is the simplest design for combining air revitalization and active thermal control. Using a flight-proven structure as a baseline defines operational boundaries and environmental considerations. However, this directly exposes the algal culture to the rapid thermal shown cycles in Figure 32.

Therefore, cultures also used for air revitalization, need to have the thermal cycling effects on $CO_2$ to $O_2$ turnover characterized.

### 5.2 Background

Outdoor mass cultivation of algal biomass for use in the biodiesel industry has indicated that algae is capable of withstanding some magnitude of thermal cycling, as diurnal cycles can cause temperature fluctuations in raceway ponds (Ugwu, Aoyagi, and Uchiyama 2007). Algal photosynthesis has a positive correlation with temperature, typically doubling in photosynthetic rate for every 10°C increase, as explained by its $Q_{10}$ temperature coefficient (Davidson 1991). This occurs until a species-dependent maximum temperature is reached, at which any temperature increase past this threshold results in a rapid decrease in photosynthetic rate, as shown in Figure 17. Ras mentions that outdoor reactors can experience fluctuations between 10°C and 45°C, extending most commercially cultured species beyond their optimal growth range (Ras, Steyer, and Bernard 2013). Fortunately, algae are adaptable and withstand these diurnal oscillations occurring at above optimal conditions. Previous experiments have indicated that cultures can be successfully grown in colder temperatures, as well. For example, *Chlorella vulgaris*, the species used in this body of research, was successfully cultured at 5°C by Maxwell et. al. This cooler temperature increased the doubling time from 8 to 48 hours, however, the culture also increased its photosynthetic capacity due to alterations in carbon fixation, allowing cell sustainment (Maxwell et al. 1994).

While the acceptable ISS cabin temperature range is 18.3-26.7°C, the LTL and MTL operate between 4°C-14°C and 16°C-18°C, respectively (Figure 32) (Valenzano et al. 2003). *Chlorella's* optimal photosynthetic temperature range has been reported as 26°C-36°C, suggesting that the maximum photosynthetic rate does not occur if used for thermal control of the spacecraft cabin. Ras also comments that diurnal temperature oscillations in outdoor cultures are rapid enough that generational adaptation is difficult, suggesting that adaptation to the thermal loop's 10-30-minute period fluctuations may be challenging for the culture (Ras, Steyer, and Bernard 2013).

Previous experiments associating environmental temperature with photosynthetic rates in algal cultures were executed in steady-state conditions (Maxwell et al. 1994; Öquist 1983; Aloice W. Mayo 1997; Serra-Maia et al. 2016). While cultivation in fluctuating outdoor temperatures was acknowledged, no previous research has characterized algal metabolic rates in these dynamic environments. Therefore, culture photosynthetic response to

temperature swings was measured. The resulting $CO_2/O_2$ turnover rate could help size the photobioreactor needed for removal of respired $CO_2$ from the cabin atmosphere.

## 5.3 Materials and Methods

### 5.3.1 Culture and Associated Hardware

*Chlorella vulgaris* was used in the steady-state and dynamic temperature environment experiments. Known axenic cultures were kept in sterile 50ml Falcon tubes on orbital shaker table under a fluorescent plant bulb (F40PL/AQ/ECO 49893 Bulb, GE Lighting) with the lids cracked for gas exchange with the lab environment. The continuous culture described in Chapter 4.3.1 was used for the non-axenic experiments.

Each experiment used the same well-plate loading protocol as described in Chapter 4.3.1. Axenic test plates were loaded while in a biosafety flow hood, while the non-axenic plates were loaded in a clean lab area. Temperature control was executed through a Peltier cooler system. Figure 33 depicts the developed system using a Peltier cooler (Peltier Thermo-Electric Cooler, Adafruit) in conjunction with a resistive heating pad (Heating Pad, Sparkfun) and controlled by a microcontroller (Mega, Arduino) through a K-type thermocouple (K-type braided, Omega and K-type Thermocouple Amplifier, AdaFruit). The microcontroller turned on the cooler or the heater, depending on the thermocouple reading and pre-determined thresholds. The footprint of the Peltier cooler was smaller than the overall footprint of the 12-plate, hence filling only 3 specific wells. This ensured direct contact between the bottom of the well-plate and cooler. Placing the whole Peltier system on an orbital shaker table (7744-01000, Bellco Orbital Shaker) set to 100 RPM kept the culture lifted in the media, reduced media temperature gradients within the well, and promoted gas exchange between the environment and media.

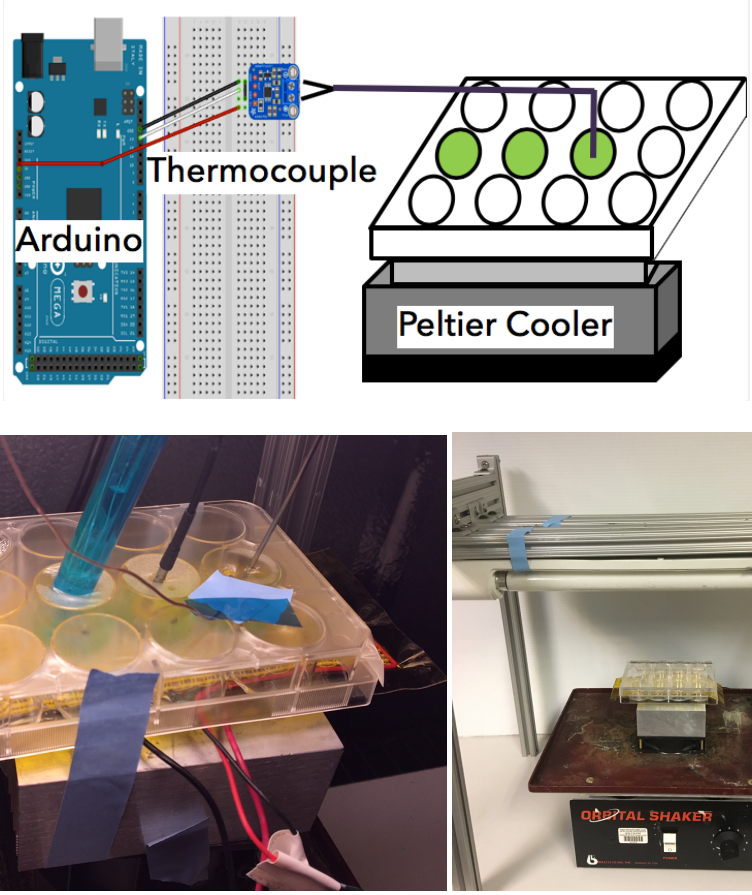


**Figure 33. Peltier cooler system controlled by an Arduino Mega through a K-type thermocouple (top). First three middle wells contain culture and fit within cooler/heater footprint. pH, dissolved oxygen, temperature probes inserted through membrane (bottom left). Peltier system on top of orbital shaker table under illumination stand (bottom right).**

The same overhead fluorescent light bank and irradiance protocol used in Chapter 4 was also used for the dynamic temperature experiments.

The lighting, shaker table, and Peltier cooler unit were placed in the BioServe Environmental Thermal Control (ETC) unit. The ETC was set to a constant temperature, depending on the requirements of the experiment.

### 5.3.2 Experiment Design

#### 5.3.2.1 Variables and Conditions

The independent variable for this series of experiments was the medium temperature, whether it be constant through the test duration or following a pre-determined cycle (Table 12). Cycle temperature and period were formulated to capture temperatures from the LTL, MTL, and cabin environment, exposing the culture to

temperature swings of +9°C to +27°C. The swings reflected temperatures experienced in the spacecraft cabin and surrounding equipment (Anderson et al. 2018). Lower temperature bounds were dictated by the cooling capabilities of the Peltier cooler and the ETC. The cycling condition inflection points were fixed just beyond the constant settings to ensure that the Peltier cooling system profile included each constant setting. The cycle period was determined by ISS Internal Active Thermal Control System (IATCS) flow rate data, system water volume, and cabin inlet and outlet water temperatures, Figure 34 depicts the resulting temperature profile. The "nominal" condition was used as the control for comparison against the cycled condition, reflecting the time-averaged temperature of the cycle plate but also found within the cabin temperature range (Table 12).

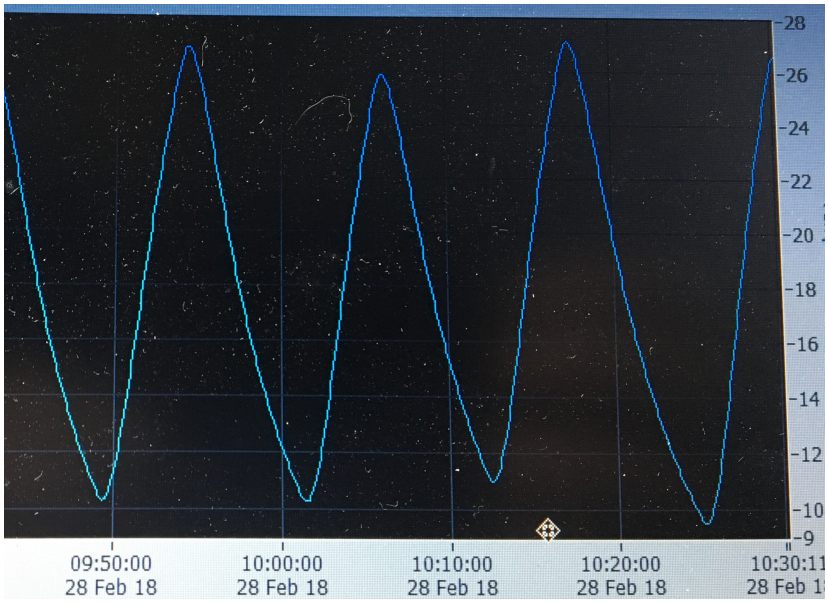


**Figure 34. Temperature plot produced by FireSting probe recording cycled well temperature (°C).**

**Table 12. Temperature range tested in this experiment, reflecting the operational conditions of a spacecraft thermal and cabin system.**

| Variable | Condition Tested | Temperature Setting (°C) | Duration |
|---|---|---|---|
| Temperature | Nominal | +19 | Constant |
| | Cycle | +9 to +27 | 14-minute Cycle Period |

The resulting measured dependent variables were culture density, growth rate, oxygen production, photosynthetic yield, and culture pH. Constants for this set of experiments were the lighting spectrum and intensity, shaking speed, and gas composition within the chamber (assumed standard atmospheric composition and pressure for Boulder, CO). Possible confounding variables were addressed in additional experiments, outlined in Table 13.

**Table 13. Possible confounding variables were identified and included in the experimental matrix. Each condition was tested but will not be extensively discussed.**

| | | Contamination Status | |
|---|---|---|---|
| | | Axenic | Contaminated |
| Daily Nutrient Addition | Yes | Cannot Execute | Completed |
| | No | Completed | Completed |

Bacterial contamination of the culture was suggested as a confounding variable. Aerobic bacteria have a symbiotic relationship with autotrophic algae, potentially benefitting and protecting algae from environmental stressors (Cole and Cole1 1982; Pisman, Galayda, and Loginova 2005). However, the goal of this research was to characterize the metabolic reaction of *Chlorella* to the environmental temperature. Experiments using both axenic cultures, where a culture is bacteria-free and single species, and non-axenic samples were conducted. An axenic culture was established by physically isolating cells of *C. vulgaris*, treating them with an antibacterial cocktail (Table 14), streaking on LB+/LB- solid substrate, and visually inspecting the substrate for any remaining heterotrophic growth (cocktail recipe, Dr. Craig Everroad, NASA Ames). The confirmed axenic stock was tested every month for heterotrophic growth using subsequent LB+/LB- solid substrate plates. Axenic status test of 12-well-plates was also conducted post-experiment to ensure cleanliness had been maintained for the duration of the experiment (Figure 35). Experiments with contaminated cultures (those containing bacteria and other heterotrophic organisms) were inoculated from a mother culture continuously maintained in a cling wrap-covered beaker on the benchtop of the Bioastronautics Laboratory.

**Table 14. Cocktail recipe, provided by Dr. Craig Everroad of NASA Ames, used to produce axenic strains of *Chlorella vulgaris*.**

| Ingredient | Amount (mg/ml) |
|---|---|
| Ampicillin | 10 |
| Kanamycin | 2.5 |
| Tetracycline | 2.5 |

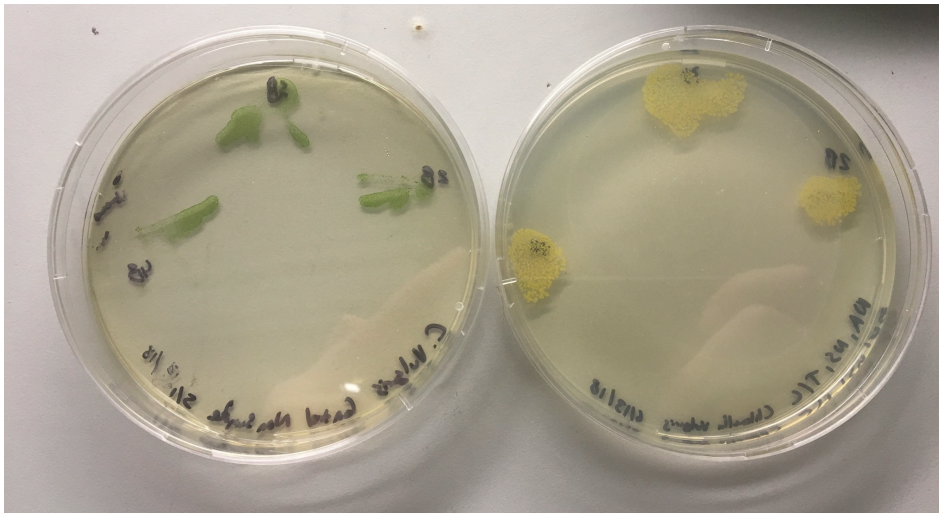

**Figure 35. Post-experiment comparison on LB+ agar of axenic temperature-cycled culture (left) and contaminated temperature-cycled culture (right). Yellow colonies on the right plate indicate heterotroph dominance, while the left plate shows vibrant *Chlorella***

Preliminary experiments also suggested a difference in wells with perforated membranes, due to the insertion of measurement probes (dissolved oxygen, pH, and temperature), versus those with unperforated membranes, indicating that the culture could be gas limited during the experiment. Experiments with all probes inserted into wells and runs with no perforations of the membrane were conducted. It was also hypothesized that back-filling the sampled wells with Bristol's media up to the 3.5ml volume after daily sampling for cell counts and optical density measurements could increase the culture viability (labeled as "nutrient-added"). However, those experiments labeled as "axenic" did not receive daily nutrients, due to the difficulty of keeping the well-plate system clean (Table 13).

While all conditions outlined in both tables (Table 12, Table 13) and descriptions were tested, this chapter focuses on the results of the axenic versus contaminated thermally cycled and nominal temperatures and contaminated thermally cycled plates with and without nutrient addition. These tests were used to suggest results of the cycled experiments and as possible operational thresholds for the culture.

#### 5.3.2.2 Test Procedure

Experiments were conducted in triplicate, with each plate containing three separate wells running simultaneously, resulting in 9 separate occurrences of each experimental condition found in Table 12. Each run was executed for at least 7 days to capture the exponential growth phase, enabling calculation of growth rate associated

with environmental conditions (Table 12). When measurement probes were necessary for the experiment, they were sanitized with a 70% Ethanol bath, rinsed with Ultrapure water, and wiped with a Kimwipe before insertion through the plate's membrane to create a seal around the probe. Probes inserted into axenic culture were allowed to air dry in the biosafety flow hood, instead of drying with a Kimwipe, before perforating membrane.

#### 5.3.2.3 Measurements

##### 5.3.2.3.1 Continuous Measurements

Continuous measurements of pH, dissolved oxygen, and temperature were conducted in the same manner as described in Chapter 4.3.2.3.1.

Before inoculating with algal culture, each of the temperature conditions (+19°C and cycled temperature) were executed with plain Bristol's media for 3 days to establish an operational baseline for dissolved oxygen and pH. Continuous temperatures for the wells were also recorded using the previously mentioned K-type thermocouple and amplifier during the Bristol's-only characterization.

##### 5.3.2.3.2 Non-continuous Measurements

Depending on the experimental conditions, the optical density, cell counts, and photosynthetic yield measurements were taken daily. Protocols for each of these measurements, including respiration and photosynthetic rate can be found in Chapter 4.3.2.3.2.

### 5.4 Data Processing

The continuous data were saved in 24-hr increments and the Bristol's dissolved oxygen baseline for that experimental case was subtracted from the collected data. The two-hour block used for measuring respiration and photosynthetic rate were removed for separate processing, and the remaining data was averaged for daily changes in pH and dissolved oxygen for steady state temperatures. The cycled cases used environmental temperature to select ranges for averaging dissolved oxygen. The "low temperature" case averaged all dissolved oxygen values associated with temperatures below 13°C and "high temperature" used values associated with temperatures above 23°C. These thresholds were determine based off of average operating temperature of the LTL and the cabin environment. The averaged "excess" $O_2$, or $O_2$ with the Bristol's baseline removed, was used to calculate the $O_2$

generation rate per day with Eq 4. Since the initial culture density was constant for all cases, the calculated $O_2$ rates for each experimental case could be compared.

Culture pH was recorded through the duration of all experiments, and is reported here, however it was not used in the final statistical significance matrix, since it does not have a direct influence on the proposed ECLS system. Optical density, cell viability, and photosynthetic yield measurements were averaged within their triplicate measurements as appropriate (only averaging within like wells -4B with 4B etc., due to the variation of probe footprints in each well, see Figure 33 and the associated standard deviation was also calculated. Cell counts were used to calculate the growth rate over the course of the experiment using the starting and ending cell count values.

Two-way ANOVA with replication was conducted, as appropriate, to determine statistical significance of the compiled results ($p<0.05$, for all tests); Student's t-test (2-tailed, assumed equal variance, independent). The tested null hypothesis was, "The treatment (temperature, axenic status, nutrient addition, etc.) has no statistically significant effect on the measured parameter," for all tested cases. All calculations and compiling of data were conducted with Microsoft Excel 2016 with the Data Analysis package. All presented data points represent averaged triplicate results, and the associated standard deviation as the error bars, unless specifically noted.

### 5.5 Results

The results of the nominal and cycled temperature cases, those that most closely align with desired spacecraft utilization, are reported. The axenic case investigated if system cleanliness impacts oxygen production rates, and daily nutrient addition suggests necessary frequency of interaction with the system. Each metabolic measurement is outlined within the experimental groups with statistical comparisons.

#### 5.5.1 Contamination Status

Table 15 outlines the four major test cases for investigating the importance of contamination status on oxygen production and viability of the culture while being subjected to space flight-like temperature swings. "Membrane penetration" means that probes were inserted into the well-plates through the gas permeable membrane, but the seal created by the membrane around the probes protected the axenic status of the culture. No sampling or nutrient addition occurred during the axenic tests, since that introduced foreign matter and risked the cleanliness of the well. The "nominal" temperature case, or +19 °C, was used as the control temperature.

**Table 15. Conditions testing importance of contamination status on thermally cycled culture metabolism**

| Temperature | Contamination Status | Membrane Penetration | Nutrient Addition |
|---|---|---|---|
| Nominal (Control) | Axenic | Yes | No |
| | Non-Axenic (contaminated) | | |
| Cycling | Axenic | | |
| | Non-Axenic (contaminated) | | |

#### 5.5.1.1 Oxygen Generation Rate and Culture pH

After removing the measured dissolved $O_2$ baseline for Bristol's media, the $O_2$ generation rate was calculated and plotted against the day measured in the experiment (Figure 36). Over the course of the experiment, $O_2$ generation rate sustains or even increases from the initial value. A two-way ANOVA with replication test was conducted, comparing the two cases but also investigating if time in experiment influenced production rates. Each case used two different experimental runs, each lasting seven days. The axenic control and contaminated control dissolved $O_2$ were not measured due to the lack of additional FireSting probes. The interaction p-value, $p = 0.06$ (df = 7), is greater than the confidence p-value ($p < 0.05$), indicating that the null hypothesis cannot be rejected. This suggests that contamination status does not affect the oxygen generation rate. However, the test did result in a rejection of the null hypothesis between days ($p = 0.03 < 0.05$). This suggests that oxygen generation rates vary from day to day. This may be an important consideration to include when designing a spacecraft photobioreactor if a constant $O_2$ production rate is required. Also, an "establishment" period might be necessary if the culture is being used for air revitalization. The trends of both cases in Figure 36 implies that oxygen generation rate increases over time. The p-value for sample is greater than the confidence p-value, indicating that there is no apparent difference between the experimental runs sampled for the test. These results indicate that a non-axenic culture may be able to meet the crew metabolic needs, which could reduce crew time to clean hardware and tend the culture.

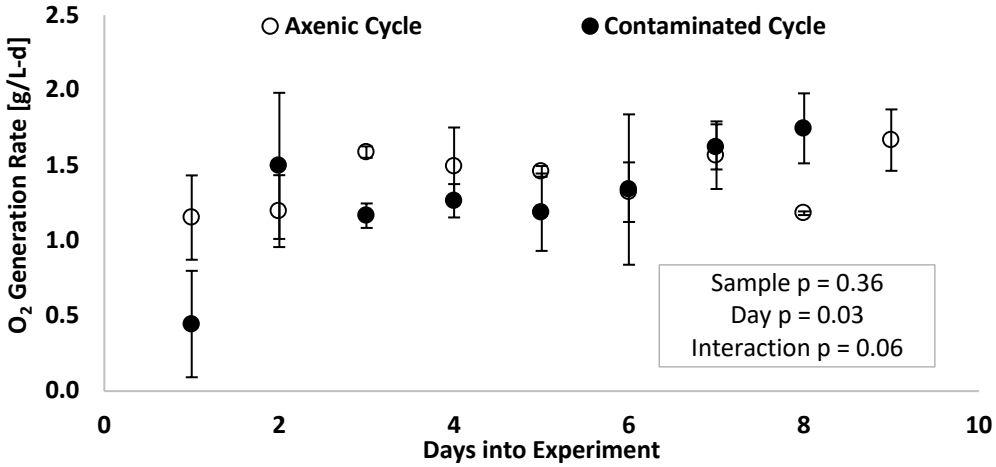


**Figure 36. Excess dissolved oxygen was measured in the well-plates after the Bristol's baseline was removed, this was then used to calculate the $O_2$ generation rate using Eq 5. Axenic control values were not measured due to probe availability. Resulting p-values indicate that there was no statistical difference overall between the two cases, and within each group, but a difference from day to day. Each data point is the average of experimental runs at each timestamp. Error bars are the standard deviation resulting from multiple runs. (Two-way ANOVA with replication, df = 7, $p<0.05$)**

The resulting pH plotted through experiment duration (presented in Figure 37) was not modified to show variation from the Bristol's baseline. Here, the axenic and contaminated control cases are included, since additional pH probes were available. All conditions experienced at least a two-day lag period before starting their exponential growth phase, as evident by sustained increases in daily pH. Both axenic cases overlapped values until day four, at which the two deviated (control reporting higher pH values than cycled) but continued to trend upward together. The increase in culture pH across all cases indicates utilization of the media's carbonic acid source during the production of biomass. These pH measurements can be used as a general proxy to assess overall health of the culture.

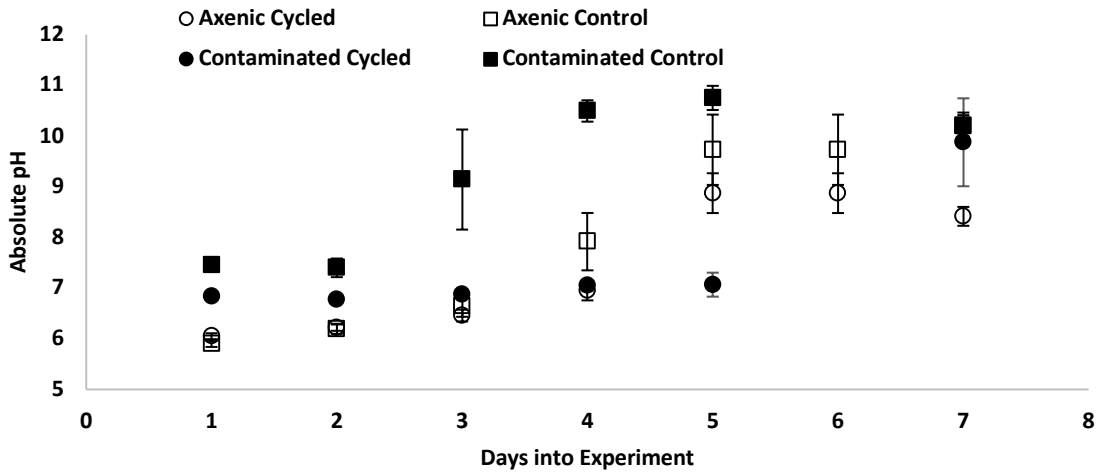


**Figure 37. Plate pH for temperature cycled and control plates for both contaminated and axenic cultures. pH values have not been adjusted to account for Bristol's media. Each data point is the average of experimental runs at each timestamp. Error bars are the standard deviation resulting from multiple runs.**

#### 5.5.1.2 Photosynthetic Yield

Both cycle cases experience a decline in yield values between day 1 and 2, this can be attributed to acclimation of the new cycling temperature environment (Ras, Steyer, and Bernard 2013). A two-way ANOVA with replication test was conducted, comparing the four cases but also investigating if time in experiment influenced photosynthetic yield rates ($df = 8$, $p < 0.05$). Each case used three different experimental runs, each lasting nine days. Each combination of cases was investigated (axenic vs contaminated, control vs cycle). The comparative list of p-values is shown in Table 16, the comprehensive list is in Appendix C. The two significant interaction cases were between axenic cycle vs contaminated control and axenic control vs contaminated control. The figure suggests that both axenic cases had higher photosynthetic yields than the contaminated control case. This is important to note, but the information should be used in conjunction with $O_2$ generation rate and cell growth rate data to understand if the yield numbers reflect effects to the overall culture. The day p-values (variation in yield measurements between days) for the cycled cases showed significance, which is reflected in the figure by the drop in photosynthetic yield in the first few days and explained as the culture acclimating to the new temperature environment. No significant interaction p-values were reported between the axenic control vs contaminated cycle and axenic cycle vs

contaminated cycle, which continues to support the idea that cleanliness of culture is not a significant factor in overall culture health in the cycled case.

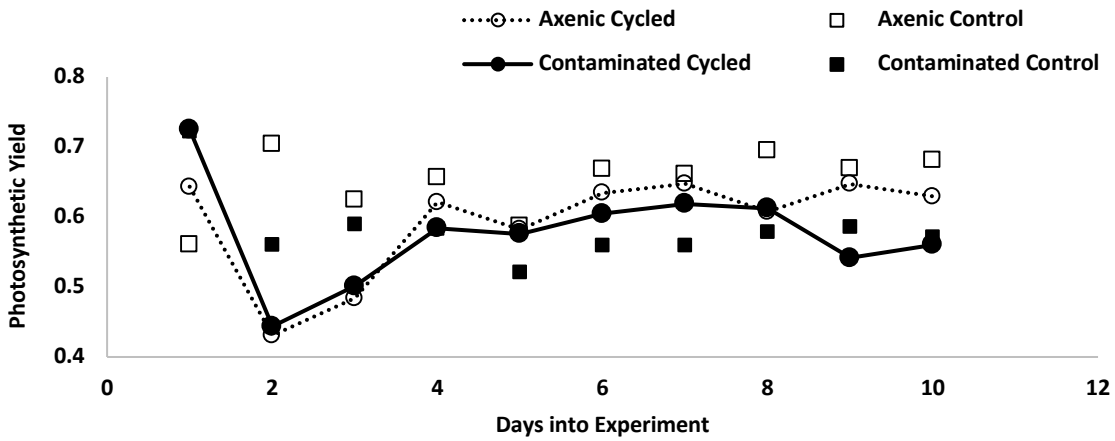


**Figure 38. Photosynthetic yield measurement over the course of the experiment. Data lines were included for the cycled cases to exemplify the decrease in yield associated with the acclimation period. Each data point is the average of experimental runs at each timestamp. (error bars omitted for clarity of trends but included in Appendix C). (Two-way ANOVA with replication, df = 8, $p<0.05$)**

**Table 16. Resulting p-values between all combinations of treatments comparing the photosynthetic yield values of the contamination status experiments. Those p-values that are significant have been listed**

| Treatment Combination | p-values |
|---|---|
| Axenic Cycle vs Contaminated Cycle | Day p = 0.003 |
| Axenic Cycle vs Axenic Control | No significant p-values calculated |
| Contaminated Cycle vs Contaminated Control | Day p = 0.003 |
| Axenic Cycle vs Contaminated Control | Day p = 0.001<br>Interaction p = 0.02 |
| Axenic Control vs Contaminated Control | Sample p = 0.01<br>Interaction p = 0.02 |
| Axenic Control vs Contaminated Cycle | No significant p-values calculated |

#### 5.5.1.3 Cell and Optical Density Growth Rate

Figure 39 has both the growth rates calculated optical density and cell counts, overlaid to show relative measure agreement. Rates were calculated from beginning and end values, since these cases did not include intermediate sampling. Unfortunately, this also prevented the specific growth rate from being determined, since the onset of exponential growth needs to be identified. Six combinations of comparisons (like for the photosynthetic yield) were conducted for the growth rates. Student's independent t-test was executed for all combinations, each

treatment used two to six experimental runs depending on the condition (df = 4, $p < 0.05$). Table 17 presents a comparison of the calculated significant p-values (all associated p-values are presented in Appendix C). The only significant difference recorded was between the axenic (OD: M = $1.3 \times 10^{-1}$ Abs/d, SD = $1.7 \times 10^{-2}$, Cell Count: M = $2.6 \times 10^{6}$ cell/mL-d, SD = $2.9 \times 10^{5}$) and contaminated control (OD: M = $3.7 \times 10^{-2}$ Abs/d, SD = $1.9 \times 10^{-2}$, Cell Count: M = $5.5 \times 10^{5}$ cell/mL-d, SD = $2.9 \times 10^{5}$), with the axenic treatment resulting in higher growth rates (approximately 245% greater). This suggests that the contamination may have been suppressing cell growth over the course of the experiment, or the sample rate was higher than the culture growth rate. However, the cycled treatments are of interest, for their potential use in the spacecraft. The cycled cases did not indicate statistical differences across the other treatments, which continues to support the suggestion that contamination status may not be a significant factor in culture operation.

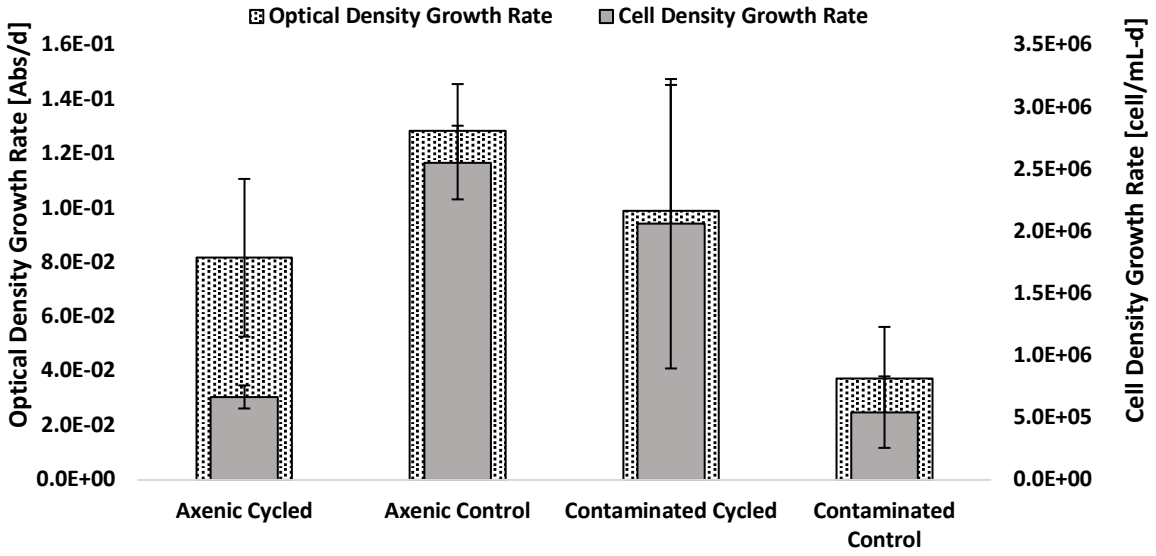


**Figure 39. Comparison of measured optical density and resulting cell counts, converted into rates by calculating daily change for contamination-status cases. Each bar is the average of experimental runs. Error bars are the standard deviation resulting from multiple runs. (Student's t-test, df = 4, $p < 0.05$)**

**Table 17. Resulting interaction p-values between all combinations of treatments comparing the growth rates of the contamination status experiments. Those p-values that are significant have been listed**

| Treatment Combination | p-values |
|---|---|
| Axenic Cycle vs Contaminated Cycle | No significant p-values calculated |
| Axenic Cycle vs Axenic Control | Cell Density Growth Rate p = 0.01 |
| Contaminated Cycle vs Contaminated Control | No significant p-values calculated |
| Axenic Cycle vs Contaminated Control | No significant p-values calculated |
| Axenic Control vs Contaminated Control | Optical Density Growth Rate p = 0.004<br>Cell Density Growth Rate p = 0.006 |
| Axenic Control vs Contaminated Cycle | No significant p-values calculated |

### 5.5.2 Nutrient Addition

Limiting inputs (irradiance, temperature, carbon dioxide) have the potential to overshadow extraneous environmental effects (nutrients, contamination status, etc.) on a culture. Therefore, an additional set of experiments were conducted that included daily sampling of the culture wells for cell counts and optical density measurements. Results also suggest how often a bioreactor needs to be tended or media added. Well volume was kept consistent by back-filling them with Bristol's media (i.e. the 200μL removed for a cell count was replaced with 200μL media). This daily introduction of media meant that axenic versions of this experiment could not be conducted, since bacteria-free culturing could not be ensured. The membrane was still penetrated by the dissolved $O_2$, pH, and temperature probes (Table 18). Nutrient addition experiments were conducted using the same hardware set-up and duration as the axenic trials.

**Table 18. Conditions testing importance of daily nutrient addition on thermally cycled culture metabolism**

| Temperature | Contamination Status | Membrane Penetration | Nutrient Addition |
|---|---|---|---|
| Nominal (Control) | Non-Axenic (contaminated) | Yes | No |
| | | | Yes |
| Cycling | Non-Axenic (contaminated) | Yes | No |
| | | | Yes |

#### 5.5.2.1 Oxygen Generation Rate and Culture pH

Oxygen generation rate for the nutrient addition experiments were calculated in the same manner as the contamination status experiments. Two-way ANOVA with replication was conducted to compare the cycled cases for the nutrient-added and non-added treatments. There were two runs per treatment, each lasting at least seven

days. The resulting p-values indicated that there was a significant difference between the nutrient-added and non-added treatments at each day but not a significant difference between each day for each treatment (sample p = $7.7x10^{-7}$, day p = 0.39, interaction p = 0.33, df = 5). This indicated that a second statistical test should be conducted to examine the difference between the two treatments. A Student's independent t-test was conducted with the averaged values of each treatment (two tailed, assumed equal variance, $p<0.05$). The subsequent p-value for the t-test indicated that each treatment resulted in significantly different oxygen generation rates, with the non-added case having the higher rate (approximately 224% greater). This may be confirmed by reviewing Figure 40. The difference between the two generation rates suggests that adding daily nutrients may be suppressing oxygen production. Extrapolating these results into spaceflight design, minimal nutrients and crew interaction may be beneficial to the oxygen generation rate of the photobioreactor, therefore, saving crew time and launched mass.

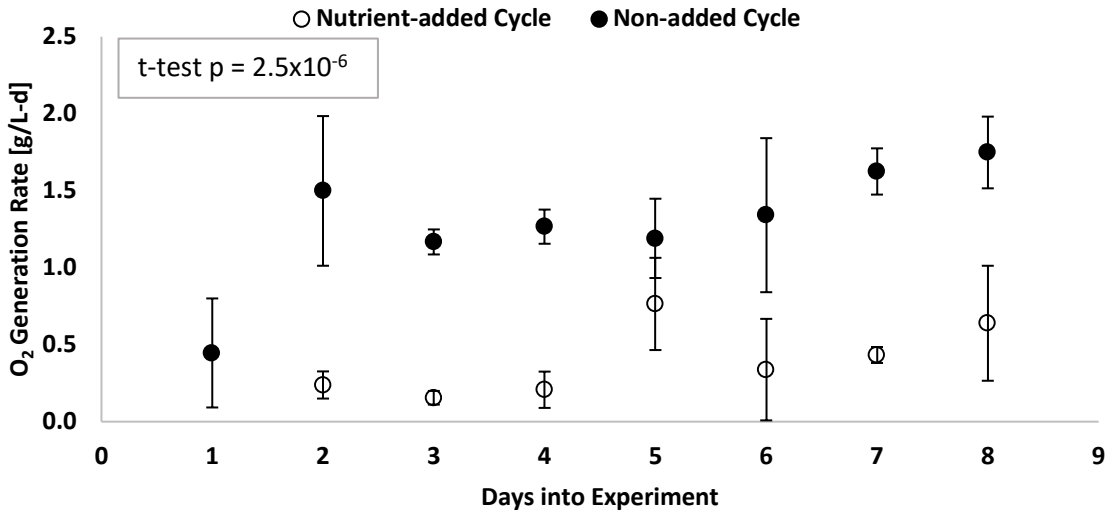


**Figure 40. $O_2$ generation rate was calculated using Eq 5 and the measured excess $O_2$ in each well per day. Each data point is the average of experimental runs at each timestamp. Error bars are the standard deviation resulting from multiple runs. (Two-way ANOVA with replication, df = 5, $p<0.05$)**

Absolute pH for the nutrient-added/non-added set of experiments followed the same trends as observed in the axenic set, where all cases experienced at least a two-day lag time before showing an increase in pH. The two non-added cases showed the greatest increase in pH over the entire experiment duration, indicating some amount of pH control resulting in the daily media addition. It is hypothesized that this is due to the inherently acidic pH of the Bristol's media (pH of about 5.6). Data from day 6 for the non-added cases was not saved to the data set.

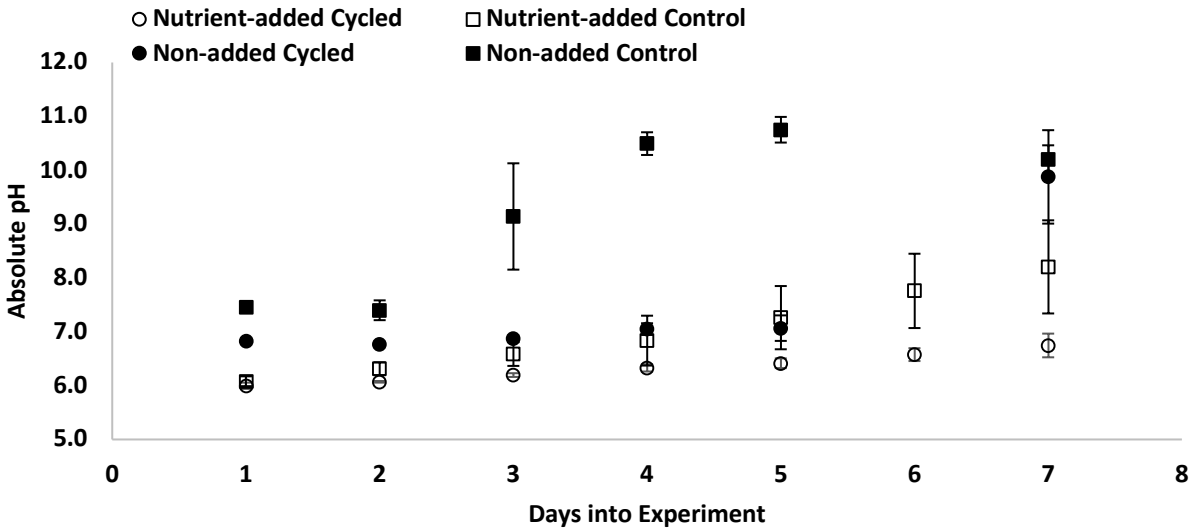


**Figure 41. Absolute pH measurements are plotted over the duration of the experiment for the four cases. Each data point is the average of experimental runs at each timestamp. Error bars are the standard deviation resulting from multiple runs.**

#### 5.5.2.2 Photosynthetic Yield

Similar trends were found in the nutrient-added/non-added cases as those found in the axenic tests. A slight drop in photosynthetic yield was observed in over the first two days, by all cases with system recovery over the course of the experiment (Figure 40). No statistically significant p-values were reported with the photosynthetic yield measurements when a two-way ANOVA was used to compare the six combinations previously introduced ($df = 7$, $p < 0.05$), all p-values reported in Table 20. Each data point represents two to six experiment runs, depending on the case, and each run was seven days long. The figure shows the greatest variation in measurements during the acclimation period, but a reduction in variance over the course of the experiment. The trends in the figure suggest that daily nutrient addition does not significantly influence the photosynthetic yield of this *Chlorella* culture. This supports the previously proposed idea that cultures may not need daily nutrient additions to be viable.

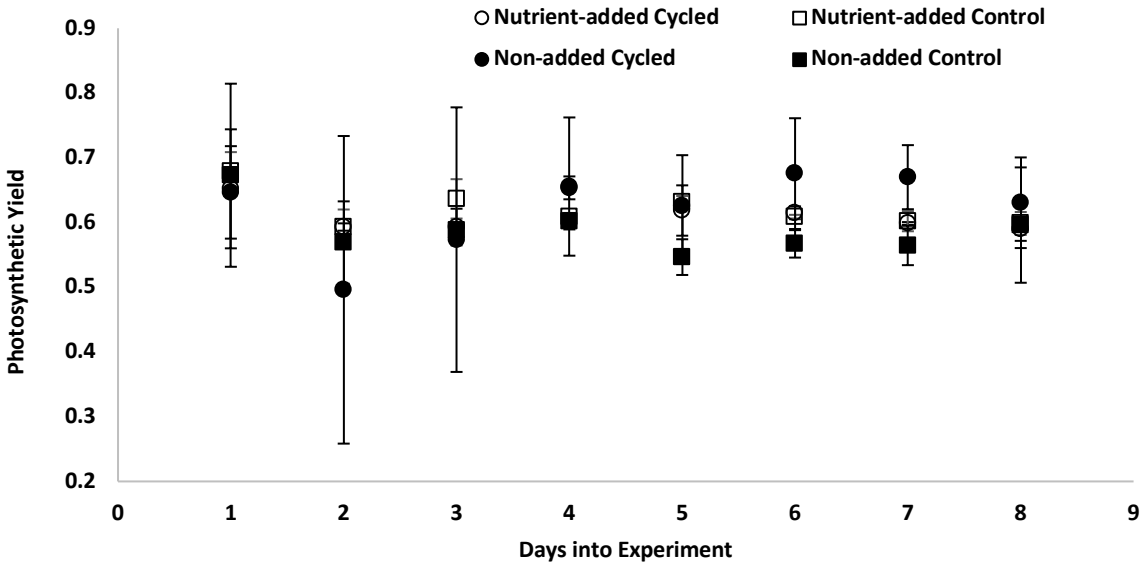


**Figure 42. Measured photosynthetic yield for each plate over the course of the experiment run examining importance of nutrient additions. Each data point is the average of experimental runs at each timestamp. Error bars are the standard deviation resulting from multiple runs. (Two-way ANOVA with replication, df = 7, $p<0.05$)**

#### 5.5.2.3 Cell and Optical Density Growth Rates

Growth rates based on optical density measurements and cell counts were calculated in the same manner as in Section 4.5.1.3 and overlain to look for correlations between the two measurements (Figure 43). Student's independent t-test was executed for all combinations, (independent, 2-tail, equal variance, $p<0.05$), each treatment used two to six experimental runs depending on the condition. Table 19 presents a comparison of the calculated significant p-values (all associated p-values are presented in Appendix C). The comparison between the two cycled cases (nutrient-added vs non-added) rejects the null hypothesis with confidence (Cycled Nutrient-added OD: M = $6.4\text{x}10^{-3}$ Abs/d, SD = $2.9\text{x}10^{-3}$, Cell Count: M = $6.5\text{x}10^{4}$ cell/mL-d, SD = $2.9\text{x}10^{4}$) (Cycled Non-added OD: M = $9.9\text{x}10^{-2}$ Abs/d, SD = $4.6\text{x}10^{-2}$, Cell Count: M = $2.1\text{x}10^{6}$ cell/mL-d, SD = $1.2\text{x}10^{6}$), with the non-added cycle case resulting in the higher growth rate (approximately 3000% greater). The other three cases that show rejection of the null hypothesis in the optical density growth rate (nutrient-added cycle vs control, nutrient-added cycle vs non-added control, and nutrient-added control vs non-added cycle) do not show rejection through the cell density growth rate. The error bars for the measurements in Figure 43 do not overlap in some of these cases. However, since the t-test did not

reject the null hypothesis, the difference between these means cannot be declared statistically significant. Therefore, as a conservative measure, these three cases should not reject the null hypothesis. The rejection of the null hypothesis by the comparison of the cycle case suggests that nutrient addition does have an effect on culture growth rate. Figure 43 suggests that nutrients are not necessary for higher cell growth rates in a temperature cycled system, when compared to the nutrient-added case.

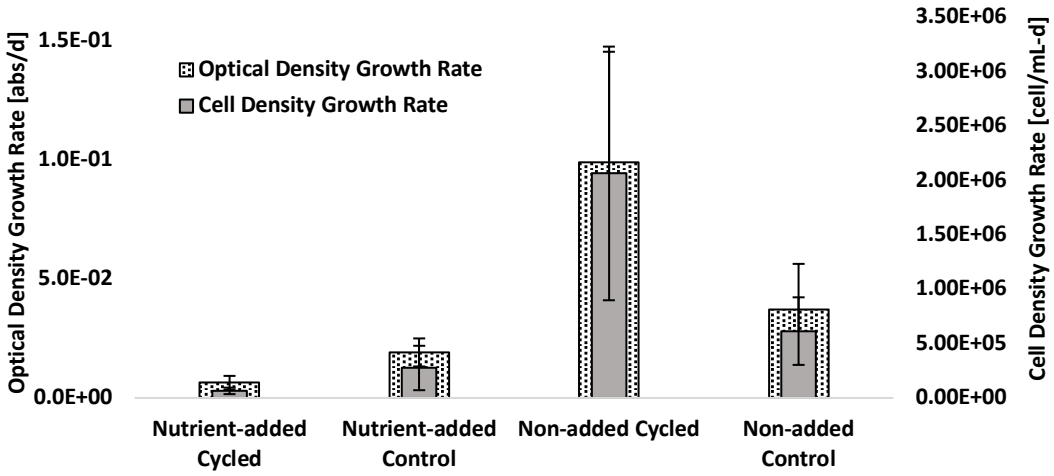


**Figure 43. Comparison of measured optical density and resulting cell counts, converted into rates by calculating daily change for nutrient-addition cases. Each bar is the average of experimental runs. Error bars are the standard deviation resulting from multiple runs. (Student's t-test, df = 4, p<0.05)**

**Table 19. Resulting p-values between all combinations of treatments comparing the photosynthetic yield values of the nutrient addition cases. Statistically significant p-values are presented, all p-values are presented in Appendix C.**

| Treatment Combination | p-values |
|---|---|
| Nutrient-added Cycle vs Non-added Cycle | Optical Density Growth Rate p = 0.01<br>Cell Density Growth Rate p = 0.01 |
| Nutrient-added Cycle vs Nutrient-added Control | Optical Density Growth Rate p = 0.01 |
| Non-added Cycle vs Non-added Control | No significant p-values calculated |
| Nutrient-Added Cycle vs Non-added Control | Optical Density Growth Rate p = 0.02<br>Cell Density Growth Rate p = 0.01 |
| Nutrient-added Control vs Non-added Control | No significant p-values calculated |
| Nutrient-added Control vs Non-added Cycle | Optical Density Growth Rate p = 0.01<br>Cell Density Growth Rate p = 0.02 |

### 5.6 Discussion

Table 20 lays out the combination of test cases and the resulting measured culture parameters. Statistical significance was tested between the cases, with either Student's t-test or two-way ANOVA with replication, as appropriate. All tested combinations used a 95% confidence interval ($p < 0.05$), and the null hypothesis that the treatment would not result in any significant differences of the measured variable between the two test cases. The results of the experiments determining the importance of contamination status on metabolic functioning suggests that contamination status (axenic vs. non-axenic) when subjecting *C. vulgaris* to rapid temperature swings does not have a measurable effect on oxygen production. These results were not surprising as Pisman et al. has shown that inclusion of heterotrophic bacteria may provide a symbiotic relationship with algae (Pisman, Galayda, and Loginova 2005). However, this finding should be further studied, since surveyed literature implies the contrary (Mouget et al. 1995). The axenic control case performed better than the contaminated control in all measured parameters. While this is interesting to note, since the steady-state control temperature is not the intended operational environment for the culture, it should not have substantial bearing on the cleanliness decision. It does suggest that an axenic status may be beneficial to the metabolic efficiency of the culture in steady-state temperatures.

The results in Table 20, investigating the importance of daily additional nutrients, suggests that for statistically significant oxygen production, daily tending is not necessary. Three possible reasons suggest this outcome. First the nutrients supplied may have a suppressing effect on the algal culture, as it may put it in a constant "acclimation" period as the culture tries to adapt to the new nutrients. Second, the sampling rate of the nutrient-added well might have been equal to or greater than the growth rate of the culture, keeping the culture at a steady-state. Lastly, daily addition of nutrients may have caused a system imbalance. Meaning, the culture may have experienced a limiting input due to the provision of nutrients. This overall result was unexpected, since the initial assumption was that an extra provision of nutrients would be needed to ensure maximum metabolic efficiency for the culture. Additional experimentation is required to isolate the reasoning behind the results.

**Table 20. Combinations of tested conditions are compared to determine environments significantly affecting *Chlorella* metabolic parameters. The interaction p-values (if ANOVA was used) and general p-values (t-tests) for all associated outcomes are listed a 95% confidence level was used as the test statistic. In the rejected cases, those characteristics with the "higher" value out of the pair were mentioned before the p-value. The null hypothesis null hypothesis that the treatment would not result in any significant differences of the measured variable between the two test cases**

| | **$O_2$ Production Rate [g/L-d]** | **Cell Growth Rate [cell/mL-d]** | **Optical Density Growth Rate [Abs/d]** | **Photosynthetic Yield** |
|---|---|---|---|---|
| Axenic Cycle vs Contaminated Cycle | Accept, p = 0.59 | Accept, p = 0.19 | Accept, p = 0.67 | Accept, p = 0.88 |
| Axenic Cycle Vs Axenic Control | N/A | Reject, Axenic Control, p =0 .01 | Accept, p =0.19 | Accept, p =0.09 |
| Axenic Cycle vs Contaminated Control | N/A | Accept, p = 0.38 | Accept, p = 0.08 | Reject, Axenic Cycled, p = 0.02 |
| Axenic Control vs Contaminated Control | N/A | Reject, Axenic Control, p = 0.01 | Reject, Axenic Control, p = 0.01 | Reject, Axenic Control, p = 0.02 |
| Axenic Control vs Contaminated Cycle | N/A | Accept, 0 = 0.61 | Accept, p = 0.45 | Accept, p = 0.2 |

| | **$O_2$ Production Rate [g/L-d]** | **Cell Growth Rate [cell/mL-d]** | **Optical Density Growth Rate [Abs/d]** | **Photosynthetic Yield** |
|---|---|---|---|---|
| Nutrient-added Cycle vs Non-added Cycle | Reject, Non-added Cycle, p =2.5E-6 | Reject, Non-added Cycle, p = 0.01 | Reject, Non-added Cycle, p = 0.01 | Accept, p = 0.94 |
| Nutrient-added Cycle vs Nutrient-added Control | N/A | Accept, p =0.09 | Reject, Nutrient-added Control, p = 0.01 | Accept, p = 0.64 |
| Nutrient-added Cycle vs Non-added Control | N/A | Reject, Non-added Control p = 0.01 | Reject, Non-added Control, p = 0.02 | Accept, p = 0.92 |
| Nutrient-added Control vs Non-added Cycle | N/A | Reject, Non-added Cycle, p = 0.02 | Reject, Non-added Cycle, p = 0.01 | Accept, p = 0.86 |
| Nutrient-added Control vs Non-added Control | N/A | Accept, p = 0.14 | Accept, p = 0.12 | Accept, p = 0.93 |
| Non-added Cycle vs Non-added Control | N/A | Accept, p = 0.09 | Accept, p = 0.05 | Accept, p = 0.88 |

### 5.7 Conclusion

This set of experiments set out to understand the effect on metabolic functioning, if any, of *Chlorella v* to temperature swings reflective of cabin thermal loop conditions. While testing the effect of this environmental

parameter, additional extraneous parameters were also studied. Contamination and nutrient addition suggested the importance of equipment cleanliness and maintenance rate, respectively, on the metabolic functioning as well. These experiments provided initial insight into biological trends, however, due to the small sample sizes, additional experiments are recommended to establish statistical significance.

Culturing *C. vulgaris* in 12-well-plates in an environmental chamber allowed for simultaneous replicates in a controlled environment. Both simultaneously tested plates were placed on-top of Peltier cooler systems for experiment consistency, but only one was turned on and cycled to replicate temperature swings of the spacecraft thermal environment. Dissolve oxygen, pH, and temperature were constantly monitored, while photosynthetic yield measurements were taken daily. Cell counts and optical density measurement were taken at the beginning and end of every experiment, and daily when appropriate.

Results indicate that contamination status nor nutrient addition affects the $O_2$ generation rate of a thermally cycled culture. This suggests that sterilization of hardware is not necessary for a culture to operate in a potentially stressful condition, and that cultures may not require constant nutrient supplementation. Both of these findings are beneficial in a spacecraft environment, since it could be time consuming and expensive to maintain axenic cultures, and additional nutrients may not need to be included in the launched mass.

### 5.8 Resulting Publications

Journal Paper

Matula, E. E., Nabity, J. A. (20XX). "Influence of a Dynamic Temperature Environment Reflecting a Spacecraft Thermal Control Loop on *Chlorella vulgaris'* Metabolic Processes", Acta Astronautica [In-Prep, Working Title]

Conference Paper (Non-refereed) and Associating Presentation

Matula, E. E., Monje, O., and Nabity, J. A. (2016). "Influence of Transient Heat Transfer on Metabolic Functions of Chlorella vulgaris used for Environmental Control and Life Support Systems of Long Duration Spaceflight," AIAA Space, Long Beach, CA, 2016.

Conference Poster

Matula, E. E. (2018) Influence of Contamination Status on Algal Culture Growth Rates and Photosynthetic Efficiency, 48th International Conference on Environmental Systems, Albuquerque, NM.

Matula, E. E. (2018) Algal Metabolic Response to Transient Thermal Environments for Long Duration Human Spaceflight Life Support, CIRES Rendezvous, Boulder, CO.

Matula, E. E. (2017) Algal Metabolic Response to Transient Thermal Environments for Long Duration Human Spaceflight Life Support, McMurdo Long Term Ecological Research Planning Meeting, Boulder, CO.

# Chapter 6 Effects of Rapid Changes in Dissolved Media $CO_2$ Concentrations on Carbon Fixation in *Chlorella*

## 6.1 Introduction

As a metabolizing organism, algae passively respond to their dynamic environment to survive, changing photosynthetic rates to match the trends of temperature, irradiance, or $CO_2$ concentration (Kimball 2011). Final design integration of a photobioreactor is unknown, but the $CO_2$ gas provision could be approached in two separate manners. First, the culture could be supplied a constant-concentration gas stream either concentrated from the CDRA or a gas-bottle-buffered stream directly from the cabin. Using this method, the metabolic reaction of the culture could be easily predicted, and models of oxygen production ranges could be established. However, this could require additional equipment to store the buffering gas or to accumulate excess $CO_2$ produced by the crew during times of excess respiration (e. g. exercise). For the second method, the culture could be exposed to the current $CO_2$ concentration in the cabin, allowing the medium to absorb the readily available cabin $CO_2$. This approach may not need as much support equipment, as the input concentration is not actively controlled. However, the response time and effect of cultures to sudden (<24hr) increases in provided $CO_2$ is unknown. Typically, these variations in cabin $CO_2$ reflect changes in crew activity, such as sleep and exercise. Ensuring that a sustained algal culture could absorb enough $CO_2$ or produce enough $O_2$ within a required timeframe is a consideration when designing a photobioreactor appropriate for dynamic environments.

## 6.2 Background

It is apparent that algal cultures are able to adapt to a changing environment, both from a diurnal standpoint for illumination (day/night) but also as the atmosphere experiences steady increase in $CO_2$ concentration (Doyle 2019). However, these changes are occurring over the course of days and years versus hours and minutes, as experienced in a spacecraft. Figure 44 presents the respiratory diurnal cycle for one crew member over two days, and total $CO_2$ respired and $O_2$ consumed per activity is tabulated in Table 21. The pressurized volume of the ISS is 916$m^3$, with a tee-shirt environment of 14.7psi and approximately 20°C. Using the Ideal Gas Law, and a standard crew of 6 people, the accumulated cabin $CO_2$ concentration could rise by 0.42 % $d^{-1}$, if left untreated. This is

potentially a problem, as NASA's allowable limit for $CO_2$ concentration on the ISS is 0.51% to limit the onset of hypercapnia (Anderson et al. 2018). While the overall trend of cabin $CO_2$ concentration is increasing, it is obvious that there are "drops" in provided concentration and $O_2$ consumption.

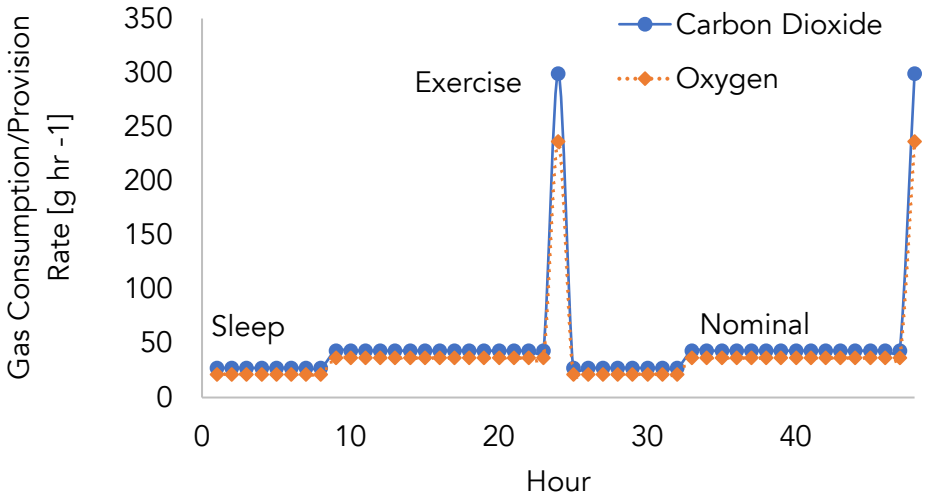


**Figure 44. Oxygen consumption and carbon dioxide production for one crewmember over 48hrs**

**Table 21. Consumed $O_2$ and produced $CO_2$ for one crew member per day during various activities**

| Activity | $O_2$ [g/CM-d] | $CO_2$ [g/CM-d] |
|---|---|---|
| Sleep | 172.8 | 218.4 |
| Nominal Work | 511.2 | 648 |
| Exercise | 236.4 | 299.1 |
| Total | 920.4 | 1165.5 |

Previous experiments have investigated the effects of various supplied $CO_2$ concentrations, showing that biomass production and $O_2$ production have a positive correlation with $CO_2$ concentrations, if there are no other limiting inputs (irradiance, nutrients, etc.). Chinnasamy (2009) shows that biomass exponentially increases from 40ug $mL^{-1}$ at 2% $CO_2$ to 225mg $mL^{-1}$ at 6% $CO_2$, but biomass production drops 200% at concentrations higher than 6%, owing it to other limiting inputs (Chinnasamy et al. 2009). One experiment, conducted by Li et al., 2013, tested the capabilities of *Chlorella* as a $CO_2$ regulator in a multi-media bioregenerative life support system. Results indicated that the culture was able to control system concentration, fed by silkworm and intermittent human respiration, between 0.03-0.2% $CO_2$. This flat-plate photobioreactor was installed in conjunction with a lettuce compartment, but an improvement in $CO_2$ stability was shown over the lettuce-only system (M. Li et al. 2013).

This non-exhaustive literature survey did not return any information about experiments describing *Chlorella*'s response to human respiration. Therefore, the following experiment focused on variations in $CO_2/O_2$ turnover rates for *C. vulgaris* when subjected to sudden but sustained changes in $CO_2$ concentration, and any indications of stress (i.e. carotenoid development or culture crash) was noted. It was hypothesized that algae respond to the increase in $CO_2$ with an increase in $O_2$ production and cell growth rate and reverses these trends if instead subjected to a sudden decrease in supplied $CO_2$. Calculated photosynthetic quotient ratios and carbon uptake measurements informs future photobioreactor performance and provide data for the calculation of the culture volume needed to accommodate changes in crew respiration.

## 6.3 Materials and Methods

### 6.3.1 Culture and Associated Hardware

The same culture stock used the experiment described in Chapter 4 was also used here, however, only the non-axenic, bench-top culture was used in all experiments. Free gas exchange with the lab environment during culture establishment more closely replicated direct exposure to ISS contamination conditions.

Figure 45 depicts the experiment's P&ID as a basic overview of the system. Three acrylic bioreactors with external illumination were placed into an environmental chamber, with external gas supply being supplied through a port in the chamber wall. Media chemical composition probes and gas exhaust were fed through the same port, while daily culture measurements were accessed through the door. The environmental chamber was held at a constant 19°C, replicating the nominal temperature condition of the thermal experiment found in Chapter 4.

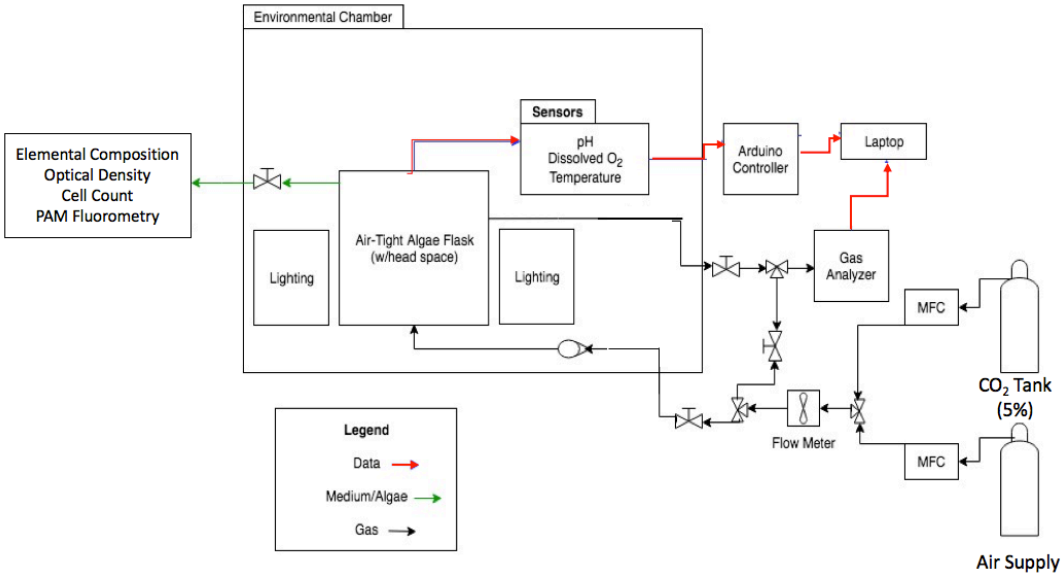


**Figure 45. The P&ID layout for the gas concentration test. Experiments were executed in the CIRES building at the University of Colorado.**

Commercially available gas-tight acrylic containers (5-in dia, 9in-height) were used as the bioreactors (2.2L, SALT). Acrylic containers were selected because they were easily modifiable, optically transparent, easy to sanitize, and non-reactive with the culture. Figure 46 shows how the tops of the containers were modified to allow for dissolved oxygen (DO kit, Atlas-Scientific), pH (pH kit, Atlas-Scientific), temperature (DS18B20, Dallas Temperature Control) probes, and a gas sample port (3/4" quick disconnect bulkhead, John Guest). A bulk-head fitting (3/4" quick disconnect bulkhead, John Guest) was inserted through a drilled hole in the bottom of the container to supply the sparge gas (Figure 47) and ¾" polyvinyl hard-wall tubing was throughout the system. All of the components selected were made of material that was non-reactive with the culture and media. The fluorescent bulbs described in Chapter 4 were used again (F40PL/AQ/ECO 49893 Bulb, GE Lighting), running along the container sides, as close to the chamber walls without touching the acrylic, as to not transfer heat via conduction. The bulbs supplied 290 μmol $m^{-2}$ $s^{-1}$, and 140 μmol $m^{-2}$ $s^{-1}$ were available inside the surface wall of the container. Experiments used 24hr illumination.

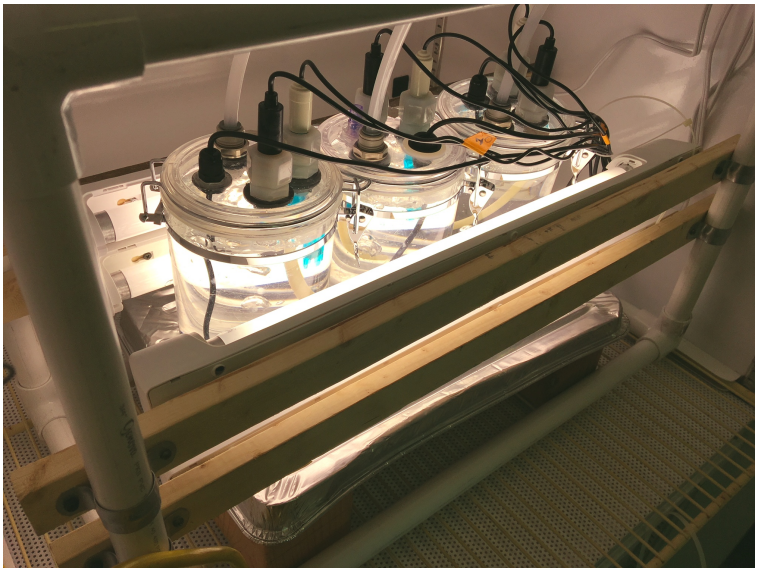

**Figure 46. Bioreactors inside of lighting structure contained inside of the environmental chamber. Measurement probes are fed through the lid through bulkhead fittings.**

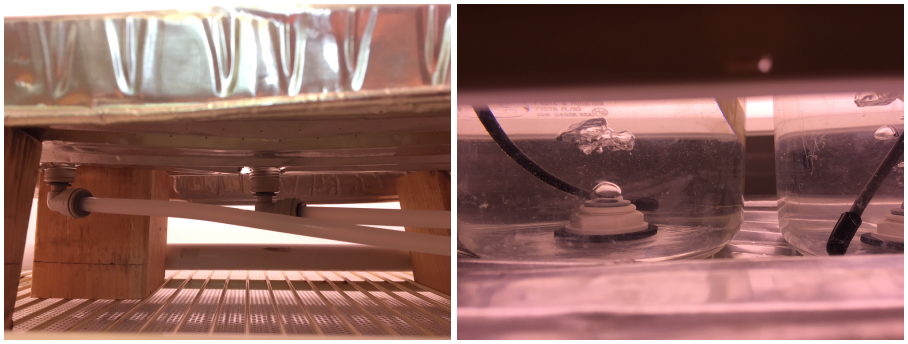

**Figure 47. Sparging system using John Guest fittings and ¾" tubing**

The gas provision system consisted of two mass flow controllers (GE50A, MKS), one controlling the flow of a dry 5.00% $CO_2$/balance air gas canister (Airgas) and the other dry air line from the lab bench (Ekeley Sciences Building, Boulder, CO). The final flow rate of the gas mix was monitored by a convection-based gas flowmeter (FMA1700A, Omega). A 3-way splitter divided the flow, between the containers, which were then controlled by rotameters (4608, CNBTR) before final delivery. The final mixture could also be diverted by way of a three-way valve, through a calcium chloride desiccant column, to the gas analyzer (902P, Quantek) for verification of gas mixture composition. The mass flow controllers, flow meter, and gas analyzer were controlled and monitored through LabView 2015 and DAQ products (NI9205 and NI9201, National Instruments).

### 6.3.2 Experiment Design

#### 6.3.2.1 Variables and Conditions

The tested independent variable for this set of experiments was the supplied $CO_2$ gas concentration. irradiance, temperature, and media solution were held constant through all experimental runs. The tested concentrations of $CO_2$ depended on two factors, flow ranges of the mass flow controllers and the sensing range of the gas analyzer. However, final $CO_2$ concentrations were scaled respiration values, to fit within this design space. Table 22 displays the flow rates used for each constituent to replicate certain human respiration conditions and were calculated using the Ideal Gas Law and Dalton's Law of partial pressures. $CO_2$ concentrations were found in literature, and then scaled to fit within the sensing capabilities of the gas analyzer (<0.5%), using the exercise condition as the maximum, and determiner of the scaling factor (Douglas et al. 1982; Anderson et al. 2018).

**Table 22. Proposed flow rates and pressures to replicate various $CO_2$ concentrations found in cyclical human respiration or the upper 1000-day $CO_2$ concentration thresholds. These can be modified to the desires of the experiment (if it's shown that 3LPM, or 1SLPM/canister is not enough to produce good sparging, the overall gas flow rate could be increased) (Douglas et al. 1982),(Anderson et al. 2018).**

| Test Parameter | Sleep (5.21% but scaled to 0.12%), Low | Nominal (7.63% but scaled to 0.29%), Medium | Exercise (18.09%, but scaled to 0.45%), High |
|---|---|---|---|
| **Total Flow rate (SLPM)** | 3 | | |
| **Flow rate of 5% $CO_2$ (SLPM)** | 0.05 | 0.15 | 0.25 |
| **Flow rate of Air Feed Line, 0.04% $CO_2$ (SLPM)** | 2.95 | 2.85 | 2.75 |

#### 6.3.2.2 Test Procedure

Using all three containers simultaneously produced triplicate replication in one experimental run. Before each experiment, containers, bulkheads, gaskets, probes, and media-contacting tubing were washed in a Liquinox solution (per package instructions) and 3x rinsed in DI water, then rinsed in a 3% hydrogen peroxide solution and rinsed 3x with DI water again for sanitizing. Components were allowed to air dry, and then were reassembled. Gas flow was initiated without culture present in containers, allowing for concentration and flow checks through the containers without culture interference. In a sanitized bucket, 8L (extra culture prepared for biomass measurements) of dilute algal culture ($10^5$ cell/ml) was prepared using the lab bench-top mother culture and Bristol's media. The prepared culture was split equally into the containers while the gas was running, to keep the sparging lines clear of

culture. Flow rates to each of the containers were checked to ensure equal flow (1SLPM), and the rotameters were adjusted as necessary. All experiments were conducted in an open-loop fashion, meaning that gas was passed through the container and then vented out to the lab environment without return. Baselines of all experimental conditions were established using clean Bristol's media, and complete 7-day runs of the concentration condition

#### 6.3.2.2.1 Steady-state $CO_2$ Concentrations

Constant concentrations of $CO_2$ at each of the three levels (Table 22) were sparged into the cultures during a 7-day experiment. These experiments established baselines at constant $CO_2$ concentrations, for comparison to the transient experiments. Results of these experiments are not presented here, but associated data can be found in Appendix D.

#### 6.3.2.2.2 Step-change in $CO_2$ Concentrations

Figure 48 shows the $CO_2$ concentration profiles delivered to the cultures. A culture was allowed to cultivate at one constant $CO_2$ concentration for 4.5 days before stepping to a different $CO_2$ constant concentration for the rest of the duration (4.5 days). First, a low-to-high experiment was conducted, to replicate a crew member switching from sleep to exercise. The culture was discarded, and the experiment was repeated with an exercise to sleep transition, to test for hysteresis. The upper-level concentration cases (exercise, Figure 44) were incorporated to ensure measurable changes in carbon fixation, as well as to establish metabolic rates at upper end of the $CO_2$ concentration range. It was also hypothesized that if the culture could endure changes in $CO_2$ concentration that fall between 0.12% and 0.45%

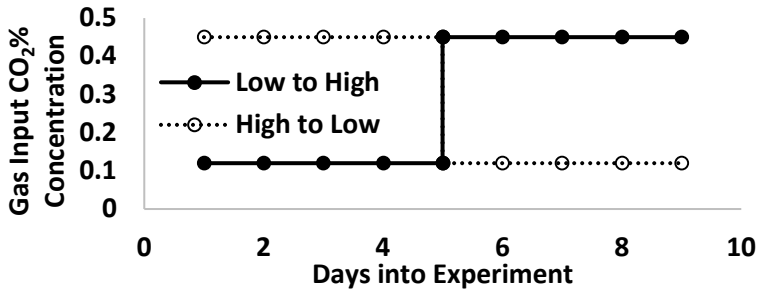


**Figure 48. Graphical representation of the inlet gas concentration for the low-to-high and high-to-low tests.**

#### 6.3.2.3 Measurements

##### 6.3.2.3.1 Continuous Measurements

Similar to the thermally cycled case in Chapter 4, the pH, dissolved oxygen, and temperature measurements were recorded into Microsoft Excel using PLX-DAQ software. All measurements were taken at a sampling rate of 0.2Hz. An Arduino shield (Tentacle Shield, Whitebox Labs) was used to connect the pH and dissolved sensor to the Arduino. The pH sensor was calibrated before each experimental run using an Atlas buffer kit. The analog gas flow rate was recorded by an NI9201 DAQ card through LabView at 10Hz, the mass flow controller settings were recorded through the same interface. Results of the dissolved oxygen, pH, and temperature measurements are not reported here but can be found in Appendix D.

##### 6.3.2.3.2 Non-continuous Measurements

Daily cell counts, optical density, and photosynthetic yield measurements were conducted in the same manner outlined in Chapter 4. However, additional mixing was required before gathering samples for optical density and cell count, due to settling that occurred when gas sparging was paused for PAM measurements. A syringe was used to "lift" settled cells before capturing with a pipette. Each reactor's inlet and outlet gas concentrations of $CO_2$ and $O_2$ were sampled daily by connecting the inlet or outlet gas stream to the gas analyzer.

Every other day, additional samples were drawn for elemental analysis (carbon and nitrogen) through flash combustion (ECS4010, Costech). Vacuum filtration deposited biomass samples onto quartz fiber filters (25mm QE200, Advantec). A sintered glass vacuum filtration apparatus (02920, Cole Parmer) held the quartz filter, processing 15mL of culture sample (Figure 49) (Growing Labs 2019). The borosilicate glass graduated cylinder used to measure the 15mL sample was triple rinsed into the apparatus using DI water. The apparatus funnel was also triple rinsed with DI water while vacuuming, to ensure no residual biomass was left on the sides of the funnel. If the culture was deemed "too dense" for the Costech, the sample was further diluted with Ultrapure water and the dilution constant noted. The quarts filters were then cryodesiccated at -50°C and $2x10^{-3}$mBar for >12hrs, cut into quarters using a razor blade, and packed into tin capsules for processing in the Costech. All surfaces touching the quartz filters were sanitized with ethanol and Ultrapure water.


**Figure 49. An example of the vacuum filtration unit used to filter biomass samples onto quartz filters for elemental analysis (Growing Labs 2019).**

Gas concentration measurements were taken daily by the gas analyzer, by diverting a slip stream of the measured gas to the analyzer. The input gas stream would be sampled for $O_2$ and $CO_2$ concentrations, then each container's outlet stream would be measured for the same constituents. It was assumed through Henry's law that the sampled headspace (container outlet stream) reflected the concentration of the constituents in the media.

#### 6.3.2.4 Data Processing

Measured parameters (dissolved $O_2$, gas concentrations, elemental analysis) were corrected with respect to values from the Bristol's-only baseline experiments. Respiration tests and photosynthetic rate tests, like the ones described in Chapter 4, were also conducted, although these data were not used to calculate average dissolved $O_2$ concentrations. Paired t-tests (2-tailed, assumed equal variance, $p<0.05$) were executed since measurements were conducted on the same container of algae before and after stepping the input $CO_2$ concentration. The statistical analyses were executed using Microsoft Excel 2016. The null hypothesis was, "The change in input $CO_2$ concentration (low-to-high or high-to-low) has no statistically significant effect on the measured parameter," for all tested cases. The photosynthetic quotient, specific growth rate and doubling time, $CO_2$ fixation and $O_2$ production rates were calculated with the measured characteristics. Averages of the triplicate experiments are presented, and the associated standard deviation are the error bars, where appropriate.

Photosynthetic quotient, presented as Eq. 5, compares the produced $O_2$ to the fixed $CO_2$. This ratio can be calculated by gas percent volume or by molar amount. For this experiment, it was easily calculated through the measured deltas in percentage in the supplied gas streams.

$$PQ = O_2 vol\% / CO_2 vol\% \tag{5}$$

Carbon fixation percentage was calculated (using Eq. 6) by multiplying the resulting elemental analysis values, which measured carbon content per ml of sample, by the ratio of $CO_2$ molar mass to carbon molar mass. This value was then divided by the dissolved $CO_2$ content in the medium, averaged over the time between element analysis measurements. The dissolved $CO_2$ content was determined using Henry's law of soluble gases and the measured partial pressure fed into the bioreactors (Royce and Thornhill 1991; L. H. Fan et al. 2008).

$$[CO_2] = \frac{P_{CO_2}}{H_{CO_2}}, \quad H_{CO_2} = e^{11.25 - \frac{395.9}{T - 175.9}} \tag{6}$$

where $[CO_2]$ is the equilibrium concentration in the culture, mol $L^{-1}$, $P_{CO2}$ is the $CO_2$ partial pressure in the gas stream, Pa, $H_{CO2}$ is the Henry's coefficient which is dependent on temperature, Pa L $mol^{-1}$, and $T$ is the temperature of the water, K.

Carbon fixation rate was calculated by using the results from elemental analysis values and dividing the differences by the time between measurements.

Daily cell counts were used to calculate the specific growth rate of the culture (since it is necessary to identify the onset of exponential growth, (Figure 50), using the following equation.

$$\mu = \frac{ln\left(\frac{N(t)}{N(t_0)}\right)}{t - t_0} \tag{7}$$

where $\mu$ is the specific growth rate, $d^{-1}$, $N$ ($t$ or $t_0$) is the cell count at time $t$ and $t_0$, cell $mL^{-1}$, and $t$ is time, d. The doubling time can be calculated from this equation by dividing the specific rate by the natural log of 2.0 (Andersen 2005).

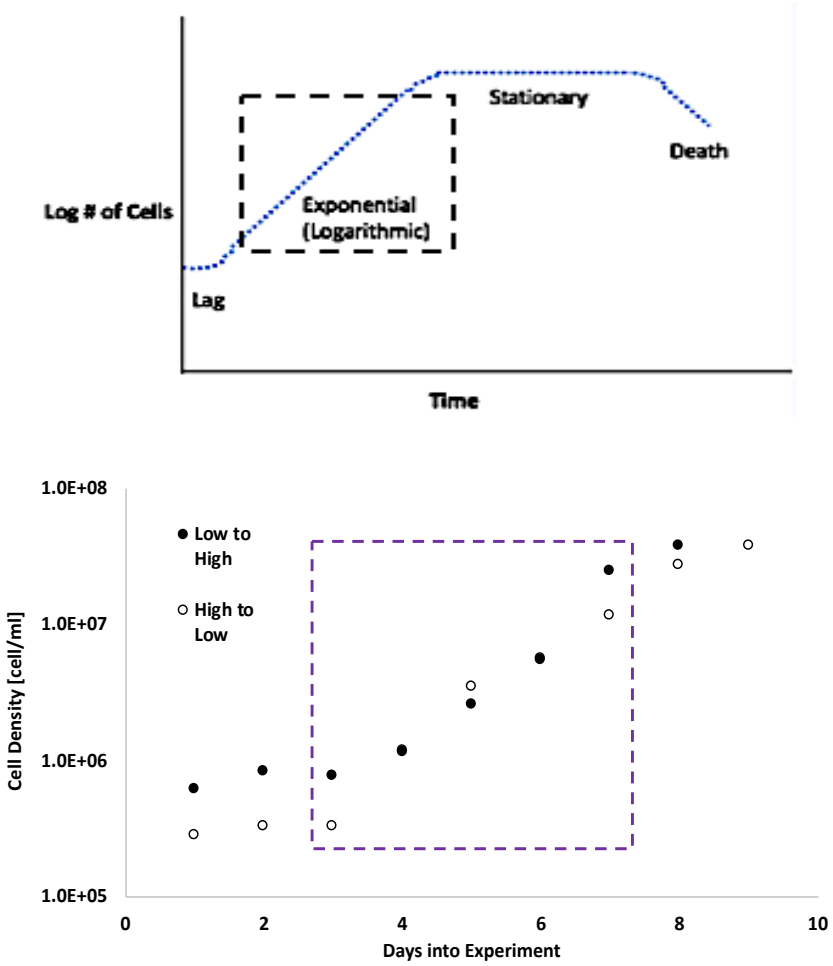


**Figure 50. Specific growth rate is calculated for the exponential growth phase of the culture. The onset of exponential growth (top) can be identified by plotting cell counts on a semi-log plot (bottom). The linearly increasing portions of the semi-log plot are the exponential phase (dotted box, bottom). During this growth period, the culture is in its most efficient growth stage with no input limitations.**

### 6.4 Results

For graphs that are plotted over the duration of the experiment, the day that gas concentration was switched from high-to-low or low-to-high is marked with a dotted line, typically offset to allow for figure clarity.

#### 6.4.1 Photosynthetic Quotient

Volumetric concentration of $O_2$ and $CO_2$ from the inlet and outlet gas streams were used to determine the photosynthetic quotient. Positive, greater than one values indicate more than one mole of $O_2$ is released per mol of $CO_2$ consumed, indicating that photosynthesis is producing excess oxygen (Sakshaug et al. 1997). While a < 1 value signifies that the $O_2$ production rate is lower than the consumption rate of $CO_2$ (Yocum and Blinks 1954; Oswald et

al. 1953). Multiple instances of negative PQ values were recorded after the switch in concentration for the "high-to-low" case, (Figure 51). There is no mention of negative PQ values in surveyed literature, however, the PQ equation suggests that there is active $O_2$ consumption or excess $CO_2$ production (possibly found in the form of cellular respiration, algal or heterotrophic cells and typically reported as respiratory quotient (RQ)) (Cramer and Myers 1948). In the high-to-low case it is hypothesized that when the gas concentration decreased on day five, excess dissolved $CO_2$ was released, increasing the concentration in the measured outlet stream (hence the initial drop in PQ on day six) (Cramer and Myers 1948). Also minimizing the carbon source, reduces the photosynthetic rate, but the culture continues to respire which consumes $O_2$ and produces $CO_2$. The resulting average values for each case, before and after the step-change in $CO_2$ concentration are: (Pre concentration change: Low-to-high (Low) PQ: M = 0.6, SD = 1.2; Post concentration change(High) PQ: M = 1.7, SD = 1.3), (Pre concentration change: High-to-low (High) PQ: M = 2.7, SD = 3.4; Post concentration change (Low) PQ: M = -1.7, SD = 4.5). Photosynthetic quotient values found in literature for similar experiments ranged from -1.1 to 1.4 (Thomas Eriksen et al. 2007; Ammann and Fraser-Smith 1968; Cramer and Myers 1948).

The varying values and standard deviations may be a result of two sources of error. The gas analyzer used to measure the gas species concentration and the measured gas flow rate to each bioreactor, which could have produced the unexpected PQ values (<-1 and >1.5) and the large (1-2x average value) variances. The gas analyzer unit had a coarse resolution (0.1% for $O_2$, 0.001% for $CO_2$) and uncertainty of $\pm$ 3% of the $CO_2$ reading. While the gas mixture was finely controlled with a mass flow controller (uncertainty of $\pm$ 1% of calibration), each container may have had a different input flow rate, since the rotameters had an uncertainty of $\pm$5%, resulting in varying molar amounts of provided $CO_2$. Including a gas analyzer with measurement finer resolution, and a mass flow controller for each algal container to meter input flow could help address unexpected values in PQ.

Paired t-tests (two-tail, df = 4, $p < 0.05$) were conducted to investigate if there was a significant change in the photosynthetic quotient after changing the input $CO_2$ concentration. The results of the t-test for each case suggest that there is no significant change in photosynthetic quotient after a step change in input $CO_2$ concentration, as the null hypothesis cannot be rejected. Trends in the averaged data points in Figure 51 suggest that if the experiment were to continue (past day 9) photosynthetic quotient may have continued to change. Results of the

statistical analysis suggest that the step change in $CO_2$ concentration does not affect the photosynthetic quotient, although, additional experiments are required to confirm this suggestion. This outcome suggests that regardless of the $CO_2$ input, the photosynthetic quotient remains constant, and providing a direct cabin feed to the photobioreactor, with its dynamic $CO_2$ concentrations, does not affect the $CO_2$ to $O_2$ ratio. Instead, this suggests that the system has the potential to passively respond to the changing gas environment (increase in $CO_2$ causes an increase in $O_2$ production). However, this idea needs to be supported by $CO_2$ fixation and $O_2$ production measurements.

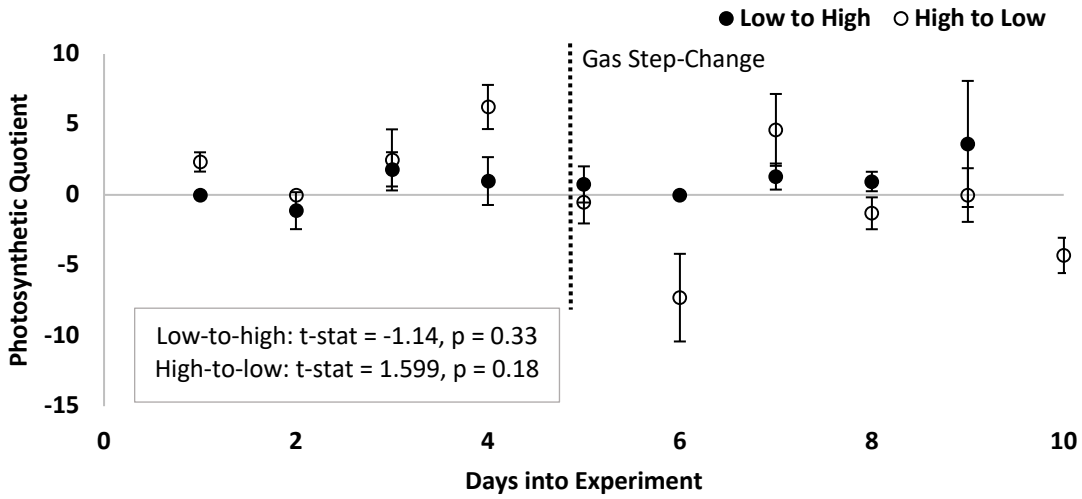


**Figure 51. The delta $O_2$ and $CO_2$ content of the inlet and outlet streams were calculated and used to determine volumetric ratio of $O_2$ produced per $CO_2$ consumed. The "step-change" cases are presented here only, to bring attention to the system responses changing inlet $CO_2$. The gas "step-change" is indicated at day 5 with a dotted line. Each data point is the average of the triplicate containers at that day. Error bars are the standard deviation resulting from the triplicate containers. (Paired t-test, df = 4, $p<0.05$)**

### 6.4.2 Cell Growth Rate

Optical density measurements and cell counts were taken for all experiments. The cell counts are featured here, since saturation of the photometer occurred in some cases which meant manual counting would be more reliable. Also, this allowed for the specific growth rate to be calculated with some confidence. The resulting calculated specific growth rates for each case were plotted together (Figure 52). Specific growth rate also provides an estimate of culture reaction to the sudden step in $CO_2$ concentration.

Paired t-tests (two-tail, df = 2, $p < 0.05$) were conducted to investigate if there was a significant change in the specific growth rate after changing the input $CO_2$ concentration. The t-test result for the low-to-high case suggests that there is no significant change in specific growth rate after a step change in input $CO_2$ concentration, as the null hypothesis cannot be rejected, and confirmed by the overlapping error bars in Figure 52. The change in specific growth rate for the high-to-low case was determined to be significant by the paired t-test, and rejected the null hypothesis (High OD specific growth rate: M = 1.1 $d^{-1}$, SD = $3.9 \times 10^{-2}$), (Low OD specific growth rate: M = $4.7 \times 10^{-1}$ $d^{-1}$, SD = $7.1 \times 10^{-2}$). This, coupled with the data presented in Figure 52, suggests that the culture significantly reduces its growth rate (approximately 137%) in response to a reduction in $CO_2$ concentration in the inlet stream. These results continue to support the suggestion that the culture is actively responding to the changing $CO_2$ environment. Figure 53 shows the cell counts plotted on a semi-log plot, and the sections used to calculate the specific growth rates. Here, the changing slopes of the exponential growth phase before and after the gas step-change are illustrated by the trendlines. Each culture stayed within the exponential growth regime after the step-change in $CO_2$ concentration, suggesting that the culture was not input limited. This implies that for the given lighting and temperature, the $CO_2$ concentration was the limiting input. Connecting this result with the calculations of the photosynthetic quotient implies that, depending on the step-change direction, $O_2$ production would trend with $CO_2$ consumption, positively correlating with the previously presented human respiration trends (Figure 44). For a spacecraft application, these results suggest that the photobioreactor system may be able to actively respond to decreases in $CO_2$ concentration (exercise to sleep) through reduction in cell growth rate. However, for an increase in $CO_2$ concentration (sleep to exercise), the growth rate appears to remain constant. A constant growth rate might be problematic if the culture is unable to consume the increased amount of $CO_2$, allowing for buildup in the atmosphere.

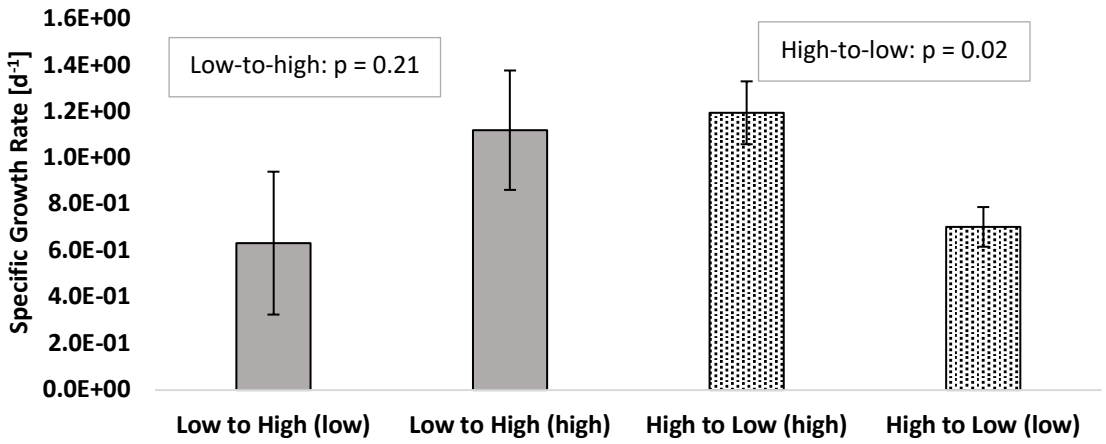


**Figure 52. Specific growth rate plotted for each test case. Splitting the "switching" cases into their subcomponents (low) and (high) allowed for the direct comparison to the steady state values. Each bar is the average of that $CO_2$ level in the experimental case. Error bars are the standard deviation resulting from the triplicate containers. (Paired t-test, df = 2, p<0.05)**

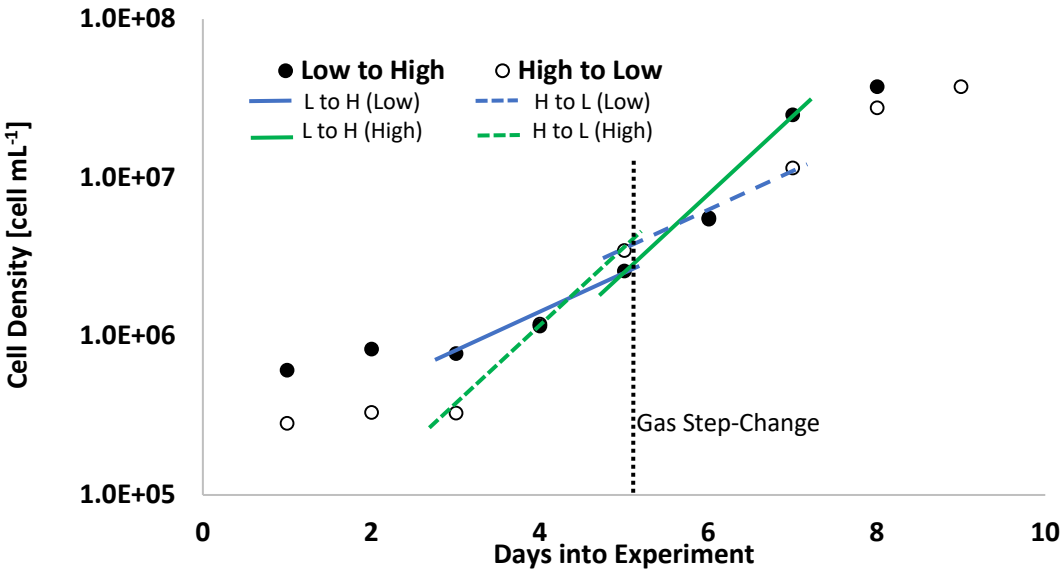


**Figure 53. Cell counts plotted on a semi-log plot to identify the onset exponential growth. Those areas associated with exponential growth are highlighted for each gas step-change case (line type), with each gas level indicated by color.**

### 6.4.3 Photosynthetic Yield

The photosynthetic yield results follow the trends described in Chapter 4, where an acclimation period is recorded within the first few days, with a subsequent rebound to steady state values. Paired t-tests (two-tail, df = 3, p <0.05) were conducted to investigate if there was a significant change in the photosynthetic yield after changing the input $CO_2$ concentration. While the statistical results do not indicate that changing the $CO_2$ concentration in the

high-to-low case significantly affects photosynthetic yield (t = 3.18, p = 0.28), but does affect yield in the low-to-high case (t = 3.18, p = 0.04). Figure 54 indicates a positive correlation between yield and the increase of $CO_2$. Figure 54 also implies a difference between the two cases. A Student's t-test (independent, 2-tail, equal variance, p<0.05) suggests that before the step-change there is no significant difference (p = 0.62) in photosynthetic yield values between the low-to-high and high-to-low cases. However, another Student's t-test test (independent, 2-tail, equal variance, equal sample size, p<0.05), suggested that there was a significant difference (p = 0.01) between the two cases after the gas step-change, rejecting the null hypothesis (Post gas change: Low-to-high (High) PY: M = $7.2x10^{-1}$, SD = $2.5x10^{-2}$; High-to-low (Low) PY: M = $6.7x10^{-1}$, SD = $1.8x10^{-2}$). Figure 54 post gas step-change shows an increase in the yield values for the low-to-high case and a decrease in values for the high-to-low case. This implies that the $CO_2$ concentration is a limiting input, and actively controls the overall health of the culture, which aligns with conclusions of the specific growth rate section. This also suggests that if the $CO_2$ concentration were to go too low, it may impart stress on the culture (reported by low photosynthetic yield measurements) which may cause failure with the system.

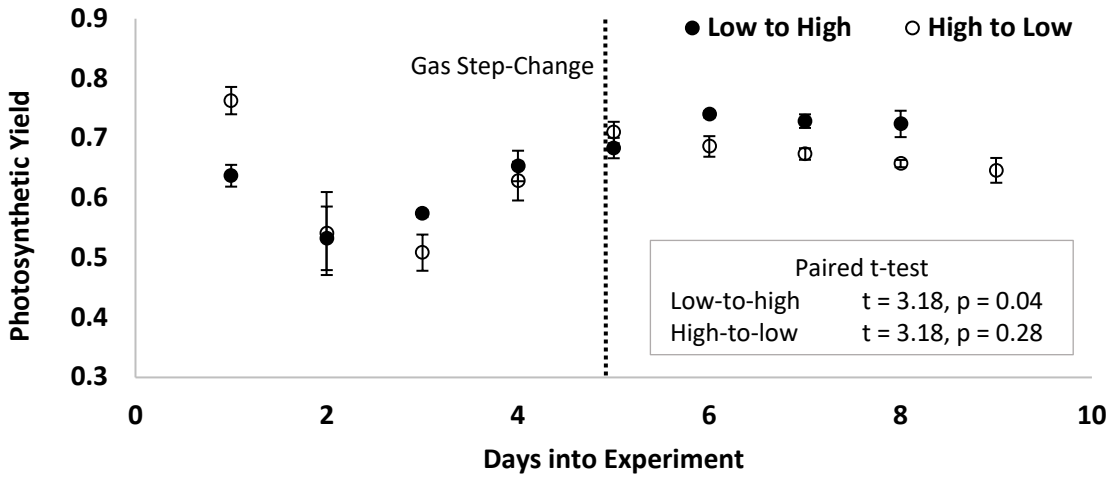


**Figure 54. Photosynthetic yield measurements across experiment duration for the gas step-change cases. Each data point is the average of the triplicate containers at that day. Error bars are the standard deviation resulting from the triplicate containers. (Paired t-test, df = 3, p<0.05)**

### 6.4.4 Carbon Biofixation Percentage

Understanding how much of the $CO_2$ provided by the gas stream was fixed by the culture helps inform future bioreactor designs. It also alludes to culture efficiency in these dynamic environments. Paired t-tests (two-

tail, df = 1, p <0.05) were conducted to investigate if there was a significant change in the carbon fixation percentage after changing the input $CO_2$ concentration. The t-tests results suggest that in either case there is no significant difference in the percentage of the $CO_2$ stream fixed by the biomass when comparing percentages before and after the step-change (Low-to-high: t = 12.71, p = 0.32; High-to-low: t = 12.71, p = 0.8). However, the low number of degrees of freedom (df = 1) indicates that additional experiments and samples are required to increase confidence in these findings. Overall, Figure 55 shows the percentage of $CO_2$ fixed increases as the experiment progresses. This suggests that as the culture becomes more established, and past the "acclimation phase", it may be able to fix more than 50% of the $CO_2$ that is dissolved into the media. Figure 55 also shows the error bars of the two cases overlapping, suggesting that there may not be a difference in the percentage fixed between the two cases. This supports the idea that algal cultures passively regulate biomass production in relation to environmental parameters. Passive regulation could benefit the spacecraft environment by not requiring additional hardware or crew time to adjust $CO_2/O_2$ turnover in relation to the dynamic cabin environment.

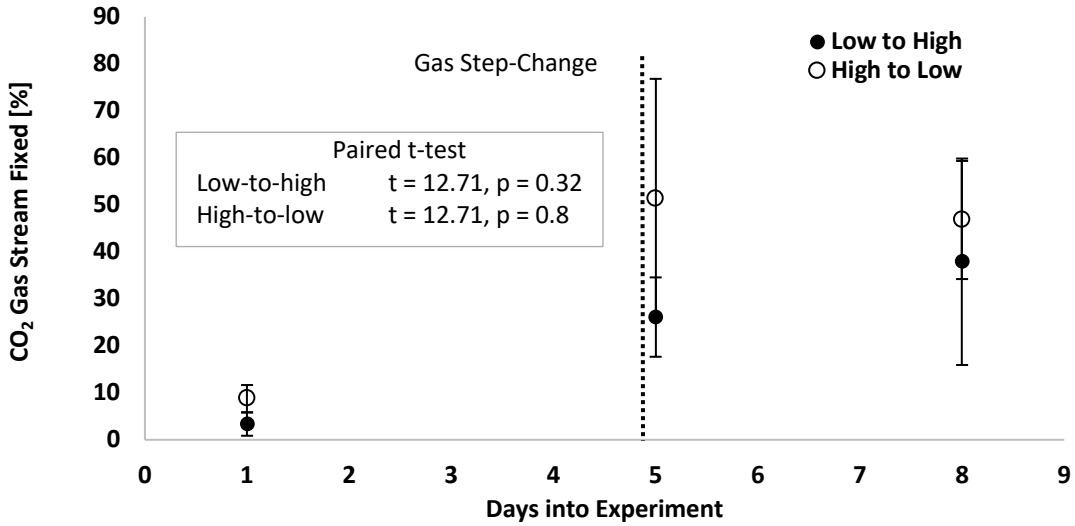


**Figure 55. $CO_2$ fixation percentage calculates the amount of carbon fixed from the provided gas stream by comparing the amount of $CO_2$ dissolved in the algal media to the amount of $CO_2$ (measured as carbon) found in the produced biomass. Each data point is the average of the triplicate containers at that day. Error bars are the standard deviation resulting from the triplicate containers. (Paired t-test, df = 1, p<0.05)**

### 6.4.5 Carbon and Nitrogen Biofixation Rate

Carbon and nitrogen fixation rates were calculated through elemental analysis of sampled biomass using a CN elemental analyzer and dividing by the number of days between measurements. This rate was first used as a

proxy for culture function but could be later used as a reference for photobioreactor design, to size the reactor properly for the spacecraft environment. The carbon is supplied both by the input gas stream and bacterial respiration (since the culture was non-axenic). Therefore, the assumption was made that a majority of the carbon was provided by $CO_2$, which informed $CO_2$ fixation rates. The majority of nitrogen was supplied by the Bristol's media (supplying nitrogen in the form of sodium nitrate, or $NaNO_3$).

Paired t-tests (two-tail, df = 1, $p < 0.05$) were conducted to investigate if there was a significant change in the fixation rates after changing the input $CO_2$ concentration. Both cases when comparing the before and after gas step-change carbon fixation rates resulted in the inability to reject the null hypothesis (Low-to-high: t = 12.71, p = 27; High-to-low: t = 12.71, p = 0.53). Both cases when comparing the before and after gas step-change nitrogen fixation rates also resulted in the inability to reject the null hypothesis (Low-to-high: t = 12.71, p = 0.54; High-to-low: t = 12.71, p = 0.74). However, the very low degrees of freedom (df=1) indicate that more experiments and samples are required to bring confidence to this result. Additional samples were not taken over the course of the experiment due to the lab workload and the schedule of sharing lab equipment. Figure 56 and Figure 57 indicate a significant change in carbon and nitrogen fixation rate through the distance in the error bars, unfortunately the minimal samples do not provide confidence. Here, the figure only suggests that there is a positive correlation between $CO_2$ fixation rate and $CO_2$ provision concentration. The high-to-low case shows a stagnation in $CO_2$ fixation rate after the gas step-change, which implies that the culture is trying to consume all provided $CO_2$, and suggests $CO_2$ is a limiting input. The reduction in nitrogen fixation rate for the high-to-low case also implies that $CO_2$ is the limiting input, as the culture does not require as much nitrogen to perform photosynthesis. The stagnation in the nitrogen fixation rate (Figure 57) for the low-to-high case, is unexpected, as this trend suggests that nitrogen is a limiting input.

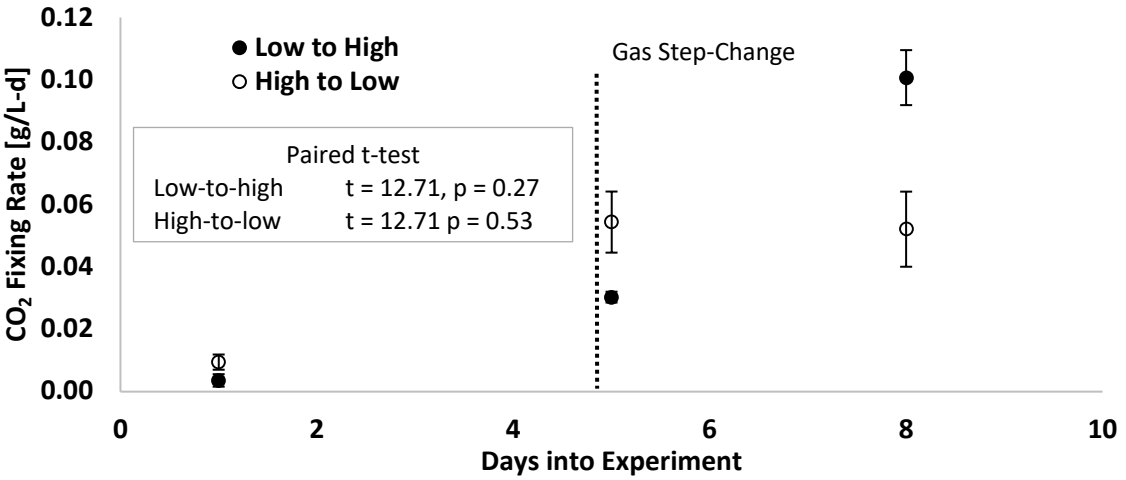


**Figure 56. $CO_2$ fixation rates were developed using the elemental analysis result and dividing by the time between analysis samples. Each data point is the average of the triplicate containers at that day. Error bars are the standard deviation resulting from the triplicate containers. (Paired t-test, df = 1, p<0.05)**

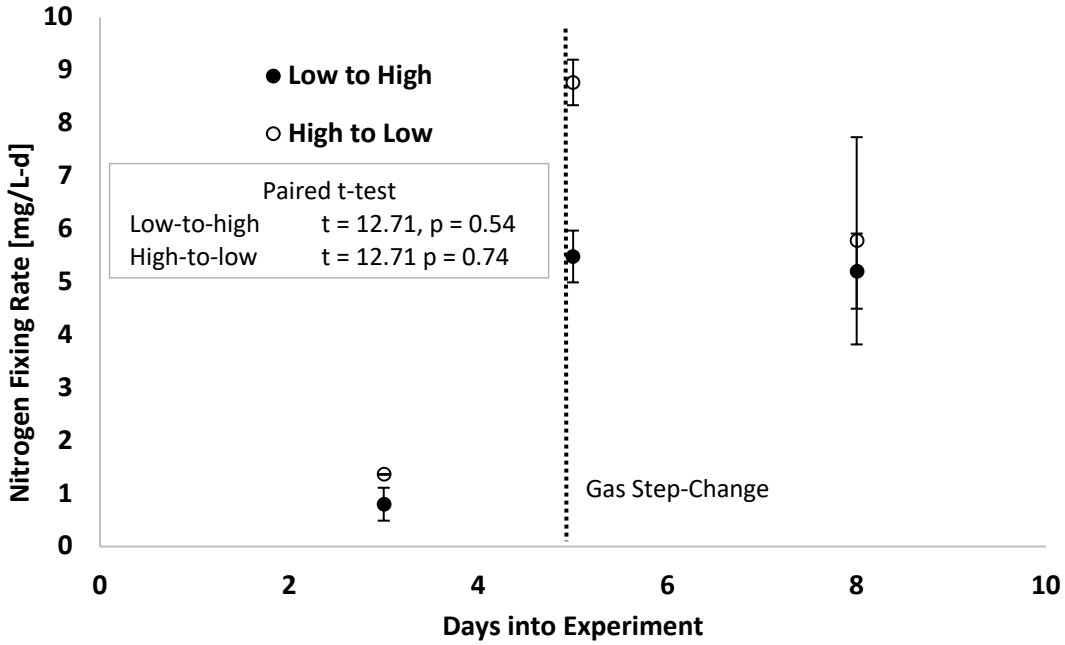


**Figure 57. Nitrogen content of the biomass was determined through elemental analysis. A rate was developed by dividing the change in nitrogen mass by the time between samples. Each data point is the average of the triplicate containers at that day. Error bars are the standard deviation resulting from the triplicate containers. (Paired t-test, df = 1, p<0.05)**

### 6.5 Discussion

Measurable responses to changing $CO_2$ concentrations were recorded during the execution of these experiments. As hypothesized, the culture modified its cell growth rate in positive correlation to the inlet $CO_2$

concentration. The results of the carbon fixation rate, photosynthetic yield, and specific growth rate all suggested that $CO_2$ inlet concentration was a limiting input for this system.

The calculated PQ values indicated that the culture would adjust its metabolism to account for the dynamic $CO_2$ environment, suggesting that a step-change in $CO_2$ concentration would not affect PQ values. The large variation (>1.5 and <0) in reported values from these PQ calculations are an anomaly, which could be attributed to the resolution of the $O_2$ channel on the gas analyzer. The resolution on the $O_2$ channel is large enough (0.1%), that it could contribute to poor estimation of $O_2$ concentration. Additional experiments using a finer resolution could hone these PQ values. Also, constantly monitoring the inlet and outlet gas stream instead of daily checks helps to better capture the active response of the culture. Unfortunately, due to humidity constraints of the gas analyzer, this was not possible at the time of experimentation.

A few of the issues experienced in these experiments came with gas provision. It was also shown through different points of the experimental run that the lab shop air experienced changes (drops) in $CO_2$ concentration. The building managers and facility technicians were contacted, but the issue was never fully resolved. Gas flow rate to the containers sometimes varied because of the liquid level in the containers. Without fine tuning, it was possible to have unequal air flow through containers. Rotameters upstream of the inlet of the containers and daily maintenance was implemented to correct this.

Longer lag times than expected were recorded in these experiments. Previous experience (Chapter 4) indicated that a *Chlorella* lag phase be closer to 1-2 days, not the 3-4 observed here. This proved to be an issue for the gas-stepped cases, since exponential growth was not initiated until after the concentration switch, skewing results. Longer experimental runs should be conducted to allow for the culture to be in exponential growth for at least 4 days before implementing a gas step-change. This ensures the culture is in that stage of growth and potentially increases the accuracy of the specific growth rate calculation with more data points.

Multiple step-changes should be conducted in future experiments to investigate the accrual of effects. It is unknown if the culture will recover to its original metabolic rates if it goes through a gas concentration cycle. The equipment available at the time was not able to execute these multiple step-changes.

No record of any of the cultures “crashing” or significant carotenoid production -indicating stress. However, a reduction in $CO_2$ fixation was recorded in the high-to-low gas-stepped case, which was also reflected in its PQ and

produced oxygen values. If using this type of system in a spacecraft, larger volumes of media or cabin gas could be used to help buffer the transient $CO_2$ levels.

### 6.6 Conclusion

Exposing an algal culture directly to the cabin environment could reduce the amount of required gas provision hardware to support the cultures. This direct exposure could subject the culture to a dynamic $CO_2$ environment, as human respiration goes through diurnal cycles, influenced by effort in daily activities. Therefore, this set of experiments set out to characterize the response of *Chlorella vulgaris* to various $CO_2$ concentrations, both steady-state and dynamic. Gas-tight, acrylic commercially available containers were modified to hold dissolved oxygen, pH, temperature probes and gas provision lines. Seven-day experiments were conducted, using three different constant levels of inlet $CO_2$ concentration, and one low-to-high and high-to-low stepwise test. The hypothesis that as inlet $CO_2$ concentration increased, an increase in culture metabolism is observed, was supported. The same was true for the opposite case (reduction in metabolic processes with a reduction in inlet $CO_2$ concentration) but it took longer than expected for these results to become measurable (3 days vs the expected 1). Reaction rate to changing $CO_2$ concentration was not quantified due to the gas sampling rate being limited by equipment allowable humidity thresholds. Constant, or an increased rate from one sample per day, monitoring of the gas stream allows the response rate to be calculated with better resolution and accuracy.

At this time, algal culture response to constant gas concentrations is better understood than that to dynamic environments, and results in more refined models. Additional experimentation using longer test durations (>7days) and multiple step changes in a row are more indicative of the spacecraft environment and better informs similar models.

### 6.7 Resulting Publications

No publications are planned at this time

# Chapter 7 Heat and Mass Transfer Across a Nonporous Silicone Membrane

## 7.1 Introduction

Volume-constrained habitats in confined settings (i.e. submarines and spacecraft) are required to support human metabolic needs by scrubbing the environment of respired $CO_2$ and providing $O_2$ (Wieland 1998; NASA 2015). In the case of human spacecraft and surface habitats, microgravity and reduced gravity environments limit the use of bubble-forming technologies for environmental control and life support systems, since buoyancy may be dominated by surface tension, and inertial or viscous forces (I. Wagner et al. 2016). To avoid the use of mixed-phase media, human-rated spacecraft have used physicochemical solid sorbents for removal of $CO_2$ and trace gas contaminants from the cabin atmosphere (Wieland 1998). However, their utilization can come at a cost due to waste streams and hazardous operation regimes (Samplatsky et al. 2011). Bioregenerative technologies (algal photobioreactors) have been suggested as a replacement for the physicochemical systems due to their multifunctionality and compatibility with the cabin environment (NASA 2015). Typically, gases are bubbled through the culture for $CO_2$ provision, posing an issue for culture use in microgravity. Contactor membranes do not rely on buoyancy and thus, are promising for performing bubble-free gas transfer to or from liquids during spaceflight missions (Lee and Palsson 1995). Recently, polydimethylsiloxane (PDMS) membranes have become of interest for spaceflight missions due to their nonporous construction, eliminating voids for potential biological growth (i.e. biofouling), allowing for consistent mass transfer over long periods (Attaway, Gooding, and Schmidt 2002). Reliable gas transport then ensures sustained culture growth within photobioreactors, suitable for long-duration spaceflight. The relatively large surface area-to-volume ratios provided by the interstitial contact surface area from the fibers (from 500 to 9,000 $m^2\ m^{-3}$), allows for greater gas transfer within a smaller footprint, an additional benefit for a volume-constrained spacecraft (S. Zhao et al. 2016; Henley, Seader, and Roper 1998).

Industries using membrane distillation have shown that gas-liquid contactors can also be utilized for heat transfer and, therefore, gas cooling (Schofield, Fane, and Fell 1987). Volume-constrained environments seek multifunctional technologies for efficient utilization of space. A suggested use of nonselective PDMS membranes would concurrently transfer $CO_2$ and heat from a cabin gas stream to a cooling water loop containing algae. The cabin gas simultaneously strips dissolved oxygen from the water. Typically, membranes distillation contactors use

microporous or use composite materials. Porous membranes allow for greater mass transfer, but the void-sites leave the membrane vulnerable to biofouling over long periods of operation (Ho and Sirkar 1992; Schofield, Fane, and Fell 1987; Leitch, Lowry, and Mauter 2017).

Characterization of a PDMS membrane for oxygen or $CO_2$ separation has been previously conducted, but these studies did not demonstrate concurrent transfer of both species (Yeom, Lee, and Lee 2000; Ito et al. 1998). Yang and Cussler set the precedent for mass transfer correlations using a microporous membrane for transport of concurrent oxygen and $CO_2$ (M. Yang and Cussler 1986). Characterization of simultaneous $CO_2$, oxygen, and heat transfer would inform the potential of nonporous membranes for use in spacecraft life support systems.

The following experiments studying heat and mass transfer in a gas-liquid contactor system used a commercially available, nonporous PDMS membrane. Using the published membrane physical and dimensional data, analytical models were developed to predict the transfer rates for a relevant range of gas and liquid flow rates. Mass transfer was first studied using manufacturer-provided data, which was then verified experimentally. Concurrent heat and mass transfer were characterized with a simulated cabin atmosphere gas stream through the lumen side of the fibers and coolant water flowing through the shell side of the contactor. Experimental results are compared to the developed models, and equation coefficients revised to better characterize the experimental system. The resulting empirically modified models could be used to predict contactor performance at other conditions.

## 7.2 Model Development

Each aspect of transfer (mass and heat) were addressed separately with models, as described below. These derivations were used to predict expected results of the experiments. Post-test, the model empirical coefficients were revised for better agreement with experiment results, enabling their use in future system designs.

### 7.2.1 Mass Transfer

Drioli et al. present an overview of membrane technologies, including the first-order equation (Eq. 8) for describing mass transport across the membrane.

$$J = B\left(C_{eq} - C_L\right) \tag{8}$$

where $J$ is the mass flux (mg $s^{-1}$ $m^{-2}$), $B$ is the local overall mass transfer coefficient (m $s^{-1}$), $C_{eq}$ is the gas species concentration in the liquid in equilibrium with the bulk concentration found in gas (mg $m^{-3}$), $C_L$ is the gas species concentration found in the liquid (mg $m^{-3}$).

The following assumptions were informed by the overview to develop the overall model (Drioli, Criscuoli, and Curcio 2006; Shirazian, Moghadassi, and Moradi 2009; Mahmud et al. 2004; Tan and Capar 2005; K. Li, Tai, and Teo 1994).

Model Assumptions:

1. Membrane temperature and flow conditions are at steady state.
2. Ideal gas law for gas stream.
3. Negligible initial amounts of oxygen in the process gas stream
4. Initial concentration of carbon dioxide in the process gas stream is higher than the dissolved concentration of carbon dioxide in the cooling water.
5. Flow rates of gas and liquid are constant.
6. The liquid stream is in crossflow over the hollow fibers.
7. Instantaneous equilibrium between the bulk gas and liquid side is obtained through Henry's law.
8. Axial concentration gradients in the gas and liquid stream are negligible.
9. Pressure drop in the membrane system is negligible. (Confirmed with PermSelect PDMSXA 7500 pressure drop figure in Appendix E)
10. Gas is physically absorbed/desorbed in the water stream. Chemical interactions are negligible.

Using these assumptions, and the first-order equation found in the literature, the concentration ratio equation (Eq. 9) describes oxygen removal from the liquid side.

$$\textit{Oxygen liquid-to-gas transport:} \frac{C_{O2out}}{C_{O2in}} = exp\left(\frac{AK_{o_2}}{Q_w}\right) \tag{9}$$

where $C_{O2in}$ and $C_{O2out}$ are the inlet and outlet concentrations, respectively, of dissolved oxygen in water (mg $m^{-3}$), $A$ is the interfacial area of the membrane ($m^2$), $Q_w$ is the volumetric flow rate of the water side ($m^3$ $s^{-1}$), and $K_{O2}$ is the overall mass transfer coefficient of oxygen (m $s^{-1}$). Similarly, Eq. 10 describes $CO_2$ removal from the gas side using the same assumptions and similar form of the equation.

$$\textit{Carbon dioxide gas-to-liquid transport:} \frac{C_{CO2out}}{C_{CO2in}} = 1 - exp\left(-\frac{AK_{CO_2}}{Q_g}\right) \tag{10}$$

here $C_{CO2in}$, $C_{CO2out}$ are the inlet and outlet concentrations of $CO_2$, respectively, measured in the gas stream (%, converted to mg $m^{-3}$ through the Ideal Gas Law), $Q_g$ is volumetric flow rate of the gas side ($m^3\ s^{-1}$) and $K_{CO2}$ is the overall mass transfer coefficient of $CO_2$ (m $s^{-1}$). Mass transfer in gas-liquid membrane contactors occurs in three distinct areas, and the direction of the mass transfer is dependent on the concentration of the species in each of the phases. Figure 58 depicts the movement of $CO_2$ from the process gas stream through the fiber wall to the coolant water. Conversely, this figure can also describe the transfer of oxygen from water to the gas phase (Rathnasiri and Ottøy 2003).

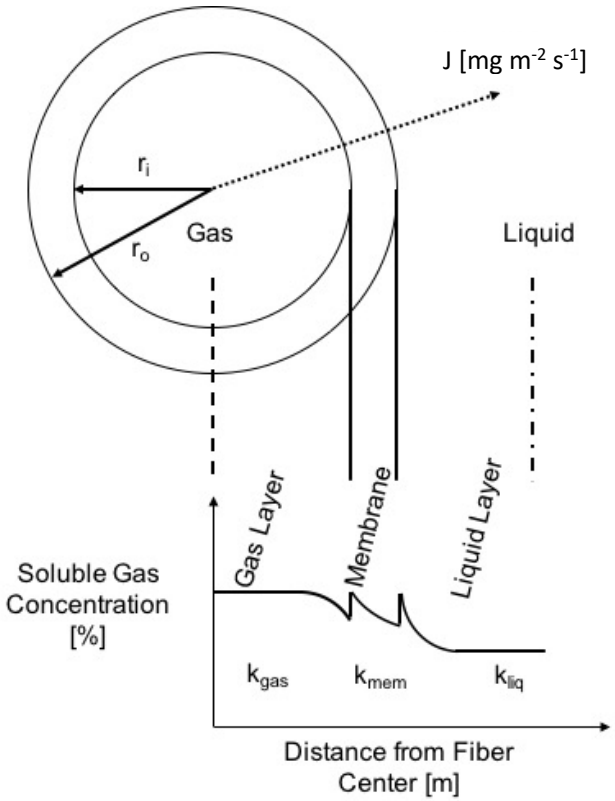


**Figure 58. Resistance-in-series diagram for carbon dioxide being stripped from the lumen-side gas stream by the water stream flowing shell-side of the contactor. Dominating resistances ($k_{gas}$, $k_{mem}$, $k_{liq}$) are indicated in their respective locations. (Figure derived from Rathnasiri and Ottøy 2003)**

The overall mass transfer coefficient for each species can be described as a sum of mass transfer resistances (depicted in Figure 58 and given by Eq. 11) based on the resistance-in-series model.

$$\frac{1}{K} = \frac{1}{k_m H} + \frac{1}{k_l} + \frac{1}{k_g H} \quad (11)$$

where $k_m$ is the mass transfer coefficient through the membrane (m $s^{-1}$), $k_l$ is the mass transfer coefficient through the liquid side (m $s^{-1}$), $k_g$ is the mass transfer through the gas side (m $s^{-1}$) and $H$ is the Henry's constant of the species being studied (Pa $m^{-3}$ $mol^{-1}$). While values for liquid and gas resistance can be modeled and verified empirically, membrane resistance can be estimated by Eq. 12 (Heile et al. 2014).

$$k_m = P/\delta \quad (12)$$

where $P$ is the gas species permeability through the membrane (mol $m^{-2}$ $Pa^{-1}$ $s^{-1}$), and $\delta$ is the membrane thickness (m). Since the membrane resistance equation does not contain any gas or liquid flow rate-dependent variables, an additional assumption was made that the membrane resistance remains constant regardless of the flow rate. Li et al. suggest membrane resistance would be negligible for the flow pattern (liquid on the shell side, across fibers) and regimes appropriate to this model (K. Li, Tai, and Teo 1994). Still, since values for the membrane parameters were available, membrane resistance was included in the model.

Liquid resistance values can be modeled and empirically defined through a Sherwood number equation. The membrane included in this experiment has a crossflow pattern across the hollow fibers, as verified by the manufacturer. This allows use of Eq. 13 for estimation of the liquid mass transfer coefficient

$$k_l = Sh * \frac{D_g}{d_e} \quad (13)$$

where $Sh$ is the Sherwood number, $D_g$ is the diffusivity of the gas of interest ($m^2$ $s^{-1}$), and $d_e$ is the equivalent diameter (m) as defined and calculated in Table 23. Since the flow of water is on the outside of the fibers, the internal diameter cannot be used as the characteristic length. The outside diameter of the fiber is not used as the characteristic length due to the complex shell-side crossflow pattern. Instead, an equivalent diameter is calculated, to take into consideration the shell diameter and number of fibers in the bundle (Table 23) (Tan and Capar 2005; Price 2013). The Sherwood number relates the ratio of convective mass transfer to diffusive mass transport. The Sherwood number can be characterized in terms of the non-dimensional Reynolds and Schmidt numbers Eq. 14.

$$Sh = \alpha Re^{\beta} Sc^{0.33} \quad (14)$$

where *Re* is the Reynolds number of the flow, *Sc* is the Schmidt number, and $\alpha$ and $\beta$ are coefficients dependent on the flow pattern through the membrane module. presents the coefficients associated with a crossflow pattern for both equations found in literature and those empirically developed. The Sc number had an established power dependence of 1/3, as informed by Tan, 2005 (Tan and Capar 2005). Kreith and Black (1980) established the correlation for cross-flow in closely packed tube bank heat exchangers, which was referenced to establish the Sherwood number model equation (Kreith and Black 1980). With $Sc^{0.33}$ omitted, a least-square regression established the relationship between Re and Sh numbers (Figure 59). Oxygen transfer data for the PermSelect PDMSXA 7500 membrane module used in the experiments was also plotted for comparison. The calculated coefficients for the Sh equation using the PermSelect data informed the expected results for the gas transfer experiment, and the simultaneous heat and mass transfer experiment. As can be seen in Figure 59, the PermSelect data agrees well with the Kreith and Black correlation (root mean square error = 0.09).

Previous experiments using similar membrane setups and flow regimes suggest gas-phase resistance to mass transport may be neglected. This ability to disregard gas-phase resistance can be tested by producing a Wilson plot of the resulting overall mass transfer coefficient against gas velocities (Tan and Capar 2005). If the plot results show constant gas transfer across the membrane for all gas flow rates, gas-phase resistance can be neglected. For that reason, it was initially assumed that Eq. 13 or liquid-phase resistance to gas transport would be appropriate for both oxygen and $CO_2$, as long as the appropriate diffusivity values were used for the respective species.

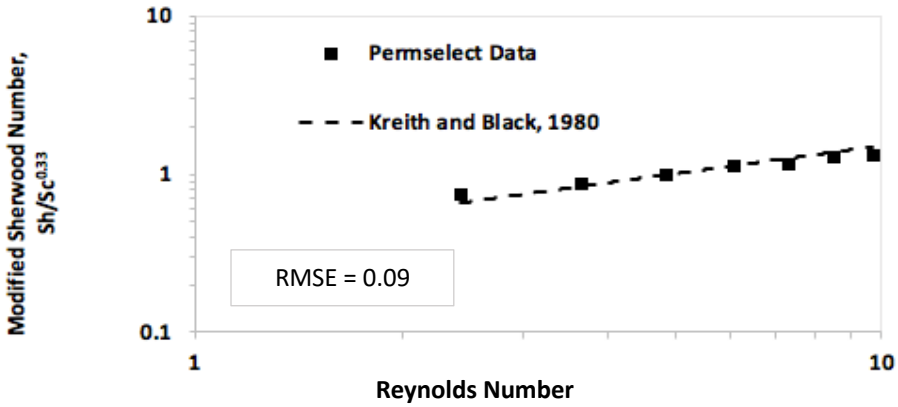


**Figure 59. Comparison of PermSelect to the Kreith and Black 1980 model, given the same membrane characteristics and flow rates for the transfer of oxygen. The calculated root mean square error between the model values and the provided data values is 0.09.**

**Table 23.Characteristics of membrane, gas species, and water with experiment operational regime**

| Characteristic, Symbol, Unit, equation (if provided) | Value |
|---|---|
| Fiber outside diameter, $d_o$, (m) | $3.00x10^{-4}$ |
| Fiber inside diameter, $d_i$, (m) | $1.90x10^{-4}$ |
| Equivalent diameter, $d_e$, (m) $d_e$ = [(4*Cross-sectional Area)/Wetted Perimeter)] | $3.722x10^{-4}$ |
| Fiber wall thickness, $\delta$, (m) | $5.50x10^{-5}$ |
| Module effective length, L, (m) | 0.123 |
| Module shell side diameter, $d_s$, (m) | 0.044 |
| Packing Fraction, $\phi$ | 0.445 |
| Number of Fibers, N | 9600 |
| Interfacial Area, A, ($m^2$) | 0.75 |
| Oxygen's Henry's constant, $H_{OXYGEN}$, (Pa $m^3$ $mol^{-1}$) | $7.468x10^4$ |
| Carbon dioxide Henry's constant, $H_{CARBON\ DIOXIDE}$, (Pa $m^3$ $mol^{-1}$) | $2.813x10^3$ |
| Oxygen diffusivity in water, $D_{OXYGEN}$, ($m^2$ $s^{-1}$), 0°C, 20°C | $1.014x10^{-9}$, $1.699x10^{-9}$ |
| Carbon dioxide diffusivity in water, $D_{CARBON\ DIOXIDE}$, ($m^2$ $s^{-1}$), 0°C, 20°C | $9.274x10^{-10}$ $1.920x10^{-9}$ |
| Permeance of oxygen through membrane, $P_{OXYGEN}$, (mol $m^{-2}$ $Pa^{-1}$ $s^{-1}$) | $2.010x10^{-13}$ $1.608x10^{-13}$ |
| Permeance of carbon dioxide through membrane, $P_{CARBON\ DIOXIDE}$ (mol $m^{-2}$ $Pa^{-1}$ $s^{-1}$) 0°C, 20°C | $1.139x10^{-12}$ $1.089x10^{-12}$ |
| Kinematic viscosity of water, $\mu_w$, (Pa s), 0°C, 20°C | $1.732x10^{-3}$ $1.00x10^{-3}$ |
| Kinematic viscosity of nitrogen gas, $\mu_{OXYGEN}$, (Pa s), 0°C, 20°C | $1.668x10^{-5}$ $1.758x10^{-5}$ |
| Specific isobaric heat capacity of water, $c_{pw}$, (kJ $kg^{-1}$ $K^{-1}$), 0°C, 20°C | 4.2199 4.1844 |
| Specific isobaric heat capacity of nitrogen, $c_{pn}$, (kJ $kg^{-1}$ $K^{-1}$), 0°C, 20°C | 1.039 1.040 |
| **Experiment Operational Regime** | |
| Water flow rate (membrane shell), $Q_l$, LPM | 0.5-2.0 0.25 increments |
| Input water Temperature, $T_{wi}$, K | 274, 292 |
| Gas flow rate (lumen flow), $Q_g$, LPM | 2.0-6.0 2.0 increments |
| Input gas temperature, $T_{gi}$, K | 296 |

**Table 24.Resulting empirical correlation of Sherwood equation using PermSelect oxygen transfer data compared to the correlation developed by Kreith and Black, 1980**

| | Correlation | |
|---|---|---|
| Conditions | Kreith and Black, 1980 | Best fit to PermSelect Data |
| PermSelect Data<br>*296K gas and 292K water*<br>*Aerated water*<br>*100% nitrogen sweep gas* | $Sh = 0.39Re^{0.59}Sc^{0.33}$ | $Sh = 0.522Re^{0.41}Sc^{0.33}$ |

### 7.2.2 Heat Transfer

A 1-D model was developed for the overall heat transfer across the membrane. Assuming steady state, a reduced thermal energy equation results for each fluid (Bergman, T., Lavine, A., Incropera, F., Dewitt 2011).

$$\dot{Q} = \dot{m} c_p (T_{out} - T_{in}) \tag{15}$$

where $\dot{Q}$ is the rate of heat transfer to or from the liquid or gas (W), $\dot{m}$ is the fluid mass flow rate (kg $s^{-1}$), $c_p$ is the specific isobaric heat capacity of the fluid (kJ $kg^{-1}$ $K^{-1}$), $T_{in}$ and $T_{out}$ are the inlet and outlet temperatures, respectively, of the fluid (K). Establishing the following assumptions allows for the use of this equation:

1. The liquid or ideal gas has negligible changes in potential or kinetic energy, and experiences negligible work (other than flow work)
2. Conditions are steady state
3. No changes in latent energy
4. No internal generation thermal or mechanical energy
5. Adiabatic system; negligible heat interaction between membrane and the outside environment

It was hypothesized the greatest change in temperature across the module would be recorded in the gas phase, due to the smaller specific heat value when compared to the liquid value, making it easier to characterize the overall heat transfer.

In conjunction with Eq. 15, the logarithmic mean temperature difference can be utilized to develop an overall heat transfer coefficient of the module Eq. 16.

$$\dot{Q} = UA \frac{(T_{gi} - T_{wf}) - (T_{gf} - T_{wi})}{ln\left(\frac{T_{gi} - T_{wf}}{T_{gf} - T_{wi}}\right)} \tag{16}$$

where $\dot{Q}$ is the rate of heat transfer as calculated in Eq. 15 (W), $U$ is the membrane module's overall heat transfer coefficient ($Wm^{-2}K^{-1}$), $A$ is the contact area of the membrane module ($m^2$), $T_{gi}$ and $T_{gf}$ are the inlet and outlet module gas temperatures, respectively (K), $T_{wi}$ and $T_{wf}$ are the inlet and outlet module water temperatures (K), respectively. Once established, this coefficient could be used with the module geometry and operational conditions to predict performance of future designs.

### 7.3 Materials and Methods

Experiments were conducted to investigate simultaneous mass and heat transfer using atmospheric conditions found in human-rated spacecraft. Water temperatures were reflective of spacecraft thermal loop regimes.

#### 7.3.1 Test Article Set-Up and Instrumentation

The experimental set-up was centered around a nonporous polydimethylsiloxane (PDMS) hollow fiber membrane module (PDMSXA 7500, PermSelect, Ann Arbor, MI, USA), with an effective surface area of 0.75$m^2$ and a cross-flow pattern around the fibers (Figure 60). The membrane module was covered with aluminized insulation (R-3.7 to R-21, Refletix) to reduce heat transfer to/from lab environment. The temperatures of the inlet and outlet gas and water streams were measured with thermistors (MC65F103AN, Amphenol Advanced Sensors), and the relative humidity of the gas streams were measured with Honeywell humidity sensors (HIH-4000-001, Honeywell). A single-use stream of pure, dry nitrogen (99.9% $N_2$) was fed into the lumen side of the module, with varying concentrations of dry $CO_2$ (0% or 0.5%) (Airgas). The gas flow was controlled by a mass flow controller and monitored by a mass flow meter (GE50A, MKS, Andover, MA, USA and FMA 33109, Omega). Species concentrations were monitored by a gas analyzer (902P, Quantek and NI 9219, National Instruments) after flowing through a calcium chloride desiccant tube. Single-use aerated tap water was pumped into the counterflow, shell-side inlet, by a diaphragm pump (1GPM, SHURflo) controlled by a power supply (DIGI 35A, Electro Industries) and monitored by a rotary flow meter (FLR 1012-D, Omega). The inlet and outlet pH and dissolved concentrations of the water stream were measured with Atlas sensors (EZO pH and EZO Dissolved Oxygen, Atlas Scientific). Instrumentation diagram of the test article set-up can be found in Figure 61.

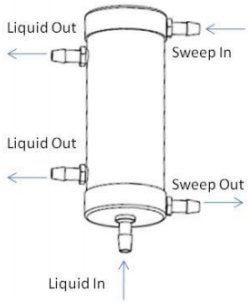


**Figure 60. Flow configuration used in experiment. Gas is fed into the lumen of the membrane, with liquid shell-feed. (PermSelect)**

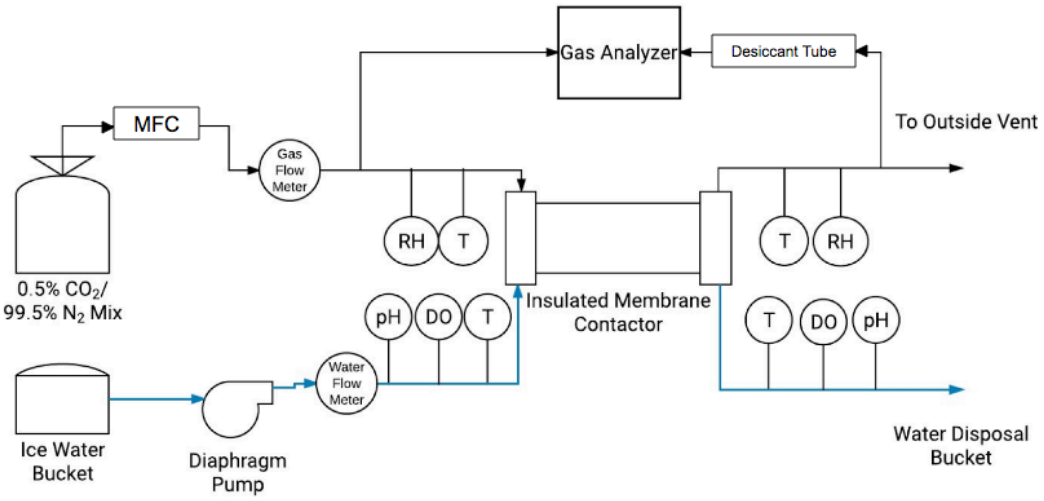


**Figure 61. Schematic of experimental apparatus used for all experimental runs. Both gas and water streams are single-pass through the membrane, as an open-loop system.**

### 7.3.2 Experiment Operation

All experiments had gas flow through the lumen side of the membrane fibers, and water in a shell-side flow configuration. Initially a baseline for the system was characterized. The first experiment replicated the manufacturer's experiment described in the membrane module's data sheet, using room-temperature gas and water (100% $N_2$, aerated tap water). Another gas composition (99.5% $N_2$ and 0.5% $CO_2$) was also used in these gas transfer experiments at room temperature. The simultaneous heat and mass transfer experiments used ice-cold water and a room-temperature gas mixture (again, 99.5% $N_2$ and 0.5% $CO_2$) (Figure 61). Temperatures of the inlet and outlet gas, water, and membrane were allowed to come to steady state (constant temperature within $\pm$ 0.5°C for 2 minutes) before changing gas/liquid flow parameters. Water and gas were not recycled through the

experiment, instead only passing once through the membrane unit. describes the gas and water flow regimes used in the experiment, while Table 25 defines “temperate” and “ice bath” conditions. Every experimental condition was conducted in triplicate for statistical significance. LabView 2015 and NI DAQ products were used to produce gas mixtures, and measure gas/water flow and inlet and outlet gas composition. Windows Microsoft Excel 2016 and MATLAB 2017 were used to calculate heat and mass transfer rates and develop flow equations, using gathered data.

**Table 25. Definition for experimental conditions**

| Experiment Condition | Approximate Input Temperature (K) |
|---|---|
| Temperate | Gas: 296<br>Water: 292 |
| Ice bath | Gas: 296<br>Water: 274 |

### 7.4 Results and discussion

Reflecting the order of the modeling section, results of mass transfer are addressed first, focusing on $O_2$ then $CO_2$. While the ice bath mass transfer results are also discussed in the gas sections, heat transfer across the membrane are the focus of a subsequent section. Data at each experimental condition were used to determine the coefficients of Eq. 14. Final equations are documented in Table 26 and Table 28. Membrane resistance was calculated to account for variation in membrane temperature, but the value was assumed constant through experimental series. Water vapor was expected to transfer into the dry gas feed. Relative humidity of the overall gas stream was measured for personal use, but the results are not reported here.

#### 7.4.1 Oxygen Transfer

Results focusing on the oxygen transfer portion are presented here and compared to the membrane manufacturer-provided transfer data. Equations describing experimental results are tabulated after the data has been presented.

##### 7.4.1.1 Oxygen Transfer with Temperate Inlet Water

After conducting the two series of experiments, one characterizing mass transfer with temperate inlet conditions and the other characterizing mass transfer between a room temperature gas feed and ice-cold water shell flow, the mass transfer for each species was compared to liquid flow rate. The hypothesis that mass transfer

would be more sensitive to liquid flow rate than gas flow rate or membrane characteristics would be readily apparent from this type of plot. Figure 62 compares the oxygen transfer in the temperate and ice bath regime to that of the provided PermSelect data. While the results indicate the module used was less efficient than the advertised data, the comparison established two major observations. Both display a similar downward trend in transferred oxygen as liquid flow increases, and no dependence upon gas flow rate. The negligible change in mass transfer with respect to the gas flow rates supports the assumption that liquid resistance dominates oxygen transfer.

It is expected that if the oxygen stripping system were to be used in a spacecraft environment, oxygen would also be present in the cabin feed gas stream reducing the delta in species concentration across the membrane, and therefore the amount of oxygen transferred.

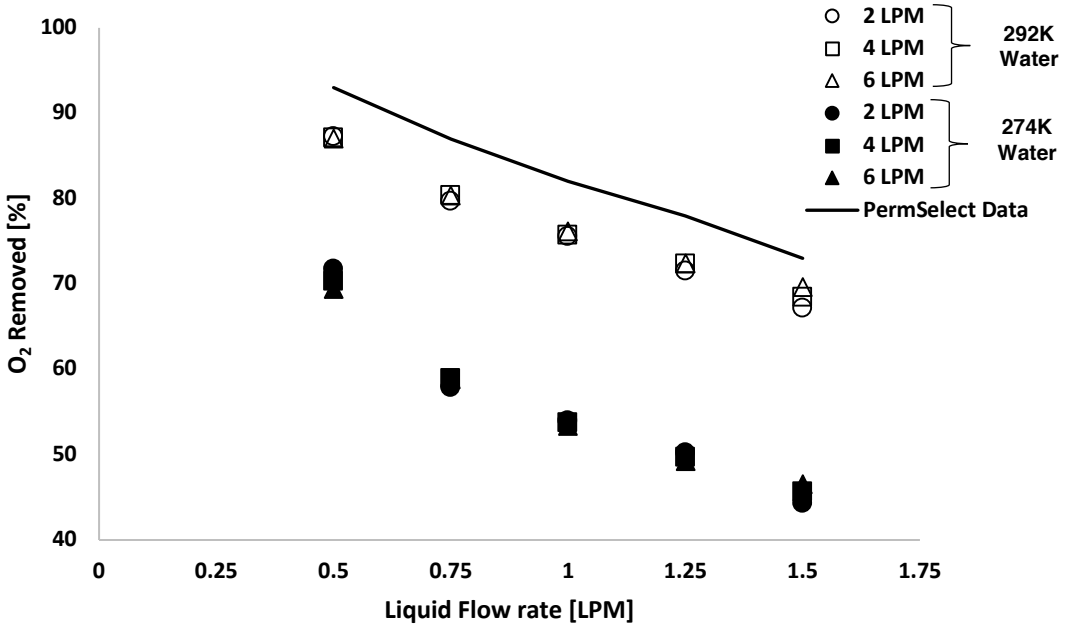


**Figure 62. Percent oxygen removal from water side plotted against the water flow rate for both water conditions. Data is grouped by gas flow rate and water temperature. A curve fitting the PermSelect data is plotted for reference. Each data point is the average of experimental runs at each flow rate. Error bars were omitted for clarity of trends.**

#### 7.4.1.2 Oxygen Transfer with Ice Bath Inlet Water

Referring to Figure 62 the percentage of oxygen transferred from the water to the gas stream during the ice bath case is compared to the liquid flow rate. Diffusivity and membrane permeance values of temperate case equation were modified to capture the characteristics of the ice bath environment. Again, these mass transfer results

are lower than that of the PermSelect data. This lower amount of transfer could be attributed to the temperature-dependent increased solubility and decreased diffusivity of oxygen in water. However, both the resulting temperate and ice bath oxygen transfer data follow the same trend as the PermSelect data and seem to be dominated by liquid flow rates, as seen by the lack of difference in transfer amounts between gas flow rates.

#### 7.4.1.3 Empirical Model for Oxygen Transfer

Liquid resistances for temperate and ice bath cases were calculated using log-log Sherwood vs Reynolds number plots (Figure 63). The Sherwood number correlation was determined using the overall resistance values determined by Eq. 11, removing the membrane resistance calculated with Eq. 12, then converting the liquid resistance to a Sherwood number using Eq. 13. The Sherwood number was then plotted against the liquid Reynolds number in a log-log plot, allowing for the determination of the coefficients found in Eq. 14.

This graph (Figure 63) includes the equation by Kreith and Black, indicating that the empirical results follow the trends for a packed bed. The Sherwood values for the temperate and ice bath conditions are similar across all gas flow rates, demonstrating that a general equation would be appropriate for oxygen and membrane. The developed empirical model uses averaged Sherwood values across both series of experiments, simplifying future calculations. Comparing this resulting model to the Kreith and Black solution in Figure 63, the slopes of the two trend lines are within 70% of each other; reaffirming that the Kreith and Black solution may be an acceptable first-order approximation for this type of membrane. Table 26 presents the final equations for oxygen transport.

Figure 64 depicts the liquid flow rate-normalized results of the temperate and ice bath oxygen transfer experiments (previously presented in Figure 62 as percent transferred). Normalizing the transfer values and concentration values (mg $L^{-1}$) allowed for direct comparison of transfer rates between the two temperature cases, and for simpler utilization in future mission designs.

Two groups of Student t-tests (two-tail, assumed equal variance, independent, $p < 0.05$, $df = 8$) were conducted to investigate if there was a significant change in the amount of $O_2$ transferred between each gas setting, and then between each temperature case. The results of the t-tests for each group suggest that there is no significant difference in the $O_2$ amount of transferred between the gas flow rates of each temperature case, as the null hypothesis cannot be rejected (null hypothesis stating that, “The treatment (fluid temperature, flow rate, etc.) has

no statistically significant effect on the measured parameter"). However, there is a significant difference in the amount of $O_2$ transferred between the two temperature groups (approximately 50% more $O_2$ transferred over the tested liquid flow rates). The matrix of p-values associated with the statistical tests can be found in Appendix E.

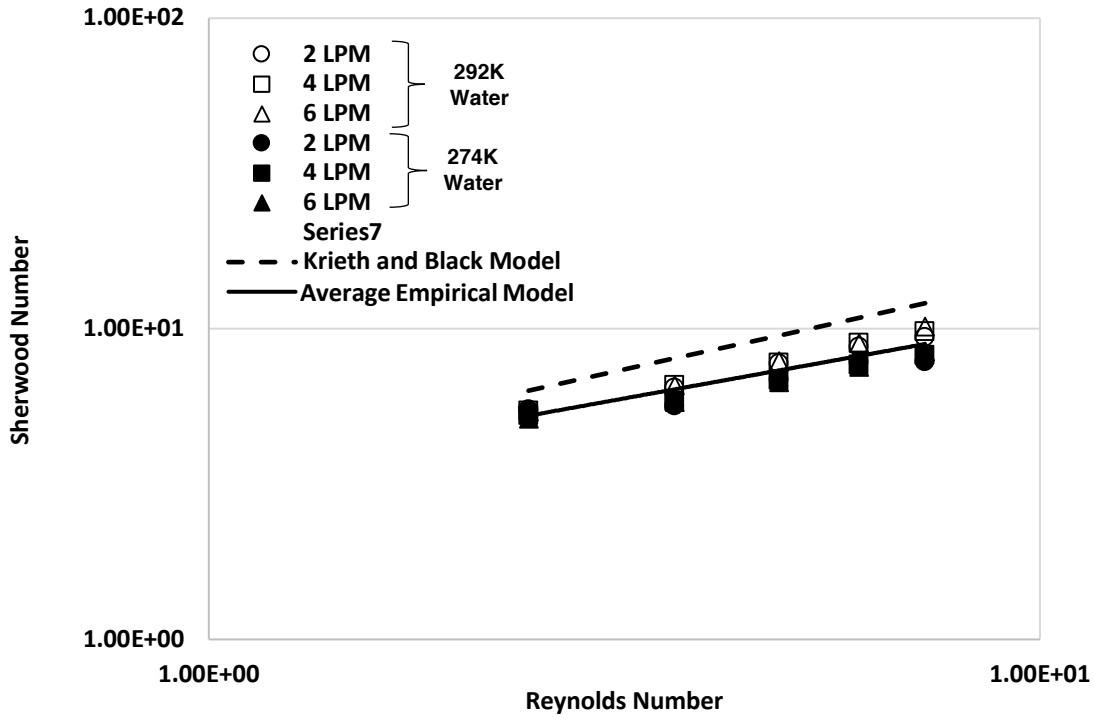


**Figure 63. Correlation of non-dimensional numbers for oxygen transport at laminar flow conditions. Developed oxygen transport model and the Kreith & Black model are shown for comparison.**

**Table 26. Sherwood equations for liquid resistance developed from oxygen transfer data**

| | Correlation | |
|---|---|---|
| Experiment Conditions | This Work | Kreith & Black, 1980 |
| PermSelect | $Sh = 0.52Re^{0.41}Sc^{0.33}$ | $Sh = 0.39Re^{0.59}Sc^{0.33}$ |
| Averaged Empirical Model | $Sh = 0.32Re^{0.48}Sc^{0.33}$ | |

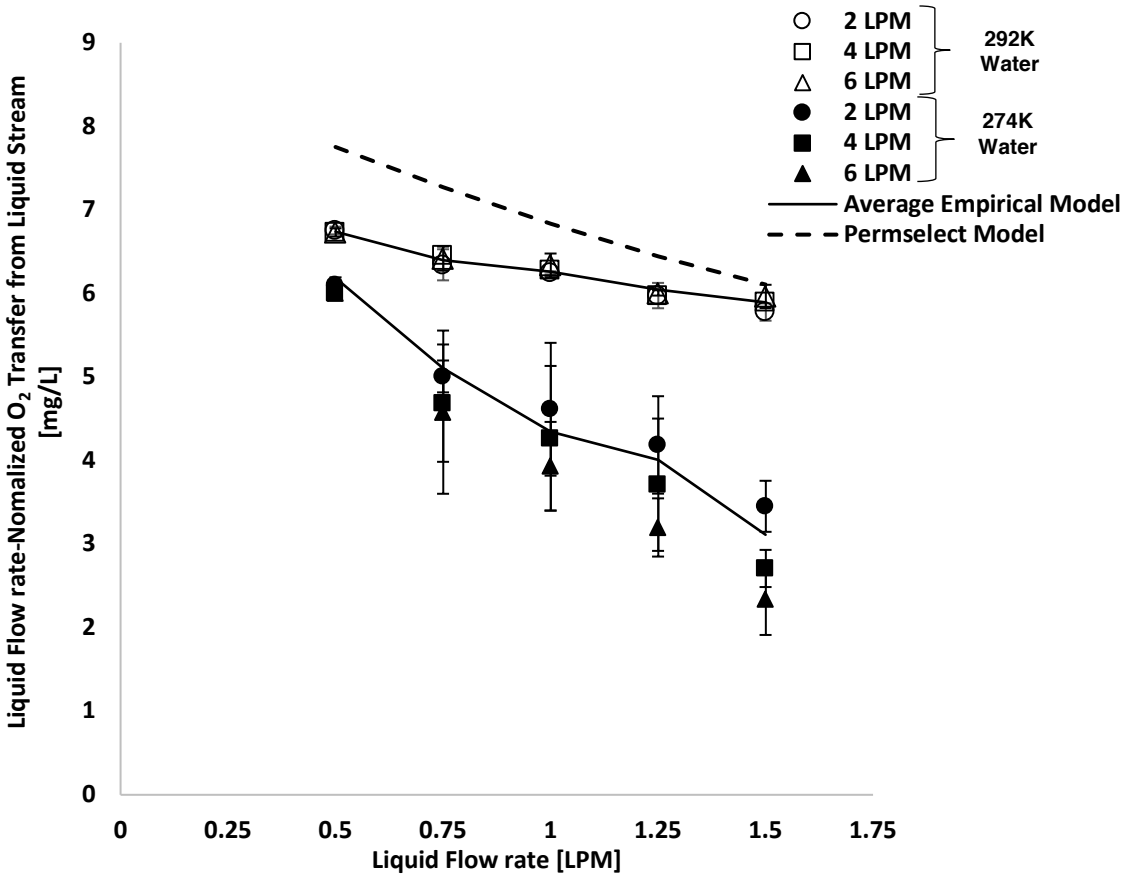


**Figure 64. The liquid flow rate-normalized oxygen transferred from the water stream into the gas stream is plotted against the water flow rates. The average empirical model was fitted to represent both the temperate and ice bath experimental results. The PermSelect model was included for reference. Data points are the averaged results of triplicate experimental runs. Error bars are the standard deviation of these multiple experimental runs.**

### 7.4.2 Carbon Dioxide Transfer

Experimental data was not available from PermSelect for $CO_2$ transport, so diffusivity and permeability coefficients were calculated for $CO_2$ to develop an initial model for transfer across the membrane. However, data from $CO_2$ transfer experiments showed this model to be in error (see Figure 65) and an empirical model, like that for $O_2$, was developed. The over-estimation may be in part due to aeration of the tap water, introducing some $CO_2$ from the atmosphere into the water source. The tap water may also have dissolved minerals and salts that affect $CO_2$ sorption.

From Figure 65, the difference in transfer values for those measured at 2LPM and those at 4LPM and 6LPM indicate there is a non-negligible amount of gas resistance present due to the statistically significant difference between transfer amounts of different gas flow rates (approximately 125% difference).

In the following section, an approach to modeling gas resistance is presented and empirical equations are formulated to describe the resulting $CO_2$ transfer data.

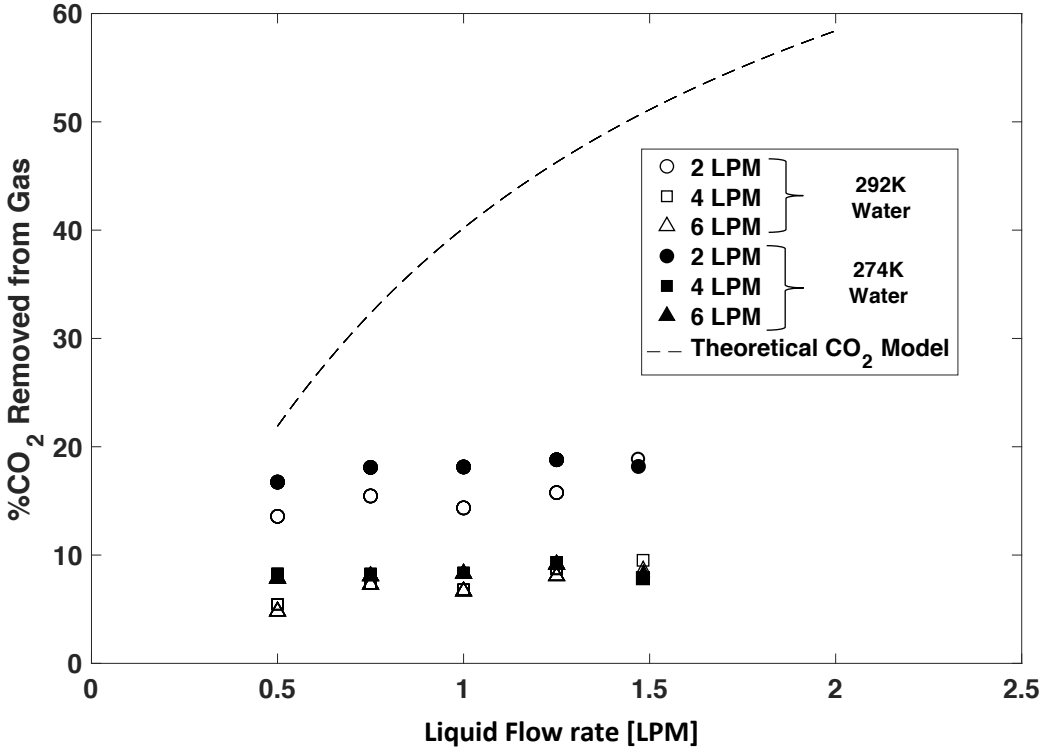


**Figure 65. Carbon dioxide removal data from both series of experiments are plotted versus water flow rate. Theoretical carbon dioxide model is included for comparison. Each data point is the average of experimental runs at each flow rate. Error bars are the standard deviation resulting from multiple runs.**

#### 7.4.2.1 Carbon Dioxide Transfer Modeling with Graetz Number

Carbon dioxide removal from the gas stream by the shell-side water flow was measured by comparing the species' inlet and outlet gas concentrations. Figure 66 shows the $CO_2$ removal against gas flow rate, which suggests that gas flow rate may affect $CO_2$ transfer, contrary to the initial assumption. There is a measurable drop in the $CO_2$ transfer when the gas flow rate is increased from 2LPM to 4LPM, but no further measurable reduction in $CO_2$ transfer when the gas flow rate is increased from 4LPM to 6LPM. A Wilson-type plot was produced (Figure 66) to confirm

that gas flow does affect transfer rates (K. Li, Tai, and Teo 1994). In Figure 66, oxygen transfer does not show sensitivity to gas flow rate, as the percent transferred stays constant across the three gas flow rates (single water flow rate presented, 1LPM). However, $CO_2$ percent transferred decreases as gas flow rate is increased for the same constant water flow rate (1LPM).

Calculating the Graetz number (*Gz*) informed which equation was appropriate to capture gas film resistance through the Sherwood number. Literature suggests the use of the Lévéque equation Eq. 17 for Graetz numbers above 20 (C. Y. Wang et al. 2017).

$$Sh = 1.6151 * Gz^{\frac{1}{3}} \tag{17}$$

Table 27 presents the calculated Graetz numbers for each gas flow within each experimental condition and indicates that Eq. 17 is appropriate for all tested conditions. Resistance of gas into the liquid is also present, as depicted in Figure 65, as $CO_2$ percent transferred changes with increasing water flow rate. After determining the gas Sherwood number with Eq. 17, the film resistance can be calculated with Eq 13. Subtraction of the calculated membrane and gas resistance from the overall mass transfer coefficient Eq. 11 allows for the calculation of the liquid mass transfer coefficient Eq. 13. The internal diameter of a membrane fiber was used as the characteristic diameter to calculate the Sherwood number for gas flow inside the lumen.

Figure 67 shows the resulting correlation of liquid Sherwood number against Reynolds number correlation, after removing gas and membrane resistances from the overall mass transfer coefficient. Differences between the two series of experiments determined the need for water temperature-specific empirical models. These models were also included in Figure 67, demonstrating the need for the series-specific equations through differences in slope and location on plot.

Table 28 presents the Sherwood equations developed from experimental results to calculate the gas and liquid resistance of $CO_2$ transfer across the PDMS membrane. The Reynolds numbers found in Table 28 for the Sherwood number formulas decrease with a decrease in temperature, which would result in a decrease in gas transferred into the liquid side. However, there is an increase of $CO_2$ solubility into water with the decrease of water temperature, the data suggests that this physical characteristic dominates and allows increased $CO_2$ transfer when compared to the temperate series. The Kreith and Black correlation for liquid resistance was included for comparison

to the empirical equations. Contrasting the coefficients used in each equation, it confirms that the equations used for oxygen transfer would not be appropriate to describe $CO_2$ transfer.

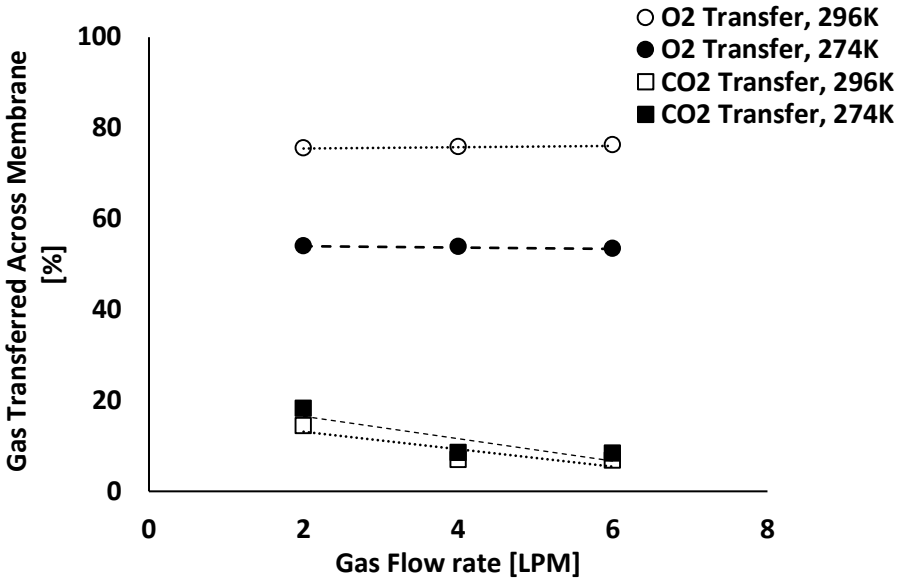


**Figure 66. Testing gas transfer sensitivity to changes in gas flow by plotting transferred concentration against gas flow rate. Water flow rate is 1.0LPM for all plotted data, and marker opaqueness indicates water temperature. Each data point is the average of experimental runs at each flow rate. Error bars were omitted for the clarity of trends**

**Table 27. Calculated Graetz numbers for the feed gas through the lumen for both experiment series.**

| Experimental Condition | Gas Flow rate [LPM] | Graetz Number |
|---|---|---|
| Temperate Experiment<br>Gas: 296K<br>Water: 292K | 2 | 22 |
| | 4 | 43 |
| | 6 | 65 |
| Ice Bath Experiment<br>Gas: 296K<br>Water: 274K | 2 | 48 |
| | 4 | 97 |
| | 6 | 145 |

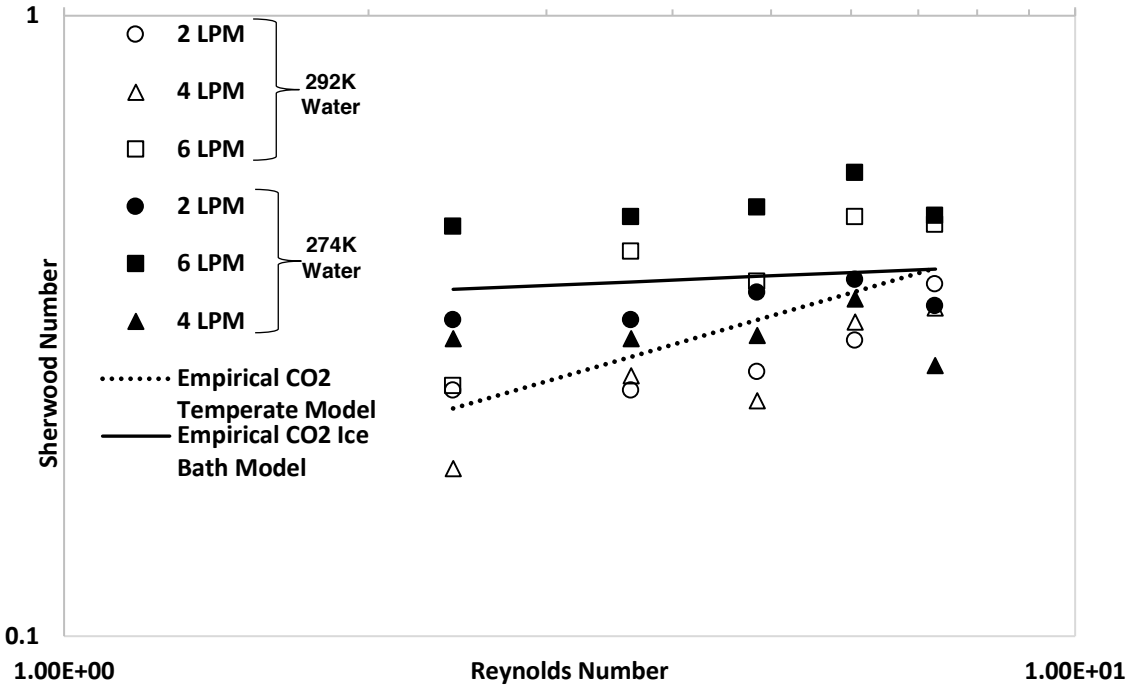


**Figure 67. Water-side Sherwood numbers for both experiment series against their corresponding Reynolds number. Resulting average empirical models for each water condition included for reference.**

**Table 28. Sherwood equations for gas and liquid resistance developed from averaged resulting carbon dioxide transfer data for each liquid temperature case**

| | Gas Correlation | Water Correlation | |
|---|---|---|---|
| Experiment Conditions | Lévéque, 1928 | This Work | Kreith & Black, 1980 |
| Temperate | $Sh = 1.6151Gz^{0.33}$ | $Sh = 0.153Re^{0.47}Sc^{0.33}$ | $Sh = 0.39Re^{0.59}Sc^{0.33}$ |
| Ice Bath | | $Sh = 0.341Re^{0.07}Sc^{0.33}$ | |

#### 7.4.2.2 Empirical Correlation for Carbon Dioxide Transfer from Gas to Liquid Stream

A reduction in $CO_2$ transfer is apparent in Figure 68, after plotting the liquid flow rate-normalized transfer measurements against the liquid flow rate between the tested gas flow rates. The transfer results were Again, this suggests a flow rate-dependent, non-negligible amount of gas-side resistance. Liquid-side resistance is also illustrated in Figure 68 as the amount of $CO_2$ transferred into the liquid stream significantly decreases as the liquid flow rate increases. Differences in the $CO_2$ transfer quantities are prevalent between the two temperature cases, supporting the understanding that media temperature is a non-negligible characteristic in membrane mass transfer. The 6 LPM case for the ice bath experiment showed a higher transfer rate than the tested 2 LPM and 4 LPM.

Gas flow rate-specific models were determined for liquid resistance of each temperature case, and then the coefficients were averaged to obtain a general equation for $CO_2$ transfer. This temperature-specific empirical model gives an estimate of transfer magnitude for all the tested gas flow rates. This suggests that the general model could be used to describe $CO_2$ transfer. However, coefficients specific to each gas flow rate should be use if the models are to be used for more accurate calculations of $CO_2$ transfer.

As in the $O_2$ tests, two groups of Student t-tests (two-tail, assumed equal variance, independent, $p < 0.05$, $df = 8$) were conducted to investigate if there was a significant change in the amount of $CO_2$ transferred between each gas setting, and then between each temperature case. The results of the t-tests for each group suggest that there is no significant difference in the $CO_2$ amount of transferred between the gas flow rates of each temperature case or within each of the temperature cases, as the null hypothesis cannot be rejected (the null hypothesis states, "The treatment (fluid temperature, flow rate, etc.) has no statistically significant effect on the measured parameter"). While the figure suggests that there may be a significant difference, the standard deviation and low degrees of freedom associated with each averaged data point was too great to establish this. The matrix of p-values associated with the statistical tests are found in Appendix E.

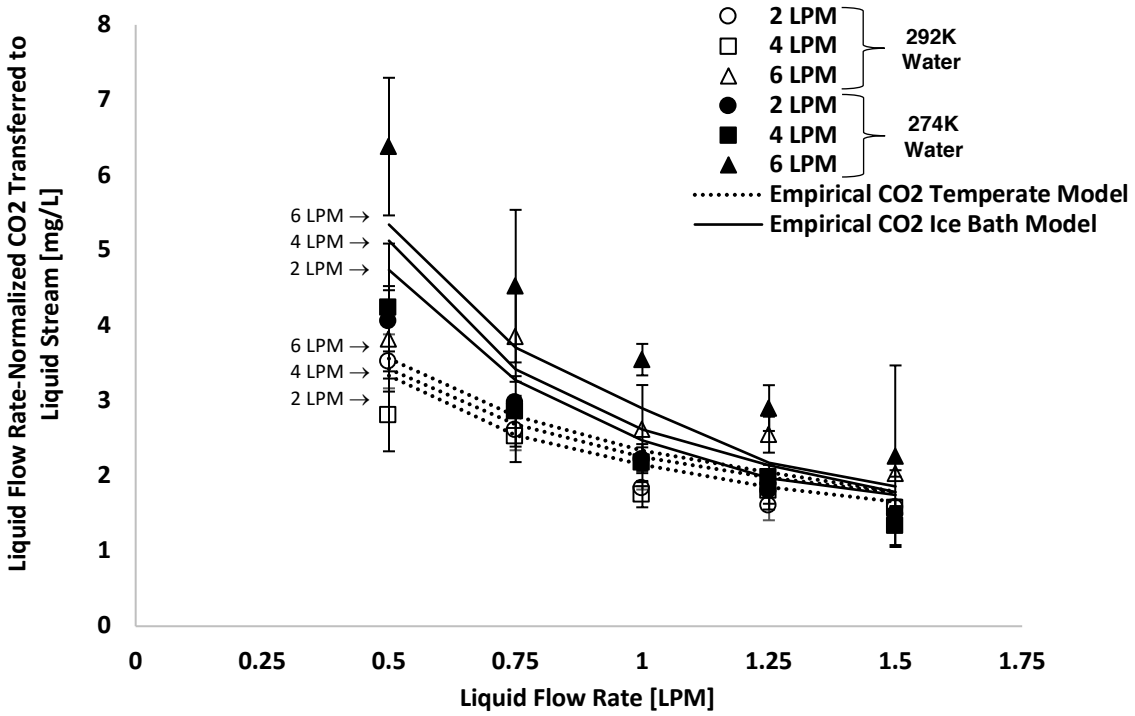


**Figure 68. Liquid flow rate-normalized carbon dioxide removal from the gas phase plotted versus water flow rate for both temperature cases. Empirical carbon dioxide model predictions are included for comparison, each line associated with a gas flow rate is signified with the arrowed text. Each data point is the average of experimental runs at each flow rate. Error bars are the standard deviation resulting from multiple experiment**

### 7.4.3 Heat Transfer

The input and output temperatures were measured for both the gas and liquid streams during temperate and ice bath experiments. Significant differences between inlet and outlet temperature were measured in the gas stream during the ice bath experiments. Using the recorded temperature differences and Eq. 15, 16, the heat transferred across the membrane was calculated. A gas flow rate-dependent correlation using a linear regression was developed for the overall heat transfer coefficient (Eq. 18).

$$U = 3.45 \times 10^{-3}\dot{V} - 3.52 \times 10^{-3} \quad (18)$$

Figure 69 plots the calculated heat transfer rate against the tested gas flow rates. The results confirm the hypothesis that the heat transfer would be most sensitive to changes in gas flow rate, rather than liquid flow rate, and that as

the gas flow rate increased, the heat transfer rate would also increase. The theoretical model, which was Eq. 15 using the maximum possible gas stream temperature delta, was also plotted for comparison. The resulting data followed the trend of the theoretical model; however, the model over-estimated the heat transfer. This was expected, as the theoretical model assumed perfectly effective transfer, with negligible losses. While the membrane unit was insulated, and the experiment was allowed to come to steady state before recording data, heat lost to the environment and thermistor error (± 0.05°C) could have contributed to the lower than predicted rates of heat transfer.

Using a nonselective membrane for gas-liquid contacting with water-based liquid, some amount of water vapor (dependent on the initial relative humidity of the gas stream) permeates to the gas side. This may be an issue for systems using a constant volume of water on the liquid side. The transfer of water vapor modifies the amount of water on the liquid side, either changing the concentration of the fluid (if a media) as well as flow dynamics. Additionally, if there is a temperature gradient across the membrane (in the case of heat transfer) the humidity in the gas stream may condense on the surface of the membrane, possibly modifying flow dynamics, and mass and heat transfer.

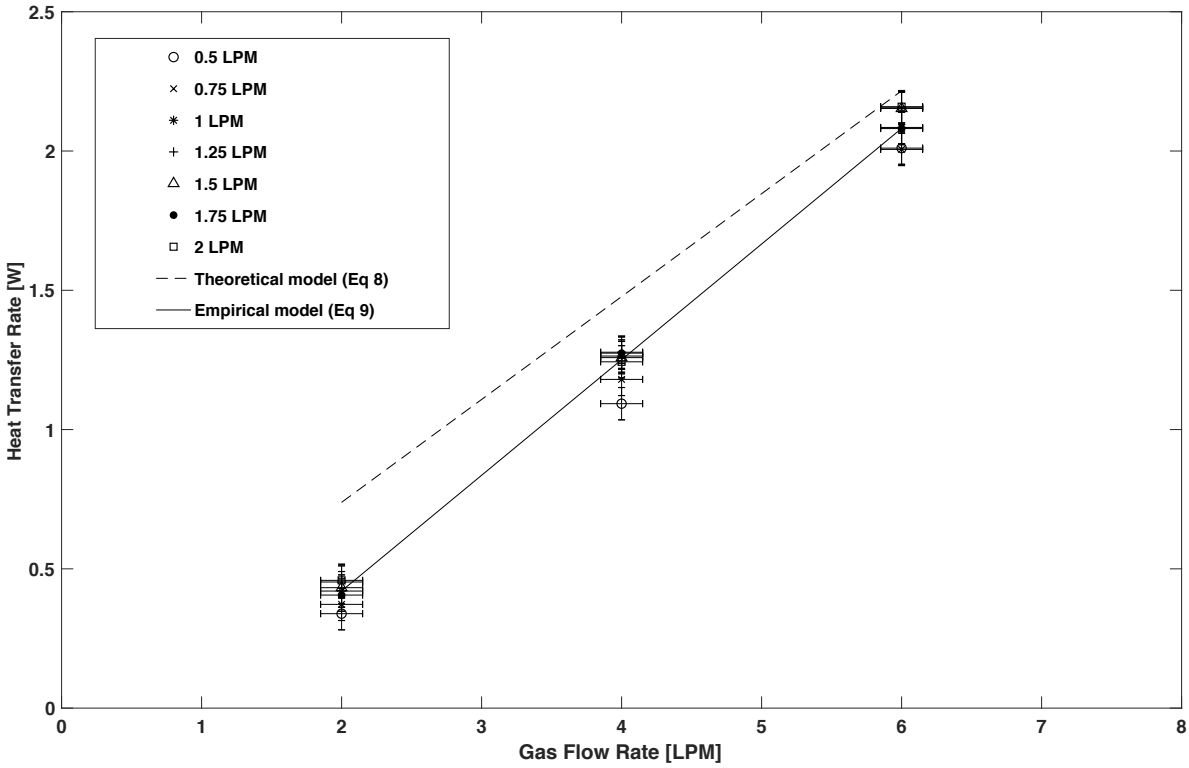


**Figure 69. Overall heat transfer rate for the membrane unit during the ice-bath experiment against the feed gas flow rate, with each water flow rate represented. The theoretical model (Eq. 15) and the log-mean temperature difference solution (Eq. 16) are plotted for reference. Each data point is the average of experimental runs at each flow rate. Error bars are the standard deviation resulting from multiple runs.**

### 7.5 Conclusion

The ability to simultaneously transfer oxygen, $CO_2$, and heat across a nonporous PDMS membrane was characterized experimentally, with the development of empirical models based off of established membrane relations. Overall mass transfer of both species was dominated by water flow rate on the shell-side, while $CO_2$ permeance was also influenced by gas flow rate. Oxygen transfer from the water side to the gas side decreases as water flow increases. A decrease in water temperature also reduces the desorption of oxygen due to the diffusion coefficient dependence on temperature, increasing oxygen solubility. An empirical equation was developed to describe the liquid resistance to mass transfer.

Transfer of $CO_2$ from the gas stream to the water side decreases with an increase of water flow rate, but transfer increases as the water temperature decreases. The diffusion coefficient for $CO_2$ in water is negatively correlated, since cooler water retains dissolved gases better. Gas resistance was important for $CO_2$ transfer, in both

gas, and heat and gas transfer. Resulting trends for $CO_2$ transfer were as expected, suggested by established membrane models. Maximum overall heat transfer was accomplished with the maximum gas flow rate (6LPM) but was not significantly influenced by changes in water flow rate. Operational regimes of this system should depend on the mass and heat transfer requirements of the system. For example, maximum heat transfer, $O_2$ removal, and $CO_2$ would require high gas flow rate coupled with low water flow rates.

## Nomenclature

| | |
|---|---|
| $A$ | interfacial area of membrane ($m^2$) |
| $B$ | overall mass transfer coefficient ($m\ s^{-1}$) |
| $C_{eq}$ | gas species concentration in the liquid in equilibrium with the bulk concentration found in gas ($mg\ m^{-3}$) |
| $C_L$ | gas species concentration found in the liquid ($mg\ m^{-3}$) |
| $C_{CO2in}$ | concentration of carbon dioxide in gas stream inlet (%) |
| $C_{CO2out}$ | concentration of carbon dioxide in gas stream outlet (%) |
| $C_{O2in}$ | concentration of dissolved oxygen in liquid stream inlet ($mg\ L^{-1}$) |
| $C_{O2out}$ | concentration of dissolved oxygen in liquid stream outlet ($mg\ L^{-1}$) |
| $c_p$ | specific heat of fluid ($J\ kg^{-1}\ K^{-1}$) |
| $d_e$ | equivalent diameter of membrane, shell feed $d_e = (4\pi(d_s^2/4 - Nd_{oxygen}/4)/(N\pi d_o)$, lumen feed $d_e = d_i$ (m) |
| $D_g$ | diffusion coefficient of gas species ($m^2\ s^{-1}$) |
| $d_i$ | inner diameter of membrane fiber (m) |
| $d_o$ | outer diameter of membrane fiber (m) |
| $d_s$ | membrane module inner shell diameter (m) |
| $Gz$ | Graetz number, $D_g/LReSc$ |
| $H_{CARBON\ DIOXIDE}$ | Henry's constant for carbon dioxide ($Pa\ m^3\ mol^{-1}$) |
| $H_{oxygen}$ | Henry's constant for oxygen ($Pa\ m^3\ mol^{-1}$) |
| $J$ | mass flux ($mg\ s^{-1}\ m^{-2}$) |
| $K_{CARBON\ DIOXIDE}$ | overall mass transfer coefficient of carbon dioxide ($m\ s^{-1}$) |
| $K_{OXYGEN}$ | overall mass transfer coefficient of oxygen ($m\ s^{-1}$) |
| $k_g$ | mass transfer through gas ($m\ s^{-1}$) |
| $k_l$ | mass transfer through liquid ($m\ s^{-1}$) |
| $k_m$ | mass transfer through membrane ($m\ s^{-1}$) |
| $L$ | effective membrane fiber length (m) |
| $\dot{m}$ | mass flow rate of fluid ($kg\ s^{-1}$) |
| $N$ | number of membrane fibers |
| $P$ | permeability of membrane to species ($mol\ m\ m^{-2}\ Pa^{-1}\ s^{-1}$) |
| $Re$ | Reynolds number, $d_e u\rho/\mu$ |
| $Sc$ | Schmidt number, $\mu/\rho D_g$ |
| $Sh$ | Sherwood number, $k_l d_e/D_g$ |
| $T_{in}$ | fluid inlet temperature (K) |
| $T_{out}$ | fluid outlet temperature (K) |
| $Q$ | volume flow rate of water (LPM) |
| $q$ | rate of heat transfer across medium (W) |
| $U$ | Overall heat transfer coefficient ($W\ m^{-2}\ K^{-1}$) |
| $\dot{V}$ | Volume flow rate of gas ($m^3\ s^{-1}$) |

*Greek Letters*

| | |
|---|---|
| $\alpha$ | Sherwood number equation coefficient |
| $\beta$ | Sherwood number equation coefficient |
| $\delta$ | fiber wall thickness |
| $\phi$ | packing fraction |
| $\mu$ | fluid viscosity (Pa s) |
| $\rho$ | fluid density ($kg\ m^{-3}$) |

## 7.6 Resulting Presentations and Publications

Journal Paper

**Matula, E. E.,** Nabity, J. A. (2019). "Characterization of heat and mass transfer across a nonporous polydimethylsiloxane (PDMS) hollow fiber membrane, "International Journal of Heat and Mass Transfer, [In Preparation].

Conference Poster

47th International Conference on Environmental Systems, "Characterization of heat and gas transfer through a silicone membrane," Charleston, SC, 2017.

# Chapter 8 Operation of a Gravity-Independent Algal Bioreactor Providing Simultaneous Air Revitalization and Thermal Control

## 8.1 Introduction and Background

Parametric experiments have demonstrated aspects of a multifunctional algal bioreactor for ECLSS. *Chlorella* can photosynthesize in dynamic temperature and $CO_2$ concentration environments. Nonporous gas-permeable membranes allow simultaneous mass and heat transfer. The final step integrates these two systems to test operation of the system within the previously determined environmental ranges and identify potential design challenges.

Using a membrane to culture algal cells, with the intent of spaceflight purposes has been investigated before (I. Wagner et al. 2016; L. H. Fan et al. 2008; Mori et al. 1987). The gas permeable membrane has proven attractive for bubble-free gas transfer in a microgravity setting. Early designs separated the gas provision system (membrane) from the main bioreactor for ease of irradiance (Javanmardian and Palsson 1992). The advancement of LEDs and illumination systems specific for plant growth have led researchers to opt towards culturing inside the membrane system instead of separating out the two. This reduces the footprint and volume of the bioreactors, which is appealing for space-constrained spacecraft.

Chapter 7 mentioned that the distillation industry regularly uses membranes to execute membrane distillation, stripping away chemicals from exhaust streams (Schofield, Fane, and Fell 1987). The approach is economical since the membranes are able to simultaneously transfer heat and mass while maximizing the contact area to system volume ratio (dependent on packing and contactor diameter, varying between 1500-3000 $m^2/m^3$) (Westerterp, van Swaaij, and Beenackers 1984). While these membranes are typically porous (allowing for greater mass transfer), Chapter 7 reported the simultaneous heat and mass transfer capabilities of a nonporous membrane.

This chapter presents the developed benchtop photobioreactor designed to minimize gravity-dependent effects and utilizes materials and components appropriate for the spacecraft cabin environment. Design and material selection considerations are also described. The benchtop system was used to test spacecraft operational regimes for simultaneous air revitalization and thermal control. Three experiments were executed using this system:

a short test (12 days) cycling both inlet $CO_2$ concentrations (replicating human respiration) and temperature (replicating algal operation in the thermal control loop), a constant inlet $CO_2$ concentration test with cycled temperature (7 days), and an additional $CO_2$ and temperature cycling test but for a longer duration (21 days). The longer duration test data is presented and discussed here, investigating the potential of using the system for an extended period (data for shorter tests are located in Appendix F). Issues arising from both the design and the experiments are also described. Finally, suggestions for future implementation and design improvements are offered.

## 8.2 Design Considerations

Utilizing the photobioreactor in a spacecraft or surface habitat environment requires considerations for use in microgravity and confined environments.

### 8.2.1 Operational

Table 29 outlines operational challenges experienced during spaceflight that could directly impact a photobioreactor system. Solutions to each identified issue were implemented in the benchtop design.

**Table 29. Necessary considerations for utilizing a photobioreactor in microgravity and spaceflight environments**

| Environmental Parameter | Issue | Solution |
|---|---|---|
| Microgravity | Chaotic bubble formation | Gas-permeable membranes, non-bubble forming |
| | Lack of natural convection | Pressurized gas, fans, and diaphragm pumps |
| Confined Space | Volume/surface area limited | Gas-permeable membrane, repurposing ISS cooling loops |
| Location of Habitat | LEO, transit to Mars, Lunar or Martian Surface | Closed loop for minimal resupply |

### 8.2.2 Hardware

Referencing the inputs and outputs of an algal culture outlined in Chapter 3, Table 30 was developed to map necessary hardware to inputs or functions of the bioreactor. The environmental parameters from Table 29 were referenced during the design selection of Table 30.

**Table 30. Hardware selected for a bioreactor system design in microgravity**

| Input or Function | Design Selection | Reasoning |
|---|---|---|
| Movement of Fluid | Diaphragm pump, flippers inside reactor | Less cell stress |
| Illumination | Fluorescent plant bulb | Emittance curve matches absorbance curve, fits in environmental chamber |
| Containment | Annular reactor | Wraps around bulb for efficient light utilization, minimal corners for flow stagnation |
| Material Selection | Acrylic tubing, plastic components | Nonreactive with culture |
| Media Temperature Control | Stainless steel wort chiller | Nonreactive material, thermal control |
| Gas Provision | Nonporous gas permeable membrane | Gravity independent, resistant to biofouling, simultaneous heat and mass transfer |
| Sampling | Sample-port box | Easy access to culture, allows for addition of nutrients |

## 8.3 Materials and Methods

### 8.3.1 Culture and Associated Hardware

Non-axenic *Chlorella vulgaris* from the continuously maintained culture from the Bioastronautics Lab was used in all experiments. Bristol's media was used as the diluting media. All experiments, except for the 25-day experiment, started with a $10^6$cell/mL (OD = 0.03 Abs) culture, the 25-day experiment started with a much denser culture (OD = 0.5 Abs) to test system sustainment of a dense culture.

The combined membrane/reactor system (made in duplicate, one for temperature cycling and one as a control) had three major components, the algal photobioreactor, chiller loop, and membrane contactor (Figure 70).

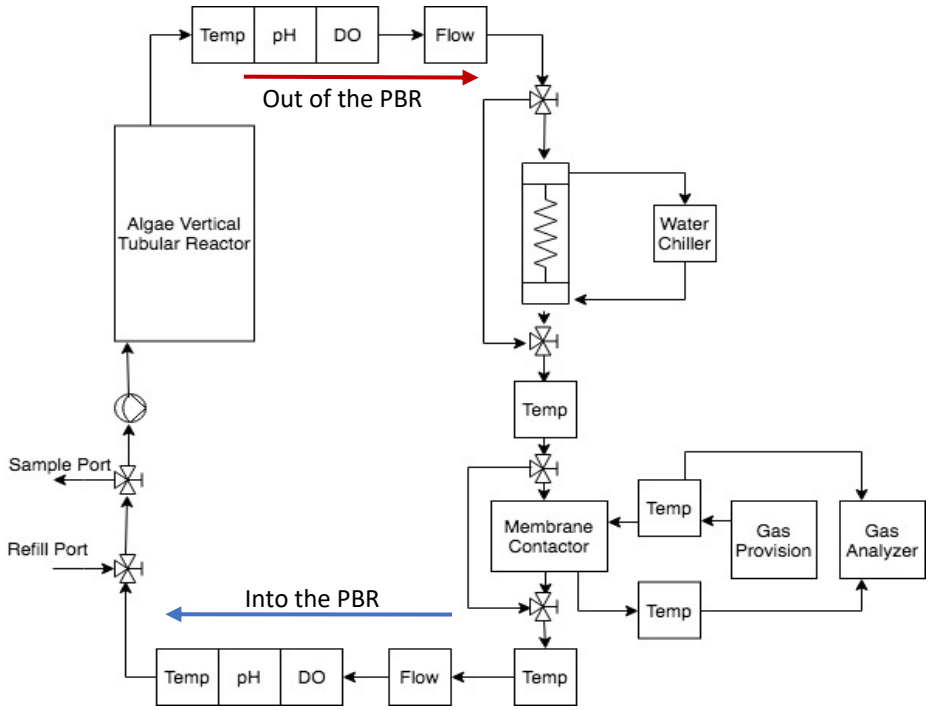


**Figure 70. P&ID for the combined air revitalization and thermal control benchtop system appropriate for microgravity environments.**

The annular photobioreactor was made out of clear acrylic and was sized to be 1L. The spacing between the outer and inner wall was equal to the maximum penetration length, or 1 cm, reported by Palsson (Lee and Palsson 1995). The plant-specific fluorescent bulb described in Chapter 4 was inserted through the center of the annulus (Figure 71).

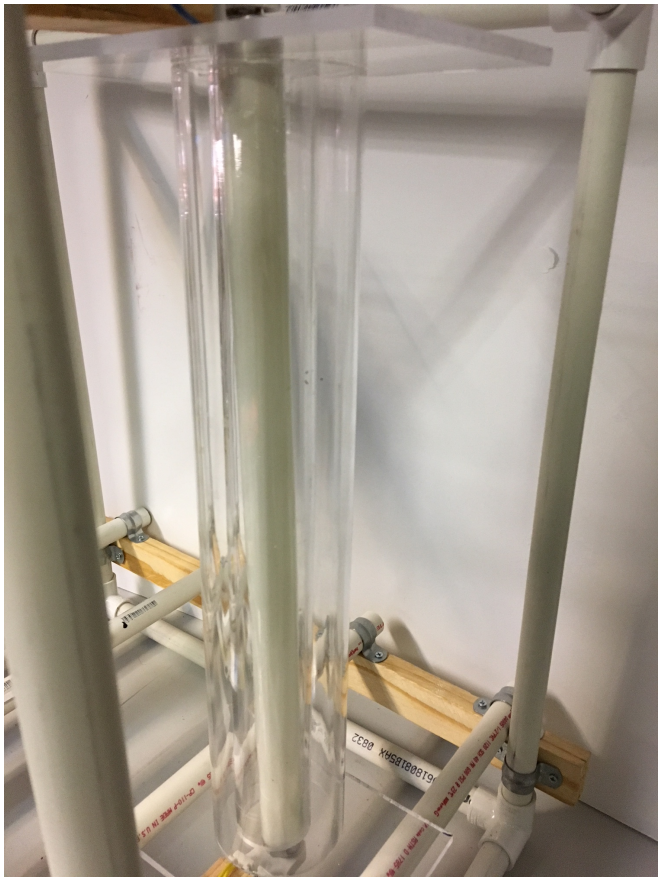

**Figure 71. Fluorescent plant bulb inserted into acrylic annulus on support stand.**

A horizontal reactor would likely reduce the potential effects of gravity gradients; however, the reactors were oriented vertically to fit within the dimensions of the environmental chamber in the Bioastronautics Laboratory. A diaphragm pump (1GPM, SHURflo) used in the Chapter 6 experiments, pumped the algal media up through the bottom of the reactors. A small angled vane was glued over the inlet port to help induce mixing within the reactor (Figure 72).

**Figure 72. Plastic vane glued to bottom of acrylic annulus, over the inlet port (boxed).**

Repurposed stainless steel, counterflow wort chillers (B07GSHZ34Y, Northern Brewer), in conjunction with a propylene glycol chiller (c50p, ThermoHaake), controlled the temperature of the algal medium. The same PermSelect membranes, gas analyzer, aluminized insulation, thermistors, and NI DAQ system from the simultaneous heat and mass transfer experiments of Chapter 6 were used in this system. The vertical tubular reactors were placed inside of an environmental chamber (Elite G, Russell Environmental Chambers) to be kept at a constant 19°C (Figure 73). The gas provision system used the same setup with MKS mass flow controllers and NI products as the gas provision system in Chapter 6. Unfortunately, in the middle of the experiment, the $CO_2$ sensor of the gas analyzer stopped working and was replaced with a different $CO_2$ sensor (EZO-CO2, Atlas Scientific).

**Figure 73. Vertical tubular bioreactors filled with dense culture, placed in environmental chamber. Start of long-term culturing experiment. Lighting at the top of the environmental chamber is for photographic clarity only and were turned off during the experiment.**

### 8.3.2 Experiment Design

#### 8.3.2.1 Variables and Conditions

The general purpose of this experiment was to test the system operation, and to identify operational or scaling challenges. Additionally, the starting culture density and $CO_2$ provision were varied to observe their effect on operation. Effects of algae and nutrients on operation were also studied, since the heat and mass transfer experiments of Chapter 7 were with water. Table 31 outlines the operational parameters and highlights independent variables. One of the photobioreactors (PBRs) was held at a constant 19°C as the control case, while the other experienced temperature cycles using a temperature profile that replicated the thermal loop (Chapter 5). The $CO_2$ provision control system was updated with new LabView code for this series of experiments, and allowed for $CO_2$ cycling, matching Figure 74, that shows the $CO_2$ profile used in the short-term and long-term tests. An additional

experiment was conducted using a steady-state 0.285% $CO_2$ concentration for comparison. $CO_2$ concentration values used for the cycling profile are found in Table 22.

**Table 31. Membrane photobioreactor operational settings.**

| System Parameter | Setting |
|---|---|
| Liquid Flow rate | 0.5 SLPM |
| Liquid Temperature | 4°C-28°C (cycled temperature), or 19°C (control) |
| Gas Flow rate | 4.5 SLPM |
| Gas Temperature | 23°C |
| $CO_2$ Concentration* | 0.12-0.45 (cycled), or 0.285 (constant) |
| Environmental Chamber Temperature | 19°C |
| Illumination Level | 280 µmol $m^{-2}$ $s^{-1}$, 24hr |
| Initial Culture Density* | Optical Density = 0.03Abs (constant), 0.5Abs (cycled) |

***Values used in experiments with either constant or cycled levels of $CO_2$**

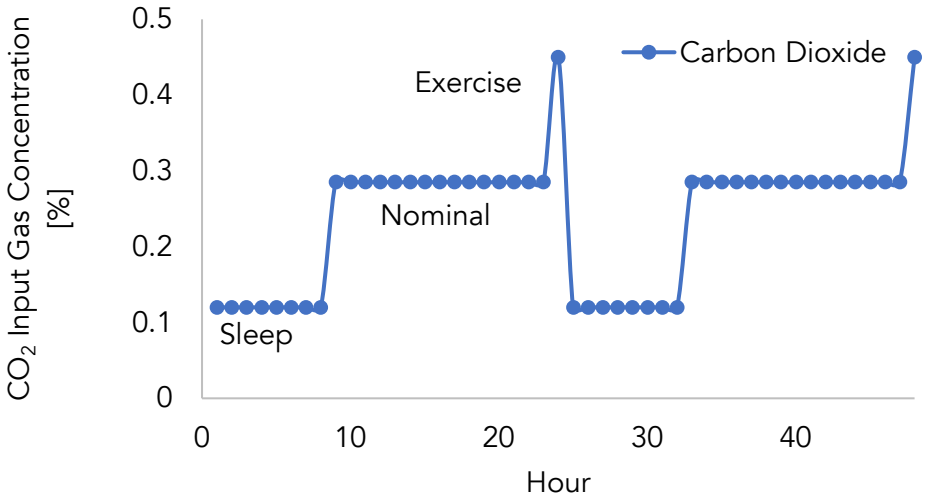


**Figure 74. Carbon dioxide concentration profile for concentration-cycled experiments. The levels are labeled with their respective conditions.**

#### 8.3.2.2 Test Procedure

Calibration of all necessary probes (dissolved oxygen and pH), per manufacturer's instructions, occurred before cleaning the probes. A hydrogen peroxide ($H_2O_2$) solution was made from 30% $H_2O_2$ and DI water, the final concentration of $H_2O_2$ was approximately 10%; the maximum allowable concentration of hydrogen peroxide for the silicone membrane fibers. Each reactor system was filled with the $H_2O_2$ solution and was pumped through the closed-loop system for at least 3 hours. The solution was drained, and the system was filled with clean DI water that was then allowed to circulate for an hour. The rinse cycle was then repeated. A dilute culture (Bristol's media and Bioastronautics Lab culture) was prepared in a sanitized 5-gallon bucket. The bioreactors were filled with the diluted

culture, the input gas was turned on, and the measuring system started. Pre-set gas cycles, controlled by LabView 2015, were fed into the membrane system. At two separate times (day 5 & day 12-13) in the "long-term" experiment the buffer air was accidentally shut off, which meant 100% $CO_2$ at a very low flow rate (approximately 0.3 SLPM) was fed into the membrane. This was an accidental disruption to the controller's $CO_2$ concentration cycle and can be seen as a drop in dissolved $O_2$ on day 5 and day 12 in Chapter 7.4.1.

#### 8.3.2.3 Measurements

##### 8.3.2.3.1 Continuous Measurements

The inlet and outlet media streams for each bioreactor had a sensor sweep containing pH, DO, temperature, and flow rate sensors (EZO-pH, Atlas, EZO-DO, Atlas, DS18B20, Dallas Temperature Control, Liquid Flow Meter 828, Adafruit respectively), and had a sampling rate of 0.2Hz. The data were sampled by an Arduino Mega at 0.2 Hz and stored in an Excel 2016 spreadsheet. The membrane had inlet and outlet sensors on the gas and liquid side. The dissolved $O_2$, pH, and water temperature were measured using the same sensors as the bioreactor sensor sweep. Gas stream temperature was measured using the same thermistors as Chapter 6 (MC65F103AN, Amphenol Advanced Sensors).

##### 8.3.2.3.2 Non-continuous Measurements

Before daily samples of culture were taken, DI water was added to the system to replace water vapor lost through the membrane. The date, time, and amount of water added were recorded in a lab notebook. Daily cell counts, optical density, and photosynthetic yield measurements were conducted in the same manner as in Chapters 4 and 5. Photosynthetic yield measurements were taken in triplicate each day, to allow for a standard deviation per day. Gas concentration ($CO_2$ and $O_2$) measurements were taken for the inlet and outlet streams of each membrane module system. The gas concentration measurements for the temperature cycled reactor were taken at the hottest and coldest point of a temperature cycle, to capture any effects of temperature on the outlet gas concentration.

#### 8.3.2.4 Data Processing

The recorded data were saved daily. The Bristol's baseline was removed from the dissolved oxygen measurements. The averages for each continuous variable were determined using the same protocol as Chapter 4. Photosynthetic quotients were determined using the measured values of $CO_2$ and $O_2$ for the inlet and outlet streams of each bioreactor and calculated using the same protocol as presented in Chapter 6. Heat transfer rates used the temperatures and gas flow rates collected via the NI DAQ system. Heat transfer data for a selected 4-6 days per

experiment (beginning, end, and a few intermittent days) was processed the same format as Chapter 7 to determine heat transfer rate. Student's t-test (independent, 2-tail, equal variance, equal sample size) was utilized when appropriate with a confidence interval of 95% ($p<0.05$). Multiple measures were averaged, and the standard deviation reported as the error. Linear regressions were used to detect changes in measurement deltas through the experiment. Microsoft Excel 2016 and the included Data Analysis package executed the statistical analyses. The null hypothesis for the statistical tests states "The treatment or independent variable has no statistically significant effect on the measured parameter" for all tested cases.

Data and measurements are presented as "into Photobioreactor (PBR)" and "out of PBR" to indicate direction of media flow. "Into the PBR" means the media is moving out of the membrane system, past the measurement probe and into the illuminated PBR. "Out of the PBR" means the media is leaving the illuminated PBR, flowing past the measurement probe and into the membrane system (Figure 70). Results and data for the long-term experimental run (25-day) are presented in this chapter's result section, unless noted otherwise.

## 8.4 Results

### 8.4.1 Photosynthetic Quotient

The photosynthetic quotients of the two bioreactors were calculated in the same manner as Chapter 6.4.1. Changes between the inlet and outlet stream of $CO_2$ and $O_2$ of each reactor were used to calculate daily PQ values. Figure 75 shows the average of all the PQ values over the 25-day experiment for each reactor (control and temperature-cycled), error bars are the standard deviation of the overall experiment. A Student's t-test (independent, 2-tail, equal variance, $p<0.05$) was implemented to determine any significance between the two bioreactors (control and temperature-cycled). The test with respect to temperature was unable to reject the null hypothesis ($t = 2.0$, $p = 0.12$, $df = 42$). This suggests that bioreactor temperature does not have an effect on the rates of $CO_2$ consumption or $O_2$ production. The Quantek 902P gas analyzer was used to measure the $O_2$ in the gas stream, and $CO_2$ was measured by the new Atlas $CO_2$ sensor (with a higher resolution of 0.0001%, accuracy 30ppm). It is hypothesized that using the Quantek gas analyzer for the $O_2$ measurement (resolution is 0.1%) contributed to the variance. However, when compared to values found in the literature for similar operational conditions, the range of

PQ's bounded by the error bars are within the range of those reported values (E. B. Sydney et al. 2011; Eduardo Bittencourt Sydney et al. 2013).

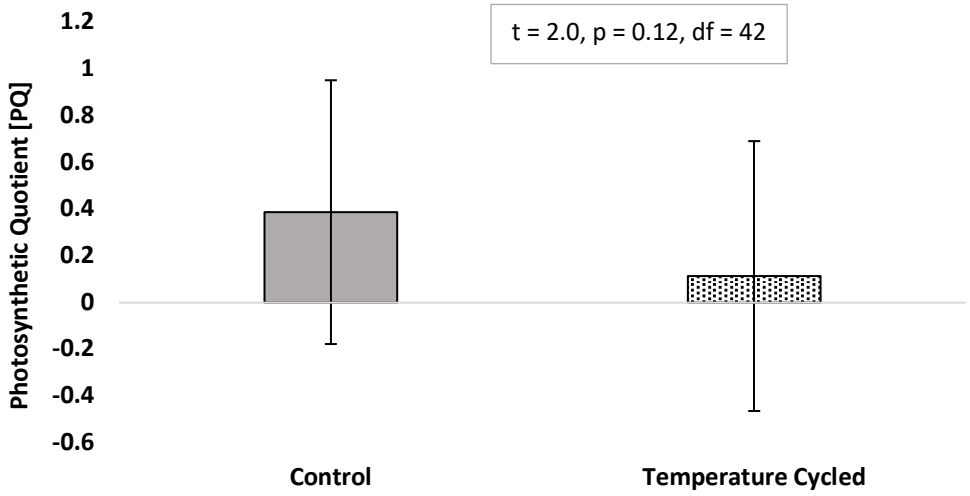


**Figure 75. Photosynthetic quotient average for the long-duration experiment is separated between the control and temperature cycled reactor. The error bars are the standard deviation of the PQ values for the 21-day experimental run.**

### 8.4.2 Optical Density

The two cases (control and temperature-cycled) depicted in Figure 76 suggest the membrane actively filtered cells from the media. This is corroborated with Figure 77, showing the membrane at the beginning and end of an experimental run. Both cases in Figure 76 have the same operational conditions, but one had an initial dilute culture (top) while the other was much denser (bottom). Each data point represents an average of experimental runs at each time stamp. Error bars are the standard deviation of the averaged data. While a statistical comparison of the optical density of the two photobioreactors was conducted (Student's t-test (independent, 2-tail, equal variance, $p<0.05$) with ($t = 0.43$, $p = 0.67$, $df = 48$)) and unable to reject the null hypothesis, due to the filtering of the biomass, it is believe that this is not a valid representation of the optical density of the overall culture.

The dilute culture experienced an initial drop in optical density but began to recover back to initial conditions by the end of the 12-day experimental run. The denser culture slowly decreased in optical density until it reached a plateau and sustained the same optical density (0.03 Abs) for 15 days. The measured absorbance was above the sensing threshold of the spectrophotometer, or 0.001 Abs (Thermo Scientific Multiskan FC, Fisher Scientific). The membrane was observed to filter algae from the culture, but some biomass did remain in the reactor.

The optical density measurements may also indicate a balance of operational conditions, growth rate, filtering, and cell density.

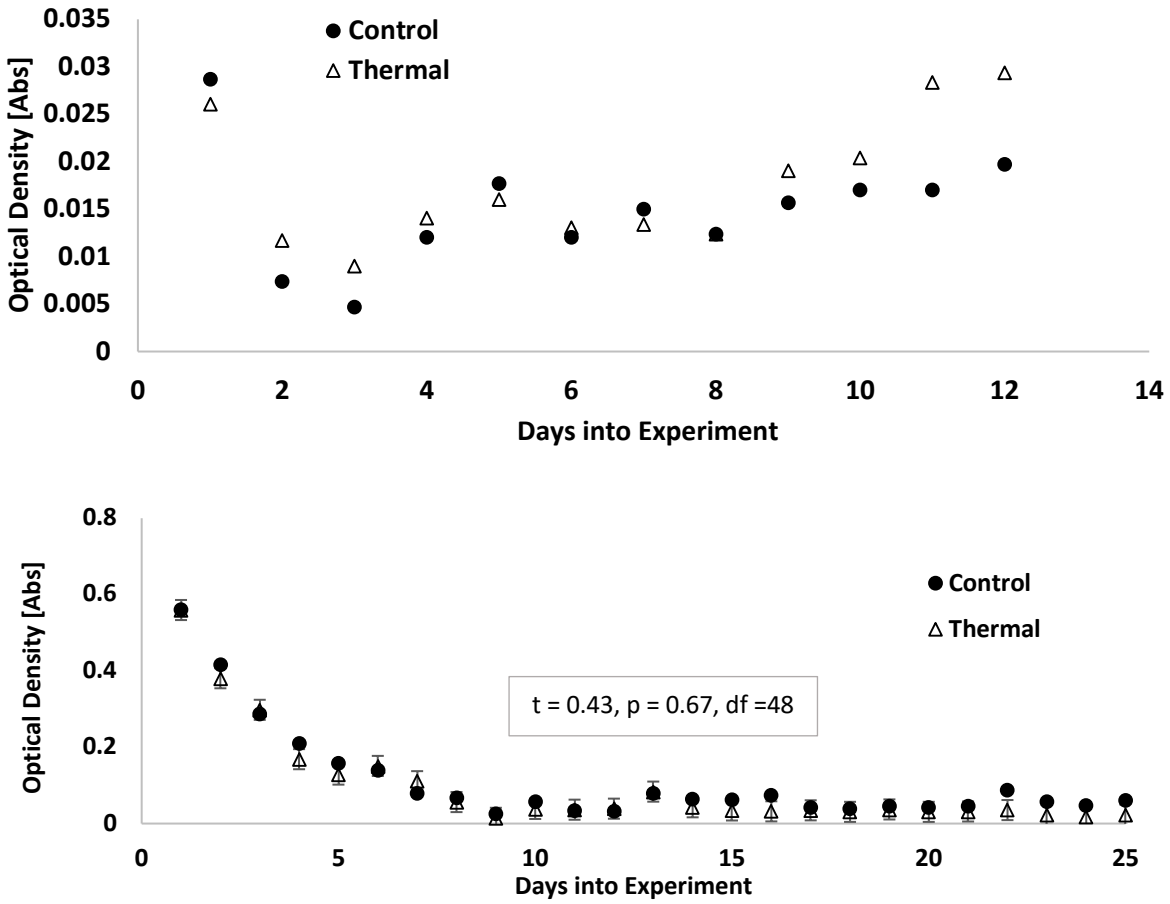


**Figure 76. The optical density for both cases (same operational process, cycled gas concentrations and temperature cycle). One experiment was operated for 12 days (top figure), while the other for 25 (bottom figure).**


**Figure 77. The nonporous membrane actively filtered out cells from the photobioreactors. New membrane before the start of an experimental run (left) and the same membrane at the end of the 25-day trial (right).**

### 8.4.3 Photosynthetic Yield

The control and the temperature cycle case trend together for photosynthetic yield. The acclimation period for this system took approximately 10 days, from which both systems returned within 10% of the initial fluorometry values. A slight increase in yield values was noted on days 6 and 13, after the known, accidental spikes in $CO_2$ content. An independent Student's t-test was conducted to compare the photosynthetic yield of the two reactors (2-tail, equal variance, $p<0.05$). The results were unable to reject the null hypothesis ($t = 2.0$, $p = 0.68$, $df = 46$). This suggests that the same photosynthetic yield values result, regardless of temperature environment. A two-way ANOVA was not conducted due to the lack of replicate experiments, but Figure 78 suggests that yield does vary with time, which reflects the results of Chapter 4. Each data point represents an average of experimental runs at each timestamp. Error bars are the standard deviation of triplicate measurements recorded each day.

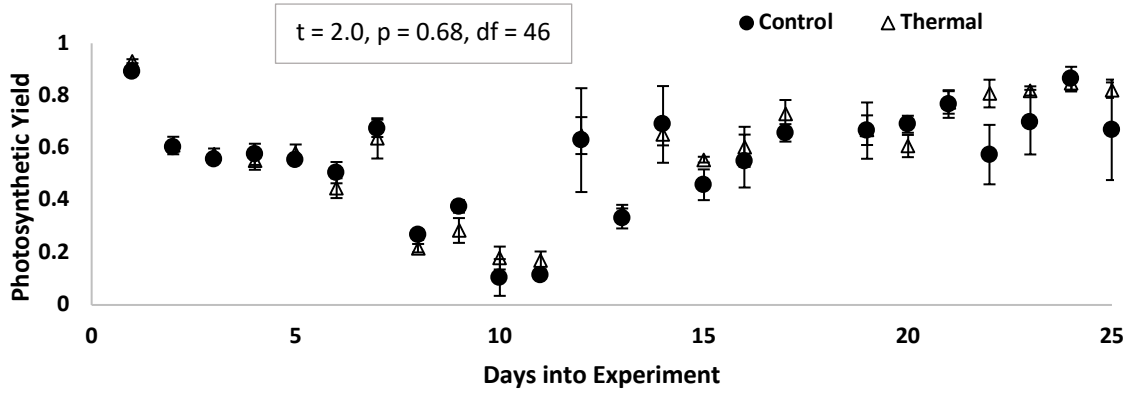


**Figure 78.The photosynthetic yield for the long-term experiment. Error bars are the standard deviation of the average of daily triplicate measurements.**

### 8.4.4 Gas Transfer

A raw value comparison of the $CO_2$ gas transferred across the membrane and the $CO_2$ gas supplied to the membrane indicated steady values across the duration of the experiment (Figure 79). The amount of $CO_2$ transferred across the membrane was calculated from the difference of the inlet and outlet gas concentrations. A linear regression was conducted between the inlet $CO_2$ concentration and the concentration delta values of each of the bioreactors ($p<0.05$). The $R^2$-value indicates that both reactors have a significant correlation between input and delta $CO_2$ concentrations. This is confirmed through an F-test and p-values (Control: $F = p = 5.9x10^{-27}$, df = 20; Temperature cycled: $F = p = 4.4x10^{-14}$, df = 21). This ability to reject the null hypothesis suggests that the accumulation of biomass did not have a significant effect on the mass transfer capabilities of the overall system.

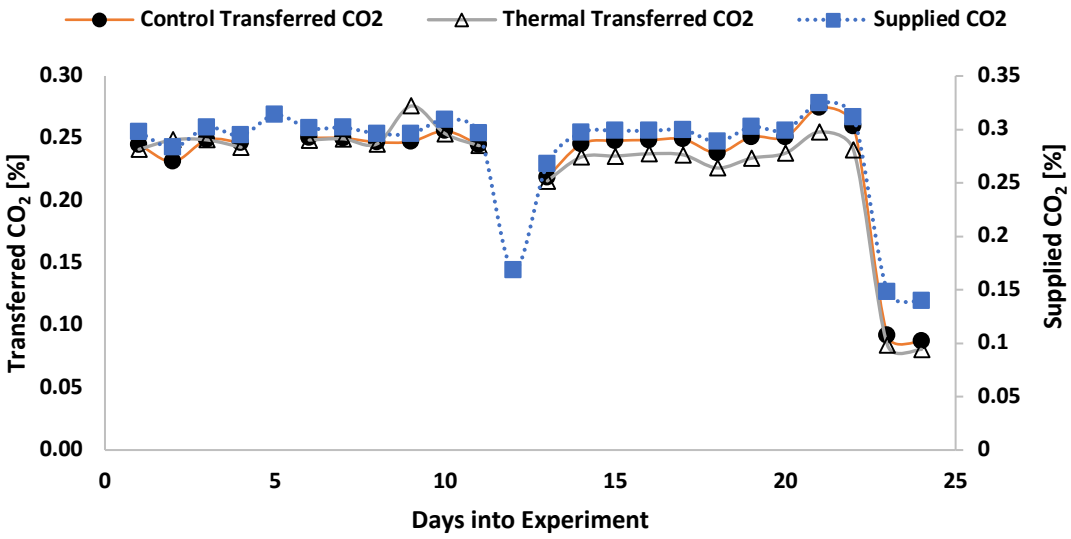


**Figure 79. $CO_2$ transferred across the membrane for all experimental cases is compared to the supplied $CO_2$. Plotted along experiment duration to check for any decline in transfer.**

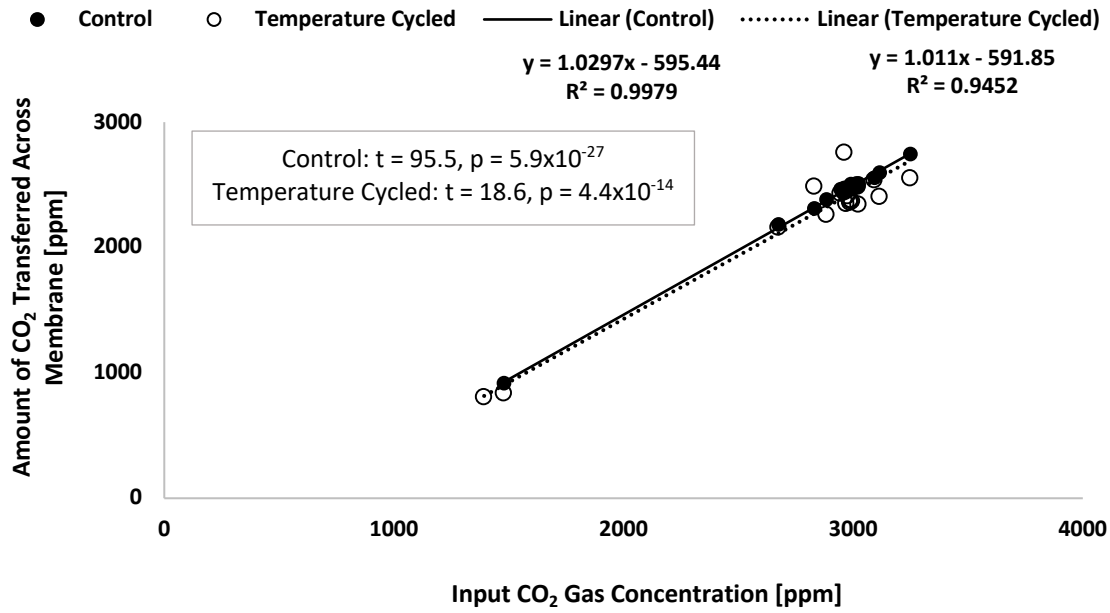


**Figure 80. Linear regression maps $CO_2$ transferred across the membrane [ppm] to initial $CO_2$ concentration. R-values indicate the "goodness" of the linear fit. (Linear regression: $p<0.05$, df = 21)**

### 8.4.5 Heat Transfer

Heat transfer across the membrane was calculated with values from the thermally-cycled photobioreactor, since the control photobioreactor was kept at a constant 19°C. Figure 81 depicts the calculated heat transfer over

the duration of the long-term case (25-day), graphed against the model result (q = 1.27W ± 0.33W) from the overall heat transfer equation presented in Chapter 6. Values were averaged when the feed water temperature was below 6°C; a regime predicted to maximize heat transfer. The horizontal solid line is the Chapter 6 model prediction given the experiment's operational regimes; the dashed lines are the corresponding uncertainty bounds for the model. The dotted line is the linear regression of the experimental data. Error bars reflect uncertainty contributed from the gas temperature sensors and gas flow meter.

The empirically determined heat transfer rates were significantly less than predicted by the model. It was hypothesized that this may be due to the buildup of biomass in the membrane. A linear regression was fitted to the data to investigate any degradation in heat transfer performance due to the biomass buildup. However, the positive slope and low $R^2$ value are not significant enough to confidently determine if there was any performance degradation. However, the overlapping error bars suggest that the heat transfer rate may be constant across the experiment duration. Algal cells are mainly comprised of water (86-91%), which may have similar heat transfer properties to the water-based media, explaining the similarity in heat transport for these two experiments (Tran, Chen, and Chang 2013).

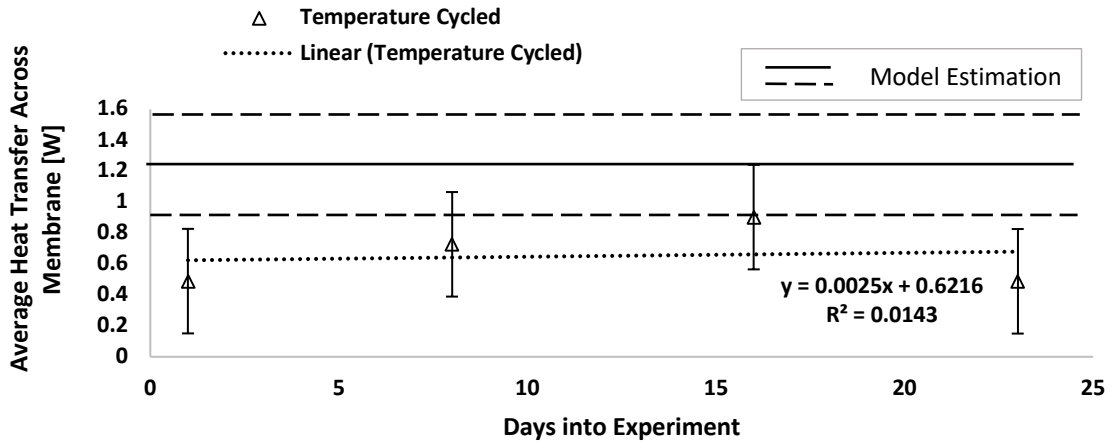


**Figure 81. Heat transfer across the thermally cycled membrane over the duration of the 25-day experiment. The solid line is the model estimation, with the error range of the model in dashed lines**

### 8.4.6 Relative Humidity

It was acknowledged that water vapor would permeate through the membrane during the duration of the experiment. The daily need to replenish bioreactor volumes corroborated this, after checking the units for any leaks.

The measurements taken for water lost through vapor transport were recorded for an understanding of the system, not a comparison of the two operational cases. Replenishment volumes averaged approximately 125mL $d^{-1}$ for the control reactor and approximately 100mL $d^{-1}$ for the temperature cycled reactor. It is hypothesized that the gas stream's dew point would fluctuate with the cycling water temperature, changing the amount of water vapor absorbed by the gas stream (Ch 7). Changing the gas stream's temperature affects the gas's relative humidity, and may reduce the amount of water lost out of the system (Kawasaki 2019).

### 8.5 Discussion

This system was an initial attempt at combining air revitalization and thermal control within a single bioregenerative system. During the design phase of this reactor, it was hypothesized that the selected commercially available membrane could filter out the biomass. It was decided that if the biomass was filtered into the membrane that it would also give insight into the operational capabilities of the membrane system, and if stable gas transport rates and ratios would still be attainable. The membranes did filter out biomass but did not have a significant effect on the amount of $CO_2$ or $O_2$ transferred across the membrane.

The average PQ values between the two cases were not significantly different over the course of the experiment. The variance for both cases were broad relative to the averaged value, however, these results still fell within the range of PQ values reported in the surveyed literature. It is hypothesized that this broad variance is a result of the resolution of the $O_2$ sensor in the gas analyzer.

It is uncertain if heat transfer was significantly affected by the buildup of biomass in the membrane. Some of the resulting heat transfer values are significantly lower than those calculated by the empirical model developed in Ch 7 (Eq 18). Additional heat transfer values could be calculated with the remaining data to investigate the data's fit to the model, since some resulting values did overlap with the model and were within the model uncertainty. However, there was not a significant degradation in the transfer values as the biomass continued to collect in the membrane.

The original design of the photobioreactor was modified to take the results of these experiments into consideration. Originally, the bioreactor was separate from the contacting membrane because it was hypothesized that the reactor would parallel the operation and installation of the current cooling loops in the ISS, encircling the

cabin interior and absorbing environment heat. However, the results of the experiment showed biomass collected in the membrane and it's not clear if the separate bioreactor was actually beneficial to the entire system. While it was the only location for the culture to receive irradiance in this design, this could be modified to irradiate the membrane module instead. Literature has suggested that the culturing could be entirely supported through just the membrane module (L. Fan et al. 2007). The culture should continue to be free-floating in the entire system (not actively restrained to the membrane module through filters or other barriers), as this minimizes necessary parts in the system, but with the understanding that a majority of the culture is trapped in the membrane.

This system also used a semi-continuous approach to algal culturing. Daily removal of biomass (for measurements) and addition of media and water (to replenish culture volume, and nutrients) allowed the culture to operate in a semi-steady state. Continuous culturing would have had a constant removal and replenishment stream, reflecting the operation of a chemostat. This could be automated in a spacecraft system, but for the purposes of benchtop validation, the semi-continuous approach was more appropriate. If a continuous design were desired for a spacecraft, an approach to biomass harvesting should also be considered.

### 8.6 Conclusion

An algal photobioreactor was designed to support simultaneous air revitalization and thermal control in reduced gravity and microgravity environments. A benchtop version of this design was prototyped and used in three different experimental runs. This accomplished two functions, testing the benchtop version of the design and investigating the effects of the photobioreactor on the air revitalization capabilities of a culture when using this type of bioreactor for culturing. It was observed that the commercially available nonporous membrane filtered out the biomass but was able to continue to transfer heat and gas within statistical boundaries of the nominal (no biomass) operation case. System stability in dynamic operational conditions was observed through the reactor's ability to return to nominal after accidental increases in supplied $CO_2$ concentration. This system was able to support a *Chlorella* culture with nominal photosynthetic yield for 25 days, suggesting the ability to sustain culture health while imparting temperature and $CO_2$ cycles reflective of the spacecraft atmosphere, which addressed the original purpose of the experiment.

### 8.7 Resulting Publications

Conference Poster

Matula, E. E. (2015) Design of a membrane photobioreactor for air revitalization and thermal control of a spacecraft cabin, AIAA Rocky Mountain Annual Technical Symposium, Golden, CO.

Matula, E. E. (2015) Design of a membrane photobioreactor for air revitalization and thermal control of a spacecraft cabin, 45h International Conference on Environmental Systems, Seattle, WA.

# Chapter 9 Feasibility of Utilizing an Algal Photobioreactor for Bioregenerative ECLSS in a Spacecraft Cabin or Surface Habitat Environment

## 9.1 Introduction

With almost 20 years in Low Earth Orbit (LEO), the International Space Station (ISS) continues to be the longest duration human spaceflight project to date. Over the course of the Station's history, hardware and systems have been upgraded to reflect advancements in science and technology. Typically, these upgrades involve increased system efficiency or reliability, or decreased volume or power consumption. Nonetheless, environmental control and life support (ECLS) systems are typically single function. The inclusion of ECLS systems with multifunction capabilities could provide the benefits of robust, closed loop ECLS systems to human spaceflight.

By their very nature, algal photobioreactors are multifunctional. They can potentially revitalize air, provide food, treat wastewater, provide radiation shielding, and be part of the thermal control system. This could offer improved reliability, along with consumable and power savings, when compared to the current ECLSS technologies on the ISS. It may also reduce the number of actuated components, which are the most likely to fail in a system, by instead using laminar flow and capillary action for fluid movement.

Photosynthetic systems metabolically respond to changing environmental factors such as: temperature, irradiance, mixing, $CO_2$, $O_2$ content, and pH in real-time. This could give system control to the crewmembers and provide increased efficiency in certain cabin environments. Due to algae response to dynamic environments, a certain level of autonomy could be expected. For example, an increase in respired $CO_2$ (and consequently an increase in $O_2$ consumption) induces an increase in algal $O_2$ production.

The following discussion compares the use of an algal photobioreactor as an ECLS system to the current ISS ECLS system for the following functions, air revitalization, wastewater management, food production, radiation shielding, and thermal control. Specifications of technologies used on the ISS, including mass, power, and volume, were used as a baseline for comparison. The assumption of sustaining a crew of six males, 70 kg/person, defined the human metabolic requirements. Where applicable, the NASA Baseline Values and Assumptions Documentation (BVAD) provided values concerning current spaceflight systems or metabolic standards.

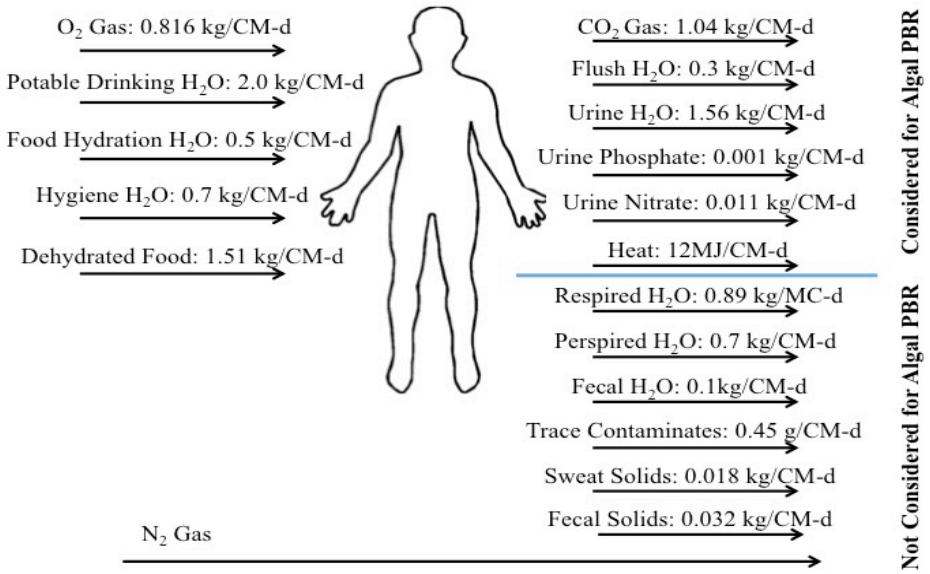


**Figure 82.The metabolic inputs and outputs of one 70kg male human (Anderson et al. 2018)**

In Figure 82 the metabolic requirements for one 70kg male crewmember per day is presented for reference (Anderson et al. 2018). While all aspects of the human metabolic inputs and outputs are presented in the figure, not all wastes are considered in the algal photobioreactor ECLS system for this discussion. These items do not have a direct involvement with an algal photobioreactor system and, in this study, are instead processed by the current ISS technologies specific to those wastes.

In an effort to standardize all the compared systems, the species *Chlorella vulgaris* was used for all algal systems. This allows for the investigation of the hypothesis that one algal system could fulfill multiple functions. Tailoring a species selection for a specific function produces single-function systems and parallels the current ISS single-function approach.

The algal photobioreactor system mass and volume values presented in the following tables include the amount of algae medium required to fulfill a functionality requirement and the estimated amount of infrastructure. The infrastructure estimate was calculated using a scaling constant developed by referencing the ISS cooling loop, since it is the ISS system closest in design to an algal photobioreactor. The percentage of the total mass that was water was determined and used as a scaling constant to size equipment for algal medium volumes. The density of

the algae and algal medium was assumed to be 1021 kg/m$^3$ based off of the mass of a cell and common cellular densities (Tuantet et al. 2014).

Algal system power requirements presented in the tables were calculated by scaling a terrestrial algal system used in Dr. Bernhard Palsson's research to the size appropriate for a space system. The culturing techniques used in Dr. Palsson's experimental photobioreactor are gravity independent, and are the same used in the discussed benchtop photobioreactor (Javanmardian and Palsson 1991). These estimated values need to be verified through experimentation and updated as necessary. The conclusion of this report assesses the feasibility of using an algal system as a replacement for multiple ECLS systems, and it is expected that as culturing technology evolves, this feasibility will advance.

### 9.2 Air Revitalization

The crew metabolic requirements dictating the production of these systems are detailed in Table 32 (Anderson et al. 2018). It was assumed that the metabolic rates are constant over time and per crewmember. For the purpose of this study, trace contaminants and humidity control were excluded from the atmospheric requirements.

#### 9.2.1 Current ISS Air Revitalization Technologies

Air revitalization on the ISS follows a very distinct flow of operation. First the air is pulled into the Carbon Dioxide Removal Assembly (CDRA) system, and scrubbed of $CO_2$, and scrubbed air is pushed back out into the cabin. The Sabatier reaction receives the removed $CO_2$, and with the addition of hydrogen ($H_2$), reduces it into methane ($CH_4$) and water ($H_2O$). Finally, the water is electrolyzed for the release of $O_2$ into the cabin.

**Table 32. Average metabolic atmospheric requirements for a crew of 6.**

| Item | Amount for Crewmember (kg/CM-d) | Amount for Crew of 6 (kg/d) |
|---|---|---|
| Input $O_2$ | 0.82 | 4.89 |
| Output $CO_2$ | 1.04 | 6.24 |

The following assumptions were made while compiling the air revitalization tables. The rates presented are constant over time in the ISS. Data for ISS components have not been scaled to support a certain crew size, but instead the current, on-orbit data is listed. This is able to support at least the assumed crew of six.

**Table 33. I/O for ISS CDRA system.**

| | Item | Amount |
|---|---|---|
| Input | Air ($m^3$/day) | 833 |
| Outputs | Consumed $CO_2$ (kg/day) | 6.3 |
| | Scrubbed Air ($m^3$/day) | 828 |

### 9.2.2 Carbon Dioxide Removal Assembly (CDRA)

The Carbon Dioxide Removal Assembly (CDRA) is the first step of the current air revitalization process on the ISS. Cabin air is pulled into the CDRA, flows through a desiccant bed, and a $CO_2$ adsorbent bed. The scrubbed air flows through a second desiccant bed before returning to the cabin to re-humidify the stream. When the zeolite adsorbent is saturated with $CO_2$, the air stream is diverted to a second $CO_2$ adsorbent bed, and the first bed is regenerated using a pressure/swing method. The released $CO_2$ is then fed into a Sabatier reactor for reduction. Table 33 details the input and output flow rates of the scrubbed air and consumed $CO_2$ (Sherif and Knox 2005; Knox and Stanley 2015; Coutts et al. 2015).

The CDRA system was supposed to require maintenance no more than once every three years, but due to zeolite dust contamination and pump failure, the system has failed more than four times in a year, on average. One of the main concerns with the CDRA system is the propagation of zeolite dust through the system. This clogs filters and creates friction in CDRA blower bearings (Gentry and Cover 2015). Each of these repairs requires extra consumables, including crew time.

### 9.2.3 Sabatier System

Prior to the Sabatier system installation, the captured $CO_2$ was vented overboard as waste. The Sabatier system uses $CO_2$, provided by the CDRA, and supplied hydrogen to synthesize $H_2O$ and methane $CH_4$. At this time, $CH_4$ is treated as a waste product and vented overboard. The water is stored either for potable use or to be reduced into oxygen and hydrogen by electrolysis. The $CO_2$ consumption rates and water production rates are presented in Table 34 (Abney and Mansell 2011; Gatens et al. 2015; Samplatsky et al. 2011).

**Table 34. I/O for ISS Sabatier system.**

| | Item | Amount (kg/day) |
|---|---|---|
| Inputs | $CO_2$ | 6.25 |
| | $H_2$ | 0.39 |
| Outputs | $H_2O$ | 2.49 |
| | $CH_4$ | 1.03 |

For the Sabatier reaction, the major consumable is hydrogen. It is delivered to the system as a product from water electrolysis. Methane is vented overboard because there are currently no onboard plans for its utilization. The Sabatier reaction is exothermic, which means it produces heat during the chemical reaction. The resulting reaction temperature can exceed 500°C. A portion of the waste heat is used to warm up the Sabatier reactants before initiation through the reaction, while the rest of the heat must be removed by a condensing heat exchanger. In addition to these wastes, the low recovery rate of $O_2$ (about 50%) also reduces the overall effectiveness of the system (Gatens et al. 2015).

### 9.2.4 Water Electrolysis System

Oxygen and hydrogen are currently produced on the ISS by way of water electrolysis. Water can be supplied from the Sabatier reaction, and the wastewater processing system. Current is passed through an electrochemical cell. The cathode reduces water to produce $H_2$, while the water around the anode oxidizes and produces $O_2$. This is by use of a proton exchange membrane, transporting the hydrated protons from the anode to the cathode side (Zoulias et al. 2004). The amount of $O_2$ produced per day is detailed in Table 35 (Bagdigian and Cloud 2005). Excess $O_2$ can be stored for later use, and produced $H_2$ can be used to fuel the Sabatier reaction (Gentry and Cover 2015).

**Table 35. I/O for ISS Electrolysis System**

| | Item | Amount (kg/day) |
|---|---|---|
| Input | $H_2O$ | 10.3 |
| Outputs | $O_2$ | 9.2 |
| | $H_2$ | 1.14 |

### 9.3 Algae for Air Revitalization

Algae readily consume $CO_2$ and water to produce $O_2$ and biomass. Since the beginning of human spaceflight history, researchers have been interested in using algae for ECLS systems due to their high $CO_2$ turnover efficiency. Unfortunately, they did not have the illumination technology to produce the highly dense cultures needed to support the crew aboard spacecraft or within the available volume on station. As culturing techniques have progressed, algae have become more viable for photosynthetic bioreactors. An example of the reduction rates of $CO_2$ and $O_2$ production is given in Table 36 (Javanmardian and Palsson 1991). This particular experiment cultured a relatively high cell density of $8x10^8$ cells/mL in order to produce these reduction rates. A concentrated gas stream (5% $CO_2$ v/v) was provided to the system to support this density. The highest densities seen today are $10^9$ cells/mL and are typically limited by irradiance penetration of the entire culture (about 1cm) (Javanmardian and Palsson 1991; Eckart 1995).

Algae require nitrate and phosphate to sustain the biomass. There have been some studies on using urine to provide these nutrients, but typically they are added to the algal medium as a consumable (Jaatinen, Lakaniemi, and Rintala 2015). The resulting biomass could be considered a waste, if it is not processed into nutritional supplements for the crew or suspended in media for radiation shielding use.

**Table 36. I/O for photobioreactor for air revitalization.**

| | Item | Amount (g/L-day) |
|---|---|---|
| Input | $CO_2$ Consumption | 2.84 |
| | Nitrate | 0.26 |
| | Phosphate | 0.74 |
| Output | $O_2$ Production | 3.85 |
| | Biomass Productivity | 1.5 |

### 9.4 ISS Requirement as Fulfilled by Algae

Using the $CO_2$ consumption rate and $O_2$ production rate recorded during Palsson's high culture density experiment, and the metabolic requirements of a crew of six, the amount of algae required for human sustainment was calculated (Anderson et al. 2018; Javanmardian and Palsson 1991). Table 37 shows that additional liters of algae

are necessary to provide for the oxygen requirements previously shown in Table 32. Fulfilling the oxygen requirement will necessitate an additional $CO_2$ source, as the metabolic fuel will become a limiting factor.

Figure 83 suggests an approach to integrate an algal photobioreactor into the ISS. It is assumed that the cabin air fed to the gas membrane contains a high enough concentration of $CO_2$ to support algal cultures, and the $O_2$ removed by the gas removal membrane could be vented directly into the cabin. Cabin air used in the membrane that is not depleted of $CO_2$, below the allowable maximum (0.5% v/v), is recirculated through the membrane. (Cronyn, Watkins, and Alexander 2012) This is compared to the current ISS technology operation. The operational temperatures of various components have been detailed, to highlight the extreme operational temperatures of the ISS system versus the ambient operational temperatures of the algal system.

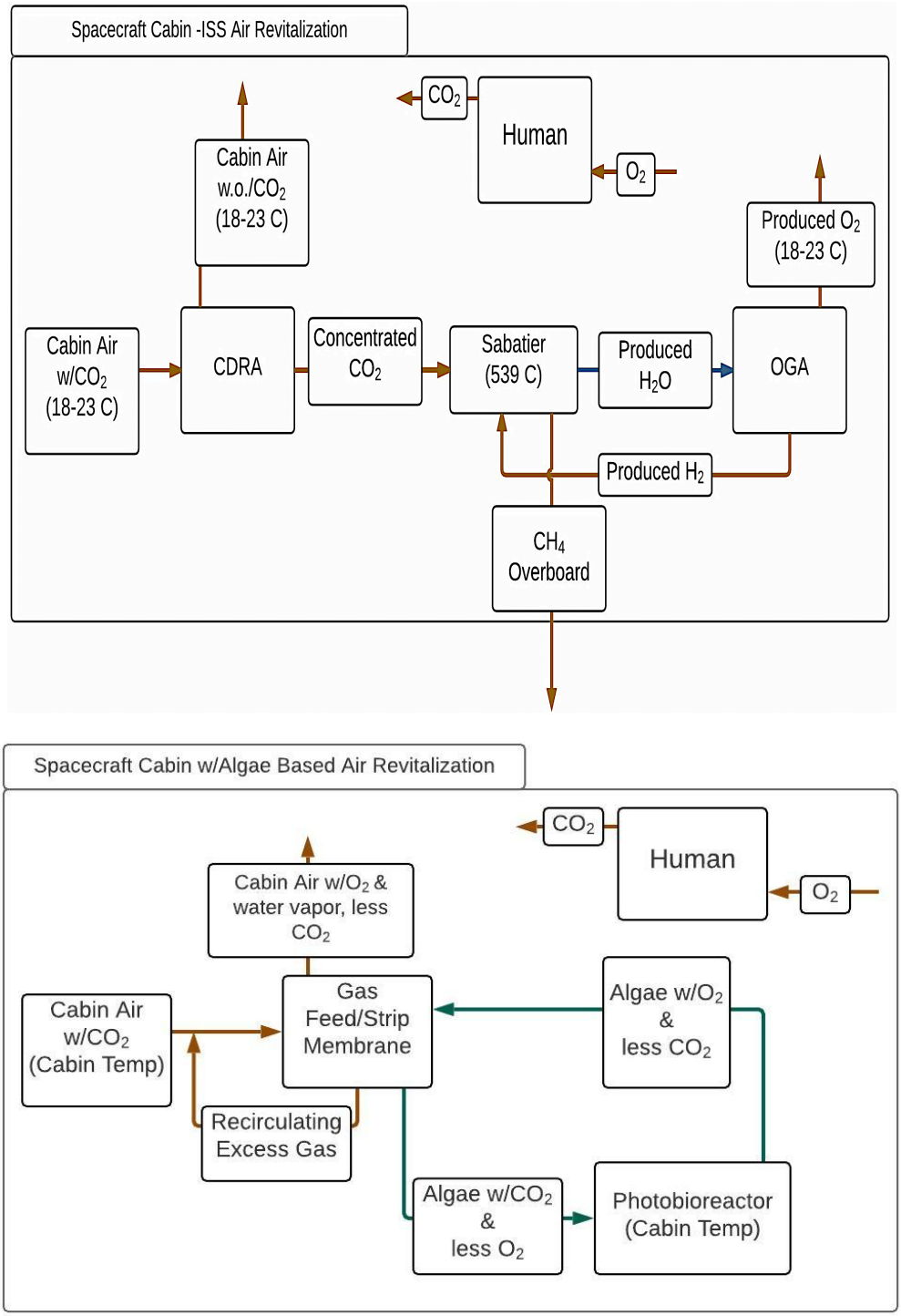


**Figure 83. Algal photobioreactor process diagram for air revitalization in the spacecraft cabin (bottom) compared to the current ISS processes (top).**

**Table 37. ISS air revitalization requirement fulfilled by *Chlorella.***

| Function | Amount of Algae Medium Required (L) | Amount Absorbed/Produced (kg/day) |
|---|---|---|
| $CO_2$ Absorption | 2,200 | 6.24 |
| $O_2$ Production | 1,300 | 4.89 |

### 9.5 Feasibility of Using an Algal System Replacement

Comparing the volume, mass, and power of both systems in Table 38 (Jones 2012, 2011) gives a better indication of the benefit that an algal system could give to a spacecraft cabin or surface habitat. The volume, mass and power required for the ISS systems have been combined into one ISS air revitalization value for each parameter. The table indicates that the current ISS air revitalization technology has less mass and uses less volume than the proposed algal system. While the table presents limited volume and mass benefits to switching to an algal system, additional potential benefits of a bioregenerative system should be considered before disregarding the algal system. Other potential of a photobioreactor include, the algal system's potential for closing the carbon loop and operation within the cabin environment.

**Table 38. Specification comparison of ISS technology to algae technology for air revitalization.**

| | | Volume ($m^3$) | Mass (kg) | Power (kW) |
|---|---|---|---|---|
| ISS Air Revitalization | CDRA<br>Sabatier<br>OGA | 1.57 | 786 | 5.26 |
| | Algae | 2.85 | 2,900 | 7.02 |

While the reliability of an algal system for air revitalization has not been completely characterized, commercial biomass producers have been able to sustain cultures for years (Borowitzka 1999). Typically when cultures fail, it is either due to a bacterial contamination, or reduction in availability of a limiting resource such as light or nutrients (Chisti 2008). Mean time between failures is not well documented for algal photobioreactors, but

commercial algal biodiesel photobioreactors shut down once a year to perform maintenance and cleaning (Chisti 2007).

The data presented in Table 7 indicates that use of an algal photobioreactor for air revitalization is not a mass or volume-saving decision. Although, when more functions of the algal system, the safe operating temperature, and no hazardous gas requirements are considered, an algal system may be acceptable.

### 9.6 Wastewater Management

History of water provision, and management of wastewater in spaceflight has followed the path of air revitalization. Shorter duration missions with fewer crewmembers could launch enough water to supply the mission in its entirety. Wastewater was vented out to space to reduce returning mass. The Space Shuttle's fuel cells' main purpose was to produce electricity, but they also produced potable water. The water recovery system was developed to recycle water to close the loop, and to reduce the dependency on resupply.

**Table 39. Water requirements and output for crew of 6.**

| Item | Amount for Crewmember (kg/CM-d) | Amount for Crew of 6 (kg/d) |
|---|---|---|
| Potable Drinking $H_2O$ | 2.0 | 12.0 |
| Food Hydration $H_2O$ | 0.5 | 3.0 |
| Hygiene $H_2O$ Consumption | 0.7 | 4.2 |
| Payload $H_2O$ Consumption | 2.18 | 13.1 |
| Urine $H_2O$ Production | 1.56 | 9.36 |

The potable water consumed and wastewater production numbers are detailed in Table 39 (Jaatinen, Lakaniemi, and Rintala 2015; Anderson et al. 2018). The production of nitrogen and phosphorus from urine (wastewater) is also listed in Table 40; as these are nutrients consumed by algae, but is considered a contaminant in drinking water (Gentry and Cover 2015).

**Table 40. Algal nutrient content found in urine stream.**

| Item | Amount for Crewmember (g/CM-d) | Amount for Crew of 6 (g/d) |
|---|---|---|
| Production of Nitrogen (as Nitrate) | 11 | 66 |
| Production of Phosphorus (as Phosphate) | 1 | 6 |

### 9.6.1 Current ISS Wastewater Processing Technologies

The ISS has two different wastewater processes depending on the type of waste produced. Hygiene, Sabatier water, and cabin condensate go through the Water Processor Assembly (WPA), and urine and flush water pass through the Urine Processor Assembly (UPA) before going to the WPA, as well.

#### 9.6.1.1 Water Processor Assembly

The Water Processor Assembly (WPA) treats hygiene and dishwater and is the final step for all other water such as the UPA stream. The water is pumped through particulate beds, multifiltration beds, a catalytic reactor, and an ion exchange bed before being stored in a potable tank. The daily rates of the water processor assembly are found in Table 41 (Gentry and Cover 2015).

**Table 41. I/O for ISS water processor assembly.**

| | Item | Amount (kg/day) |
|---|---|---|
| Input | Hygiene/Payload/Medical Wastewater | 9.1 |
| Output | Potable $H_2O$ | 7.7 |

Fouling of the filtration system causes the need for filter exchange in the WPA system. Once breakthrough of the filter is detected, the filter is switched out and the old one is disposed of, creating a need for spares and storage for used units. Fortunately, this does not happen every time a batch of wastewater is processed, but instead every few months. Oxygen is also used as a consumable in the system to oxidize organics not filtered out of the water. This increases the amount of oxygen required for launch above the human metabolic requirements (Gentry and Cover 2015).

#### 9.6.1.2 Urine Processor Assembly

The Urine Processor Assembly (UPA) treats water from experimental waste, flush water, and urine. Wastewater is first treated with phosphoric acid (originally sulfuric acid) and chromium trioxide to control microbial growth (Gentry and Cover 2015; Carter 2009). The distillation assembly is the core of the UPA and evaporates the wastewater at a low pressure and condenses the water on the walls of the assembly. Leftover brine (salts from urine) is stored in a Temporary Urine Brine Storage System (TUBSS) and the distilled water is directed to the WPA for further processing. The disparity in the input and output masses in Table 42 is reflective of how much mass is attributed to brine (Gentry and Cover 2015).

**Table 42. I/O for ISS urine processor assembly.**

| | Item | Amount (kg/day) |
|---|---|---|
| Input | Urine/Flush $H_2O$ | 5.07 |
| Output | Non-Potable $H_2O$ | 3.8 |

Every time the assembly is operated it produces a brine puck that cannot be further reduced, which is stored for incineration upon reentry, meaning both the brine and container are lost (Bagdigian and Cloud 2005; Anderson et al. 2018).

#### 9.6.1.3 Algae for Wastewater Processing

Algae use the nitrate and phosphate compounds dissolved in the growth medium to support cellular growth. Human and animal urine also contains these compounds and could be used to support the production of biomass, which is why streams and ponds contaminated by fertilizer typically have dense algal cultures.

In prior research, the urine was diluted before using it as algal media. Dilution ratios ranged from 1:2 to 1:200, urine to water. Very few studies have been conducted to characterize algal growth on non-diluted urine (Jaatinen, Lakaniemi, and Rintala 2015). Table 43 (Tuantet et al. 2014; Jaatinen, Lakaniemi, and Rintala 2015) presents the nitrogen and phosphorus reduction of two different species of algae, both within the same genus. While this chapter uses the species *Chlorella vulgaris* for its baseline of algae comparison, *Chlorella sorokiniana* was also included due to its recognition as an efficient reducer of nitrogen and phosphorus compounds (Jaatinen, Lakaniemi, and Rintala 2015).

**Table 43. I/O for photobioreactor for wastewater processing.**

| | Item | Amount (*Chlorella vulgaris*) | Amount (*Chlorella sorokiniana*) |
|---|---|---|---|
| Inputs | Gas Stream $CO_2$ Concentration % | 0.03% | 10% |
| | Nitrogen total post dilution (g/L) | 0.173 | 1.77 |
| | Phosphorus total post dilution (kg/L) | 0.014 | 0.130 |
| | Urine: Water Dilution Ratio | 1:25 | 1:3 |
| Outputs | Nitrogen Reduction | 40% | 45% |
| | Phosphorus Reduction | 35% | 70% |
| | Turn over time (days) | 21 | 200 |
| | Biomass Productivity (g/L-day) | 0.06 | 15 |
| | Biomass Density (cell/ml) | $1.93x10^7$ | $2.44x10^8$ |

### 9.6.2 ISS Requirement as Fulfilled by Algae

The amount of algae and medium required to fulfill the metabolic requirements of six crewmembers is presented in Table 44 (Tuantet et al. 2014; Jaatinen, Lakaniemi, and Rintala 2015). Equation 19 was developed to calculate the reduction rate of the species to determine the amount of algae needed to process the urine.

$$L_A = N_{crew}/(N_T * \%_R/n_{day}) \quad (19)$$

where $L_A$ is the amount of algae/algae medium required to reduce the compound in L, $N_{crew}$ is the amount of the compound produced by the crew in kg/day, $N_T$ is the amount of the compound found in the medium after dilution in kg/L, $\%_R$ is the percent reduced by the algae, $n_{day}$ is the number of days needed to consume the compound. It can be noted that while both amounts necessary to reduce urine may be excessive, the *Chlorella sorokiniana* is more efficient at compound turnover than *Chlorella vulgaris*.

**Table 44. ISS wastewater processing fulfilled by *Chlorella*.**

| Item | *Chlorella vulgaris* | *Chlorella sorokiniana* |
|---|---|---|
| Algal Medium for Reducing Total Nitrogen (L) | 19,600 | 16,200 |
| Amount of Total Nitrogen Reduced (g/day) | 66 | 66 |
| Algal Medium for Reducing Total Phosphorus (L) | 26,500 | 13,800 |
| Amount of Total Phosphorous Reduced (g/day) | 6 | 6 |

Table 45 compares the wastewater reduction stream of the ISS to that of an algal photobioreactor system (Carter 2009; Javanmardian and Palsson 1991; Anderson et al. 2018). The algal system is assumed to use a non-hazardous sterilization procedure, such as Pasteurization, to reduce microbial growth in the urine stream before feeding to the algae. This is in contrast to the harsh chemicals that are used on the ISS to stave off growth. Also, both pre-WPA water and urine could be introduced into the algal photobioreactor concurrently, reducing the number of redundant processes.

**Table 45. Specification comparison of ISS technology to algae technology for wastewater processing.**

| | | Volume ($m^3$) | Mass (kg) | Power (kW) |
|---|---|---|---|---|
| WPS | WPA | 3.14 | 850 | 0.32 |
| | UPA | | 530 | 0.24 |
| | Algae | 21.0 | 24,050 | 85.7 |

### 9.6.3 Feasibility of Using an Algal System Replacement

Biologically, algae have the ability to reduce nitrogen- and phosphorus-based compounds, but the process is rate-limited. Due to this slow-moving process, a higher volume is required to consume the same number of compounds as found in human urine. Table 45 presents the volume, mass, and power requirements of the algae system versus the Water Recovery System (WRS) (Javanmardian and Palsson 1991; Carter 2009; Anderson et al. 2018). The volume for the UPA and the WPA were combined since they are located in the same two racks. Increasing the biomass density may be a way to resolve the slow turnover rate since algae use the nutrients for cell health and growth. Some studies have indicated a way to increase the culture density through either increasing irradiance or

the addition of magnesium to the medium. This increase in biomass has allowed researchers to reduce the needed amount of dilution. However, the power consumed was much higher, compared to that of the current system; this is due to the amount of irradiance required for the culture (Jaatinen, Lakaniemi, and Rintala 2015). This number could be reduced if the experimentally used florescent lights were replaced with LEDs tuned to algal growth.

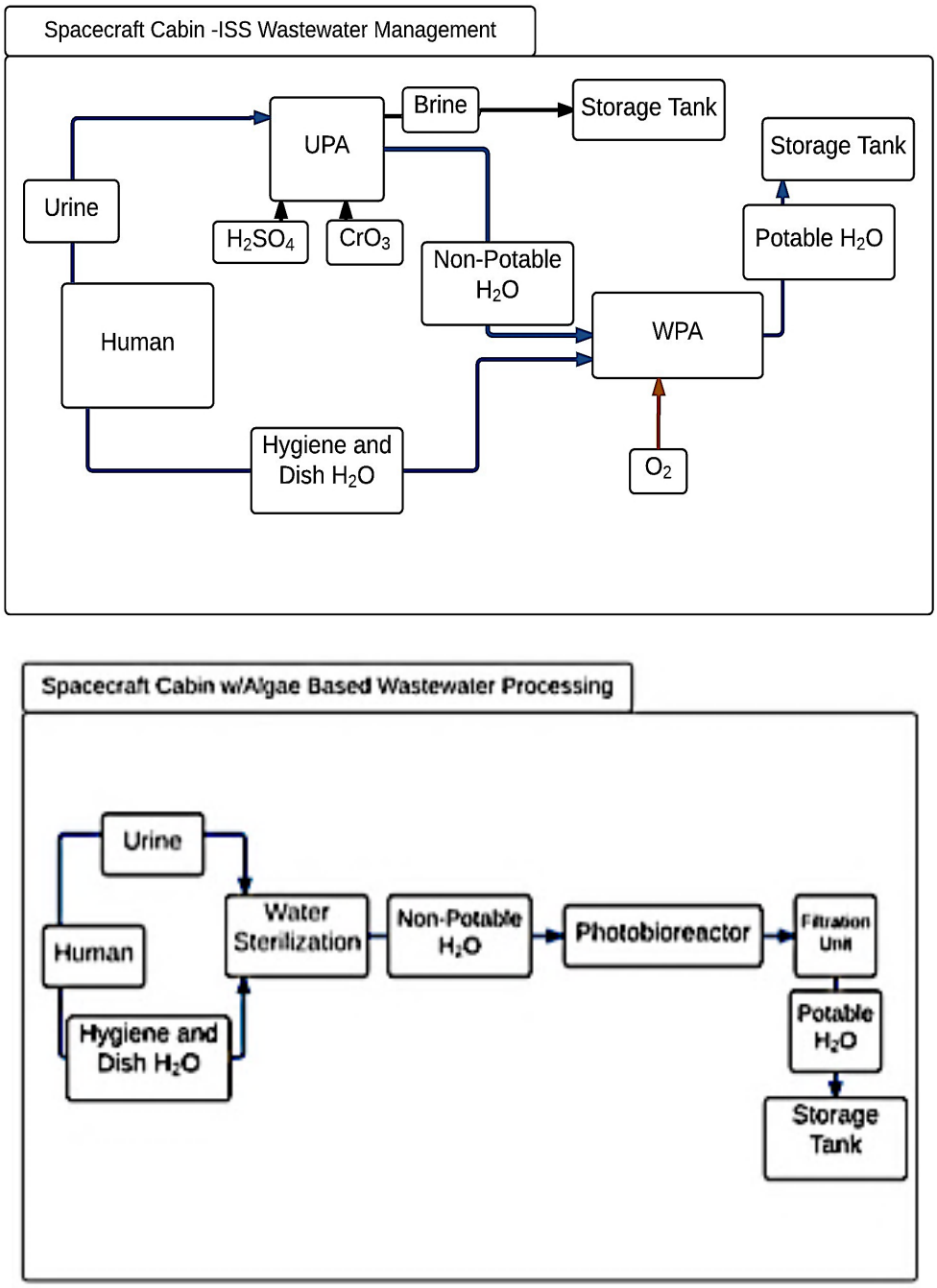


**Figure 84. Process diagram of the current ISS wastewater management system (top) compared to a wastewater system using algae (bottom).**

Even with the reduction of nitrogen and phosphate, algae are unable to completely inhibit bacterial cultures that might be found in urine or experimental water. This may pose a problem if the spacecraft or habitat were hoping to use the water directly from the algal stream. It will need treatment through the onboard water processing assembly or Pasteurization before used as potable water. The current system on the ISS also experiences biofouling, which could cause failure of valves and filters.

## 9.7 Food Production

The nutritional requirements of astronauts have stayed relatively constant through evolution of the space program. Although great strides have been made to improve food variety, taste, and smell, the means of food preparation has not. The current nutritional requirements for an astronaut can be found in Table 46 (Anderson et al. 2018). Food is important to the morale of the crew since it may be the only thing they have control over in a mission (Logan 2004).

### 9.7.1 Current ISS Food Provision

Currently, food is transported up to the ISS and stored in the galley cupboards. The ISS could continue resupply procedures, or incorporate onboard production of fresh produce, like algae.

Early in the space program, food was processed into paste form and stored in squeeze tubes. Dehydrated food replaced the squeeze-tube meals due to the disgust expressed by the astronauts (Logan 2004). The freeze-dried meals save on storage volume, have increased shelf life, and do not need refrigeration. Unfortunately, the dehydrated food does have an eventual expiration, leftover packaging contributes to waste, and the food fails to have the full sensory effect of fresh produce. Limited quantities of fresh food are sent to the ISS, but only when resupply missions launch every few months. These types of launches are not possible for a mission to Mars, so preliminary experiments involving produce growth are currently being conducted on the ISS (Massa et al. 2015).

**Table 46. Nutritional requirements for a crew of 6.**

| Item | Amount for Crewmember | Amount for Crew of 6 |
|---|---|---|
| Protein (kg/CM-d) | 0.057 | 0.344 |
| Carbohydrates (kg/CM-d) | 0.30 | 1.80 |
| Fat (g/CM-d) | 43.8 | 263 |
| Vitamin K (mg/CM-d) | 0.145 | 0.873 |
| Calcium (g/CM-d) | 0.370 | 2.22 |
| Magnesium (g/CM-d) | 0.380 | 2.28 |
| Iron (mg/CM-d) | 19 | 113 |
| Chromium (mg/CM-d) | 0.07 | 0.42 |
| Copper (mg/CM-d) | 1.9 | 11.4 |
| Zinc (mg/CM-d) | 6.9 | 41.4 |
| Manganese (mg/CM-d) | 5.2 | 31.2 |
| Selenium (mg/CM-d) | 0.07 | 0.42 |
| Phosphorus (g/CM-d) | 0.984 | 5.90 |

### 9.7.2 Algae for Food Provision

Developing areas use algae as a food source due to its ease of cultivation, high production rates, and high protein and nutrient content (Tokusoglu, Ö., Unal 2003). Recently, nutritionists have been studying the anti-inflammatory effects of consuming algae. The FDA has approved using algae as a food supplement (16.8 g/day for a 70kg male), but not as a sole food source (Carlson 2011).

The cellular physiology of certain algae species restricts it from being a primary food source. *Chlorella vulgaris* cells contains a thick cellulose wall, which is difficult for humans to digest in large quantities, leading to dyspepsia and diarrhea. Post-harvest processing, such as grinding the dried culture into a powder increases the digestibility. Ingesting smaller doses of *Chlorella* also reduce the digestive side effects. The species also has a slightly

fishy odor and taste, making it unappetizing in large quantities. Fortunately, the biomass growth rate of *Chlorella* is fast enough (approximately 1.5 g DM/L-day) that it can support one human with approximately 11L, fulfilling the FDA allotment (Javanmardian and Palsson 1991).

### 9.7.3 ISS Requirement as Fulfilled by Algae

The values displayed in Table 47 show the amount of algae and medium required to fulfill the FDA limitation of algae consumption, the amount provided of the listed nutrient, and the percent daily value that it satisfies (Anderson et al. 2018; Tokusoglu, Ö., Unal 2003). In order to fulfill the FDA approved amount of biomass, 11 L/CM-d of algae and medium are needed, assuming the biomass growth rate is 1.5 g dry mass/L-d.

Figure 86 compares the food provision of the ISS operation against the biomass production from a photobioreactor. It was assumed the biomass did not need any further processing after filtration, since the algae culture concentrate could be mixed into food or drinks.

**Table 47. Nutritional benefits of the FDA suggested amount of *Chlorella vulgaris* per person per day.**

| Item | Amount of Nutrient Provided with FDA Allowance (16.8 g) | Percent Daily Value |
|---|---|---|
| Protein | 8.03 g | 14% |
| Carbohydrates | 1.35 g | 0.45% |
| Fat | 2.23 g | 5% |
| Vitamin K | 8.4 mg | 5,763% |
| Calcium | 99.7 mg | 27% |
| Magnesium | 57.8 mg | 15% |
| Iron | 43.5 mg | 230% |
| Chromium | 0.003 mg | 4.8% |
| Copper | 0.010 mg | 0.53% |
| Zinc | 0.200 mg | 2.9% |
| Manganese | 0.350 mg | 6.75% |
| Selenium | 0.011 mg | 17% |
| Phosphorus | 0.30 g | 30% |

### 9.7.4 Feasibility of Using an Algal System Replacement

Production for use as a nutritional supplement could be sustained with the biomass produced from an algal photobioreactor designed for air revitalization. However, trying to completely transition to algae as a single food source is unreasonable. Daily consumption of biomass would have to be on the order of approximately 3kg/CM-d. This is approximately 1 kg/CM-d more food than what the crew currently consumes. Furthermore, the flavor and texture would be monotonous with daily consumption and could degrade crew morale (La Vone 2014).

Using algae as a nutritional supplement could reduce the amount of food to be launched, without losing the variety through other sources. Table 48 presents the amount of biomass required to fully replace launched food, the amount of algae prescribed by the FDA, and how much food is currently consumed daily by a crew of six. It is assumed that the astronauts receive 100% of their daily nutritional requirements from a day's worth of packaged food. The power requirements for food preparation and preservation were not included in the table, as it is assumed that the packaged materials do not require refrigeration (Anderson et al. 2018).

**Table 48. ISS food provision fulfilled by *Chlorella*.**

| | | Volume ($m^3$) | Mass (kg/day) | Power (kW) |
|---|---|---|---|---|
| | Prepackaged Food/Water | 0.028 | 9.06 | |
| Algae | Complete Food Replacement | 0.178 | 210 | 0.467 |
| Algae | FDA Restricted Replacement | 0.037 | 44 | 0.098 |

The main concern with the current ISS standard for food provision is the reliance on regular launches for resupply. If a resupply mission were to be postponed, terminated, or lost, it puts a strain on the astronauts' diet, eventually leading to malnourishment, if not resolved. Cultivating algae in the spacecraft could help mitigate that risk.

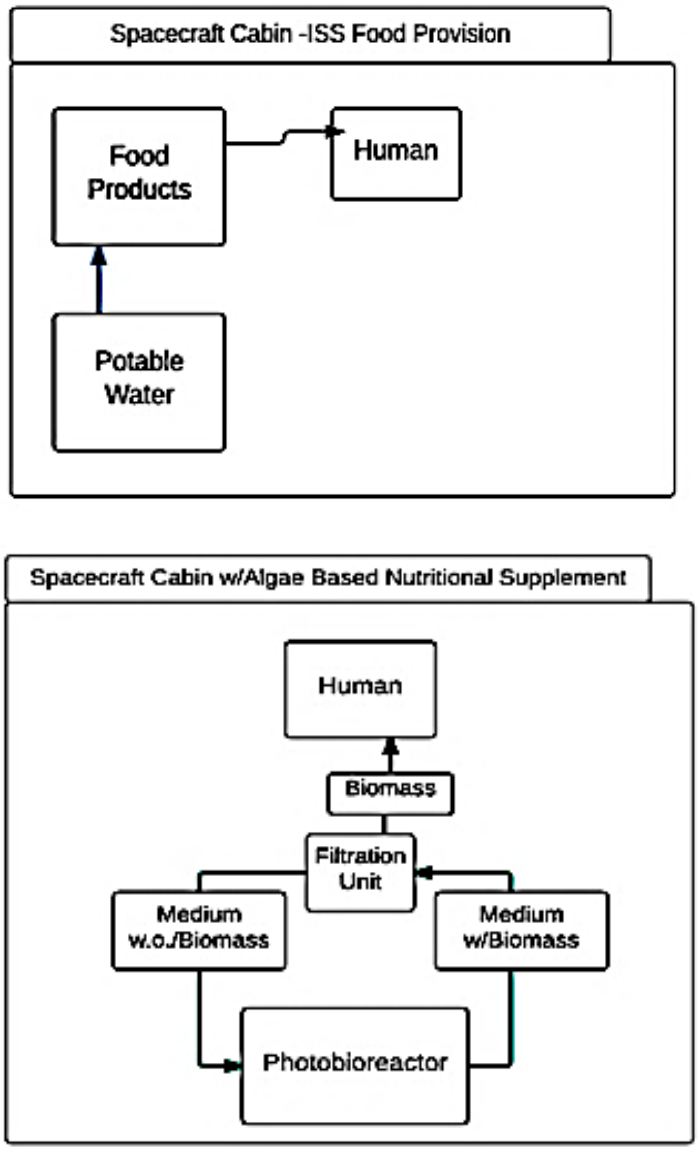


**Figure 85. Process diagram of the current ISS food provision system (top) compared to algal food provision (bottom)**

### 9.8 Radiation Shielding

NASA's approach to radiation dosage limits have been based on the concept of "as low as reasonably achievable" (ALARA). Table 49 details these dosage limits for both men and women (Beville 2014). Selecting a crewmember age of 30 gives the minimum allowable dosage per year, for as the crewmember grows older, the limits increase. Currently, only passive radiation shielding has been included in the design of spacecraft. The amount of shielding provided depends on the material selected and the thickness of the materials incorporated in the craft.

Figure 86 shows the amount of protection provided by thickness of a material type during both a solar-minimum year and the September 1989 solar particle event (Barghouty and Thibeault 2006). As the figure shows, liquid hydrogen theoretically provides the most mass-effective choice (Barghouty and Thibeault 2006).

**Table 49. Radiation dose equivalent limits.**

| Item | Amount for one Crewmember (Sv/year) |
|---|---|
| Radiation Dose Limit (Men) | 0.78 [Age 30] |
| Radiation Dose Limit (Women) | 0.6 [Age 30] |

### 9.8.1 Current ISS Radiation Shielding

Both ISS radiation shielding technology and the algal photobioreactor are examples of passive shielding; meaning layers of material line the inside of the spacecraft as a "wall" between radiation and the crew. In reality, all materials on board contribute to total radiation shielding, but are not selected primarily for their shielding qualities. Rather, they are chosen for other attributes or characteristics important to the component or subsystem design.

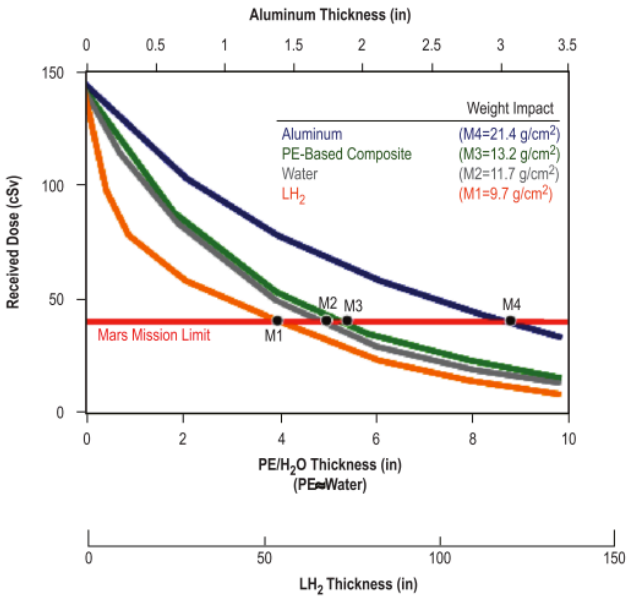


**Figure 86. Received dose versus the thickness of PEM, $H_2O$, and $H_2$ for radiation shielding. The mass impact is also indicated (selected from (Barghouty and Thibeault, 2006)).**

With 0.6 Sv/year as the allowable radiation threshold, the thickness of the most popular shielding material is presented in Table 50 ("Polyethylene (PE) Typical Properties Generic HDPE | UL Prospector" 2016; Simonsen and

Nealy 1991), (Richard S. Williams 2015). The threshold was selected based off of the year limit of a 30-year-old woman, since it provides the minimum required amount of shielding for a year-long mission. The inner surface area of the ISS was used for the volumetric and mass study.

**Table 50. Material specifications for passive ISS radiation shielding**

| Item | Thickness (cm) | Mass (kg) |
|---|---|---|
| High Density Plastic (HDPE) | 9.9 | 119,390 |

While High Density Polyethylene is a lightweight material for radiation shielding, it is combustible. Material selection for cabin use must consider the associate hazards and have potential for mitigation. Current combustibility considerations have the HDPE wrapped in aluminum foil.

### 9.8.2 Algae for Radiation Shielding

From the previously presented Figure 86, liquid hydrogen is the most mass effective choice for shielding but it can take up a sizeable amount of volume. Also, cryogenics for hydrogen liquefaction continually "leak" into space and thus, have relatively short lifetimes. Water contains hydrogen and, from the figure, is a good choice for radiation shielding, because it provides a tradeoff of mass for volume savings. Pockets filled with algae and water could line the inside of a structure, much like the Water Walls design proposed by Dr. Michael Flynn (Cohen, Flynn, and Matossian 2012). A concern about this design is the reaction of algae to radiation. No extensive studies have been conducted to look at the influence of radiation on algae culturing. Those that have been conducted indicate that *Chlorella vulgaris* could withstand acute exposure to gamma radiation but not chronic exposure (exposure lasting more than approximately 3 days with a dose of 75 kr/20-hr day (Posner and Sparrow 1964).

### 9.8.3 ISS Requirement as Fulfilled by Algae

Table 51 displays how many liters of algae and medium are required to line the inside surface of the ISS to only allow a 0.6 Sv/year dose of radiation, assuming equal organ dose equivalents (Posner and Sparrow 1964; Barghouty and Thibeault 2006),(Richard S. Williams 2015). The minimum dosage limit was selected to produce the estimate for the maximum amount of shielding required for a yearlong mission. The thickness of water was determined by using the previously presented Figure 86 and the minimum dosage limit. The inner surface area of the ISS was used to produce the volume estimate.

**Table 51. ISS radiation protection requirement fulfilled by *Chlorella*.**

| Item | Thickness (cm) | Volume of Algae Required (L) |
|---|---|---|
| Volume of water (L) | 9.4 | 116,870 |

The assumptions for this table include: the water thickness does not cause a limitation for algal irradiance, and culture density did not influence the amount of shielding provided. The correlation between algal culture densities and radiation shielding have not been experimentally established.

### 9.8.4 Feasibility of Using an Algal System Replacement

A comparison of the volume, mass, and power needed for each shielding material is presented in Table 52. The materials were presented as an "all or nothing" approach, instead of including a combination of all materials for shielding.

**Table 52. Specification comparison of ISS technology to algae technology for radiation shielding.**

| | Volume ($m^3$) | Mass (kg) | Power (kW) |
|---|---|---|---|
| HDPE | 123 | 119,390 | 0 |
| Algae | 152 | 138,000 | 400 |

Including water for radiation shielding in future mission provides increases the radiation protection for same mass in comparison to HDPE. Culturing that much algae has diminishing returns, but with the larger water volumes, the density of algal culture could be reduced and still adequately address the other ECLSS functions. If water were to be used as a radiation shield, it may be more beneficial to reserve only a portion of the shield for use as an algal photobioreactor, so as to reduce power consumption and avoid over production of biomass. One suggestion, to avoid the over-commitment of power and mass to the photobioreactor, restricts the radiation shielding benefits to one specific area. Using the algal photobioreactor as a "safe zone" for solar particle ejections (SPE) takes advantage of the system's radiation shielding but not require an entire lining of the spacecraft. Table 53 details internal volume required for a radiation "safe zone" for a crew of six, assuming the habitable volume is provided by the Celentano curve for a mission of 2 days, or the typical max for a coronal mass ejection (CME) event (Akin 2013),("Coronal Mass Ejections | NOAA / NWS Space Weather Prediction Center" n.d.). Using the medium volume required to fulfill air revitalization functions, the thickness of the radiation shielding was determined using

a rectangular box design for the shielding module. The height of the crew was assumed to be less than 1.8m to assist with volumetric calculations. Figure 86 was used to determine the amount of additional shielding provided by the calculated thickness. Comparing the water thickness values of the "safe zone" to previously developed designs in research, the shelter could reduce an effective dose by more than 50%, when used in an Xapsos 95% event (Simon, Walker, and Clowdsley 2013).

**Table 53. Specifications for a radiation event shelter employing a PBR sized for air revitalization.**

| | Internal Volume for Crew of 6 ($m^3$) | Internal Dimensions (m) | Medium Volume ($m^3$) | Mass (kg) | Power (kW) | Medium Thickness (m) | Amount of Shielding Provided (Sv) |
|---|---|---|---|---|---|---|---|
| Safe Zone | 5.67 | 1.77x1.77x1.8 | 1.66 | 1,700 | 4.08 | 0.08 | ~0.7 |

While an algal photobioreactor should not be considered for primary radiation protection, due to previously provided volume and power concerns, the secondary function of protection while using a photobioreactor for other means (air revitalization, food production, etc.) should not be overlooked.

### 9.9 Thermal Control

Avionics, equipment, and crew generative heat and necessitate the need for a cooling system to keep the cabin within the set temperature range. Table 54 exhibits the required temperature range for the cabin, and the metabolic and equipment waste heat produced (Anderson et al. 2018). This table assumes that the heat production rates are constant, scale linearly with crewmember number, and characterize a 70kg man.

#### 9.9.1 Current ISS Thermal Control Technologies

Both the current ISS thermal control system, the Low Temperature Loop (LTL) and the Moderate Temperature Loop (MTL), and the algal photobioreactor are subject to heat transfer principles. The LTL and MTL were used as the ISS systems for thermal comparison to an algal photobioreactor. The entire Internal Active Thermal Control System (IATCS) was not included, since it is assumed that the algal loops use the radiator aspects of the current system.

**Table 54. Thermal requirements and outputs for a crew of 6.**

| Item | Amount for Crewmember | Amount for Crew of 6 |
|---|---|---|
| Temperature (°C) | 18-27 | |
| Metabolic Waste Heat (kW) | 0.139 | 0.833 |
| Equipment Waste Heat (kW) | 2.0 | 12.2 |

#### 9.9.1.1 Internal Active Thermal Control System (IATCS)

Cabin cooling capabilities are provided by a system that uses clean water loops to remove heat from the cabin. The heat from the water is transferred to an ammonia loop (via an Interface Heat Exchanger, IFHX), then to a radiator, from which the heat is rejected into space. Having two separate cooling loops, the MTL and the LTL, allows for quicker heat removal, depending on the area's temperature requirements and allowable temperature swings. The following discussion focuses on the water loop system of the IATCS since it is the most parallel to the algae system.

#### 9.9.1.2 Low Temperature Loop (LTL)

The Low Temperature Loop (LTL) removes heat from the ECLS system, Common Cabin Air Assembly (CCAA), and certain payload experiments. Heat removal rates, temperature limitations, and the amount of water in the system are presented in Table 55 (The Boeing Company, n.d.; Patel et al. 2001).

**Table 55. I/O for ISS low temperature loop of the internal active thermal control.**

| | Item | Amount |
|---|---|---|
| Inputs | Heat Removal (kW) | 3 |
| | Water (L) | 63 |
| | Minimum Temperature for Supply to Cabin (°C) | 4 |
| Output | Maximum Temperature for Supply to Heat Exchanger (°C) | 21 |

#### 9.9.1.3 Moderate Temperature Loop (MTL)

The Moderate Temperature Loop (MTL) absorbs heat from the avionics and the remaining payload experiments. Heat removal rates, temperature limitations, and the amount of water in the system are presented in Table 56 (Patel et al. 2001).

**Table 56. I/O for ISS moderate temperature loop of the internal active thermal control.**

| | Item | Amount |
|---|---|---|
| Inputs | Heat (kW) | 12 |
| | Water (L) | 200 |
| | Minimum Temperature for Supply to Cabin (°C) | 16 |
| Output | Maximum Temperature for Supply to Heat Exchanger (°C) | 49 |

### 9.9.2 Algae for Thermal Control

The photobioreactor could have two different approaches to thermal management, depending on system size. If the photobioreactor is small, a more active approach is needed to remove heat by cycling the medium through a heat exchanger, e.g. the Interface Heat Exchanger (IFHX), and returning the cooler medium to the cabin. This requires higher flow rate pumps than a system with a larger water mass requiring less cabin volume. The second approach uses a larger water mass, approximately 320 L photobioreactor, as a thermal sink. This amount of water could absorb the thermal energy for one 70kg man for one day, by increasing its temperature by 9°C (temperature range of ISS). Eventually, the water mass needs to be cooled down or the heat transferred away, since cabin components are always producing heat, but this could be done over much larger time scales, requiring pumps with smaller flow rates and power consumption. This thermal sink estimate did not include other contributors of heat in a spacecraft cabin, including the avionics, experiments, or the lighting system of the photobioreactor itself.

Various species of algae, especially *Chlorella vulgaris*, are capable of living in warmer temperatures. Research has shown that *Chlorella vulgaris* air revitalization efficiency improves as the environmental temperature increases up to 40°C under atmospheric $CO_2$ conditions (Chinnasamy et al. 2009). Typically *Chlorella* is cultivated in outdoor tubular or raceway ponds, that while exposed to sunlight, can increase in temperature from 28° to 40°C over the course of the afternoon, without any detriment to culturing (Ugwu, Ogbonna, and Tanaka 2005). Cultivating algae in warmer temperatures (15-50°C) has been well documented in the literature, but cultivation in the lower end of the temperature spectrum (4-15°C) has not. This could be due to the possible reduction in algae metabolic efficiency, but this temperature regime should still be fully characterized before dismissing algae and its medium as an insufficient multifunctional thermal control method.

### 9.9.3 ISS Requirement as Fulfilled by Algae

This discussion assumes that the water in the IATCS and the algae medium have approximately the same heat transfer characteristics. However, it is understood that the culture density and biofouling may effect heat transfer. Future experimentation is required to determine these trends. With this assumption, Table 57 presents the amount of algal medium required to control the temperature of the ISS, which are the same amounts as the current system (The Boeing Company, n.d.). The density of the algal medium and culture was assumed to be 1021 kg/m$^3$.

**Table 57. ISS thermal transport fulfilled by *Chlorella.***

| Item | Amount of Algae Medium Required |
|---|---|
| *Chlorella* for LTL (L) | 63 |
| *Chlorella* for MTL (L) | 200 |
| Mass of Media and Algae Culture (kg) | 269 |

Figure 87 presents how the algal system is incorporated into a spacecraft, and how that compares to the current ISS design. The proposed integration for the algal system is very similar to the current ISS design. The algal loop is in contact with the cabin air, with fans moving the air across the reactor. The gas transport system, feeding $CO_2$ enriched air from the cabin to the algae, also containing heat from the cabin environment and transferred into the medium.

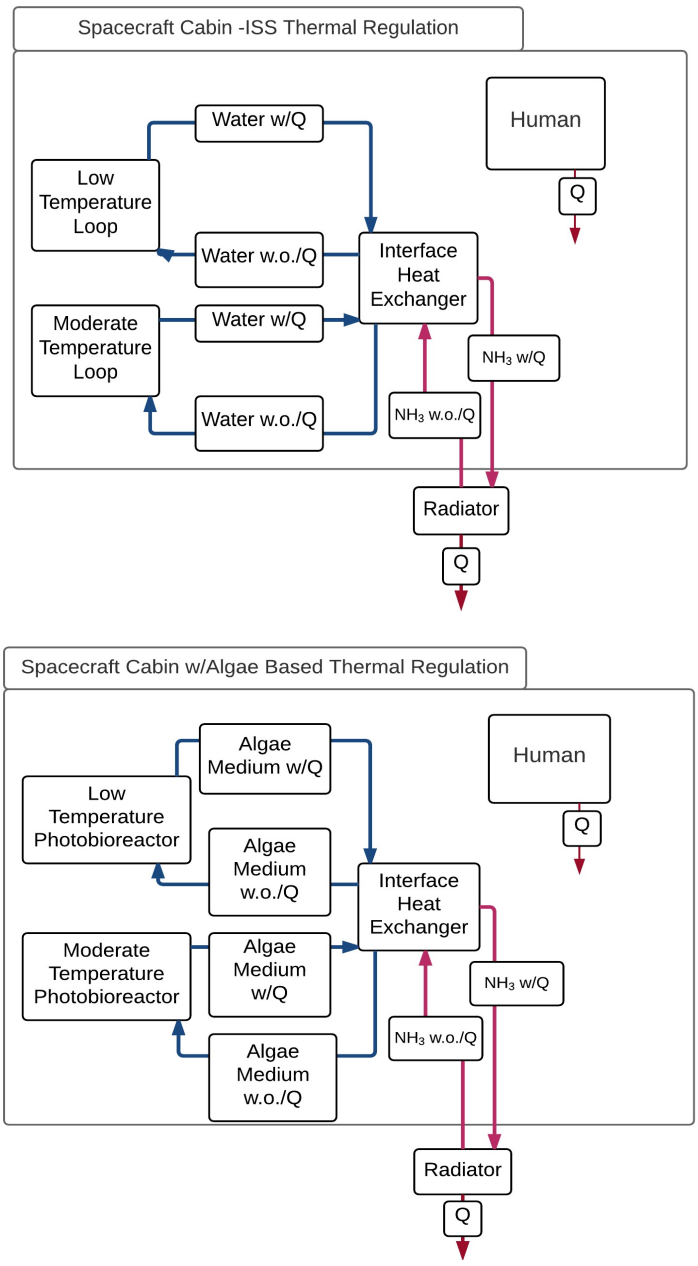


**Figure 87. Process diagram of the current ISS thermal control system compared to an algal-based system**

### 9.9.4 Feasibility of Using an Algal System Replacement

Algae have been grown in various steady-state temperatures, including temperatures spanning the range of the ISS coolant loops. However, the effect of time-varying temperature and concurrent heat loads has not been extensively studied. In order to fully assess the feasibility of using algae medium in the thermal control system, algal

response to cycling temperatures needs to be known. These swings can range from +4 to +42°C over a few minutes to a few hours, depending on the heat loads.

Table 58 presents the volume, mass, and power requirements of both the current ISS thermal system and the proposed algal photobioreactor system. It was assumed that the piping and pumps be similar between the current ISS system and the algal system. The need for increased power for the algal system can be attributed to added lights and the standard pumps, while IATCS only requires pumps (Patel et al. 2001).

**Table 58. Specification comparison of ISS technology to algae technology for thermal transport.**

| | Volume ($m^3$) | Mass (kg) | Power (kW) |
|---|---|---|---|
| LTL | 0.082 | 1,880 | 0.11 |
| MTL | 0.26 | | |
| Algae | 0.342 | 1,890 | 0.897 |

Heat attributed to the lighting system also needs to be considered when developing the thermal budget of the algal photobioreactor. Based off of the irradiance capacity and efficiency of current light emitting diodes (LED), a "grow-light" LED tuned for photosynthetic activation typically has a wall-plug efficiency of approximately 42% (when using the designed ratio of red/blue LEDs) (LUMILEDS 2015). This leads to an additional 0.50 kW, based off of 58% of the 0.861 kW required for lighting, of heating needed to be accounted for in the spacecraft thermal budget.

Failures for either system is attributed to loss of circulation pressure or the ability to circulate cooling water through the cabin. Algae has a unique failure, in that, if the algae do not survive temperature swings or there is a loss of lighting, the algal photobioreactor thermal control loses all secondary functions including food production and air revitalization but could continue to perform the thermal control function.

If the algae are able to withstand thermal cycling, this could be a viable option for multifunctioning thermal control.

### 9.10 Comparison

Table 59 presents the volume, mass, and power consumption of the current ISS ECLS systems, and an algal photobioreactor designed to provide these functions.

### 9.10.1 Current ISS ECLSS Technologies

The specifications of the current ISS ECLS systems were compiled as a reference for a comparative discussion in Table 59. It is to be understood that this is a high-level overview of the systems and is to support a crew of six.

**Table 59. Volume, mass, and power specifications for used ISS subsystems.**

| | | Volume ($m^3$) | Mass (kg) | Power (kW) |
|---|---|---|---|---|
| ECLSS Functions | Atmospheric Revitalization | 1.57 | 786 | 5.26 |
| | Waste Management | 3.14 | 1380 | 0.56 |
| | Food Provision | 0.028/day | 9.06/day | 0 |
| | Thermal Control | 0.263 | 1880 | 0.11 |
| | Radiation Shielding | 123 | 119,390 | 0 |
| | Total | 128 | 123,445 | 5.93 |

### 9.10.2 Replacing All Current ISS Technologies with Algal System

Table 60 was included to exemplify the downfalls of including a very large algae system, these values are estimated, but are for comparisons of magnitude. Radiation shielding required an amount of power, mass, and algal medium volume 100 times greater than that of the algal atmospheric revitalization system. Sizing for the requirements of algal radiation shielding also encapsulated the requirements of the other algal ECLS system functions, assuming algae replaces all food. The power, mass, and volume of the system are 10-100% more than that of the current ISS ECLS system. The mass and volume amounts of the algal system are dependent on the volume of water required to protect against a certain radiation threshold. These values could be reduced if more risk were acceptable with radiation shielding, effectively reducing the required material/water thickness. Illumination systems required to cultivate an algae culture to this size contributes to the excessive power requirements.

Fortunately, while the amount of water needed for radiation shielding is 20% more volume than the current shielding system, not all of the water has to be either occupied by algae at all times or made to be the most efficient algal system. Up to a certain threshold, algae efficiency scales with the irradiance received (Bartosh and Banks 2007). If the other ECLSS functions could be met with a less efficient algal photobioreactor by reducing the irradiance amount, it provides an energy saving and could increases the attractiveness of an all-inclusive algae system.

**Table 60. Volume, mass, and power specifications if all ISS ECLSS functions were fulfilled by an algal photobioreactor.**

| | | Volume ($m^3$) | Mass (kg) | Power (kW) |
|---|---|---|---|---|
| ECLSS Functions | Atmospheric Revitalization | 152 | 138,000 | 400 |
| | Waste Management | | | |
| | Food Provision | | | |
| | Thermal Control | | | |
| | Radiation Shielding | | | |
| | Total | 152 | 138,000 | 400 |

### 9.10.3 Only Replacing Air Revitalization and Thermal Control Technologies with an Algal System

In the previous sections, it was presented that with the current culturing technology; air revitalization and thermal control could be replaced with an algal photobioreactor. Table 61 shows that using a multifunction system may not provide a system savings. Using the amount of medium required to fulfill air revitalization, it encapsulated the algae volumetric requirement for thermal control as well. This is compared to the total of the two parallel ISS systems.

**Table 61. Specification comparison of replacing the current ISS air and thermal systems with one algal photobioreactor**

| | | ISS Subsystems | | | Algae Photobioreactor | | |
|---|---|---|---|---|---|---|---|
| | | Volume ($m^3$) | Mass (kg) | Power (kW) | Volume ($m^3$) | Mass (kg) | Power (kW) |
| ECLSS Functions | Atmospheric Revitalization | 1.57 | 786 | 5.26 | 2.85 | 2,900 | 7.02 |
| | Thermal Control | 0.26 | 1,880 | 0.11 | | | |
| | Total | 1.83 | 2,666 | 5.37 | 2.85 | 2,900 | 7.02 |

Through the previous overview of the waste management and radiation shielding, it was made apparent that the amount of algae required to fulfill those functions was just too massive to be reasonably considered. However, the water management and radiation shielding contributions of the algae used for air revitalization and thermal control should not be overlooked.

### 9.10.4 Benefit of a Portion of All ISS ECLSS Technologies Being Algal System Based

Table 62 has taken into consideration the support supplied to waste management and radiation shielding in terms of volume, mass, and power reduction while also covering air revitalization and waste management. Using an algal photobioreactor to support or replace ECLS systems required for human spaceflight provided a savings of 0.99 $m^3$ and 1,630 kg. These savings were calculated as the difference between specifications of the current ISS ECLS system and a system augmented with algae involvement. The system with algae involvement calculations used the medium volume amount for air revitalization to scale the benefit to other functions (food provision, waste management, and radiation shielding). However, more power (1.59 kW) is required for supporting an algal photobioreactor due to required lighting and pumps. Developing capillary systems, cycling pumps and irradiance systems instead of constant operation may help to reduce this power requirement.

**Table 62. Specifications of an ISS ECLSS that includes an algae photobioreactor and current technologies**

| | | ISS Subsystems | | | Algae Photobioreactor | | |
|---|---|---|---|---|---|---|---|
| | | Volume ($m^3$) | Mass (kg) | Power (kW) | Volume ($m^3$) | Mass (kg) | Power (kW) |
| ECLSS Functions | Atmospheric Revitalization Thermal Control | Algae system | | | 2.85 | 2,900 | 7.02 |
| | Food Provision | 0.03 | 8.96 | 0 | Provided by ISS | | |
| | Waste Management | 2.83 | 1235 | 0.50 | | | |
| | Radiation Shielding | 121.3 | 117,671 | 0 | | | |
| | Total Combined Systems | 127.01 | 121,814 | 7.52 | | | |
| | ISS-Only Systems | 128 | 123,445 | 5.93 | | | |
| | System Savings with Algae | 0.99 | 1,630 | -1.59 | | | |

### 9.11 Current and Future Work

Demonstration of the previously mentioned functions could be accomplished with a benchtop experiment. Figure 70 shows the process flow diagram of the developed benchtop apparatus for operational research. While designing a photobioreactor to be used for functionality testing, it is imperative to consider some of the limitations or challenges associated with spaceflight or surface habitation. Figure 88 illustrates the potential to integrate a photobioreactor into the spacecraft environment for simultaneous air revitalization and thermal control. It includes

some design considerations (gas-liquid contactor membrane, mixing pumps, and inclusion of the ISS ammonia loop) for gravity-independent operation and utilization of currently established spacecraft hardware.

### 9.11.1 Gas Transport

For terrestrial applications, sparging small bubbles of $CO_2$ enriched gas into the algae medium effectively mixes, feeds the algae, and knocks produced $O_2$ out of the medium. In microgravity, sparging gases into liquid results in inefficient large bubble formation. Contactor membranes are able to enrich a liquid with $CO_2$ and degasify the $O_2$ without bubble formation by using the principle of Henry's Law. The proposed photobioreactor system uses two contactor membranes, one specifically to introduce $CO_2$ into the medium and one to strip away the produced $O_2$. A horizontal tube is used as the culturing portion of the photobioreactor in an effort to minimize the influence of gravity on the culture and provide a better analogue to one for use in microgravity. To maximize light utilization, the diameter of the tube is equal to the maximum light penetration length through algae.

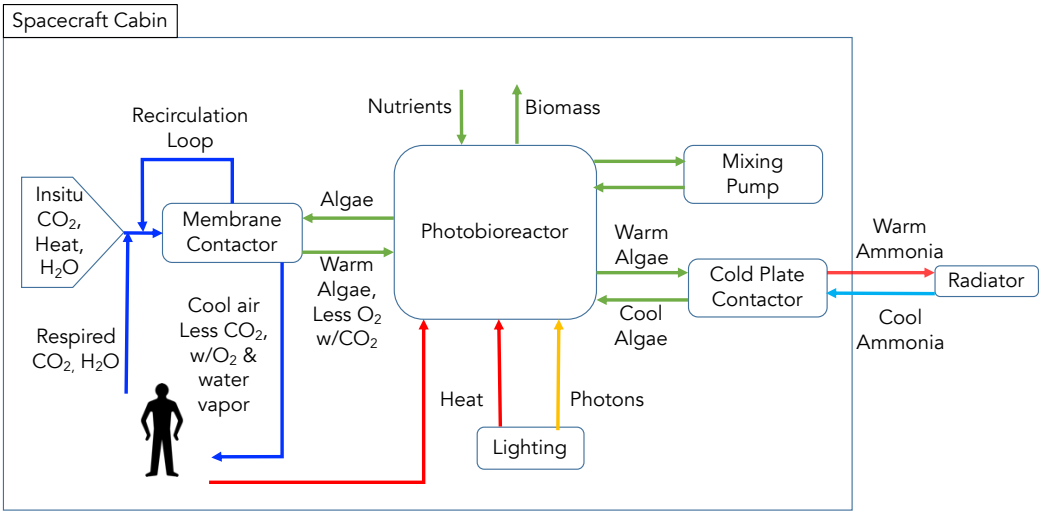


**Figure 88. Process diagram of proposed photobioreactor for simultaneous air revitalization and thermal control in the spacecraft cabin.**

### 9.11.2 Radiation and Microgravity Considerations

This system could then be used to test air revitalization, thermal control, biomass production/food production, and possibly waste reduction. Radiation shielding studies should first be completed by computational modeling due to limited laboratory radiation resources. Due to the inherit gravity influence in a terrestrial lab, this

benchtop photobioreactor would be an excellent algal photobioreactor for a surface habitat. A microgravity flight should be conducted to fully corroborate the feasibility for using a photobioreactor in a spacecraft cabin.

### 9.11.3 Large Scale System Issues

While many feasibility topics are investigated, scaling up the system is a concern not covered in a benchtop experiment. Instead, scaling concerns are examined through study of literature or commercial bioreactor facilities, and modeling.

### 9.11.4 Denser Biomass Culture

Future work in algae studies would benefit by creating denser cultures. A reduction in algal system volume and mass could be achieved by increasing the biomass output of the culture. Since air revitalization rates, waste management, and food production all scale with biomass amounts, denser cultures may be able to provide these functions with less mass, and volume cost. The effect of a denser culture on power consumption needs to be investigated, since denser cultures require increased irradiance for metabolic support. A denser biomass could also provide additional radiation shielding. Thermal management may become more difficult with increased biomass if the heat transfer characteristics are different than water and could be tested with resistive heating of the culture. Further studies need to be conducted on how to achieve increased culture densities.

### 9.11.5 Equivalent System Mass Estimate

In the future, with the findings of the benchtop experiment, in addition to the information found in this chapter, an Equivalent System Mass (ESM) review could be conducted. At this time, the algal photobioreactor for ELCSS use is novel enough that definitive mass equivalency factors have not been established.

## 9.12 Conclusion

An algal photobioreactor was sized to fulfill the ECLSS requirement of the ISS and compared to the current ISS ECLSS technologies. The ISS ECLS system was used as reference architecture due to its history in LEO and its purpose as a scientific test bed for microgravity experiments. Reviewing the volume, mass, and power requirements of a photobioreactor sized to fulfill all ECLSS functions for a crew of six shows that it could theoretically be accomplished, albeit with increased mass, power, and volume than the current technologies. Alternative algal system designs were discussed to reduce these values, including reduced irradiance and increasing the radiation

threshold. The suggestion is not being made that current ECLS technologies on the ISS should be replaced by algal photobioreactors, but instead that algal photobioreactors be considered for ECLSS purposes in future spacecraft and habitat designs.

### 9.13 Resulting Presentations and Publications

Conference Paper

**Matula, E. E.,** Nabity, J. A. (2016). "Feasibility of photobioreactor systems for use in multifunctional environmental control and life support system for spacecraft and habitat environments," 46th International Conference on Environmental Systems, Vienna, Austria, 2016.

Conference Presentation

Matula, E. E. (2016) Feasibility of photobioreactor systems for use in multifunctional environmental control and life support system for spacecraft and habitat environments, 46th International Conference on Environmental Systems, Vienna, Austria.

# Chapter 10 Characterization of Antarctic Chlorophyta in Dynamic Thermal Environments

## 10.1 Introduction and Background

Inclusion of algae in spaceflight may seem difficult due to viability and clumping issues but selection of the proper species for the mission may increase the success rate of bioregenerative technologies (Niederwieser, Kociolek, and Klaus 2018). Choosing species that have acclimated to extreme thermal environments, such as below freezing temperatures, or intense UV exposure, might allow researchers to take advantage of their robustness and adapted metabolic processes. This idea of selecting species or investigating the underlying mechanisms that allow execution of biological processes in their surrounding environments is called bioprospecting (Beattie et al. 2011).

Ras did suggest in their 2013 paper that species may be able to generally adapt to a new environment over the course of a season, allowing enough generations to acclimate to the environment. Although they do suggest that, "Optimal temperature should therefore be associated to the environmental conditions for which they [algae] have been obtained' (Ras, Steyer, and Bernard 2013).

Since there is an interest in using algae in spaceflight applications, the bioprospecting approach would suggest considering species that are acclimated to extreme temperatures (including the potential to freeze), able to withstand high doses of radiation, thermal cycling, viable after long dormancies, and can be transported with minimal support systems. Antarctic species have the potential to fulfill the needs of an extreme (spaceflight) environment due to their natural environment. In a recent study conducted by Leya, partially desiccated, Antarctic-native *Nostoc* and *Sphaerocystis* were placed on the outside of the ISS in a glovebox to test viability, radiation shielding, and extreme thermal cycling. Concurrently, laboratory controls were exposed to diurnal temperature cycles between -25°C to +10°C, vacuum pressure of $4.1 \times 10^{-5}$ Pa, and UV radiation of $UVR_{200\text{-}400nm}$ with >1200 $Wm^{-2}$ for over 4 days. Results indicated that the species did survive the ground tests replicating space environments. Returned samples of *Nostoc* and *Sphaerocystis* were undergoing post-flight tests during the time of publication, but similar species *Chroococcidiopsis* returned from spaceflight were showing signs of viability after return (de Vera et al. 2019; Rabbow et al. 2017).

The McMurdo Dry Valleys outside of McMurdo Station, Antarctica are home to glacial-fed streams where various types of algal mats are found. Desiccated and cryopreserved for the winter, these mats photosynthesize within 10-20 min of rewetting in the spring, when the first glacial melt water seeps into the stream bed (Darling et al. 2017; McKnight et al. 1999). Through the summer, these species experience daily thermal swings between +6° to +15°C with 24-hr sunlight. The conditions, along with the nutrients distributed along the stream bed by rocks weathering upstream, support this cold-environment photosynthesis (Figure 89).

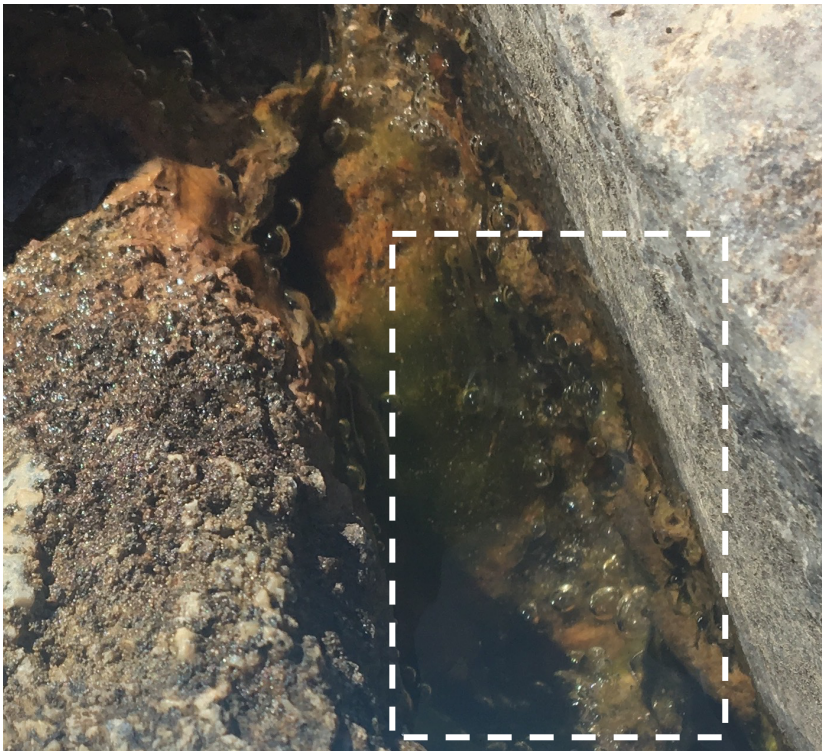

**Figure 89. Small $O_2$ bubbles nucleating on the top of the green mat in Delta Creek in the Dry Valleys (boxed).**

Currently, NASA transports freeze-dried food for mid to long duration spaceflights. Algal photobioreactors could take a similar approach by traveling with desiccated algal mats ready to be rehydrated and revived for culture. A selection of mats from this region were sampled and brought back to be used in part for experiments, including characterization of oxygen production under various temperature conditions. Here the algal samples were subjected to temperature swings previously outlined in Chapter 4. However, instead of +9°C to +28°C, the swings were set +4°C to +14°C. This more closely reflects the ISS LTL temperature profile and the mat's natural thermal environment.

## 10.2 Materials and Methods

### 10.2.1 Culture and Associated Hardware

Triplicate experiments were conducted using a naturally-occurring mixture of the phylum Chlorophyta and Cyanophyta (green algae and blue-green algae, respectively) gathered from Von Guerard Stream (S 77°50.907', E 166°40.557') during the 2018-2019 Antarctic season (Figure 90) (McKnight et al. 1999). Samples were taken from the main thalweg of the stream under approximately 1.5-in of water. A plastic spatula and kitchen knife, triple-rinsed in stream water, were used to gather up three 1-in x 3-in sections of mat. Mat sections were each placed in three 200ml Nalgene screw-top bottles were triple-rinsed in stream water, filled with approximately 100mL of stream water, and tops screwed on tightly. Bottles were transported to the field camp (F6), wrapped in tinfoil, and placed in a +7°C refrigerator. Samples were hand-carried back to the University of Colorado – Boulder in a +4°C cooler with icepacks. When the bottles arrived at the Sustainability, Energy, and Environmental Community (SEEC) Phycology Lab at the University of Colorado, the lids to the bottles were loosened to allow for ventilation, and the foil-wrapped bottles were placed on a dark shelf of a +7°C refrigerator.

Biomass from one of the bottles (Von Guerard E2) was transferred to a 125mL Erlenmeyer flask of sterile Bristol's media and lightly capped with foil, placed on an orbital shaker table under a fluorescent bulb providing 50 $\mu$mol $m^{-2}s^{-1}$ of irradiance -still inside the +7°C refrigerator. The flask was allowed to culture in the refrigerator for 14 days.

After 14 days, samples of mat biomass from the flask were diluted in additional volumes of sterile Bristol's media, and partitioned out into plates for the temperature cycling experiment. 12-well-plates of the Antarctic green mat were prepared using procedures previously described in Chapter 4. The experiments also utilized the FireSting dissolved oxygen unit, pH probes, and PAM fluorometry unit as outlined in Chapter 4. In addition, the experiments used the same orbital shaker table, Peltier cooler system, and irradiance system. However, a different environmental chamber was used, housed in the Phycology Lab, and was set to +5°C, instead of the previous +10°C due to chamber specifications.

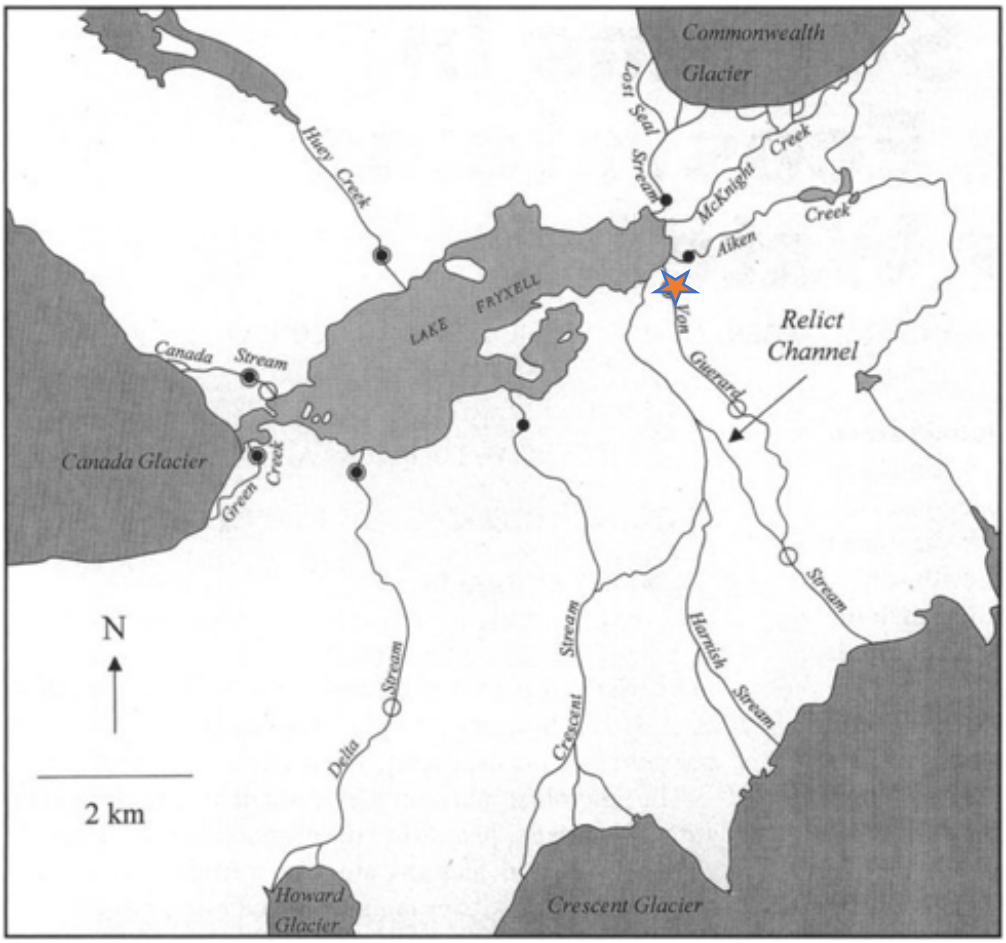


**Figure 90. Map of the Dry Valleys, Antarctica. Samples used in this series of experiments came from Von Guerard Stream in the South East corner of the valley (marked with a star) (selected from (McKnight et al. 1999)).**

### 10.2.2 Experiment Design

The following experiments replicate those conducted in Chapter 4 but using Antarctic Chlorophyta instead of the previous *Chlorella*. While the sampled Antarctic mat may contain *Chlorella*, the previously tested culture (Chapter 4) had *Chlorella* v. as the dominant species.

#### 10.2.2.1 Variables and Conditions

The medium temperature was the independent variable for this series of experiments. The temperature-cycled plate followed a similar pre-determined temperature cycle profile as the *Chlorella* experiments (these plates will be referred to as "Antarctic Cycled" in the following results section). However the temperature range was adjusted to the temperature extremes of the LTL (+4°C to +14°C), while the control was kept at +7°C (Anderson et

al. 2018). This adjustment parallels the temperatures of the culture's natural environment and the Low Temperature Loop on the ISS. Effects of contamination and daily nutrient supplementation were not studied in these experiments.

The constant-cold *Chlorella* case that is referenced in the following sections was one of the constant-temperature cases for the *Chlorella* experiments (this case is referred to as "*Chlorella* Cold" in the results section). These plates were cultured in a constant +10°C and used the same hardware, and measurement and culturing protocols as the cycled *Chlorella* experiments.

#### 10.2.2.2 Measurements

##### 10.2.2.2.1 Continuous Measurements

The continuous measurement protocols described in Chapter 4.3.2.3.2 (dissolved $O_2$, pH, temperature) are used here.

##### 10.2.2.2.2 Non-continuous Measurements

Photosynthetic yield measurements were replicated per the Chapter 4 protocol.

Due to the clumping nature and various species found in an algal mat, it was difficult to complete an accurate cell count. Thus, 3.5mL samples were drawn from a prepared culture, from which biomass was obtained using the vacuum filtration method outlined in Chapter 5.3.2.3.2. Used filters were placed in Whirl-pak bags and placed in a -19°C freezer for preserving before processing. All filters were dried out in a 60°C oven for >24hrs to obtain the dry mass.

*Chlorella* biomass was not measured during the temperature cycling experiments. However, the amount of biomass produced was estimated using an empirical equation (Eq. 20) converting cell counts to biomass by Sharma et al.

$$m_{cell} = c_{cell} * 1E10^{-4} - 19.61 \quad (20)$$

where $m_{cell}$ is the calculated amount of biomass, mg/L and $c_{cell}$ is the number of cells in a specific volume, cell/mL (Sharma 2012). The resulting calculated biomass was used to determine the $O_2$ produced/biomass ratio.

### 10.3 Data Processing

Data for these experiments were processed in a similar manner to Chapter 4.4.

No dissolved oxygen measurements were recorded for the Antarctic Control (constant +7°C) case, due to the lack of FireSting probes.

The ratio of produced $O_2$ to quantity of dry biomass was calculated for the Antarctic Cycled, *Chlorella* Cycled, and *Chlorella* Cold cases to normalize $O_2$ production and allow for the comparison of $O_2$ generation capabilities.

Two-sample t-Tests (2-tailed, assumed equal variance, independent, $p < 0.05$) were conducted since the duration of experimental runs varied between cases. The null hypothesis was, "The treatment (temperature, algal species) has no statistically significant effect on the measured parameter," for all tested cases. All calculations and compiling of data were conducted with Microsoft Excel 2016 with the Data Analysis package. All presented data points represent averaged triplicate results, and the associated standard deviation as the error bars, unless specifically noted.

## 10.4 Results

### 10.4.1 Produced Oxygen Rate

The $O_2$ generation rate for each experimental case (Antarctic Cycled, *Chlorella* Cycled, *Chlorella* Cold) were plotted over the course of the experiment (Figure 91). Two-way t-tests were conducted to compare the three cases ($p < 0.05$). Each case used three different experimental runs, each lasting at least 6 days. Each combination of cases was investigated. The comprehensive list of p-values, degrees of freedom, and associating t-values, are shown in Table 63. The results suggest that the Antarctic Cycle case produced a significantly greater amount of $O_2$ (approximately 80% more) than the *Chlorella*-dominant cases.

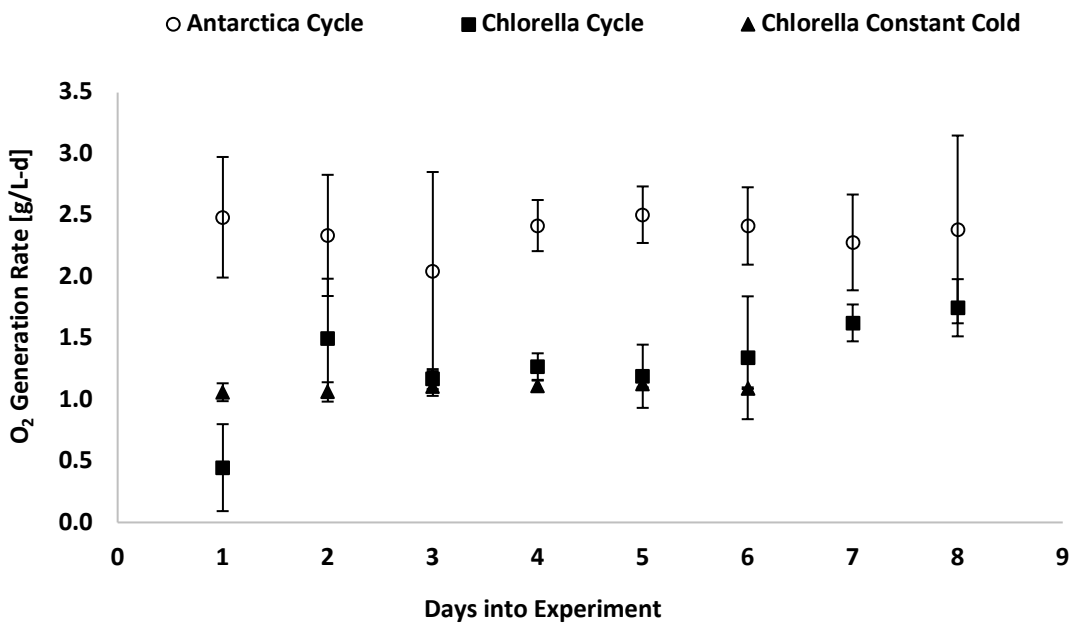


**Figure 91. $O_2$ generation rate of Antarctic Chlorophytes compared to the $O_2$ generation rate of *Chlorella vulgaris* cultured in similar conditions. Each data point is the average of experimental runs at each timestamp. Error bars are the standard deviation resulting from multiple experimental runs.**

**Table 63. Resulting p-values between all combinations of treatments comparing the oxygen production values of the Antarctic and *Chlorella* experiments. All p-values have been listed.**

| Treatment Combination | p-values |
|---|---|
| Antarctic Cycle vs *Chlorella* Cycle | $t = 2.13$, $df = 15$, $p = 1.53 \times 10^{-6}$ |
| Antarctic Cycle vs *Chlorella* Constant Cold | $t = 2.16$, $df = 13$, $p = 1.15 \times 10^{-11}$ |
| *Chlorella* Cycle vs *Chlorella* Constant Cold | $t = 2.18$, $df = 12$, $p = 0.27$ |

### 10.4.2 Oxygen Production to Biomass Ratio

The two-way t-tests compared the three experimental cases after determining the oxygen production to biomass ratio ($p<0.05$). The comprehensive list of p-values, degrees of freedom and associated t-values are shown in Table 64. Every combination rejected the null hypothesis, which suggests that each calculated ratio is significantly different. The *Chlorella* cases had wide variance, which may be a result of the biomass estimation approach. Directly measuring biomass content would reduce these variances. These results suggest that Antarctic mat may not be as efficient at producing $O_2$ per amount of biomass when compared to the constant-cold *Chlorella* case. However, since this result is not consistent across all the *Chlorella* cases, further experimentation is required.

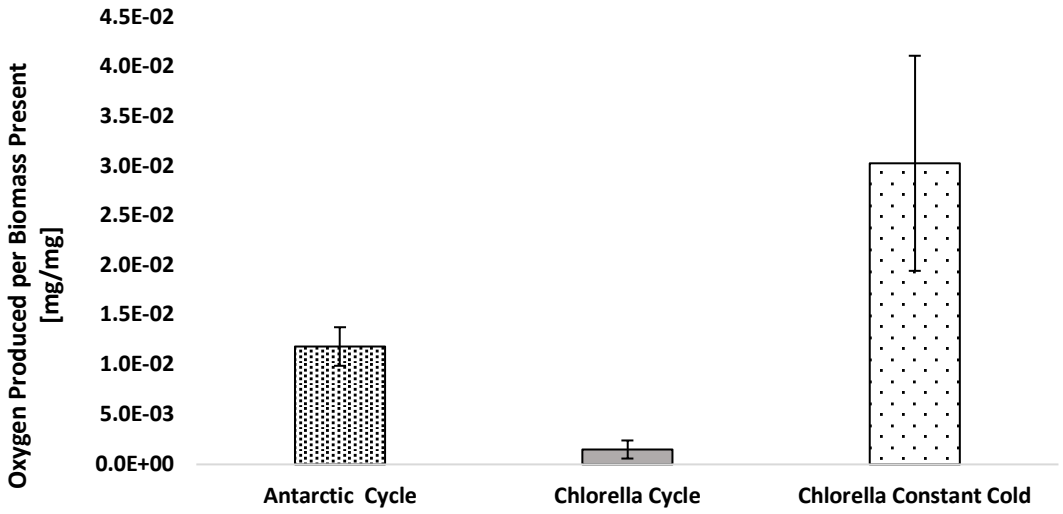


**Figure 92. The ratio of final oxygen production rate to the final biomass amount for each temperature case. Each data point is the average of each experimental run using final biomass and oxygen production rate measurements. Error bars are the standard deviation resulting from multiple experimental runs.**

**Table 64. Resulting p-values between all combinations of treatments comparing the oxygen production to biomass ratio for the Antarctic and *Chlorella* experiments. All p-values have been listed**

| Treatment Combination | p-values |
|---|---|
| Antarctic Cycle vs *Chlorella* Cycle | t = 3.18, df = 3, p = 0.01 |
| Antarctic Cycle vs *Chlorella* Constant Cold | t = 2.77, df = 4, p = 0.04 |
| *Chlorella* Cycle vs *Chlorella* Constant Cold | t = 3.18, df = 3, p = 0.04 |

### 10.4.3 Photosynthetic Yield

The Antarctic species experience an acclimation period drop within the first two days of culturing, just like the *Chlorella* species. The Antarctic cases, and *Chlorella* cycle and control trended together over the experiment duration (Figure 93). However, the constant-cold *Chlorella* case's yield values dropped over the first few days during the acclimation period and never recovered back to its original yield value. Variation of $O_2$ production among the Antarctic cases may be due to clumping. Two-sample t-tests compared the significance of the Antarctic cycle yield values to all other cases (Table 65), since its response to the cycled temperatures are of particular interest to the photobioreactor system. The Antarctic cycle versus the constant-cold *Chlorella* case was the only comparison able to reject the null hypothesis, with the Antarctic cycle providing significantly higher yield values (approximately 57% higher). All other comparisons accepted the null hypothesis. Since photosynthetic yield can be used as a proxy for

culture efficiency or health, this suggests that the Antarctic species operates better in the cold environment than *Chlorella*.

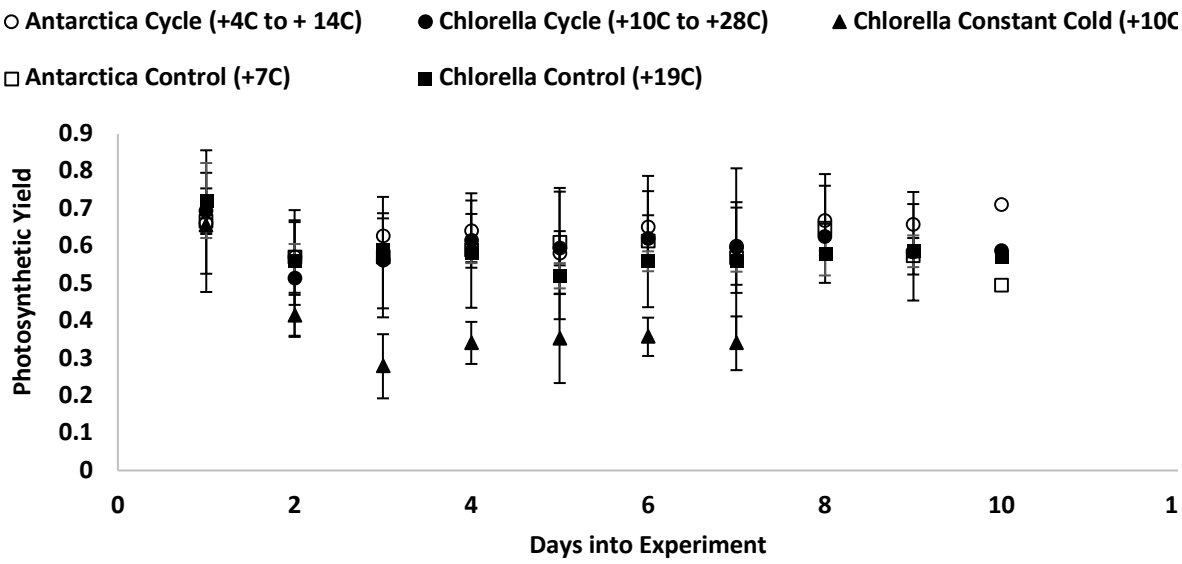


**Figure 93. Photosynthetic yield measurements for both Antarctic species and *Chlorella* tests are plotted against experiment duration. Each data point is the average of experimental runs at each timestamp. Error bars are the standard deviation resulting from multiple experimental runs.**

**Table 65. Resulting p-values between all combinations of treatments comparing the photosynthetic yield values of the Antarctic and *Chlorella* experiments. Those p-values for the Antarctic cycled comparisons have been listed**

| Treatment Combination | p-values |
|---|---|
| Antarctica Cycle vs *Chlorella* Cycle | t = 2.12, df = 16, p = 0.2 |
| Antarctica Cycle vs Antarctica Control | t = 2.12, df = 16, p = 0.14 |
| Antarctica Cycle vs *Chlorella* Constant Cold | t = 2.15, df = 13, p = 0.002 |
| Antarctica Cycle vs *Chlorella* Control | t = 2.12, df = 16, p = 0.07 |

### 10.5 Discussion

Preliminary results suggest that the mixture of Chlorophyta and Cyanophyta sampled from the Antarctic Dry Valleys continued to be viable while being subjected to temperature swings between +4°C to +14°C. The $O_2$ generation rate for the Antarctic algal mat was significantly higher (approximately 80%) than the *Chlorella* values when comparing the temperature cycled cases and the constant-cold *Chlorella* case. However, when $O_2$ generation was normalized by biomass amount, the constant-cold *Chlorella* case had a higher $O_2$/biomass ratio than the

Antarctic cycle case. The biomass of *Chlorella* was estimated with an empirical equation from literature which converted cell counts to biomass, which increases the uncertainty of these results. Conversely, the Antarctic cycle case reported significantly higher photosynthetic yield values (approximately 57%) than the constant cold case. This disparity in the outcomes, indicates that additional experimentation is required to increase the confidence in these results.

Aggregation of the Antarctic mat made it challenging to evenly distribute the biomass across each of the wells and increased the variance in the initial biomass measurements. A more homogenous sample could be accomplished through culture agitation for future experiments.

The *Chlorella* samples cultured in a constant cold environment cases were included in this chapter's comparisons for two reasons. First, the *Chlorella* cultured in a constant-cold environment could be thought of as a *Chlorella* counterpart to the Antarctic control, since both were cultured in environments of ≤+10°C. Second, coolant can take up more heat when delivered at its lowest temperature. If algal medium is utilized as the heat-transfer working fluid, may be cultured at constant, cold temperatures (between +4°C and +10°C). Thus, requiring the constant-cold *Chlorella* case to be included in the comparison to Antarctic species, cultured in similar conditions.

The Antarctic green mat's extremophilic capabilities by inhabiting cold (between +4°C and +10°C) and high UV environments, while also planning for mat transportation through cryopreservation may be advantageous to extreme environments, such as spaceflight. While the results of these experiments do not guarantee that Antarctic algal mat is better suited for spaceflight applications than *Chlorella*, they have shown that these cold-acclimated species were viable in the LTL thermal conditions.

### 10.6 Conclusion

These experiments were conducted to compare the metabolic performance of algal mat already acclimated to cold environments to their temperate-*Chlorella* counter parts. Preliminary findings from culture experiments suggest that Chlorophytes, green algal mat, collected from the McMurdo Dry Valleys of Antarctica may have higher $O_2$ production rates and comparable photosynthetic yields to the *Chlorella* temperature-cycled case. Additional experimentation could corroborate these findings and provide stronger characterization of these Antarctic algae.

## 10.7 Resulting Publications

Journal Papers

Matula, E. E., Nabity, J.A. McKnight, D. M. (20XX). "Comparison of the oxygen production of *Chlorella vulgaris* and Antarctic Chlorophyta for use in a spaceflight environment "[In-Prep, Working Title], Polar Biology

## 10.8 Special Acknowledgement

Cultures for this chapter were provided by the McMurdo Long-Term Ecological Research (MCM-LTER) group, which is supported by NSF Grant #OPP-1637708. Special thanks to Dr. Diane McKnight, Dr. Michael Gooseff, and the C-509 team for their guidance and support.

# Chapter 11 Conclusion and Recommendations for Future Work

## 11.1 Dissertation Summary

This body of research investigated the ability to utilize an algal culture for simultaneous air revitalization and active thermal control of a spacecraft or surface habitat. Integration of a photobioreactor into a spaceflight mission design has the potential to offer closure of the carbon loop through photosynthesis and edible biomass. Furthermore, algal culturing techniques such as growth in water-based media, could offer additional ECLSS functionalities. Utilizing the algal media as a thermal transport media and paralleling the operation of the current ISS thermal control system, the algal culture could be used for active thermal control of the spacecraft environment. Developing a multifunctional system, such as using an algal culture for simultaneous air revitalization and active thermal control, has the potential to save on mass, power, and volume by addressing multiple ECLSS functionalities with one volume of algae. The conducted literature reviews, and subsequent experimentation investigated an algal culture's metabolic response to dynamic thermal and $CO_2$ concentration environments, reflecting the transient environment of a spacecraft cabin, to understand the potential benefits and shortcomings of this type of integrated system.

Reviewing failure causes and modes of utilizing an algal bioreactor for ECLSS purposes informed the experiments going forward, as well as potential bioreactor designs for spaceflight. Experiments subjecting cultures to temperature swings and changes to supplied $CO_2$ concentrations indicated that algal cultures continued to be viable in dynamic environments. Testing the simultaneous heat and mass transfer capabilities of a nonporous gas to liquid contacting membrane characterized its capabilities for non-bubbling gas transfer, suitable for use in spaceflight. Development of a benchtop photobioreactor, minimizing the amount of included gravity-dependent designs, allowed for testing of a comprehensive system for air revitalization and active thermal control. Here, the design of the reactor was studied to understand potential difficulties in operation and its ability to support an algal culture in a dynamic environment. In conjunction with the lessons learned from operation of the benchtop photobioreactor, a literature review was conducted to execute a first-order comparison of the mass, power, and volume of current ISS ECLSS systems to that of an algal photobioreactor fulfilling those same functions. Finally,

replications of the previously conducted temperature cycling experiments were executed using Antarctic algal samples to compare the extremophile's metabolic response to that of the previously tested *Chlorella*.

Conclusions from this work indicate that algae, specifically *Chlorella*, are viable in dynamic temperature and $CO_2$ concentration environments. Adapting to the surrounding environment, the culture was able to measurably shift its metabolic processes to sustain itself through the duration of various experiments. While the implementation of photobioreactors into human spaceflight designs are just commencing, this research has indicated algal cultures can withstand the tested cabin environments and may still be sustainable for simultaneous air revitalization and thermal control of a spacecraft cabin environment.

## 11.2 Review of Objectives and Chapters with Conclusions

### 11.2.1 Research Objectives

1. *Investigate the reliability of an algal photobioreactor system used in nominal cabin atmospheric and thermal environments through literature surveys and experimental results.*
2. *Determine the influence of steady-state and dynamic environmental temperatures on the algal system's $CO_2$ removal and reduction, $O_2$ regeneration, and cell growth rate.*
3. *Characterize the effects of time-varying the input $CO_2$ concentrations on an algal photobioreactor system's $CO_2$ removal, $O_2$ regeneration, and metabolic rates.*
4. *Characterize simultaneous heat and mass transfer capabilities of a non-porous membrane suitable for gravity independent gas transfer.*
5. *Develop a bench-top algal system, designed to minimize gravity effects, that allows for the study of closed-loop simultaneous algal air revitalization and thermal control.*
6. *Consider the first-order feasibility of an algal photobioreactor system as a closed loop $CO_2$ reduction and $O_2$ regeneration system under nominal spacecraft cabin atmospheric and temperature conditions.*

### 11.2.2 Summary of Chapters

Chapter 1 started with NASA's request for closed loop, robust ECLSS to service manned missions farther than before. It was suggested in the same call-to-action that algae and microbiological organisms may be an appropriate solution. It was hypothesized that combining air revitalization through algae photosynthesis, and active

thermal control, using the liquid medium, two systems could share one footprint. This could possibly create a mass, power, volume, savings. An overview of the proposed research topic, using an algal photobioreactor as a simultaneous air revitalization and active thermal control unit, was presented. The research objectives first proposed at the comprehensive exam were re-introduced here. A brief overview of the dissertation connected the research objectives and the completed research

Chapter 2 restated the problem and the researched solution. The current standard for ECLSS in long duration human spaceflight was reviewed as well as the current progress in the research field. The history of bioregenerative ECLSS, and the human metabolic requirements were also introduced as considerations in future experiments.

Chapter 3 addressed research Objective 2 by creating an overview of the failure modes, causes, and effects of a photobioreactor used for ECLSS applications. This study was split into two sections, one focused the biological and cell physiology aspects of a culture failure and the other focused on the supporting hardware, and how it could fail while servicing the culture. Each presented failure was assigned a likelihood and severity position, to inform designers of biological-based failures with photobioreactors.

Chapter 4 started the investigation of the effect of temperature on *Chlorella's* metabolic rates by culturing algae in steady-state temperatures optimizing either heat transfer of the liquid medium or air revitalization qualities of the algae. Metabolic rates including $O_2$ production, cell viability, and density growth rates. Statistically significant differences between the hot (optimizing air revitalization) and cold (optimizing heat transfer) were recorded. This corroborated the trends found in literature, investigated operational boundaries for the culture, and informed results of the dynamic temperature experiments.

Chapter 5 characterized the effect to *Chlorella's* $O_2$ production, cell viability, and growth rates when subjected to temperature swings reflective of traveling through the ISS thermal control loop, directly relating to research Objective 4. Two confounding variables were also studied, biological contamination in the culture and daily nutrient addition, to see if either of them significantly influenced oxygen production. Results indicated that culture contamination with bacteria nor daily nutrient addition significantly affected the $O_2$ production, cell viability, or growth rates of the culture undergoing temperature cycles.

Chapter 6 investigated the effect of subjecting *Chlorella* to various steady-state and dynamic concentrations of $CO_2$, paralleling the atmospheric environment of a spacecraft. This work examined the question posed in Objective 3. Step-change $CO_2$ profiles were used to assess the effects of the dynamic environment on $O_2$ production, cell viability, and growth rates. Results supported the developed hypotheses, that culture $O_2$ production, cell viability, and growth rates were positively correlated with the fed concentration of $CO_2$.

Chapter 7 developed heat and mass transfer models for a nonporous, gas-permeable membrane by running combinations of water and gas flow rates and gas flow rates reflective of the flow rates found in a spacecraft. This addressed research Objective 5. Here, it was established that gas transfer rates are dominated by water flow rates, while heat transfer rates are dictated by gas flow rates. Suggesting that for the gas-liquid contacting purposes of the combined air revitalization and active thermal control photobioreactor, the media flow rate should be as slow as possible while the gas flow rate be as fast as possible for efficient transfer.

Chapter 8 presented considerations when developing bioreactors for spaceflight. With these considerations, and the lessons learned from previous experiments, bench-top closed-loop photobioreactor that minimized the inclusion of gravity dependent technologies was designed and prototyped, directly addressing objective number 6. The design was tested through experimentation, while subjecting the culture to temperature and $CO_2$ concentration cycles. The reactor was able to support algal growth for the entirety of a 25-day test, however the membrane contactor actively filtered out the biomass, and aggregated it around the membrane fibers. Fortunately, even with the buildup of biomass, the membranes were able to maintain constant rates of heat and mass transfer. Design critiques and suggestions for future bioreactor modifications were offered at the end of the chapter.

Chapter 9 presented a first order feasibility assessment of a using a photobioreactor to address multiple functionalities in one spacecraft, while predicting the resulting size, mass, and required volume. This preliminary study suggested that using a mixed technology approach, by addressing ECLSS functions through both an algal photobioreactor and current ISS technologies, has the potential for mass and volume savings.

Chapter 10 replicated Chapter 5's temperature cycling experiment, but incorporated samples of green mat (Chlorophyta and Cyanophyta) sampled from Antarctica instead of *Chlorella*. This experiment investigated if natural acclimation to cold environments would produce any potential advantages in $O_2$ production, when compared to

*Chlorella* samples cultured in temperate conditions. This preliminary work suggested that there may be some benefit to using the Antarctic-native mat for $O_2$ production, but additional experimentation is required to increase confidence in these results.

### 11.3 Future Work

This work provided an initial investigation into the feasibility of using a volume of algae for more than just air revitalization. Adding the active thermal control aspect could increase the functionality of included bioregenerative systems in spacecraft designs. The results from this work indicate that algae are adaptive to dynamic environments within the spacecraft cabin operating environment. Furthermore, selecting species whose natural environment reflects the operating environment may provide increased $O_2$ and cell viability. Consequently, this was a small body of work in comparison to what is required to establish enough statistical significance to convince the spaceflight community to include algae in ECLSS designs. Therefore, replicates of previously conducted space algal science should be executed to help develop that significance.

Using the "lab rats" of algae, *Chlorella* and *Spirulina*, for engineering experiments are great for initial investigations, but additional species that are known for surviving like-environments should also be included in the experimental matrix. This avoids prematurely discarding potential spaceflight technologies because the species selected did not survive an unsuitable environment. Conducting experiments with species found in the Antarctic, Artic, and others found in high elevations could increase the database of species with specific capabilities but could also help the microbiology world expand their understanding of algal environmental tolerances as well. Additionally, cultures used in future experimentation do not have to be monospecies, meaning combinations of algae could be explored in order to accommodate wider ranges of environmental conditions or specific ECLSS functions.

The experiments for this body of work were conducted over relatively short timescales (7-25 days) when compared to the potential of using on a long duration spaceflight mission (>90 days). Preliminary spaceflight experiments have indicated that algae can survive long duration spaceflight (experiments conducted up to 530 days), but these experiments did not include measurements that specified their capability to fulfill ECLSS functions during flight (de Vera et al. 2019). Therefore, replicating the presented experiments with longer experiment durations (>90 days) would instill confidence in the long-term sustainability in the dynamic environments but also could elucidate

any long-term culturing issues. These issues could include species or bacterial dominance (if using a non-axenic culture) or genetic modification of the culture -potentially rendering the culture unable to perform the required ECLSS functions. Additional measurements of spaceflight experiments, including continuous dissolved $O_2$, cell growth rate, and biomass content, may indicate any effects of spaceflight to the culture's metabolic processes.

The establishment period of growth may also be an important factor in utilization of algal cultures. Depending on the mission requirements, it may not be feasible to transport a fully established culture density but instead take up small samples and culture when appropriate. Establishing the required density may take a significant amount of time, which also may not be possible for a spaceflight mission. Therefore, characterization of establishment time or culture transportation techniques (such as cryopreservation) will inform culturing timelines during mission transport or utilization.

While an algal photobioreactor can passively adapt to the surrounding environment, active control may be necessary. There is the potential to control the metabolic rates of the culture through variation of irradiance, supplied $CO_2$ concentration, temperature, or concentration of nutrients in the media. Characterization of the effect of each of these inputs could allow future photobioreactor designs to implement more control, paralleling the operation of the current ISS ECLSS systems, if necessary.

The completion of this forward work, in conjunction with the presented research in this dissertation, could exemplify the resiliency of algal culture to dynamic environments. The completed experiments subjected algal cultures to transient temperature and $CO_2$ concentration environments, in an effort to determine their suitability for use in a photobioreactor designed to support simultaneous air revitalization and active thermal control. The cultures survived the dynamic environments and suggested that the specified ECLSS functions could be supported. Using the results presented here, there is the potential that algae could benefit human spaceflight through providing an approach to closed-loop, adaptive ECLSS.

### 11.4 Extraneous Presentations and Publications (Besides those mentioned under relating chapters)

**Journal Papers**

Matula, E. E., McKnight, D. M. (20XX). Chlorophyte biodiversity patterns of the green mat found in multi-Valley sampling [In-Prep, Working Title]

**Presentations**

University of Colorado -Boulder Aerospace Engineering Department's Researchpalooza, "Surviving Space with Algae," Boulder, CO, 2015.

University of Colorado -Boulder Aerospace Engineering Department's Researchpalooza, "Characterizing *Spirulina*'s Metabolic Response to Transient Thermal Environments," Boulder, CO, 2015.

Boulder County Senior Center Lecture Series, "University of Colorado's Involvement in NASA's Current Human Spaceflight Program," Boulder, CO, 2017.

**Popular Press**

Asgardia.space, "Algae might be the ingredient needed to make long-term space travel possible", Medium, March 2019, https://medium.com/life-on-the-other-planets-whats-new/algae-might-be-the-ingredient-needed-to-make-long-term-space-travel-possible-2c97aa74a845.

Beall, A.,"Clever space algae could be the key to getting humans to Mars", Wired, February 2019, https://www.wired.co.uk/article/algae-long-term-space-missions.

Matula, E. E., 'Using algae as an alternative source of environmental control and life support systems in space exploration", Science Trends, March 2019, https://sciencetrends.com/using-algae-as-an-alternative-source-of-environmental-control-and-life-support-systems-in-space-exploration/.

Wettstein, G., "A Day in the Life: Bioastronautics student Emily Matula", Science Buffs, September 2017, https://sciencebuffs.org/2017/09/20/a-day-in-the-life-bioastronautics-student-emily-matula-talks-astronauts-algae-and-mentoring-adolescents/.

### 11.5 Resulting Public Outreach

Earth Explorers –Expert Scientist (2015)
Shades of Blue –Group Leader (2015)
DSST Day –Activity Leader (2015)
NASA Remote Mentor (2015)
Houston Aerospace Scholars –Professional Mentor (2015)
Earth Explorers –Expert Scientist (2015, 2016)
Stats Tutor –Graduate Level (2015-2016)
Lockheed Martin High School Night –Tour Guide (2016)
Exploring Your Horizons -Presenter (2017, 2018)
EHS SAA Reviewer(2017-Present)
STEMRev -Mentor (2017-2018)
Girls in STEM Weekend -Presenter (2018)
Exploring Your Horizons -Presenter (2018)
Preliminary Exam Tutor (2018)
Granville High School VEGGIE -Presenter (2018)
CU Amateur Radio Club President (May 2018-December 2018)
MCM-LTER Calls from Antarctica for Kenston and Granville Schools (Jan/Feb 2019)

### 11.6 Awards

AIAA, Neil Armstrong Graduate Award -June 2018
University of Colorado, Aerospace Engineering Department, John A. Vise Graduate Award -May 2018
AAUW Brown/Ricketts/Udick Grant –April 2016

# REFERENCES


Abney, Morgan B, and J Matthew Mansell. 2011. "Evaluation of Bosch-Based Systems Using Non-Traditional Catalysts at Reduced Temperatures." In *41st International Conference on Environmental Systems*, 1–14. Portland, OR. https://doi.org/doi:10.2514/6.2011-5059.

Akin, David. 2013. "Introduction to Habitability." University of Maryland. 2013. http://spacecraft.ssl.umd.edu/academics/697S13/697S13L09.habitability1.pdf.

"Algae and the Nitrogen Cycle." 2012. 2012. http://biocyclopedia.com/index/algae/biogeochemical_role_of_algae/algae_and_the_nitrogen_cycle.php.

Ammann, Elizabeth C. B., and Antony Fraser-Smith. 1968. "Gas Exchange of Algae." *Applied Microbiology* 16 (5): 669–72.

Andersen, R.A., ed. 2005. *Algal Culturing Techniques*. New York: Elsevier Academic Press.

Anderson, Molly S., Michael K. Ewert, John F. Keener, and Sandra A. Wagner. 2018. "Life Support Baseline Values and Assumptions Document." *Nasa/Tp-2015-218570*, no. March: 1–220. https://doi.org/CTSD-ADV-484 A.

Anderson, Molly S, Michael Ewart, John F Keener, and Sandra A Wagner. 2015. "Advanced Life Support Baseline Values and Assumptions Document." *National Aeronautics and Space Administration*, no. August: 172. https://doi.org/CTSD-ADV-484 A.

Attaway, H, C H Gooding, and M G Schmidt. 2002. "Comparison of Microporous and Nonporous Membrane Bioreactor Systems for the Treatment of BTEX in Vapor Streams." *Journal of Industrial Microbiology & Biotechnology* 28 (5): 245–51. https://doi.org/10.1038/sj/jim/7000235.

Augustin, Jens. 2017. "Experiment on the ISS Algae Survive Heat, Cold and Cosmic Radiation." Munich. www.izi.fraunhofer.de.

Averner, Maurice, Yarcus Karel, Richard Radmer, and Marcus Karel. 1983. "Problems Associated with the Utilization of Algae in Bioregonerative Life Support Systems." Moffett Field.

Bagdigian, Robert M., and Dale Cloud. 2005. "Status of the International Space Station Regenerative ECLSS Water Recovery and Oxygen Generation Systems." *Society of Automotive Engineers*. https://doi.org/10.4271/2005-01-2779.

Bajguz, Andrzej. 2000. "Blockade of Heavy Metals Accumulation in Chlorella Vulgaris Cells by 24-Epibrassinolide." *Plant Physiology and Biochemistry* 38 (10): 797–801. https://doi.org/10.1016/S0981-9428(00)01185-2.

Barghbani, R., K. Rezaei, and A. Javanshir. 2012. "Investigating the Effects of Several Parameters on the Growth of Chlorella Vulgaris Using Taguchi's Experimental Approach." *International Journal of Biotechnology for Wellness Industries* 1 (2): 128–33. https://www.lifescienceglobal.com/pms/index.php/ijbwi/article/view/28/100.

Barghouty, AF, and SA Thibeault. 2006. "The Exploration Atmospheres Working Group ' s Report on Space Radiation Shielding Materials."

Barth, J.L., C.S. Dyer, and E.G. Stassinopoulos. 2003. "Space, Atmospheric, and Terrestrial Radiation Environments." *IEEE Transactions on Nuclear Science* 50 (3): 466–82. https://doi.org/10.1109/TNS.2003.813131.

Bartosh, Y., and C. J. Banks. 2007. "Algal Growth Response and Survival in a Range of Light and Temperature Conditions: Implications for Non-Steady-State Conditions in Waste Stabilisation Ponds." *Water Science and Technology* 55 (11): 211–18. https://doi.org/10.2166/wst.2007.365.

Beattie, Andrew J, Mark Hay, Bill Magnusson, Rocky de Nys, James Smeathers, and Julian F V Vincent. 2011. "Ecology and Bioprospecting." *Austral Ecology* 36 (3): 341–56. https://doi.org/10.1111/j.1442-9993.2010.02170.x.

Bennett, J, and M Klich. 2003. "Mycotoxins." *Clinical Microbiology REviews*, 497–516. https://www.ncbi.nlm.nih.gov/pmc/articles/PMC164220/pdf/0050.pdf.

Bergman, T., Lavine, A., Incropera, F., Dewitt, D. 2011. "Relationship to Thermodynamics." In *Fundamentals of Heat and Mass Transfer*, 7th ed., 17. Hoboken: John Wiley & Sons.

Beville, Terrie. 2014. "NASA - Space Radiation Analysis Group (SRAG) Web Site." Terrie Bevill. 2014. http://srag-nt.jsc.nasa.gov/spaceradiation/faq/faq.cfm.

Blüm, V., J. I. Gitelson, G. Horneck, and K. Kreuzberg. 1994. "Opportunities and Constraints of Closed Man-Made Ecological Systems on the Moon." *Advances in Space Research* 14 (6): 271–80. https://doi.org/10.1016/0273-1177(94)90038-8.

Boributh, Somnuk, Suttichai Assabumrungrat, Navadol Laosiripojana, and Ratana Jiraratananon. 2011. "A Modeling Study on the Effects of Membrane Characteristics and Operating Parameters on Physical Absorption of CO2 by

Hollow Fiber Membrane Contactor." *Journal of Membrane Science* 380 (1–2): 21–33. https://doi.org/10.1016/j.memsci.2011.06.029.
Borowitzka, Michael a. 1999. "Commercial Production of Microalgae: Ponds, Tanks, Tubes and Fermenters." *Journal of Biotechnology* 70 (1–3): 313–21. https://doi.org/10.1016/S0168-1656(99)00083-8.
Borsche, Catherine E. 2005. "ISS 5th Anniversary of Human Occupancy." NASA. 2005. https://www.nasa.gov/mission_pages/station/main/5_year_anniversary.html.
Bosma, R, J H De Vree, P M Slegers, M Janssen, R H Wijffels, and M J Barbosa. 2014. "Design and Construction of the Microalgal Pilot Facility AlgaePARC." *Algal Research* 6: 160–69.
Bretschneider, Jens, Stefan Belz, H. Helisch, G. Detrell, J Keppler, and Stefanos Fasoulas. 2016. "Functionality and Setup of the Algae Based ISS Experiment PBR@LSR." In *International Conference on Environmental Systems*, 1–11. Vienna, Austria.
Bronnenmeier, R., and H. Märkl. 1982. "Hydrodynamic Stress Capacity of Microorganisms." *Biotechnology and Bioengineering* 24 (3): 553–78. https://doi.org/10.1002/bit.260240304.
Broyan, James, David Welsh, and Scott Cady. 2010. "International Space Station Crew Quarters Ventilation and Acoustic Design Implementation." *40th International Conference on Environmental Systems*, 1–16. https://doi.org/10.2514/6.2010-6018.
Campbell, N.A., and J.B. Reece. 2008. *Photosynthesis*. 8th ed. Pearson.
Carlson, Susan. 2011. "GRAS Exemption Claim for Chlorella Vulgaris as an Ingredient in Foods." College Park, MD.
Carter, D Layne. 2009. "Status of the Regenerative ECLS Water Recovery System." In *AIAA International Conference on Environmental Systems*, 1–11. Barcelona, Spain. https://doi.org/10.2514/6.2010-6216.
Červený, Jan, Ivan Šetlík, Martin Trtílek, and Ladislav Nedbal. 2009. "Photobioreactor for Cultivation and Real-Time, in-Situ Measurement of O2 and CO2 Exchange Rates, Growth Dynamics, and of Chlorophyll Fluorescence Emission of Photoautotrophic Microorganisms." *Engineering in Life Sciences* 9 (3): 247–53. https://doi.org/10.1002/elsc.200800123.
Chambliss, Joe, Gary Rankin, Tim Bond, Cindy Cross, Mike Holt, Jerry Ling, and Leon Collins. 2003. "The State of ISS ATCS Design, Assembly, and Operation." *Journal of Aerospace* 112 (1): 193–206.
Chinnasamy, Senthil, Balasubramanian Ramakrishnan, Ashish Bhatnagar, and Keshav C Das. 2009. "Biomass Production Potential of a Wastewater Alga Chlorella Vulgaris ARC 1 under Elevated Levels of CO2 and Temperature." *International Journal of Molecular Sciences* 10 (2): 518–32. https://doi.org/10.3390/ijms10020518.
Chisti, Yusuf. 2007. "Biodiesel from Microalgae." *Biotechnology Advances* 25: 294–306. https://doi.org/10.1016/j.biotechadv.2007.02.001.
———. 2008. "Biodiesel from Microalgae Beats Bioethanol." *Trends in Biotechnology*, 2008. https://doi.org/10.1016/j.tibtech.2007.12.002.
Cloot, A. 1994. "Effect of Light Intensity Variations on the Rate of Photosynthesis of Algae: A Dynamical Approach." *Mathl. Comput. Modelling* 19 (9): 23–33.
Cohen, Marc M., Michael T. Flynn, and Renee L. Matossian. 2013. "Water Walls Life Support Architecture." In *43rd International Conference on Environmental Systems*, 1–15. Reston, Virginia: American Institute of Aeronautics and Astronautics. https://doi.org/10.2514/6.2013-3517.
Cohen, Marc M, Michael T. Flynn, and Renee L. Matossian. 2012. "Water Walls Architechture: Massively Redundant and Highly Reliable Life Support for Long Duration Exploration Missions." In *Global Space Exploration Conference*, 1–14. Washington, D.C.
Cole, Jonathan J, and Jonathan J Cole1. 1982. "Interactions Between Bacteria and Algae in Aquatic Ecosystems." *Source: Annual Review of Ecology and Systematics Ann Rev. Ecol. Syst* 13 (13). http://www.jstor.org/stable/2097070.
"Coronal Mass Ejections | NOAA / NWS Space Weather Prediction Center." n.d. Accessed April 18, 2016. http://www.swpc.noaa.gov/phenomena/coronal-mass-ejections#.
Costache, T. A., F. Gabriel Acien Fernandez, M. M. Morales, J. M. Fern??ndez-Sevilla, I. Stamatin, and E. Molina. 2013. "Comprehensive Model of Microalgae Photosynthesis Rate as a Function of Culture Conditions in Photobioreactors." *Applied Microbiology and Biotechnology* 97 (17). https://doi.org/10.1007/s00253-013-5035-2.
Coutts, Janelle, Griffin M Lunn, Leticia Vega, and Caitlin E Meyer. 2015. "Analysis of Process Gases and Trace Contaminants in Membrane-Aerated Gaseous Effluent Streams." In *International Conference on*

*Environmental Systems*, 1–12. Bellevue, WA.
Cramer, Marian, and Jack Myers. 1948. "Effects of Starvation on the Metabolism of Chlorella." *Plant Physiology* 255–264. https://www.ncbi.nlm.nih.gov/pmc/articles/PMC437368/pdf/plntphys00264-0063.pdf.
Cronyn, Patrick D, Sharmi Watkins, and David J Alexander. 2012. "Chronic Exposure to Moderately Elevated CO 2 during Long-Duration Space Flight."
Darling, Joshua P., Deena D. Garland, Lee F. Stanish, Rhea M.M. Esposito, Eric R. Sokol, and Diane M. McKnight. 2017. "Thermal Autecology Describes the Occurrence Patterns of Four Benthic Diatoms in McMurdo Dry Valley Streams." *Polar Biology* 40 (12): 2381–96. https://doi.org/10.1007/s00300-017-2151-y.
Dauta, Alain, Jean Devaux, Fran oise Piquemal, and Lhoussaine Boumnich. 1990. "Growth Rate of Four Freshwater Algae in Relation to Light and Temperature." *Hydrobiologia* 207 (1): 221–26. https://doi.org/10.1007/BF00041459.
Davidson, I. 1991. "Environmental Effects on Algal Photosynthesis: Temperature." *Journal of Phycology* 27: 2–8. https://colorado-illiad-oclc-org.colorado.idm.oclc.org/illiad/COD/illiad.dll?Action=10&Form=75&Value=834949.
Degen, Jörg, Andrea Uebele, Axel Retze, Ulrike Schmid-Staiger, and Walter Trösch. 2001. "A Novel Airlift Photobioreactor with Baffles for Improved Light Utilization through the Flashing Light Effect." *Journal of Biotechnology* 92 (2): 89–94. https://doi.org/10.1016/S0168-1656(01)00350-9.
Dixon, R., and D. Kahn. 2004. "Genetic Regulation of Biological Nitrogen Fixation." *Nature Reviews Microbiology* 2: 621–31.
Douglas, Neil J, David P White, Cheryl K Pickett, John V Weil, and W Clifford. 1982. "Respiration during Sleep," 840–44.
Doyle, A. 2019. "Ocean Algae Can Evolve Fast to Tackle Climate Change - Scientific American." Scientific American. 2019. https://www.scientificamerican.com/article/ocean-algae-can-evolve-fast-to-tackle-climate-change/.
Drioli, E, A Criscuoli, and E Curcio. 2006. *Membrane Contactors: Fundamentals, Applications and Potentials*. Amsterdam.
Eckart, P. 1996. *Spaceflight Life Support and Biospherics*. Edited by Microcosm Press. 1st ed. Torrance, CA. https://books.google.com/books?id=y3zoCAAAQBAJ&pg=PA270&lpg=PA270&dq=eckart+algal+systems&source=bl&ots=goz1SXpE9W&sig=kQrJFomsI9nBrMYZ6M_wbB0fpzs&hl=en&sa=X&ved=0ahUKEwiQqJ_jtYrQAhWKhVQKHdPJBx4Q6AEIJjAC#v=onepage&q=eckart algal systems&f=false.
Eckart, P. 1995. "Life Support and Biospherics." *Life Support & Biosphere Science : International Journal of Earth Space* 2 (2): 84–385.
Escobar, Christine M, James A Nabity, and David M Klaus. 2017. "Defining ECLSS Robustness for Deep Space Exploration," no. July: 1–15.
Etten, James L. Van, Dwight E. Burbank, Anne M. Schuster, and Russel H. Meints. 1985. "Lytic Viruses Infecting a Chlorella-like Alga." *Virology* 140 (1): 135–43. https://doi.org/10.1016/0042-6822(85)90452-0.
Fan, Li Hai, Ya Tao Zhang, Lin Zhang, and Huan Lin Chen. 2008. "Evaluation of a Membrane-Sparged Helical Tubular Photobioreactor for Carbon Dioxide Biofixation by Chlorella Vulgaris." *Journal of Membrane Science* 325 (1): 336–45. https://doi.org/10.1016/j.memsci.2008.07.044.
Fan, Lihai, Yatao Zhang, Lihua Cheng, Lin Zhang, Desong Tang, and Huanlin Chen. 2007. "Optimization of Carbon Dioxide Fixation by Chlorella Vulgaris Cultivated in a Membrane-Photobioreactor." *Chemical Engineering and Technology* 30 (8): 1094–99. https://doi.org/10.1002/ceat.200700141.
Finlay, Bland J. 2014. "Global Dispersal of Eukaryote Species Microbial" 296 (5570): 1061–63.
Fisher, Paul. 2009. "Water Treatment for Pathogens and Algae." *Horticulture*.
Gatens, Robyn L, Molly S Anderson, James L Broyan, Ariel V Macatangay, Sarah A Shull, Jay L Perry, Walter F Schneider, and Nikzad B Toomarian. 2015. "National Aeronautics and Space Administration Environmental Control and Life Support Technology Development and Maturation for Exploration : 2014 to 2015 Overview." In *45th International Conference on Environmental Systems*, 1–23. Bellevue, WA.
Gentry, Gregory J. 2016. "International Space Station (ISS) Environmental Control and Life Support (ECLS) System Overview of Events: 2015-2016." In *46th International Conference on Environmental Systems*. Vienna, Austria.
Gentry, Gregory J, and John Cover. 2015. "International Space Station (ISS) Environmental Control and Life Support (ECLS) System Overview of Events: 2010 - 2014." In *45th International Conference on Environmental Systems*, 1–12. Bellevue, WA.
Gerardi, M. 2018. "Algae, Alkalinity, and PH." In *The Biology and Troubleshooting of Facultative Lagoons*, 1st ed.,

105–10. John Wiley & Sons, Inc.
Gitelson, J. I., G. M. Lisovsky, and R.D. MacElroy. 2003. *Manmade Closed Ecological Sysems*. Edited by Peter Kleber. 9th ed. New York: Taylor & Francis Group.
Growing Labs. 2019. "All-Glass Vacuum Filter Holder Set." 2019. https://www.growinglabs.com/products/all-glass-vacuum-filter-holder-set.
Hao, Zongjie, Yanhui Li, Wenkai Cai, Peipei Wu, and Yongding Liu. 2012. "Possible Nutrient Limiting Factor in Long Term Operation of Closed Aquatic Ecosystem." *Advances in Space Research* 49 (5): 841–49. https://doi.org/10.1016/j.asr.2011.11.030.
Heile, S., S. Rosenberger, A. Parker, B. Jefferson, and E. J. McAdam. 2014. "Establishing the Suitability of Symmetric Ultrathin Wall Polydimethylsiloxane Hollow-Fibre Membrane Contactors for Enhanced CO2separation during Biogas Upgrading." *Journal of Membrane Science* 452: 37–45. https://doi.org/10.1016/j.memsci.2013.10.007.
Henley, E J, J D Seader, and D K Roper. 1998. *Separation Process Principles*. 2nd ed. Wiley. https://books.google.com/books?id=CUo8bwAACAAJ.
Hintze, P., A. Caraccio, S. Athony, A. Tsoras, M. Nur, R. Devor, and J. Captain. 2014. "Trash-to-Gas: Using Waste Products to Minimize Logistical Mass During Long Duration Space Missions CH 4." In *AIAA SPACE*, 1–6. https://ntrs.nasa.gov/search.jsp?R=20140002806.
Ho, W.S. Winston, and Kamalesh K. Sirkar. 1992. *The Membrane Handbook*. 1st ed. New York: Springer Science + Business Media, LLC.
Hörcsik, Z T, L Kovács, R Láposi, I Mészáros, G Lakatos, and G Garab. 2007. "Effect of Chromium on Photosystem 2 in the Unicellular Green Alga, Chlorella Pyrenoidosa." *PHOTOSYNTHETICA* 45 (1): 65–69. https://link.springer.com/content/pdf/10.1007%2Fs11099-007-0010-8.pdf.
Incropera, F., D. Dewitt, T. Bergman, and A. Lavine. 2007. "Heat Exchanger Analysis: The Effectiveness -NTU Method." In *Introduction to Heat Transfer*, 5th ed., 648–56. John Wiley & Sons.
Ito, Akira, Kazuaki Yamagiwa, Masato Tamura, and Michio Furusawa. 1998. "Removal of Dissolved Oxygen Using Non-Porous Hollow-Fiber Membranes." *Journal of Membrane Science* 145: 111–17. http://ac.els-cdn.com/S0376738898000684/1-s2.0-S0376738898000684-main.pdf?_tid=02c45168-5226-11e7-a9a7-00000aacb360&acdnat=1497571067_9834bbc2260e9e125298cb600f142492.
Jaatinen, Sanna, Aino-maija Lakaniemi, and Jukka Rintala. 2015. "Use of Diluted Urine for Cultivation of Chlorella Vulgaris." *Environmental Technology*, no. December: 1–12. https://doi.org/10.1080/09593330.2015.1105300.
Javanmardian, Minoo, and Bernhard Palsson. 1991. "High-Density Photoautotrophic Algal Cultures: Design, Construction, and Operation of a Novel Photobioreactor System." *Biotechnology* 38 (1): 1182–1189. https://doi.org/10.1002/bit.260381010.
———. 1992. "Design and Operation of an Algal Photobioreactor System." *Advances in Space Research* 12 (5): 231–35.
Jones, Harry. 2011. "Carbon Dioxide Reduction System Trade Studies." In *41st International Conference on Environmental Systems*, 1–12. Portland, OR. https://doi.org/doi:10.2514/6.2011-5099.
———. 2012. "Ultra Reliable Space Life Support." In *AIAA SPACE 2012 Conference & Exposition*, 1–15. Pasadena, CA. https://doi.org/AIAA-2012-5121.
Kanda, Hideki, and Peng Li. 2011. "Simple Extraction Method of Green Crude from Natural Blue-Green Microalgae by Dimethyl Ether: Extraction Efficiency on Several Species Compared to the Bligh-Dyer's Method." http://www.ep.liu.se/ecp/057/vol1/071/ecp57vol1_071.pdf.
Kawasaki, Kristy. 2019. "Physical Properties of Air." Jet Propulsion Laboratory Website. 2019. https://sealevel.jpl.nasa.gov/overview/overviewclimate/overviewclimateair/.
Keppler, J. 2015. "Entwurf, Aufbau Und Test Des Algen Medium Loops Für Das Experiment PBR@ACLS." Univeristy of Stuttgart. https://doi.org/IRS-15-064.
Keppler, Jochen, Stefan Belz, Gisela Detrell, Harald Helisch, Johannes Martin, Norbert Henn, Stefanos Fasoulas, Reinhold Ewald, Oliver Angerer, and Heinz Hartstein. 2018. "The Final Configuration of the Algae-Based ISS Experiment PBR@LSR." In *International Conference on Environmental Systems*, 1–12. https://ttu-ir.tdl.org/handle/2346/74122.
Khalil, Zeinab I., Mohsen M.S. Asker, Salwa El-Sayed, and Imam A. Kobbia. 2010. "Effect of PH on Growth and Biochemical Responses of Dunaliella Bardawil and Chlorella Ellipsoidea." *World Journal of Microbiology and Biotechnology* 26 (7): 1225–31. https://doi.org/10.1007/s11274-009-0292-z.
Kimball, J. 2011. "Discovering the Secrets of Photosynthesis." 2011. http://www.biology-

pages.info/P/Photosynthesis_history.html.
Klaus, D. 1998. “Microgravity and Its Implications for Fermentation Biotechnology.” *Tibtech* 16: 369–72. http://ac.els-cdn.com/S0167779998011974/1-s2.0-S0167779998011974-main.pdf?_tid=482e1f8c-05d1-11e7-b2b5-00000aab0f6b&acdnat=1489178387_eb9d995c2a3c3b3b69e72828c1fe5fe5.
Klaus, D M. 2004. “Space Habitat.” *Space Habitat Design*, no. July: 1–7.
Knox, James C, and Christine M Stanley. 2015. “Optimization of the Carbon Dioxide Removal Assembly ( CDRA - 4EU ) in Support of the International Space System and Advanced Exploration Systems.” In *International Conference on Environmental Systems*, 1–8. Bellevue, WA.
Krall, A. R., and B. Kok. 1960. “Studies on Algal Gas Exchangers with Reference to Space Fligh.” In *Developments in Industrial Microbiology*, edited by S. Rich, 1st ed., 33–44. State College, PA: Springer Science. https://doi.org/10.1007/978-1-4899-5073-4.
Kreith, Frank., and William Z. Black. 1980. *Basic Heat Transfer*. Harper & Row. https://books.google.com/books/about/Basic_Heat_Transfer.html?id=NgVRAAAAMAAJ.
Kumar, Kanhaiya, Sanjiv Kumar Mishra, Gang-Guk Choi, and Ji-Won Yang. 2015. “Chapter 2 CO 2 Sequestration Through Algal Biomass Production.” In *Algal Biorefinery: An Integrated Approach*, edited by D. Das, 35–57. Capital Publishing. https://doi.org/10.1007/978-3-319-22813-6_2.
Lasseur, C. 2011. “MELiSSA: The European Project of Closed Life Support System.” *Gravitational …*, 3–12. http://gravitationalandspacebiology.org/index.php/journal/article/view/487.
Lee, Choul-gyun, and Bernhard Ø. Palsson. 1995. “Light Emitting Diode-Based Algal Photobioreactor with External Gas Exchange.” *Journal of Fermentation and Bioengineering* 79 (3): 257–63. http://www.sciencedirect.com/science/article/pii/0922338X95906135.
Leitch, Megan E., Gregory V. Lowry, and Meagan S. Mauter. 2017. “Characterizing Convective Heat Transfer Coefficients in Membrane Distillation Cassettes.” *Journal of Membrane Science* 538 (March): 108–21. https://doi.org/10.1016/j.memsci.2017.05.028.
Leupold, Marco, Stefan Hindersin, Giselher Gust, Martin Kerner, and Dieter Hanelt. 2013. “Influence of Mixing and Shear Stress on Chlorella Vulgaris, Scenedesmus Obliquus, and Chlamydomonas Reinhardtii.” *Journal of Applied Phycology* 25: 485–95. https://doi.org/10.1007/s10811-012-9882-5.
Li, Gen-bao, Yong-ding Liu, Gao-hong Wang, and Li-rong Song. 2004. “Reactive Oxygen Species and Antioxidant Enzymes Activity of Anabaena Sp. PCC 7120 (Cyanobacterium) under Simulated Microgravity.” *Acta Astronautica* 55 (11): 953–57. https://doi.org/10.1016/j.actaastro.2004.04.014.
Li, K., Mona S.L. Tai, and W. K. Teo. 1994. “Design of a CO2scrubber for Self-Contained Breathing Systems Using a Microporous Membrane.” *Journal of Membrane Science* 86 (1–2): 119–25. https://doi.org/10.1016/0376-7388(93)E0137-9.
Li, Ming, Dawei Hu, Hong Liu, Enzhu Hu, Beizhen Xie, and Ling Tong. 2013. “Chlorella Vulgaris Culture as a Regulator of CO2in a Bioregenerative Life Support System.” *Advances in Space Research* 52 (4): 773–79. https://doi.org/10.1016/j.asr.2013.04.014.
Liao, Qiang, Lin Li, Rong Chen, and Xun Zhu. 2014. “A Novel Photobioreactor Generating the Light/Dark Cycle to Improve Microalgae Cultivation.” *Bioresource Technology* 161 (June): 186–91. https://doi.org/10.1016/j.biortech.2014.02.119.
Llabrés, M., and A. Susana. 2010. “Effects of Ultraviolet Radiation on Growth, Cell Death, and the Standing Stock of Antarctic Phytoplankton.” *Aquatic Microbial Ecology* 59: 151–60. https://doi.org/10.3354/ame01392.
Logan, Barry. 2004. “NASA - Food for Space Flight.” National Aeronautics and Space Administration. 2004. http://www.nasa.gov/audience/forstudents/postsecondary/features/F_Food_for_Space_Flight.html.
LUMILEDS. 2015. “General Illumination.”
Luz, E, Xavier Mayali, Brad M Bebout, Peter K Weber, Angela M Detweiler, Juan- Pablo Hernandez, Leslie Prufert-bebout, and Yoav Bashan. 2016. “Establishment of Stable Synthetic Mutualism without Co-Evolution between Microalgae and Bacteria Demonstrated by Mutual Transfer of Metabolites ( NanoSIMS Isotopic Imaging ) and Persistent Physical Association ( Fluorescent in Situ Hybridization ).” *ALGAL* 15: 179–86. https://doi.org/10.1016/j.algal.2016.02.019.
Ma, Mingyang, Danni Yuan, Yue He, Minsung Park, Yingchun Gong, and Qiang Hu. 2017. “Effective Control of Poterioochromonas Malhamensis in Pilot-Scale Culture of Chlorella Sorokiniana GT-1 by Maintaining CO2-Mediated Low Culture PH.” *Algal Research* 26 (June): 436–44. https://doi.org/10.1016/j.algal.2017.06.023.
Mahmud, Hassan, Ashwani Kumar, Roberto M. Narbaitz, and Takeshi Matsuura. 2004. “The Air-Phase Mass Tranfer

Resistance in the Lumen of a Hollow Fiber at Low Air Flow." *Chemical Engineering Journal* 97 (1): 69–75. https://doi.org/10.1016/S1385-8947(03)00111-6.
Mai, Thuy. 2015. "Technology Readiness Level." NASA. Brian Dunbar. 2015.
Mallick, Nirupama. 2004. "Copper-Induced Oxidative Stress in the Chlorophycean Microalga Chlorella Vulgaris: Response of the Antioxidant System." *J. Plant Physiol* 161: 591–97. http://www.elsevier.de/jplhp.
Mandalam, Ramkumar K., and B. Ø Palsson. 1998a. "Elemental Balancing of Biomass and Medium Composition Enhances Growth Capacity in High-Density Chlorella Vulgaris Cultures." *Biotechnology and Bioengineering* 59 (5): 605–11. https://doi.org/10.1002/(SICI)1097-0290(19980905)59:5<605::AID-BIT11>3.0.CO;2-8.
Mandalam, Ramkumar K, and Bernhard Ø Palsson. 1998b. "Elemental Balancing of Biomass and Medium Composition Enhances Growth Capacity in High-Density Chlorella Vulgaris Cultures." *-Eng* 59: 605–11.
Massa, Gioia D, Raymond M Wheeler, Gary W Stutte, Jeffrey T Richards, Lashelle E Spencer, Mary E Hummerick, Grace L Douglas, and Takiyah Sirmons. 2015. "Selection of Leafy Green Vegetable Varieties for a Pick-and- Eat Diet Supplement on ISS." In *45th International Conference on Environmental Systems*, 1–16. Bellevue, WA.
Matula, Emily E, and James A Nabity. 2016. "Multifunctional Environmental Control and Life Support System for Spacecraft and Habitat Environments." In *International Conference on Environmental Systems*. Vienna, Austria.
Maxwell, D. P., S. Falk, C. G. Trick, and Npa. Huner. 1994. "Growth at Low Temperature Mimics High-Light Acclimation in Chlorella Vulgaris." *Plant Physiology* 105 (2): 535–43. https://doi.org/10.1104/pp.105.2.535.
Mayo, A. W., and T. Noike. 1994. "Response of Mixed Cultures of Chlorella Vulgaris and Heterotrophic Bacteria to Variation of PH." *Water Science and Technology*.
Mayo, Aloice W. 1997. "Effects of Temperature and PH on the Kinetic Growth of Unialga Chlorella Vulgaris Cultures Containing Bacteria." *Water Environment Research* 69 (1): 64–72. https://doi.org/10.2175/106143097X125191.
McBrien, D, and K Hassall. 1967. "The Effect of Toxic Doses of Copper upon Respiration, Photosynthesis and Growth of Chlorella Vulgaris." *Physiologia Plantarum*, 113–17. https://colorado-illiad-oclc-org.colorado.idm.oclc.org/illiad/COD/illiad.dll?Action=10&Form=75&Value=841392.
McKnight, Diane M., Dev K. Niyogi, Alexander S. Alger, Arne Bomblies, Peter A. Conovitz, and Cathy M. Tate. 1999. "Dry Valley Streams in Antarctica: Ecosystems Waiting for Water." *BioScience* 49 (12): 985. https://doi.org/10.2307/1313732.
Meck, J V, C J Reyes, S A Perez, A L Goldberger, and M G Ziegler. 2001. "Marked Exacerbation of Orthostatic Intolerance after Long- vs. Short-Duration Spaceflight in Veteran Astronauts." *Psychosomatic Medicine* 63 (6): 865–73. http://www.ncbi.nlm.nih.gov/pubmed/11719623.
Melis, Anastasios. 2009. "Solar Energy Conversion Efficiencies in Photosynthesis: Minimizing the Chlorophyll Antennae to Maximize Efficiency." *Plant Science* 177 (4): 272–80. https://doi.org/10.1016/j.plantsci.2009.06.005.
Metcalf, J, L Peterson, R L Carrasquillo, and R M Bagdigian. 2012. "National Aeronautics and Space Administration (NASA) Environmental Control and Life Support (ECLS) Capability Roadmap Development for Exploration," no. July: 22.
Miller, R. L., and C. H. Ward. 1966. "Algal Bioregenerative Systems." In *Atmosphere in Space Cabins and Closed Environments*, 186–222. Boston, MA: Springer US. https://doi.org/10.1007/978-1-4684-1372-4_9.
Mills, W.R. 2000. "Growth and Metabolism of the Green Alga, Chlorella Pyrenoidosa in Simulated Microgravity." Clear Lake.
Miyamoto, K. 1997. *Renewable Biological Systems for Alternative Sustainable Energy Production*. Edited by K. Miyamoto. Rome, Italy.
Morgan-Kiss, Rachael M, John C Priscu, Tessa Pocock, Loreta Gudynaite-Savitch, and Norman P A Huner. 2006. "Adaptation and Acclimation of Photosynthetic Microorganisms to Permanently Cold Environments." *MICROBIOLOGY AND MOLECULAR BIOLOGY REVIEWS* 70 (1): 222–52. https://doi.org/10.1128/MMBR.70.1.222–252.2006.
Mori, K., H. Ohya, K. Matsumoto, and H. Furune. 1987. "Sunlight Supply and Gas Exchange Systems in Microalgal Bioreactor." *Advances in Space Research* 7 (4): 47–52. https://doi.org/10.1016/0273-1177(87)90031-7.
Morton, Stephen D, and Philip H Derse. n.d. "COMMUNICATION Use of Gamma Radiation to Control Algae." Accessed July 28, 2019. https://pubs.acs.org/sharingguidelines.
Mouget, Jean-luc, Azzeddine Dakhama, Marc C Lavoie, and Joel De. 1995. "Algal Growth Enhancement by Bacteria: Is Consumption of Photosynthetic Oxygen Involved?" *FEMS Microbiology Ecology* 18: 35–44.

Myers, J. 1964. “Use of Algae for Support of the Human in Space.” *Life Sciences and Space Research* 2: 323–36. https://colorado-illiad-oclc-org.colorado.idm.oclc.org/illiad/COD/illiad.dll?Action=10&Form=75&Value=988669.

Nakajima, Tomohiko, Harumi Hanawa, and Tetsuo Tsuchiya. 2015. “Plant Habitat-Conscious White Light-Emitting Devices: Dy\n 3+\n Emission Considerably Reduces Involvement in Photosynthesis.” *J. Mater. Chem. C* 3: 3371–78. https://doi.org/10.1039/C4TC02558J.

NASA. n.d. “ISS Main Systems.” https://www.nasa.gov/pdf/167129main_Systems.pdf.

———. 2010. “Reference Guide to the International Space Station.” 2010. http://www.nasa.gov/pdf/508318main_ISS_ref_guide_nov2010.pdf.

———. 2015. “TA 6: Human Health, Life Support, and Habitation Systems.” *NASA Technology Roadmaps*, no. July: 1–217.

Nelson, Mark, Nickolay S Pechurkin, John P Allen, Lydia A Somova, and Josef I Gitelson. 2009. “Closed Ecological Systems, Space Life Support and Biospherics.” *Environmental Biotechnology Edited* 10. https://doi.org/10.1007/978-1-60327-140-0_11.

Niederwieser, Tobias, Patrick Kociolek, and David Klaus. 2018. “A Review of Algal Research in Space.” *Acta Astronautica* 146 (November 2017): 359–67. https://doi.org/10.1016/j.actaastro.2018.03.026.

Ogawa, Takahira, Takao Fujii, and Shuichi Aiba. 1980. “Effect of Oxygen on the Growth (Yield) of Chlorella Vulgaris.” *Arch. Microbiol* 127: 25–31. http://download.springer.com/static/pdf/390/art%253A10.1007%252FBF00414351.pdf?originUrl=http%3A%2F%2Flink.springer.com%2Farticle%2F10.1007%2FBF00414351&token2=exp=1488498690~acl=%2Fstatic%2Fpdf%2F390%2Fart%25253A10.1007%25252FBF00414351.pdf%3ForiginUrl%3Dhttp%253A%252F%252Flink.springer.com%252Farticle%252F10.1007%252FBF00414351*~hmac=4952ef26a6e3b0fd559a7da8a752f60d4d03461cdccea748e8ad36ed0882c184.

Ojo, Ebenezer O., Hadiza Auta, Frank Baganz, and Gary J. Lye. 2015. “Design and Parallelisation of a Miniature Photobioreactor Platform for Microalgal Culture Evaluation and Optimisation.” *Biochemical Engineering Journal* 103 (November): 93–102. https://doi.org/10.1016/j.bej.2015.07.006.

Öquist, Gunnar. 1983. “Effects of Low Temperature on Photosynthesis.” *Plant, Cell and Environment* 6 (October 1982): 281–300. https://doi.org/10.1111/1365-3040.ep11612087.

Oram, B. 2014. “Well Biofouling.” Water Research Watershed Center. 2014. http://www.water-research.net/index.php/water-testing/private-well-testing/well-biofouling.

OrbitBiotech. 2018. “Bacterial Growth Curve.” Orbit Biotech. 2018. https://orbitbiotech.com/bacterial-growth-curve-generation-time-lag-phase-log-phase-exponential-phase-decline-phase/.

Oswald, William J, H B Gotaas, Harvey F Ludwig, and Victoria Lynch. 1953. “Algae Symbiosis in Oxidation Ponds: III. Photosynthetic Oxygenation.” *Source: Sewage and Industrial Wastes*. Vol. 25. https://www.jstor.org/stable/pdf/25032197.pdf?refreqid=excelsior%3Aa409941d3e7bdfa7a4039fbededa8662.

Oxford. 2018. “Edible.” The Oxford Dictionary. 2018.

Patel, Vipul P., Richard Barido, Brien Johnson, and Thomas Ibarra. 2001. “Development of the Internal Thermal Control System (ITCS) for International Space Station (ISS).” In *SAE Transactions*. https://doi.org/10.4271/2001-01-2332.

Peterson, G. P. 1987. “Thermal Control Systems for Spacecraft Instrumentation.” *Journal of Spacecraft and Rockets* 24 (1): 7–13. https://doi.org/10.2514/3.25866.

Pisman, T. I., Ya V. Galayda, and N. S. Loginova. 2005. “Population Dynamics of an Algal-Bacterial Cenosis in Closed Ecological System.” *Advances in Space Research* 35 (9 SPEC. ISS.): 1579–83. https://doi.org/10.1016/j.asr.2005.03.073.

“Polyethylene (PE) Typical Properties Generic HDPE | UL Prospector.” 2016. 2016. http://plastics.ulprospector.com/generics/27/c/t/polyethylene-pe-properties-processing/sp/5.

Posner, Herbert B., and Arnold H. Sparrow. 1964. “Survival of Chlorella and Chlamydomonas after Acute and Chronic Gamma Radiation.” *Radiation Botany* 4 (3): 253–57. https://doi.org/10.1016/S0033-7560(64)80072-7.

Powell, Richard C., Elizabeth M. Nevels, and Marion E. McDowell. 1961. “Algae Feeding in Humans.” *Journal of Nutrition* 75 (1): 7–12.

Price, R.M. 2013. “Shell and Tube Heat Exchangers: Calculations.” 2013. http://facstaff.cbu.edu/rprice/lectures/stcalcs.html.

Qian, H., J. Li, X. Pan, Z. Sun, C. Ye, G. Jin, and Z. Fu. 2010. “Effects of Streptomycin on Growth of Algae Chlorella Vulgaris and Microcystis Aeruginosa.” *Environmental Toxicology* 27 (4): 229–37. https://doi.org/10.1002/tox.

Rabbow, Elke, Petra Rettberg, Andre Parpart, Corinna Panitz, Wolfgang Schulte, Ferdinand Molter, Esther Jaramillo, René Demets, Peter Weiß, and Rainer Willnecker. 2017. “EXPOSE-R2: The Astrobiological ESA Mission on Board of the International Space Station.” *Frontiers in Microbiology* 8: 1533. https://doi.org/10.3389/fmicb.2017.01533.

Ras, Monique, Jean-Philippe Steyer, and Olivier Bernard. 2013. “Temperature Effect on Microalgae: A Crucial Factor for Outdoor Production.” https://doi.org/10.1007/s11157-013-9310-6.

Raso, Sayam, Bernard Van Genugten, Marian Vermuë, and René H Wijffels. 2011. “Effect of Oxygen Concentration on the Growth of Nannochloropsis Sp. at Low Light Intensity.” https://doi.org/10.1007/s10811-011-9706-z.

Rathnasiri, Puhulwella Gamacharige, and Magnar Ottøy. 2003. “Oxygen Transfer and Transport Resistance across Silicone Tubular Membranes.” Porsgrunn. http://www.hit.no/.

Richard S. Williams, M.D. 2015. “NASA TECHNICAL National Aeronautics and Space Administration VOLUME 1 , Revision A NASA SPACE FLIGHT HUMAN-SYSTEM STANDARD VOLUME 1 , REVISION A : CREW HEALTH MEASUREMENT SYSTEM IDENTIFICATION :” 1: 83.

Royce, Patrick N C, and Nina F Thornhill. 1991. “Estimation of Dissolved Carbon Dioxide Concentrations in Aerobic Fermentations.” *American Institute of Chemical Engineering Journal* 37 (11): 1680–87. https://aiche.onlinelibrary.wiley.com/doi/pdf/10.1002/aic.690371111.

Sakshaug, E., A. Bricaud, Y. Dandonneau, P. G. Falkowski, D. A. Kiefer, L. L. Legendre, A. Morel, J. Parslow, and M. Takahashi. 1997. “Parameters of Photosynthesis: Definitions, Theory and Interpretation of Results.” *Journal of Plankton Research* 19 (11): 1637–70. https://watermark.silverchair.com/19-11-1637.pdf?token=AQECAHi208BE49Ooan9kkhW_Ercy7Dm3ZL_9Cf3qfKAc485ysgAAAkwwggJIBgkqhkiG9w0BBwagggI5MIICNQIBADCCAi4GCSqGSIb3DQEHATAeBglghkgBZQMEAS4wEQQMwjVvEpir9F46nkjyAgEQgIIB_019jXjm68zB3YA2FMWjnU5GYolwrqmxRwNj-gNQdke9.

Salisbury, F., J. Gitelson, and G. Lisovsky. 1997. “Bios-3: Siberian Experiments in Bioregenerative Life Support.” *Bioscience*, 575–85. http://bioscience.oxfordjournals.org/content/47/9/575.full.pdf.

Samplatsky, Darren J., Kevin Grohs, Marybeth Edeen, Jason Crusan, and Russel Burkey. 2011. “Development and Integration of the Flight Sabatier Assembly on the ISS.” In *41st International Conference on Environmental Systems*, 1–9. Portland, OR. https://doi.org/doi:10.2514/6.2011-5151.

Scherholz, Megerle L, and Wayne R Curtis. 2013. “Achieving PH Control in Microalgal Cultures through Fed-Batch Addition of Stoichiometrically-Balanced Growth Media.” *BMC Biotechnology* 13 (1): 39. https://doi.org/10.1186/1472-6750-13-39.

Schofield, R W, A G Fane, and C J D Fell. 1987. “Heat and Mass Transfer in Membrane Distillation.” *Journal of Membrane Science* 33: 299–313. https://doi.org/Doi 10.1016/S0376-7388(00)80287-2.

Serra-Maia, Rui, Olivier Bernard, Ana Gonçalves, Sakina Bensalem, and Filipa Lopes. 2016. “Influence of Temperature on Chlorella Vulgaris Growth and Mortality Rates in a Photobioreactor.” https://doi.org/10.1016/j.algal.2016.06.016.

Sharma, Rekha. 2012. “Effects of Culture Conditions on Growth and Biochemical Profile of Chlorella Vulgaris.” *Journal of Plant Pathology & Microbiology* 03 (05). https://doi.org/10.4172/2157-7471.1000131.

Shen, Q., Y. Gong, W. Fang, Z. Bi, L. Cheng, X. Xu, and H. Chen. 2015. “Saline Wastewater Treatment by Chlorella Vulgaris with Simultaneous Algal Lipid Accumulation Triggered by Nitrate Deficiency.” *Bioresource Technology* 193: 68–75. https://pdf.sciencedirectassets.com/271433/1-s2.0-S0960852415X00150/1-s2.0-S096085241500841X/main.pdf?X-Amz-Security-Token=AgoJb3JpZ2luX2VjEPD%2F%2F%2F%2F%2F%2F%2F%2F%2F%2FwEaCXVzLWVhc3QtMSJGMEQCIDeN151HmcOFr%2Fz3LIdRaCvEE4LW0MWSH4gtnQ22KnthAiAYdqvNWffzJx.

Sherif, Dina El, and James C Knox. 2005. “International Space Station Carbon Dioxide Removal Assembly ( ISS CDRA ) Concepts and Advancements.” Vol. 2892. https://doi.org/10.4271/2005-01-2892.

Shirazian, Saeed, Abdolreza Moghadassi, and Sadegh Moradi. 2009. “Numerical Simulation of Mass Transfer in Gas-Liquid Hollow Fiber Membrane Contactors for Laminar Flow Conditions.” *Simulation Modelling Practice and Theory* 17 (4): 708–18. https://doi.org/10.1016/j.simpat.2008.12.002.

Simon, Matthew a., Steven a. Walker, and Martha Clowdsley. 2013. “Habitat Design Considerations for Implementing Solar Particle Event Radiation Protection.” *43rd International Conference on Environmental Systems*, 1–13. https://doi.org/10.2514/6.2013-3403.

Simonsen, Lisa C, and John E Nealy. 1991. “Radiation Protection for Human Missions to the Moon and Mars.” Hampton, VA.

Singh, S.P., and Priyanka Singh. 2014. “Effect of CO2 Concentration on Algal Growth: A Review.” *Renewable and Sustainable Energy Reviews* 38 (October): 172–79. https://doi.org/10.1016/j.rser.2014.05.043.

Smernoff, David T, Robert A Wharton, and Maurice M Averner. 1987. “An Experimental Algal Gas Exchanger for Use in a CELSS.” *Advances in Space Research* 7 (4): 17–27.

Solter, Philip F., and Val R. Beasley. 2013. “Phycotoxins.” *Haschek and Rousseaux’s Handbook of Toxicologic Pathology*, January, 1155–86. https://doi.org/10.1016/B978-0-12-415759-0.00038-8.

“Spectral Power Distribution Curves.” 2016. GE Lighting. 2016.

Sydney, E. B., T. E. da Silva, A. Tokarski, A. C. Novak, J. C. de Carvalho, A. L. Woiciecohwski, C. Larroche, and C. R. Soccol. 2011. “Screening of Microalgae with Potential for Biodiesel Production and Nutrient Removal from Treated Domestic Sewage.” *Applied Energy* 88 (10): 3291–94. https://doi.org/10.1016/j.apenergy.2010.11.024.

Sydney, Eduardo Bittencourt, Alessandra Cristine Novak, Julio Cesar de Carvalho, and Carlos Ricardo Soccol. 2013. *Respirometric Balance and Carbon Fixation of Industrially Important Algae*. *Biofuels from Algae*. Elsevier B.V. https://doi.org/10.1016/B978-0-444-59558-4.00004-8.

Tam, N., and Y. Wong. 1996. “Effect of Ammonia Concentrations on Growth of Chlorella Vulgaris and Nitrogen Removal from Media.” *Biosource Technology* 57: 45–50. http://ac.els-cdn.com/0960852496000454/1-s2.0-0960852496000454-main.pdf?_tid=77f9b762-1bd9-11e7-8664-00000aab0f6c&acdnat=1491600829_edef87153b4c939931147584b38466f7.

Tan, X, and K Capar. 2005. “Analysis of Dissolved Oxygen Removal in Hollow Fiber Membrane Modules: Effect of Water Vapour.” *Journal of Membrane Science* 251: 111–19. http://ac.els-cdn.com/S0376738804007495/1-s2.0-S0376738804007495-main.pdf?_tid=ca7c3b70-5bbe-11e7-889f-00000aacb35d&acdnat=1498626245_3cd1926b74b83a7758b9977b5a4a6893.

The Boeing Company. n.d. “Active Thermal Control System ( ATCS ) Overview.” St. Louis, MO. https://www.nasa.gov/pdf/473486main_iss_atcs_overview.pdf.

Thomas Eriksen, Niels, Frederik Kier Riisgård, William Stuart Gunther, Jens Jørgen Lønsmann Iversen, N T Eriksen, F K Riisgård, W S Gunther, and J J Lønsmann Iversen. 2007. “On-Line Estimation of O 2 Production, CO 2 Uptake, and Growth Kinetics of Microalgal Cultures in a Gas-Tight Photobioreactor.” *J Appl Phycol* 19: 161–74. https://doi.org/10.1007/s10811-006-9122-y.

Tikhomirov, A. A., S. A. Ushakova, N. P. Kovaleva, B. Lamaze, M. Lobo, and Ch Lasseur. 2007. “Biological Life Support Systems for a Mars Mission Planetary Base: Problems and Prospects.” *Advances in Space Research* 40 (11): 1741–45. https://doi.org/10.1016/j.asr.2006.11.009.

Tokusoglu, Ö., Unal, M.K. 2003. “Biomass Nutrient Profiles of Three Microalgae: Spirulina Platensis, Chlorella Vulgaris and Isochrysis Galbana.” *Journal of Food Science* 68 (4): 1144–48.

Tomsett, A, and D Thurman. 1988. “Molecular Biology of Metal Tolerances of Plants.” *Plant, Cell and Environment* 11: 383–94.

Tran, D., C. Chen, and J. Chang. 2013. “Effect of Solvents and Oil Content on Direct Transesterification of Wet Oil-Bearing Microalgal Biomass of Chlorella Vulgaris ESP-31 for Biodiesel Synthesis Using Immobilized Lipase as the Biocatalyst.” *Bioresource Technology* 135: 213–21. https://pdf.sciencedirectassets.com/271433/1-s2.0-S0960852413X00069/1-s2.0-S0960852412014514/main.pdf?X-Amz-Security-Token=AgoJb3JpZ2luX2VjEFwaCXVzLWVhc3QtMSJHMEUCIQCXHNOI4hoLyNrRSYe6g%2B7%2F37J34g8d%2B%2F0ZLS0%2Fes%2FKpAIgFieO1QgdyzI0olQ20FMvRsjGTFystEpH.

Travieso, L., R.O. Cañizares, R. Borja, F. Benítez, A.R. Domínguez, R. Dupeyrón, and Y.V. Valiente. 1999. “Heavy Metal Removal by Microalgae.” *Bulletin of Environmental Contamination and Toxicology* 62 (2): 144–51. https://doi.org/10.1007/s001289900853.

Tuantet, Kanjana, Hardy Temmink, Grietje Zeeman, Marcel Janssen, René H Wijffels, and Cees J N Buisman. 2014. “Nutrient Removal and Microalgal Biomass Production on Urine in a Short Light-Path Photobioreactor.” *Water Research* 55 (May): 162–74. https://doi.org/10.1016/j.watres.2014.02.027.

Turner, B Y J S, and E G Brittain. 1962. “Oxygen as a Factor in Photosynthesis.” *Biological Reviews* 37 (December 1960): 130–70.

Ugwu, C. U., J. C. Ogbonna, and H. Tanaka. 2005. “Light/Dark Cyclic Movement of Algal Culture (Synechocystis Aquatilis) in Outdoor Inclined Tubular Photobioreactor Equipped with Static Mixers for Efficient Production of

Biomass." *Biotechnology Letters* 27 (2): 75–78. https://doi.org/10.1007/s10529-004-6931-4.
Ugwu, C U, H Aoyagi, and H Uchiyama. 2007. "Photobioreactors for Mass Cultivation of Algae." https://doi.org/10.1016/j.biortech.2007.01.046.
United States Department of Agriculture. 2016. "Food Composition Databases Show Foods -- Seaweed, Spirulina, Raw." 2016. https://ndb.nal.usda.gov/ndb/foods/show/3305?manu=&fgcd=&ds=.
Valenzano, Giuseppe, Silvia Lombardi, Giovanni Loddoni, and Renato Martino. 2003. "ISS Node 3 TCS Analysis and Design." In *International Conference on Environmental Systems*. SAE International. https://doi.org/10.4271/1999-01-2003.
Vanhoudt, Nathalie, Hildegarde Vandenhove, Almudena Real, Clare Bradshaw, and Karolina Stark. 2012. "A Review of Multiple Stressor Studies That Include Ionising Radiation." *Environmental Pollution* 168 (September): 177–92. https://doi.org/10.1016/j.envpol.2012.04.023.
Vekshina, L.K., I.G. Kogan, E.I. Kudryashov, D.R. Pyatyshev, I.S. Sakovich, and V.A. Shevchenko. 1969. "EFFECT OF ALPHA-IRRADIATION ON CHLORELLA SURVIVAL AND MUTATION." *Kosm. Biol. Med. 3: No. 5, 34-8(Sep-Oct 1969).*, January. https://www.osti.gov/biblio/4744670.
Vera, Jean-Pierre de, Mashal Alawi, Theresa Backhaus, Mickael Baqué, Daniela Billi, Ute Böttger, Thomas Berger, et al. 2019. "Limits of Life and the Habitability of Mars: The ESA Space Experiment BIOMEX on the ISS." *Astrobiology* 19 (2): 145–57. https://doi.org/10.1089/ast.2018.1897.
Vone, Michael La. 2014. "The Future of Food on Mars." 2014. http://www.spacesafetymagazine.com/spaceflight/space-food/future-food-mars/.
Wagner, Ines, Markus Braun, Klaus Slenzka, and Clemens Posten. 2016. "Photobioreactors in Life Support Systems." *Advances in Biochemistry Engineering Biotechnology* 153 (July 2015): 143–84. https://doi.org/10.1007/10.
Wagner, S.C. 2011. "Biological Nitrogen Fixation." The Nature Education Knowledge Project. 2011.
Wang, Bei, Yanqun Li, Nan Wu, and Christopher Q. Lan. 2008. "CO2 Bio-Mitigation Using Microalgae." *Applied Microbiology and Biotechnology* 79 (5): 707–18. https://doi.org/10.1007/s00253-008-1518-y.
Wang, C. Y., E. Mercer, F. Kamranvand, L. Williams, A. Kolios, A. Parker, S. Tyrrel, E. Cartmell, and E. J. McAdam. 2017. "Tube-Side Mass Transfer for Hollow Fibre Membrane Contactors Operated in the Low Graetz Range." *Journal of Membrane Science* 523 (June 2016): 235–46. https://doi.org/10.1016/j.memsci.2016.09.049.
Wang, Gaohong, Haofeng Chen, Genbao Li, Lanzhou Chen, Dunhai Li, Chunxiang Hu, Kun Chen, and Yongding Liu. 2006. "Population Growth and Physiological Characteristics of Microalgae in a Miniaturized Bioreactor during Space Flight." *Acta Astronautica* 58: 264–69. https://doi.org/10.1016/j.actaastro.2005.11.001.
Wang, Liang, Min Min, Yecong Li, Paul Chen, Yifeng Chen, Yuhuan Liu, Yingkuan Wang, and Roger Ruan. 2010. "Cultivation of Green Algae Chlorella Sp. in Different Wastewaters from Municipal Wastewater Treatment Plant." *Applied Biochemistry and Biotechnology* 162 (4): 1174–86. https://doi.org/10.1007/s12010-009-8866-7.
Welch, B.E. 1963. "Ecological Systems." In *Physiology of Man in Space*, 309–34. https://doi.org/10.1016/B978-1-4832-0080-4.50012-1.
Wells, Mark L., Philippe Potin, James S. Craigie, John A. Raven, Sabeeha S. Merchant, Katherine E. Helliwell, Alison G. Smith, Mary Ellen Camire, and Susan H. Brawley. 2017. "Algae as Nutritional and Functional Food Sources: Revisiting Our Understanding." *Journal of Applied Phycology* 29 (2): 949–82. https://doi.org/10.1007/s10811-016-0974-5.
Westerterp, K., W. van Swaaij, and A. Beenackers. 1984. *Chemical Reactor Design and Operation*. New York: Wiley.
Wheeler, Raymond M. 2003. "Carbon Balance in Bioregenerative Life Support Systems: Some Effects of System Closure, Waste Management, and Crop Harvest Index." *Advances in Space Research* 31 (1): 169–75. https://doi.org/10.1016/S0273-1177(02)00742-1.
Whitmarsh, J., and Govindjee. 1999. *Concepts in Photobiology: Photosynthesis and Photomorphogenesis*. Edited by Govindjee Singhal, G., Renger, G., Sopory, S., Irrgang, K. 1st ed. New Delhi, India: Springer-Science + Business Media. https://books.google.com/books/about/Concepts_in_Photobiology.html?id=Da39CAAAQBAJ&printsec=frontcover&source=kp_read_button#v=onepage&q&f=false.
Wieland, P O. 1998. "Living Together in Space: The Design and Operation of the Life Support Systems on the International Space Station." Huntsville, AL. https://spaceflightsystems.grc.nasa.gov/repository/NRA/tm206956v1 living together in space.pdf.
Wolf-Gladrow, Dieter A., Richard E. Zeebe, Christine Klaas, Arne Körtzinger, and Andrew G. Dickson. 2007. "Total

Alkalinity: The Explicit Conservative Expression and Its Application to Biogeochemical Processes." *Marine Chemistry* 106 (1-2 SPEC. ISS.): 287–300. https://doi.org/10.1016/j.marchem.2007.01.006.

Xiong, Jiu Qiang, Mayur B. Kurade, and Byong Hun Jeon. 2017. "Biodegradation of Levofloxacin by an Acclimated Freshwater Microalga, Chlorella Vulgaris." *Chemical Engineering Journal* 313: 1251–57. https://doi.org/10.1016/j.cej.2016.11.017.

Yang, Chenliang, Hong Liu, Ming Li, Chengying Yu, and Gurevich Yu. 2008. "Treating Urine by Spirulina Platensis." *Acta Astronautica* 63 (7–10): 1049–54. https://doi.org/10.1016/j.actaastro.2008.03.008.

Yang, Ming-chien, and E L Cussler. 1986. "Designing Hollow-Fiber Contactors." *AIChE Journal* 32 (11): 1910–16.

Yeom, C K, S H Lee, and J M Lee. 2000. "Study of Transport of Pure and Mixed CO 2 / N 2 Gases through Polymeric Membranes." *Journal of Applied Physics* 78: 179–89. https://doi.org/10.1002/1097-4628(20001003)78:1<179::AID-APP220>3.0.CO;2-Z.

Yocum, C S, and L R Blinks. 1954. "Photosynthetic Efficiency of Marine Plants." *The Journal of General Physiology*, 1–16. https://doi.org/10.1085/jgp.38.1.1.

Zea, Luis, Nripesh Prasad, Shawn E. Levy, Louis Stodieck, Angela Jones, Shristi Shrestha, and David Klaus. 2016. "A Molecular Genetic Basis Explaining Altered Bacterial Behavior in Space." *PLoS ONE* 11 (11): 1–23. https://doi.org/10.1371/journal.pone.0164359.

Zhang, Shanshan, Chun Yong Lim, Chia Lung Chen, He Liu, and Jing Yuan Wang. 2014. "Urban Nutrient Recovery from Fresh Human Urine through Cultivation of Chlorella Sorokiniana." *Journal of Environmental Management* 145: 129–36. https://doi.org/10.1016/j.jenvman.2014.06.013.

Zhao, Shuaifei, Paul H.M. Feron, Liyuan Deng, Eric Favre, Elodie Chabanon, Shuiping Yan, Jingwei Hou, Vicki Chen, and Hong Qi. 2016. "Status and Progress of Membrane Contactors in Post-Combustion Carbon Capture: A State-of-the-Art Review of New Developments." *Journal of Membrane Science* 511 (August): 180–206. https://doi.org/10.1016/J.MEMSCI.2016.03.051.

Zhao, Yongjun, Juan Wang, Hui Zhang, Cheng Yan, and Yuejin Zhang. 2013. "Effects of Various LED Light Wavelengths and Intensities on Microalgae-Based Simultaneous Biogas Upgrading and Digestate Nutrient Reduction Process." *Bioresource Technology* 136 (May): 461–68. https://doi.org/10.1016/j.biortech.2013.03.051.

Zoulias, Emmanuel, Elli Varkaraki, Nicolaos Lymberopoulos, Christodoulos N Christodoulou, and George N Karagiorgis. 2004. "A Review on Water Electrolysis." Vol. 4. http://large.stanford.edu/courses/2012/ph240/jorna1/docs/zoulias.pdf.

# Appendix A Bristol's Media Recipe

Bristol's Media Recipe

| Component | Amount | Stock Solution Concentration | Final Concentration |
|---|---|---|---|
| $NaNO_3$ (Fisher BP360-500) | 10 mL/L | 10g/400mL $dH_2O$ | 2.94 mM |
| $CaCl_2$-$2H_2O$ (sigma C-3881) | 10 mL/L | 1g/400mL $dH_2O$ | 0.17mM |
| $MgSO_4$-$7H_2O$ (Sigma 230391) | 10 mL/L | 3g/400mL $dH_2O$ | 0.3mM |
| $K_2HPO_4$ (Sigma P 3786) | 10 mL/L | 3g/400mL $dH_2O$ | 0.43mM |
| $KH_2PO_4$ (Sigma P 0662) | 10 mL/L | 7g/400mL $dH_2O$ | 1.29mM |
| NaCl (Fisher S271-500) | 10 mL/L | 1g/400mL $dH_2O$ | 0.43mM |

# Appendix B Respiration and Photosynthetic Rate Calculation

Respiration and photosynthetic rate were calculated by linear regression using the maximum and minimum dissolved oxygen values selected for each irradiance level. These rates were used as a reference for general diagnosis of the functioning of a culture. These rates were not included as a variable for the statistical analysis.

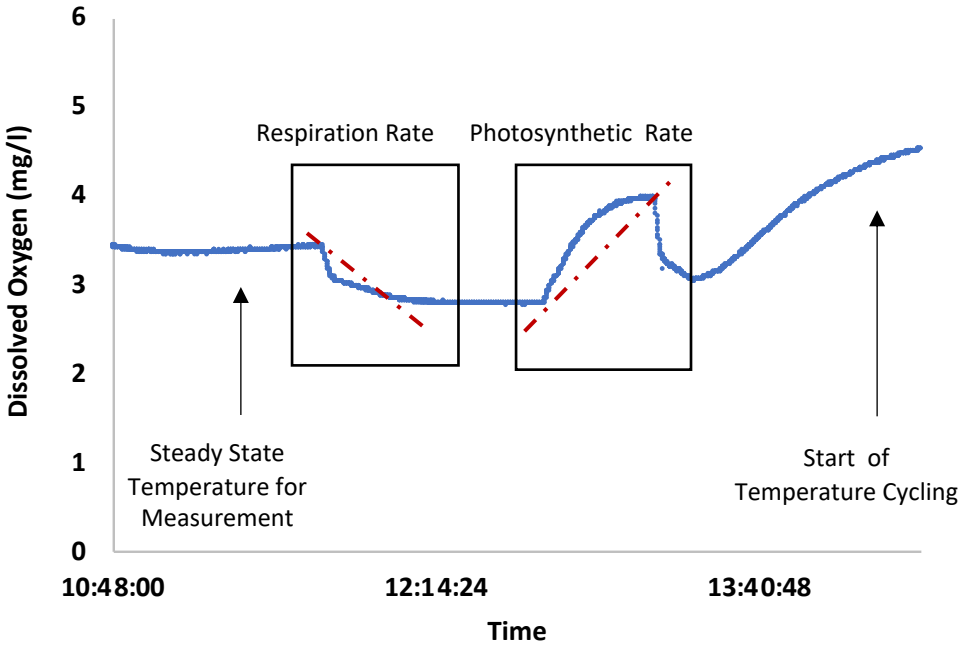


**Figure 94. Minimum and maximum dissolved oxygen measurements found in respiration rate (left) and photosynthetic rate (right) boxes used to formulate linear regression, as outlined by dashed line.**

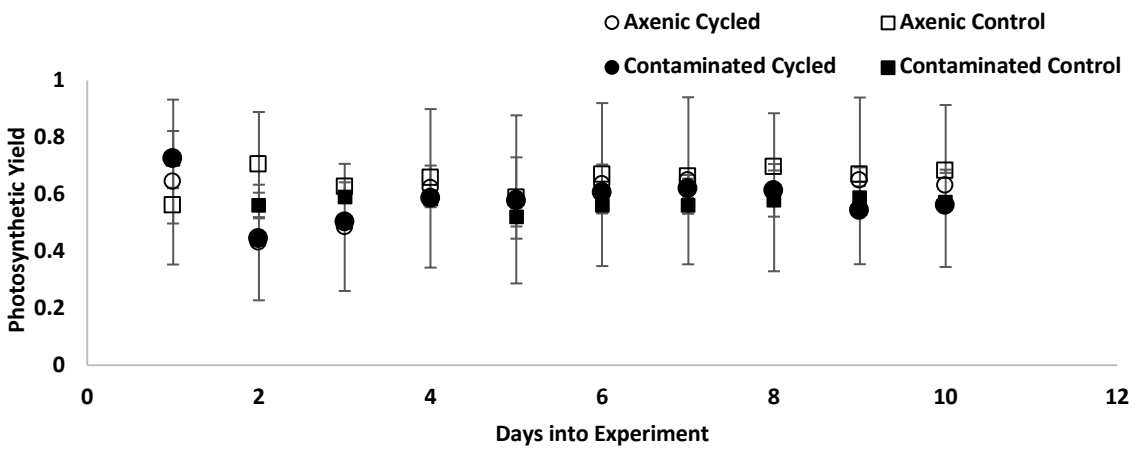


**Figure 95. The resulting photosynthetic yield values for the dynamic temperature experiment over the course of the experiment duration. Error bars represent standard deviation calculated from multiple experimental runs.**

**Table 66. Resulting p-values for each treatment combination, comparing the photosynthetic yield. Those p-values that are significant have been highlighted**

| Treatment Combination | p-values |
|---|---|
| Axenic Cycle vs Contaminated Cycle | Sample p = 0.72<br>Day p = 0.003<br>Interaction p = 0.88 |
| Axenic Cycle vs Axenic Control | Sample p = 0.18<br>Day p = 0.11<br>Interaction p = 0.09 |
| Contaminated Cycle vs Contaminated Control | Sample p = 0.04<br>Day p = 0.003<br>Interaction p =0.51 |
| Axenic Cycle vs Contaminated Control | Sample p = 0.52<br>Day p = 0.001<br>Interaction p = 0.02 |
| Axenic Control vs Contaminated Control | Sample p = 0.01<br>Day p = 0.56<br>Interaction p = 0.02 |
| Axenic Control vs Contaminated Cycle | Sample p = 0.33<br>Day p = 0.83<br>Interaction p = 0.20 |

**Table 67. Resulting p-values for each treatment combination, comparing the growth rates. Those p-values that are significant have been highlighted**

| Treatment Combination | p-values |
|---|---|
| Axenic Cycle vs Contaminated Cycle | Optical Density Growth Rate t = 0.67<br>Cell Density Growth Rate t = 0.19 |
| Axenic Cycle vs Axenic Control | Optical Density Growth Rate t = 0.19<br>Cell Density Growth Rate t = 0.01 |
| Contaminated Cycle vs Contaminated Control | Optical Density Growth Rate t = 0.05<br>Cell Density Growth Rate t = 0.09 |
| Axenic Cycle vs Contaminated Control | Optical Density Growth Rate t = 0.08<br>Cell Density Growth Rate t = 0.38 |
| Axenic Control vs Contaminated Control | Optical Density Growth Rate t = 0.004<br>Cell Density Growth Rate t = 0.006 |
| Axenic Control vs Contaminated Cycle | Optical Density Growth Rate t = 0.45<br>Cell Density Growth Rate t = 0.61 |

**Table 68. Resulting p-values between all combinations of treatments comparing the photosynthetic yield values of the nutrient addition cases. There were no statistically significant p-values in this comparison**

| Treatment Combination | p-values |
|---|---|
| Nutrient-added Cycle vs Non-added Cycle | Sample p = 0.83<br>Day p = 0.73<br>Interaction p = 0.94 |
| Nutrient-added Cycle vs Nutrient-added Control | Sample p = 0.62<br>Day p = 0.06<br>Interaction p = 0.66 |
| Non-added Cycle vs Non-added Control | Sample p = 0.37<br>Day p = 0.78<br>Interaction = 0.88 |
| Nutrient-Added Cycle vs Non-added Control | Sample p = 0.19<br>Day p = 0.37<br>Interaction p = 0.92 |
| Nutrient-added Control vs Non-added Control | Sample p = 0.08<br>Day p = 0.19<br>Interaction p = 0.93 |
| Nutrient-added Control vs Non-added Cycle | Sample p = 0.95<br>Day p = 0.76<br>Interaction p = 0.86 |

**Table 69. Resulting p-values between all combinations of treatments comparing the growth rates of the nutrient addition cases. Statistically significant cases are highlighted**

| Treatment Combination | p-values |
|---|---|
| Nutrient-added Cycle vs Non-added Cycle | Optical Density Growth Rate p = 0.01<br>Cell Density Growth Rate p = 0.01 |
| Nutrient-added Cycle vs Nutrient-added Control | Optical Density Growth Rate p = 0.01<br>Cell Density Growth Rate p = 0.09 |
| Non-added Cycle vs Non-added Control | Optical Density Growth Rate p = 0.05<br>Cell Density Growth Rate p = 0.09 |
| Nutrient-Added Cycle vs Non-added Control | Optical Density Growth Rate p = 0.02<br>Cell Density Growth Rate p = 0.01 |
| Nutrient-added Control vs Non-added Control | Optical Density Growth Rate p = 0.12<br>Cell Density Growth Rate p =0.14 |
| Nutrient-added Control vs Non-added Cycle | Optical Density Growth Rate p = 0.01<br>Cell Density Growth Rate p = 0.02 |

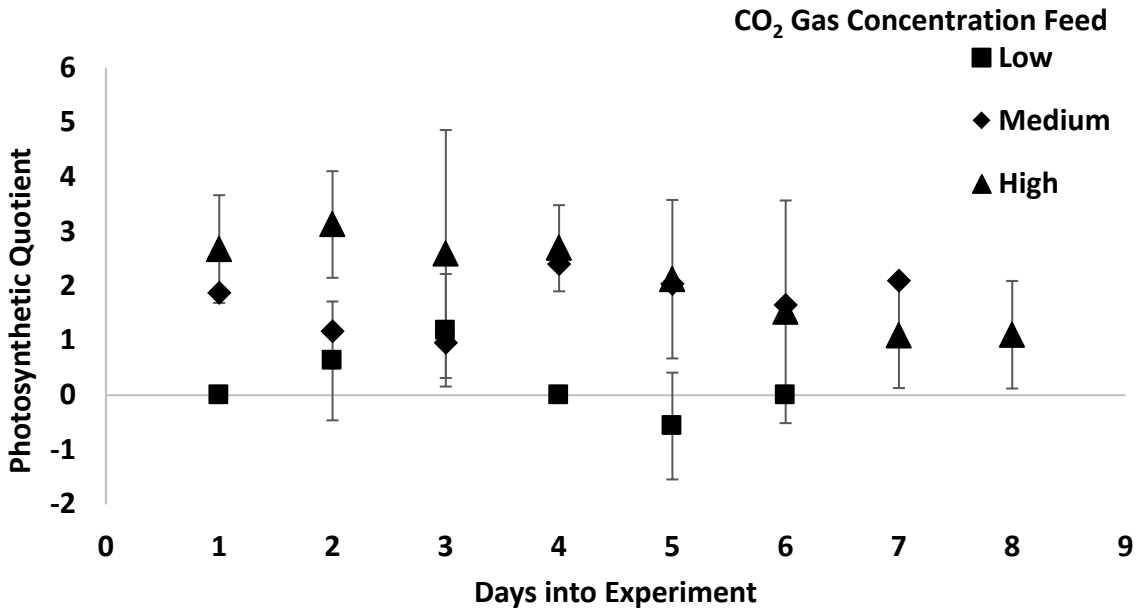


**Figure 96. Photosynthetic quotient for each tested steady-state $CO_2$ feed over the course of the experiment duration. Error bars represent standard deviation calculated from multiple experimental runs.**

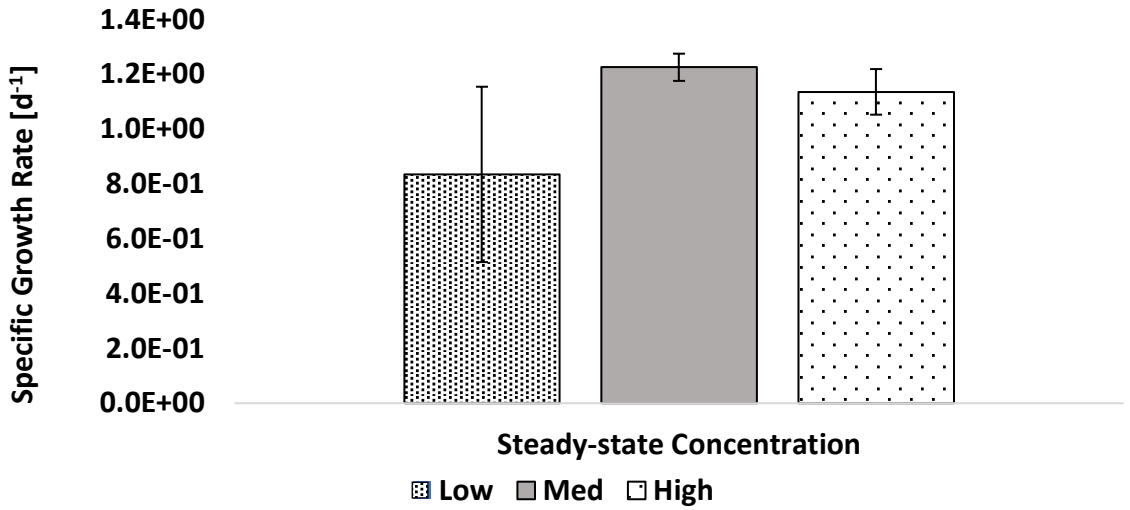


**Figure 97. Specific growth rate for each steady-state $CO_2$ concentration. Error bars represent standard deviation calculated from multiple experimental runs.**

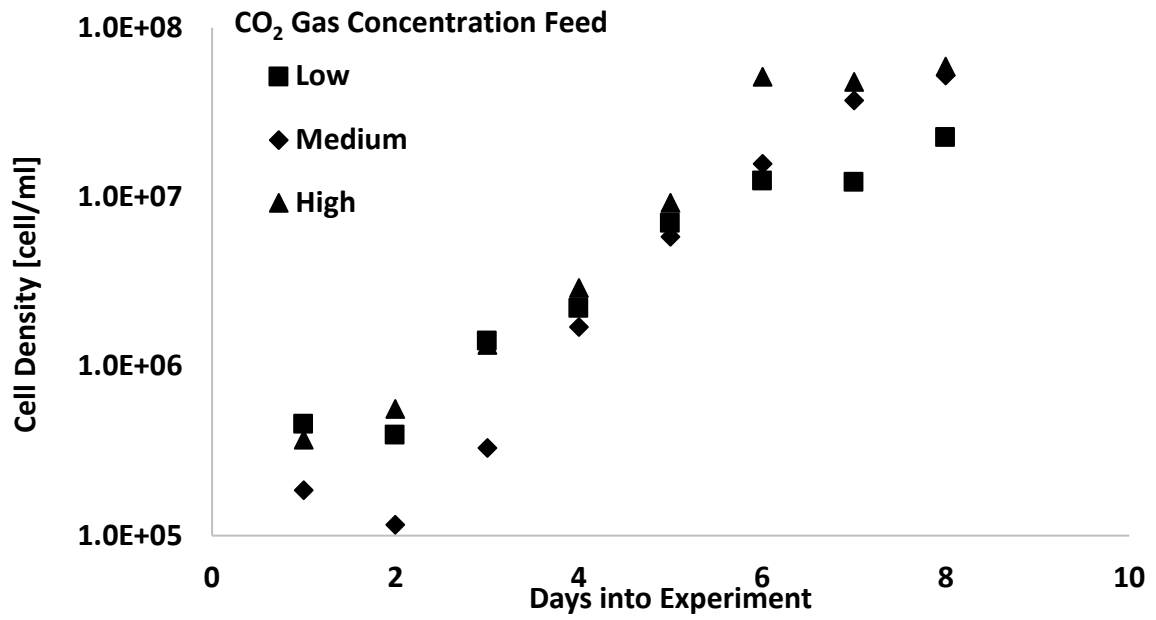


**Figure 98. Daily cell counts for each stead-state $CO_2$ concentration plotted on a semi-log plot over experiment duration**

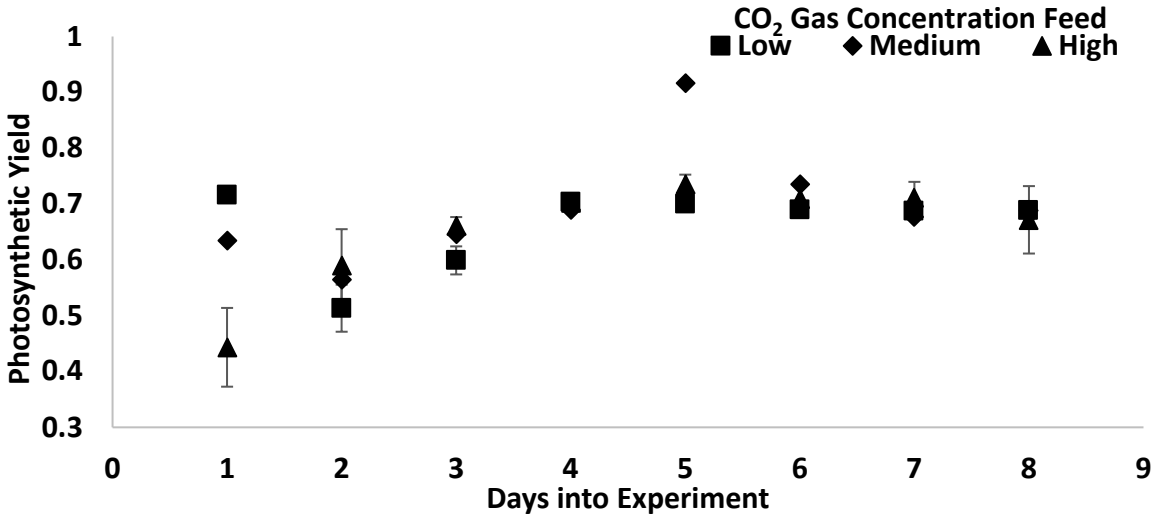


**Figure 99. Photosynthetic yield for each tested steady-state $CO_2$ feed over the course of the experiment duration. Error bars represent standard deviation calculated from multiple experimental runs.**

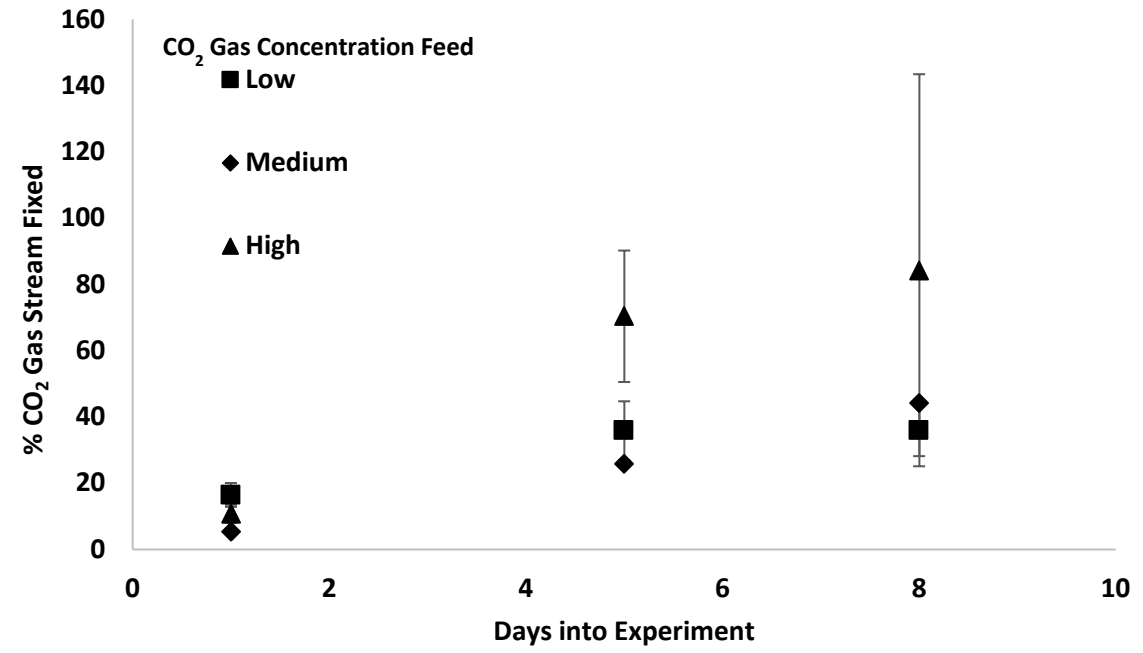


**Figure 100. $CO_2$ fixation percentage calculates the amount of carbon fixed from the provided gas stream by comparing the amount of $CO_2$ dissolved in the algal media to the amount of $CO_2$ (measured as carbon) found in the produced biomass. Each data point is the average of the triplicate containers at that day. Error bars are the standard deviation resulting from the triplicate containers.**

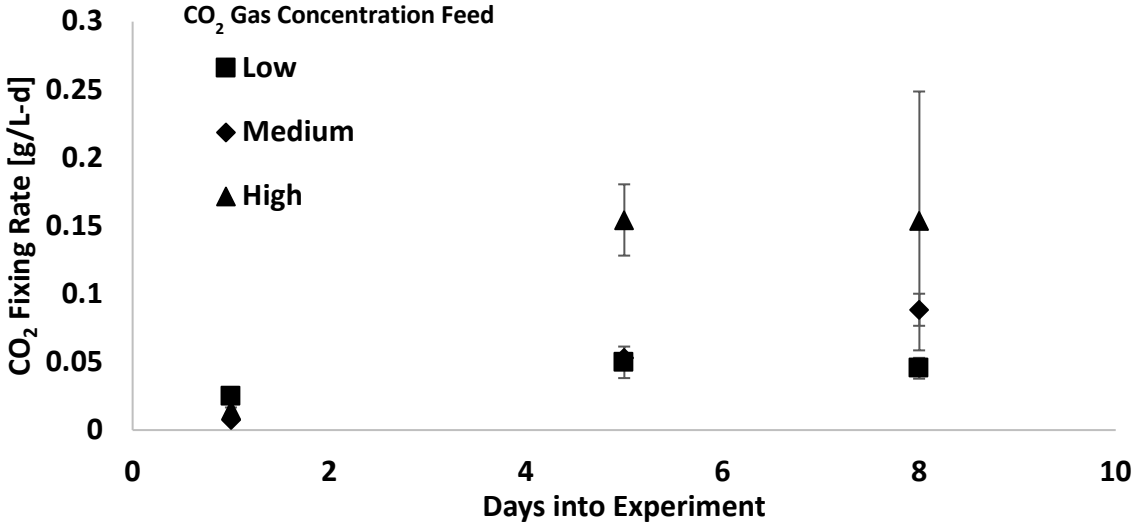


**Figure 101. $CO_2$ fixation rates were developed using the elemental analysis result and dividing by the time between analysis samples. Each data point is the average of the triplicate containers at that day. Error bars are the standard deviation resulting from the triplicate containers.**

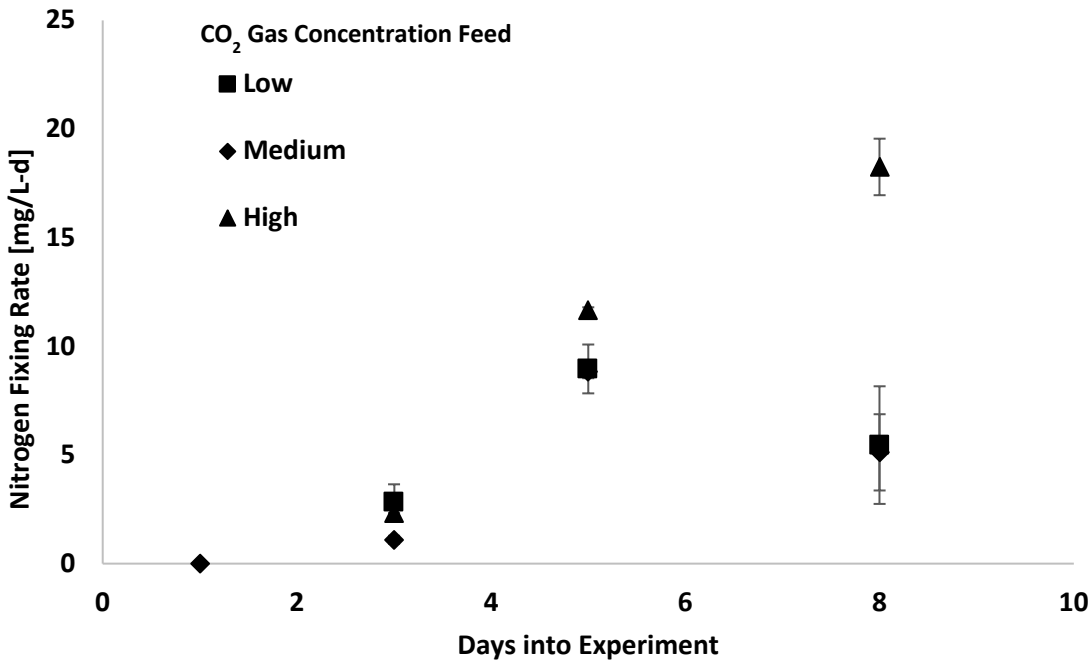


**Figure 102. Nitrogen fixation rates were developed using the elemental analysis result and dividing by the time between analysis samples. Each data point is the average of the triplicate containers at that day. Error bars are the standard deviation resulting from the triplicate containers.**

# Appendix E Additional Data for Heat and Mass Transfer Across a Nonporous Silicone Membrane

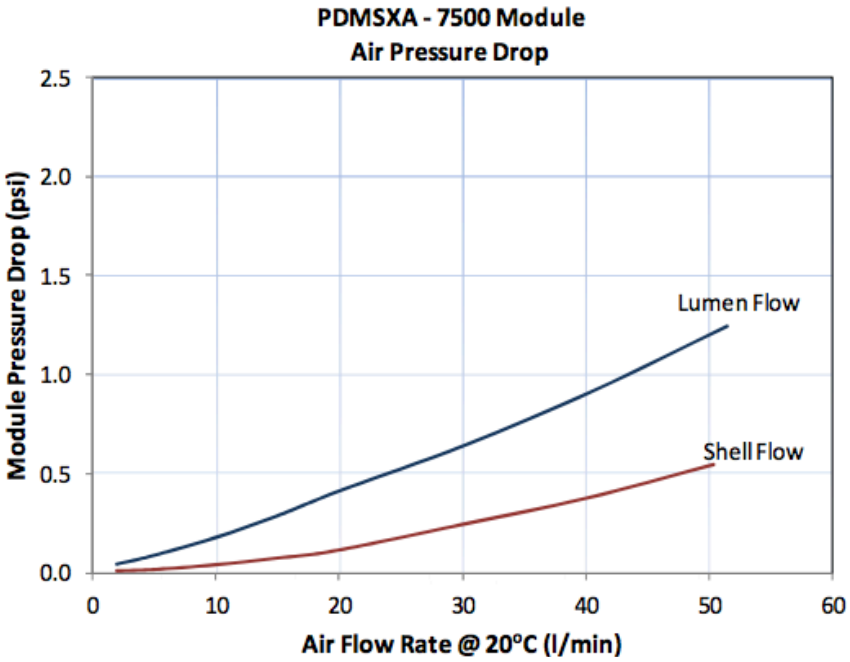


Pressure drop across PDMSXA 7500 membrane module used in experiment. Lumen-side flow of the gas within the 2-6LPM flow rang show a maximum 0.1psi pressure drop across the module. (Image credit, PermSelect)

**Table 70. Resulting p-values between all combinations gas flow rates, comparing the amount of oxygen transferred across the membrane at each temperature case. Statistically significant cases are highlighted (p<0.05).**

| | | Ice Bath (274 K) | | | Temperate Water (292 K) | | |
|---|---|---|---|---|---|---|---|
| | | **2 LPM** | **4 LPM** | **6 LPM** | **2 LPM** | **4 LPM** | **6 LPM** |
| **Temperate Water (292 K)** | **2 LPM** | 0.006 | 0.005 | 0.005 | - | 0.74 | 0.54 |
| | **4 LPM** | - | 0.002 | 0.002 | - | - | 0.76 |
| | **6 LPM** | - | - | 0.001 | - | - | - |
| **Ice Bath (274 K)** | **2 LPM** | - | 0.88 | 0.91 | | | |
| | **4 LPM** | - | - | 0.97 | | | |
| | **6 LPM** | - | - | - | | | |

**Table 71. Resulting p-values between all combinations gas flow rates, comparing the amount of carbon dioxide transferred across the membrane at each temperature case. Statistically significant cases are highlighted (p<0.05).**

| | | Ice Bath (274 K) | | | Temperate Water (292 K) | | |
|---|---|---|---|---|---|---|---|
| | | **2 LPM** | **4 LPM** | **6 LPM** | **2 LPM** | **4 LPM** | **6 LPM** |
| **Temperate Water (292 K)** | **2 LPM** | 0.64 | 0.44 | 0.45 | - | 0.99 | 0.14 |
| | **4 LPM** | - | 0.46 | 0.47 | - | - | 0.15 |
| | **6 LPM** | - | - | 0.27 | - | - | - |
| **Ice Bath (274 K)** | **2 LPM** | - | 0.76 | 0.19 | | | |
| | **4 LPM** | - | - | 0.08 | | | |
| | **6 LPM** | - | - | - | | | |

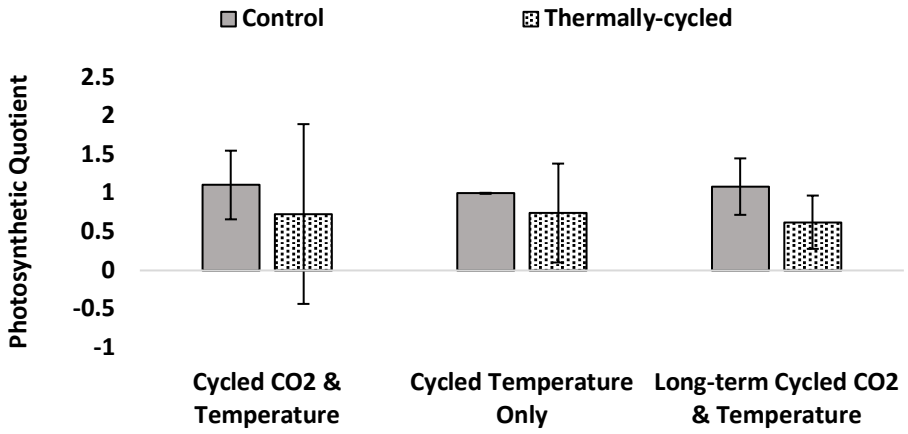


**Figure 103. Photosynthetic quotient average for each experiment is separated between the control and temperature cycled reactor. The error bars are the standard deviation of the PQ values for the associated experimental run.**

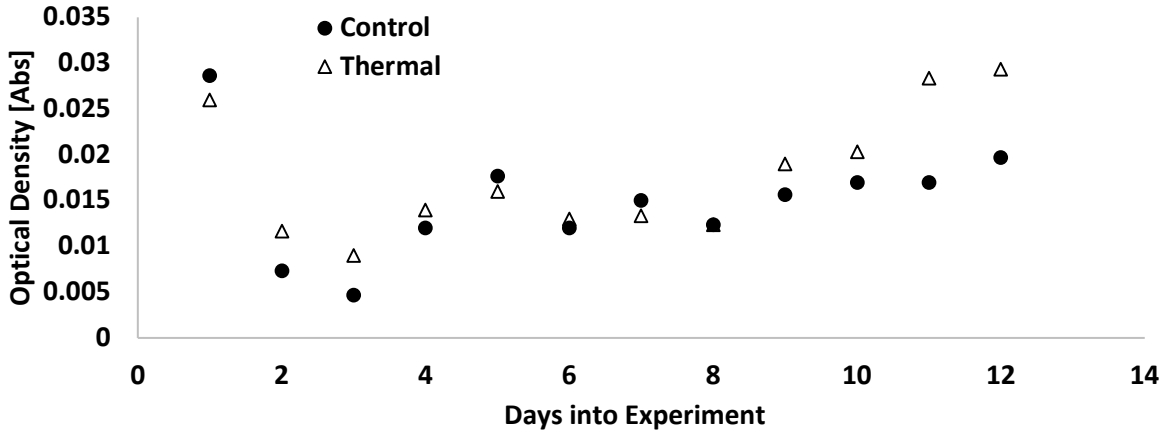


**Figure 104. Optical density of the "short" $CO_2$ and temperature cycled experiment over the course of the experiment duration**

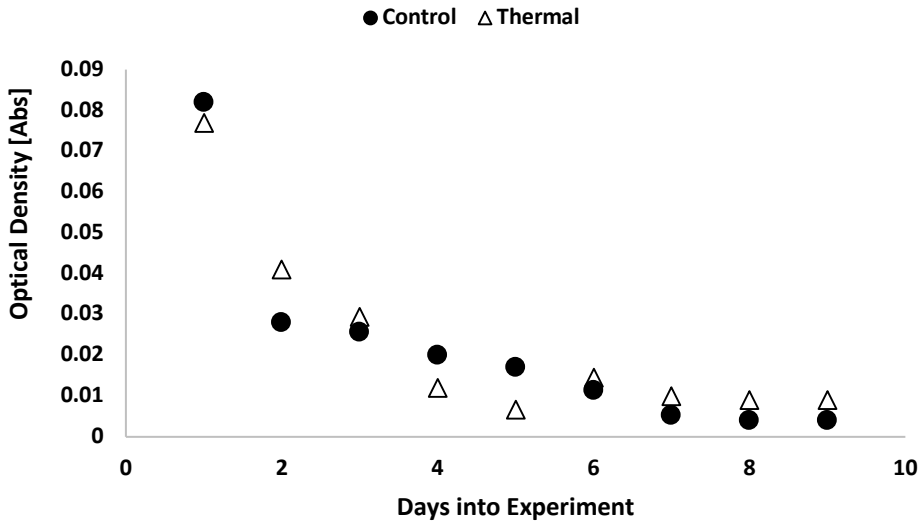


**Figure 105. Optical density as a measure of culture density for the constant $CO_2$/temperature cycled only case over the course of the experiment.**

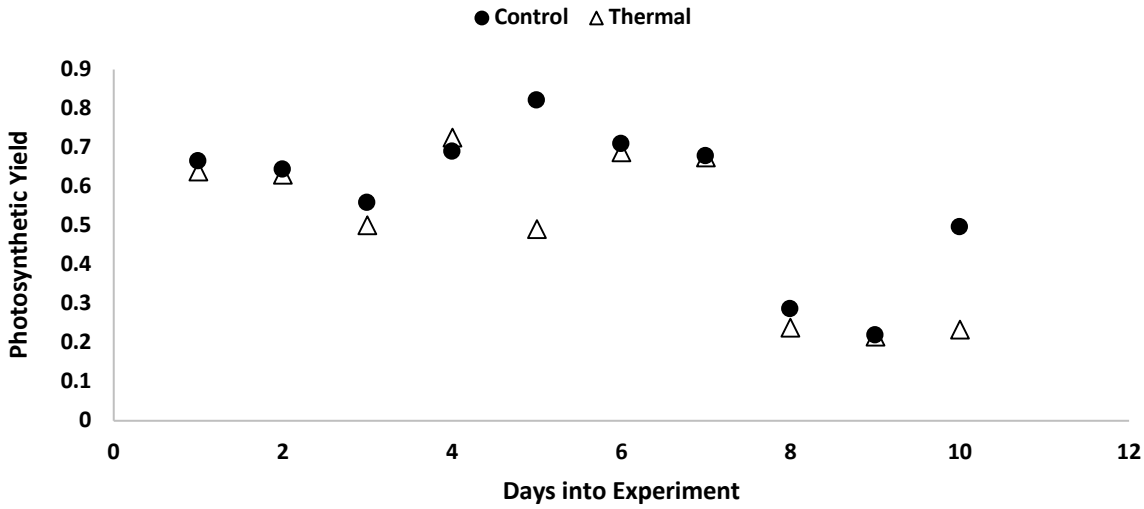


**Figure 106. Photosynthetic yield for the "short" duration $CO_2$ and temperature cycled test over the course of the experiment duration.**

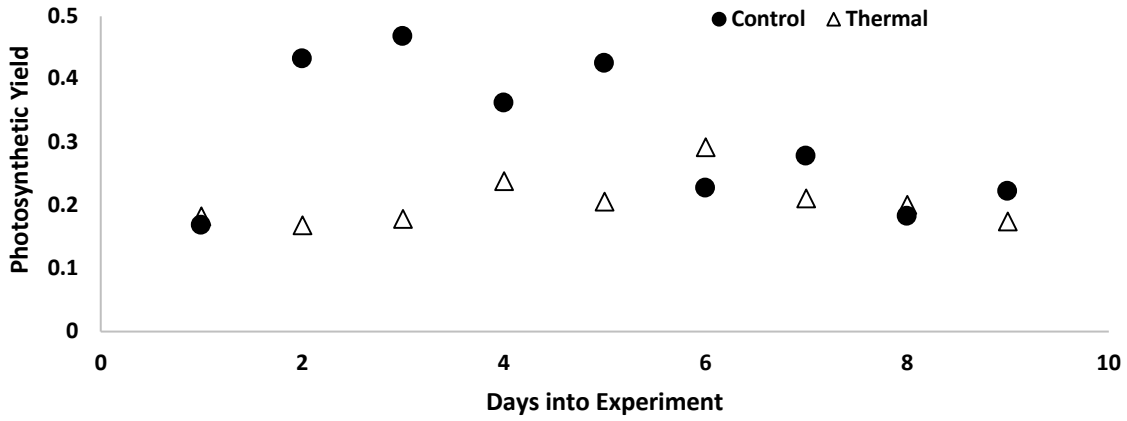


**Figure 107. Photosynthetic yield for the steady-state $CO_2$ concertation and the cycled temperature experiment over the duration of the experiment.**

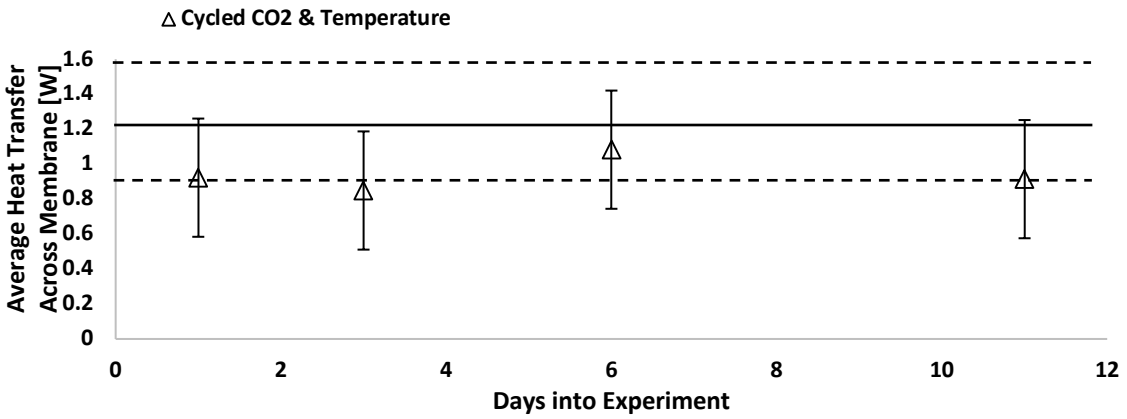


**Figure 108. Calculated heat transferred across the membrane for the "short" cycled temperature and cycled $CO_2$ case. Error bars are the calculated error from flow rate measurements, propagated through the heat transfer equation. Solid horizontal line is the calculated maximum heat transfer, and the dashed lines are the calculated error boundaries**

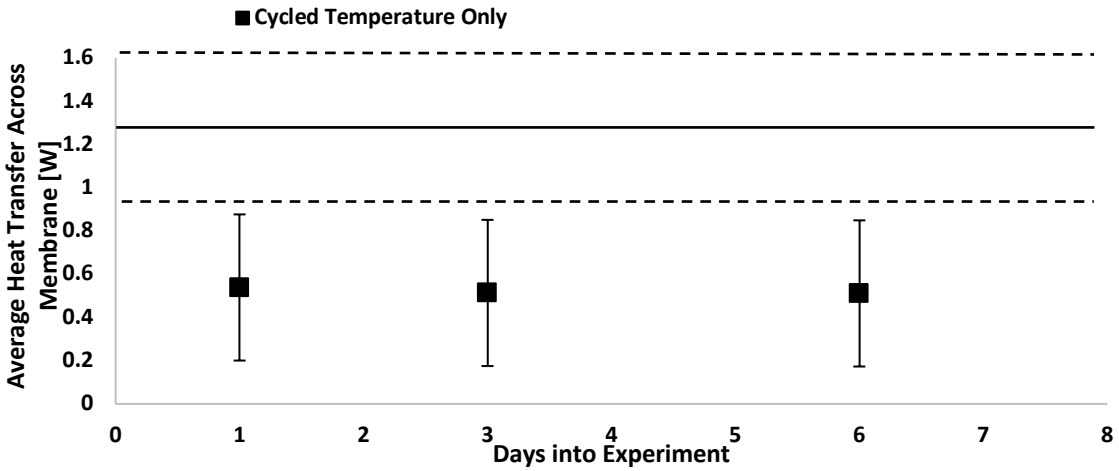


**Figure 109. Calculated heat transferred across the membrane for the cycled temperature only case. Error bars are the calculated error from flow rate measurements, propagated through the heat transfer equation. Solid horizontal line is the calculated maximum heat transfer, and the dashed lines are the calculated error boundaries**